GEOLOGIC STUDIES IN ALASKA
by the U.S. Geological Survey during 1986

U.S. Geological Survey Circular 998

Photographs on front and back covers are of 1986 eruption of Augustine Volcano.
See article on p. 4-13.

Front cover

Increasingly vigorous vapor plumes and melting of snow cover on volcano's summit were early signs of an impending eruption. View from northeast on March 21.

Back cover

Top right: Small amounts of ash were emitted along with increased vapor plume during weeks prior to eruption. Ash which fell from plume extends from summit toward foreground. View from east on February 22.

Top left: On first day of eruption, hot pyroclastic material falling on upper cone caused mudflows that extended down gullies on south and west sides of volcano. An ash-rich eruption column was almost continuous during first five days of eruption. View from southwest on March 27.

Center left: Rainfall accentuated contrast between dry, hot pyroclastic material deposited during March eruptive phase (light) and damp, lightly vegetated deposits of previous eruptions (dark). View of north side of mountain from east on April 18.

Center right: Oblique view of dark, blocky lava flow extending northward (toward bottom of picture) from summit. Photograph taken April 27.

Bottom left: Dramatic ash plume over Homer, Alaska, resulted from last large explosion of March eruptive phase which occurred at approximately 10:00 A.M. AST, March 31. Use of photograph by permission of photographer Chlaus Lotscher is gratefully acknowledged.

Bottom right: Lobate nose of a pyroclastic flow on upper slope of volcano. Flows such as this moved at estimated speeds greater than 35 meters per second (80 mph); temperature of their deposits measured several weeks after eruption exceeded 550 °C (120 °F). Photograph taken on north side of cone April 27.

GEOLOGIC STUDIES IN ALASKA by the U.S. Geological Survey during 1986

Thomas D. Hamilton and John P. Galloway

Editors

U.S. Geological Survey Circular 998

Short papers describing results
of recent geologic investigations
and lists of published reports

1987

Department of the Interior

DONALD PAUL HODEL, *Secretary*

U.S. Geological Survey

Dallas L. Peck, *Director*

Library of Congress Catalog Number 76-608093

Free on application to the Books and Open-File Reports Section,
U.S. Geological Survey, Federal Center, Box 25425, Denver, CO 80225

CONTENTS

SOUTHEASTERN ALASKA

OFFSHORE

Walrus on Round Island in Bristol Bay. Photo by S.E. Box, 1982.

GEOLOGIC STUDIES IN ALASKA BY THE U.S. GEOLOGICAL SURVEY DURING 1986

Thomas D. Hamilton and John P. Galloway, Editors

INTRODUCTION

This volume is a continuation of the annual circulars that formerly were titled "The United States Geological Survey in Alaska--Accomplishments during 19xx." The 39 short papers and three abstracts presented here report on some of the geologic studies performed in Alaska by the U.S. Geological Survey (USGS) and cooperating agencies during 1986. The reports are presented in their geographic order of occurrence, beginning with investigations that are statewide in scope and followed by papers related to five regional subdivisions of Alaska and to areas offshore on the Alaskan continental shelf. The regional papers are generally presented in sequence from north to south. Author and subject indexes and full addresses of all authors are appended at the back of the volume. We also include two bibliographies that cover (1) reports about Alaska in USGS publications released in 1986 and (2) reports about Alaska by USGS authors in other publications in 1986.

The 42 reports in this volume provide a representative sample of current U.S. Geological Survey research in Alaska. Sixteen papers are devoted to mineral resources--six on precious metals, six on other metallic resources, three on fossil fuels, and one on statewide inventory systems. Basic framework studies comprise an additional 16 papers that focus on a wide range of topics, including geochronology, structural geology, stratigraphy, petrology, and paleoclimatology. Comparable studies carried out offshore comprise seven additional papers. Geologic hazards in Alaska's dynamic environment are discussed in three reports that cover volcanic hazards, earthquake recurrence intervals, and coastal erosion.

This year we depart from custom by publishing "an article of special interest" devoted to a topic that was prominent in the news during 1986--the eruption of Augustine Volcano and its impact on population centers around Cook Inlet. That paper, which begins on the following page, is longer and more fully illustrated than the other papers in this volume, and its illustrations include the photographs on the front and back covers.

The two bibliographies that follow the short reports were compiled by Ellen R. White, and the mosaic of cover photographs was prepared by M. Elizabeth Yount and Robert F. Gilmore. We would like to particularly acknowledge the efforts of Susan Bartsch-Winkler and Katharine M. Reed, the editors of the three preceding (1983-1985) volumes in the "Accomplishments" series, who set a high standard of dedication and quality that we have been hard pressed to maintain. We have borrowed liberally from their ideas in preparing the present volume.

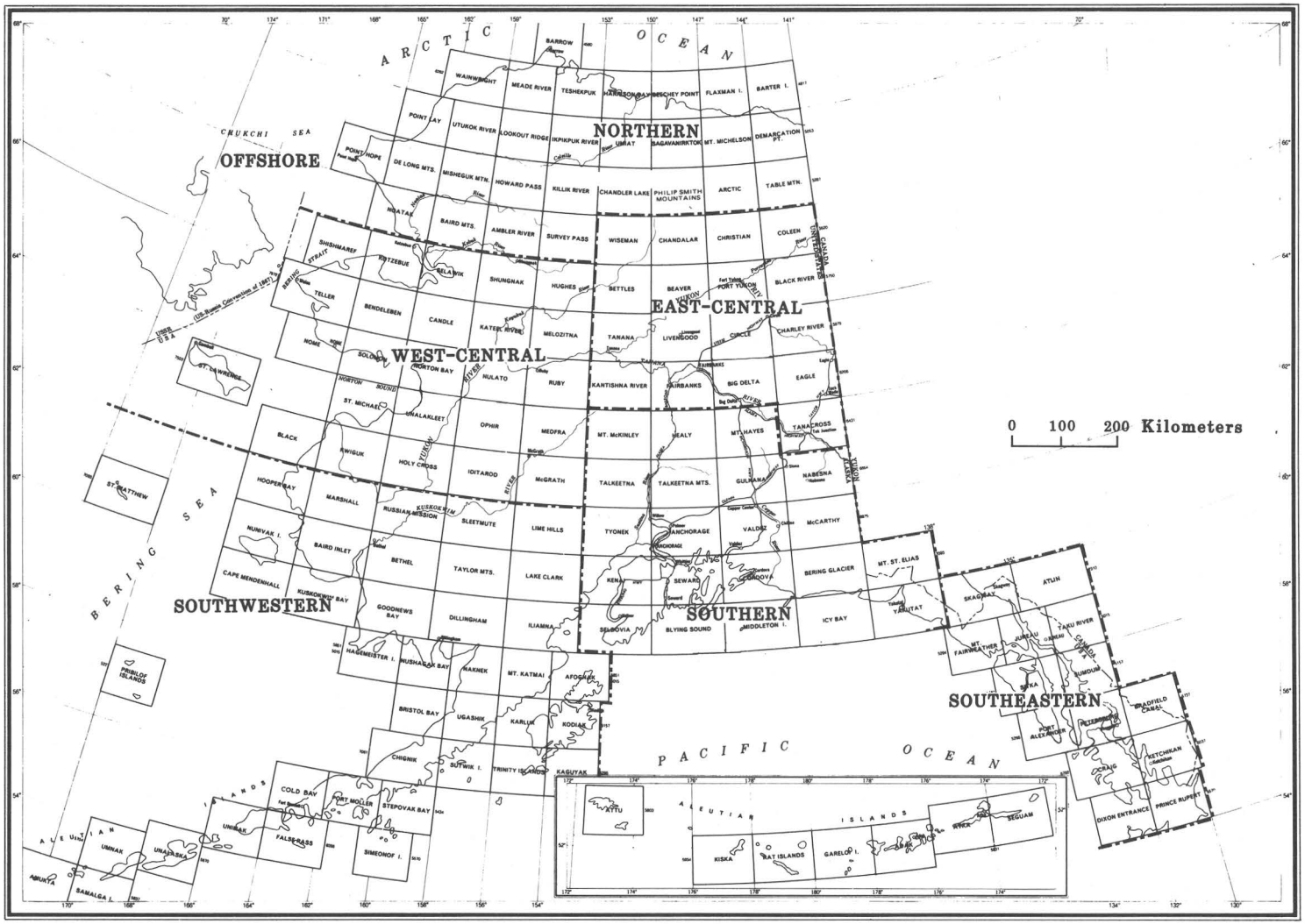

Regions of Alaska as used in this circular.

ARTICLE OF SPECIAL INTEREST

Geologist sampling steep, blocky face of lava flow that was erupted during April 1986 at Augustine Volcano. Photo by M.E. Yount, May 6, 1986.

THE 1986 ERUPTIONS OF AUGUSTINE VOLCANO, ALASKA: HAZARDS AND EFFECTS

M. Elizabeth Yount, Thomas P. Miller, and Bruce M. Gamble

Augustine Volcano, 1,227 m high, forms a 8x11 km^2 island 280 km southwest of Anchorage and is the southernmost of five volcanoes in the Cook Inlet region (fig. 1). Since its discovery by Captain Cook in 1778, Augustine has had six recorded eruptions: 1812, 1883, 1935, 1963-64, 1976, and 1986 (Kienle and Swanson, 1985). The last four eruptions have each involved explosive venting of ash, pyroclastic flows and mudflows, and, in the later phases, eruption of lava and formation of a new dome within the summit crater. The most violent historic eruption of Augustine Volcano occurred in 1883 when major explosive activity triggered a tsunami in lower Cook Inlet that caused minor damage to nearby coastal communities (Davidson, 1884). The 1986 eruption consisted of three main episodes on March 27-April 2, April 23-28, and August 22-September 1.

The following account, intended for geologists and non-geologists, briefly summarizes the perceived hazards from eruptions of Augustine volcano, the 1986 activity and its effects, and the distribution and chemistry of airborne ash from the 1986 eruption.

Potential hazards

Knowledge of Augustine Volcano's eruptive history allows inferences about the potential hazards of future activity (Kienle and Swanson, 1983, 1985). The most likely and widespread hazard is posed by airborne ash, whose abrasive and corrosive properties can cause severe damage to exposed mechanical and electronic equipment. Major disruption to transportation and communication networks can occur in areas of heavy ashfall; for example, two Boeing 747 jets over Indonesia in 1982 experienced in-flight failure of engines due to ingestion of airborne ash (Blong, 1984). Several air traffic corridors pass within 50 km of Augustine; at least five aircraft were damaged during the 1976 eruption (Kienle and Swanson, 1985, p. 31). Although unlikely to be erupted in quantities large enough to pose a major direct threat to life in lower Cook Inlet communities, ash may exacerbate existing health problems.

Eruption-induced tsunamis (sea waves), although less common, are potentially more devastating to nearby coastal communities than the ubiquitous ash. A tsunami caused by a large avalanche during the 1792 eruption of Unzen volcano in Japan resulted in a death toll of at least 700 (Blong, 1984). The 1883 explosive eruption of Augustine Volcano produced a massive avalanche into Cook Inlet (Siebert and others, 1986), causing a tsunami 7-9 m high at Port Graham, 90 km to the east on the southwest Kenai Peninsula. Damage at Port Graham was apparently limited to boats; "fortunately it was low water, or all of the people at the settlement must inevitably have been lost" (Davidson, 1884). Mounds and irregular ridges on the north shore of Augustine Island are deposits of the 1883 avalanche (fig. 2). Similar deposits on the west, northeast, and south sides of the island record as many as seven prehistoric avalanches (Beget, 1986) and emphasize the recurrent hazard of avalanche-generated tsunamis at Augustine.

Recent computer simulation of the 1883 avalanche by Zygmunt Kowalik, University of Alaska, has predicted travel times for a comparable tsunami (Kienle and others, 1986). The calculated travel time to Port Graham is approximately 1 hour (fig. 3) as compared to the 25-min travel time reported for the 1883 tsunami (Davidson, 1884). Imprecise timing estimates in 1883 or scaling problems with the controlling

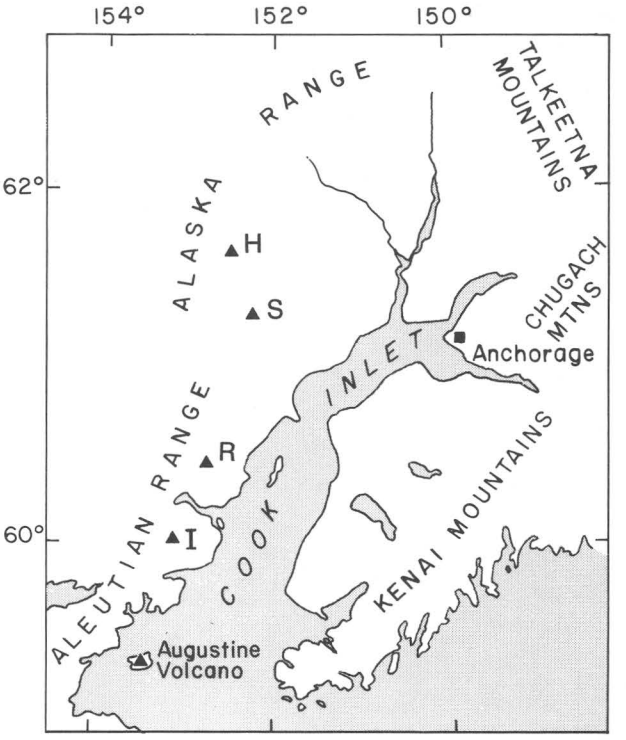

Figure 1.--Cook Inlet region, showing location of Augustine Volcano, Mount Iliamna (I), Redoubt Volcano (R), Mount Spurr (S), and Hayes volcano (H). Mountain ranges surrounding Cook Inlet caused northward-directed ash to stagnate above Cook Inlet for first three days of 1986 eruption.

Figure 2.--Northeast end of Augustine Island on April 18, 1986. In foreground are mounds and irregular ridges which resulted from 1883 avalanche. Deposits of March 1986 pyroclastic flows are light-colored material extending upslope from shoreline on left (east). Snow level is about 300 m in this picture.

parameters for the computer simulation may account for the 35-min difference. These travel-time estimates place severe constraints on warning and evacuation time, which would be shorter by the time required by observers or analysts to determine that a tsunami had likely been generated. Effects of a tsunami might be mitigated if the tide were relatively low at the time of occurrence (as it was in 1883).

The 1986 Augustine eruptions

The first of the 1986 eruptions was preceded by more than five weeks of generally increasing seismic activity and heat flow to the summit area. Most of the thousands of seismic events detected by the five seismometers on the island before and during the eruption were so small as not to be detected by a seismometer at Oil Point, 32 km to the north.

The eruption began on March 27 and was characterized by an almost continuous, ash-rich eruption plume that commonly reached elevations

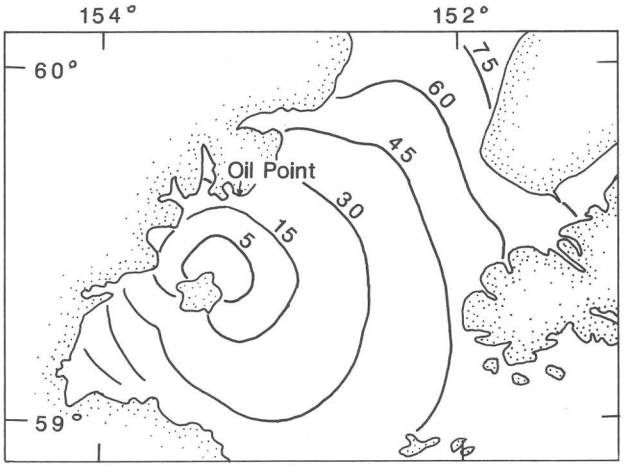

Figure 3.--Calculated travel time (in minutes) of a tsunami resulting from an avalanche of same size and location as 1883 avalanche (after Kienle and others, 1986). Computer modeling by Zygmunt Kowalik, University of Alaska Institute of Marine Sciences.

of 3,000 to 4,600 m and was punctuated by large explosions (fig. 4) that generated columns of ash as high as 12,200 m. Hundreds of small pyroclastic flows moved down the north flank of Augustine during the first few days of the eruption (fig. 5; Miller and others, 1987), the largest ones reaching the north shore, 5 km from the summit vent. Pyroclastic flow activity gradually diminished after March 31.

During the April and August episodes, lava erupted from the summit vent, fed a short, steep lava flow down a north-facing gully, and built a new dome (fig. 6; Kienle and others, 1986; Yount and Miller, 1987). The eruption column seldom exceeded 3,700 m in height, and the large explosive events of the earlier March 27-31 episode were not observed. Ash erupted in small bursts every few minutes, often followed immediately by small pyroclastic flows.

Distribution and chemistry of ash from the March 1986 eruption

The distribution of airborne ash during volcanic eruptions is determined chiefly by the height of the eruption column, wind direction and speed at various altitudes, amount of precipitation during the eruption interval, and size and shape of particles erupted. Some of these factors changed drastically during the March eruptive episode, affecting the pattern of ash distribution. Because of these changes and because much of the area surrounding Augustine Island is either ocean or sparsely inhabited, detailed mapping of the ash distribution was not possible.

Data on the timing and height of explosion columns and wind directions during the March episode do provide a general picture of the ash distribution during the explosive, ash-rich initial

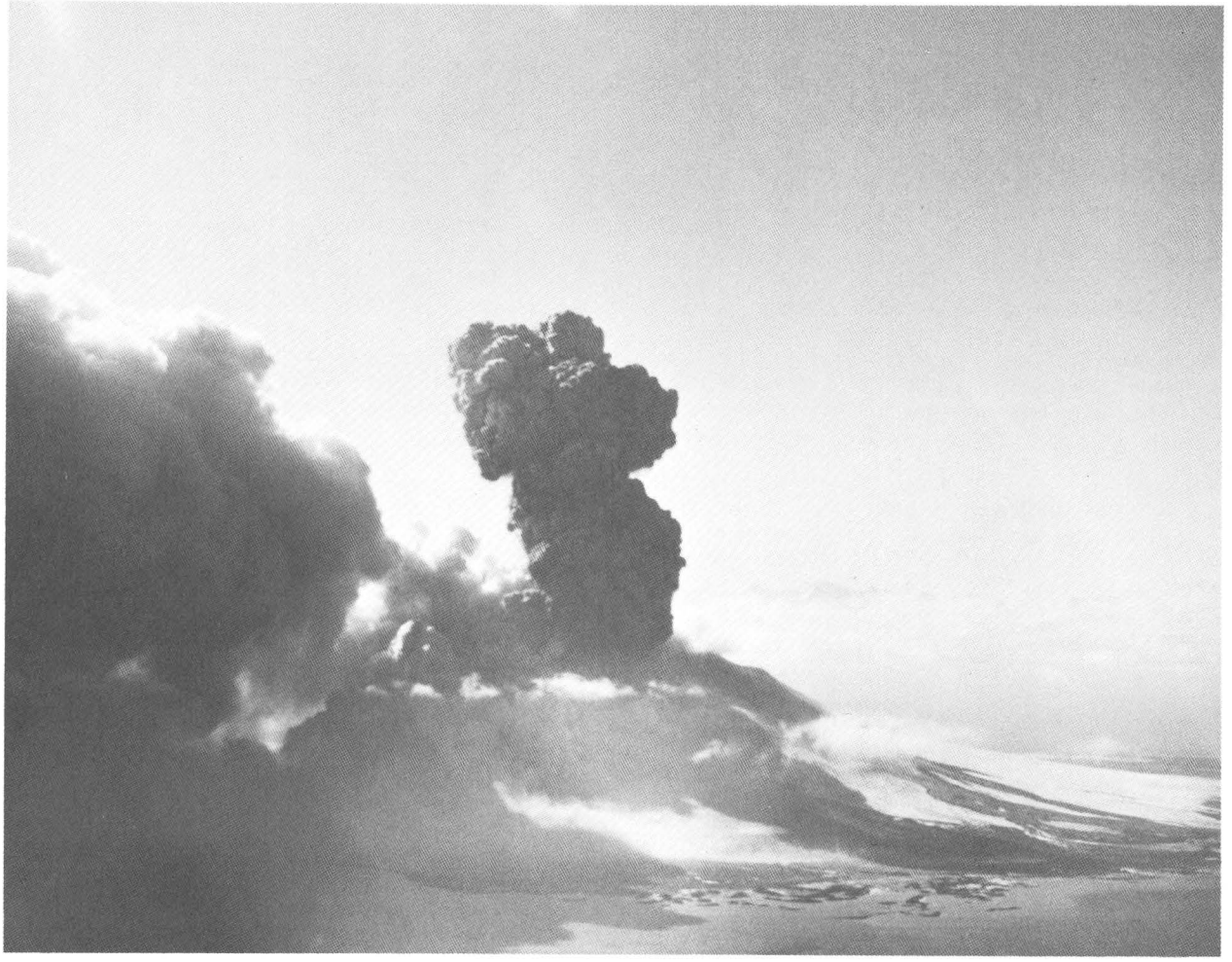

Figure 4.--Explosive burst of ash, March 28, 1986, photographed approximately 30 seconds after first appearance. During first five days of March eruption, such explosions propelled ash as high as 12,200 m into the atmosphere.

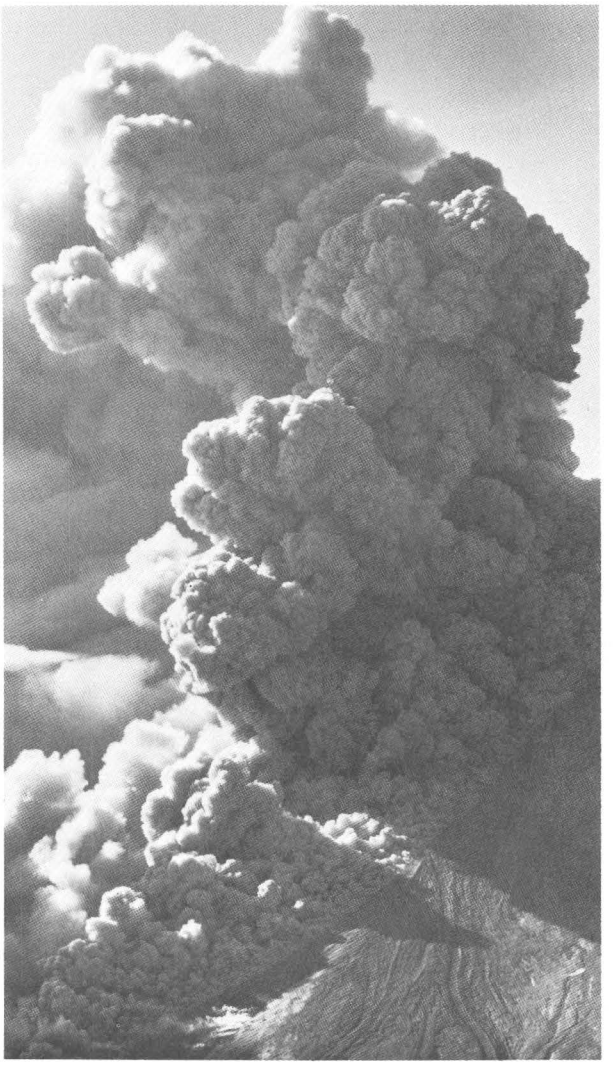

Figure 5.--Pyroclastic flow racing down north side of Augustine Volcano on March 30, 1986. Composed of hot, turbulent mixtures of rock chunks ranging from house to sand size and rapidly expanding volcanic gases, these flows travelled at estimated speeds greater than 100 km per hour.

phase. Explosion plume heights summarized in figure 7 are based on pilot reports, USGS observation flights, and radar observations from King Salmon and Kenai; the times shown on figure 7 are only approximate. The elapsed time between onset of an explosive event and decay of the subsequent eruption column varied from one-half to more than one hour. The radar station at Kenai was shut down for 24 hours March 28-29 due to ash fallout, thereby hampering recognition of major explosive events. Airborne observers were scarce during the first three days of the eruption because ash suspended in the atmosphere over Cook Inlet made aircraft operations hazardous. For these reasons, correlation of the larger seismic events with the large explosive ash bursts was limited.

General wind directions at the 1,470-m (4,500-ft) level are shown on figure 8. Winds were generally southerly during the first 36 hours of the eruption, sending the eruption plume over the western edge of the Kenai Peninsula and northward between Anchorage and Mount Spurr. The plume did not spread appreciably downwind, but remained relatively narrow (fig. 9), thereby constraining the width of the area affected by ash fallout. Airborne ash was detected as far north as the Brooks Range on March 28 (Gary Herbert, NOAA, oral commun., April 1986). Much ash remained in the atmosphere of Cook Inlet basin due to confining effects of surrounding mountains (shown on fig. 1) and to varying wind directions at different altitudes, which caused atmospheric mixing of the ash. At mid-day on March 28, winds shifted to westerly (fig. 8), sending eruption plumes toward Anchor Point and Homer and beginning to disperse ash from the upper Cook Inlet atmosphere. The final large explosion on March 31 caused spectacular ash clouds over Anchor Point (fig. 10) and deposited approximately 2-3 mm of ash on Anchor Point and Homer.

Ash samples from the 1986 eruption collected in Homer consist of 2- to 30-μm-sized fragments of rock, glass shards, and crystals of plagioclase and pyroxene; they are finer grained than those collected following the 1976 eruption. The chemical compositions of 1986 ash samples collected in Anchorage, Drift River, Homer, and Seward are shown in table 1, together with several 1976 samples for comparison. All of the 1986 samples contain greater than 64 percent silica. Samples of 1986 ash are higher in silicon dioxide, potassium oxide, and phosphorus pentoxide than 1976 ash samples, and they are lower in aluminum oxide, iron oxide, magnesium oxide, and calcium oxide. However, all analyses are within ranges typical of continental-margin calcalkaline volcanoes.

Gas sampling downwind of a volcano, when done on a regular basis, can indicate an impending eruption through changes in levels of SO_2 and CO_2 (Harris and others, 1981; Casadevall and others, 1983). Pre-eruption measurements at Augustine are not available; but on April 3, Rose and others (1987), using a plane equipped with a correlation spectrometer (COSPEC) and flying at the margins of the plume, measured a sulfur dioxide (SO_2) emission rate of 24,000 tonnes per day (one of the highest rates ever recorded from an erupting volcano) and estimated hydrogen chloride (HCl) emission at 6,000 t/d. By contrast, at Mount St. Helens on May 25, 1980, seven days after the catastrophic May 18 eruption, SO_2 emission rates were 2,500 t/d (Casadevall and others, 1981). By July 24, SO_2 emission at Augustine had dropped to 380 t/d (Symonds and others, 1987). Acidic volcanic gases containing chlorine, bromine,

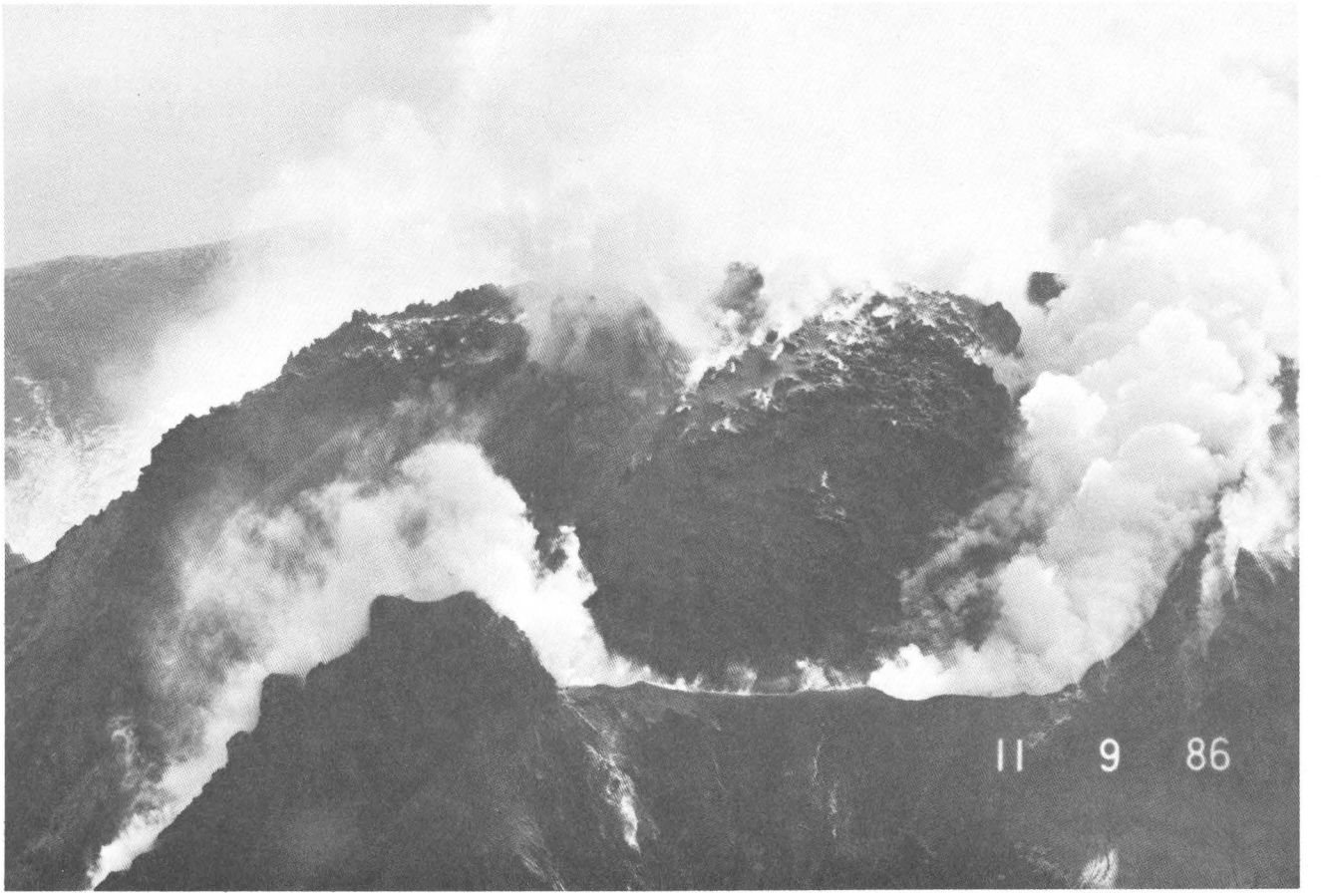

Figure 6.--View east toward new dome in summit crater, September 9, 1986. Western crater rim is in foreground, east shore of island in background.

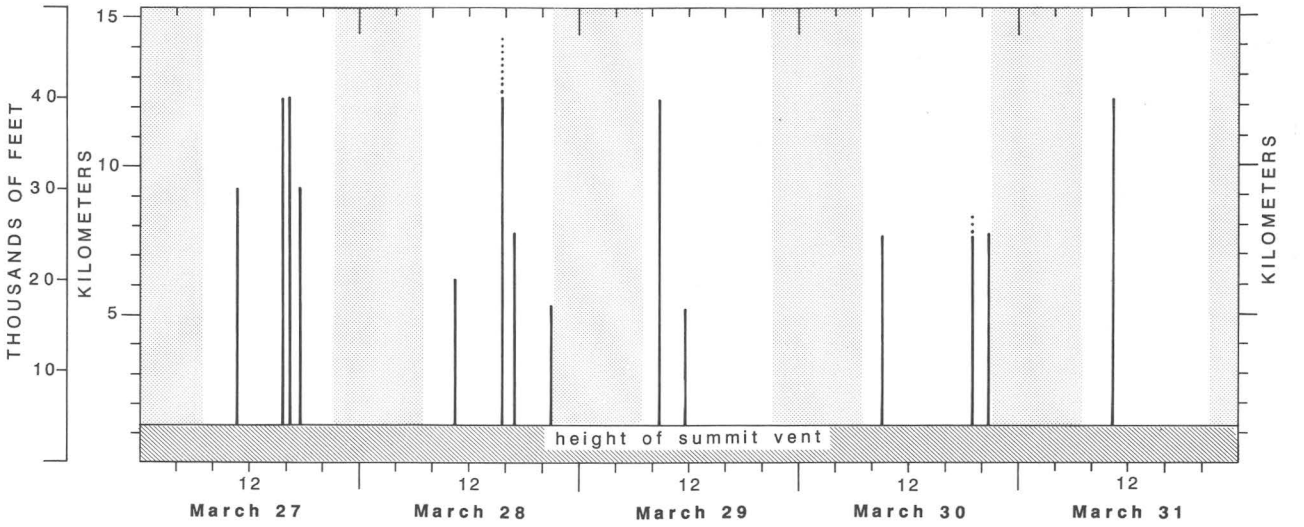

Figure 7.--Height of observed explosive eruption plumes from summit vent (elevation 1,227 m) of Augustine Volcano during March 27-31. All times are Alaska Standard Time. Nighttime hours shaded, lack of eyewitness observations accounts for apparent lack of explosive eruptive plumes during nights. Large explosive bursts of comparable magnitude were not observed during April and August eruptive episodes.

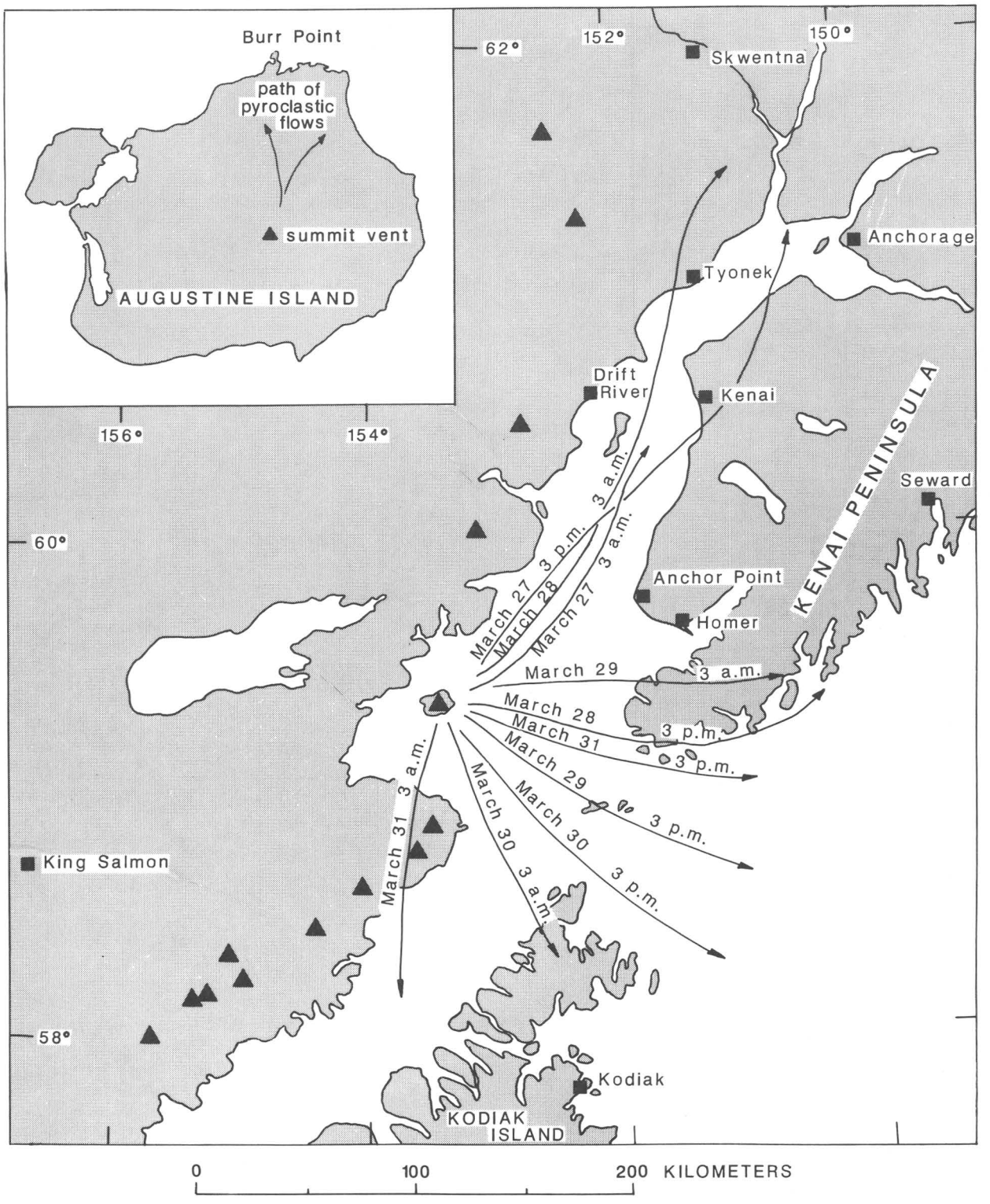

Figure 8.--General direction of winds at 1,470-m (4,500-ft) level during period March 27-31 as estimated from National Weather Service charts based on winds-aloft data from Anchorage, King Salmon, Kodiak, and McGrath. Explosive eruption plumes of up to 12,200 m were influenced by directions of higher level winds.

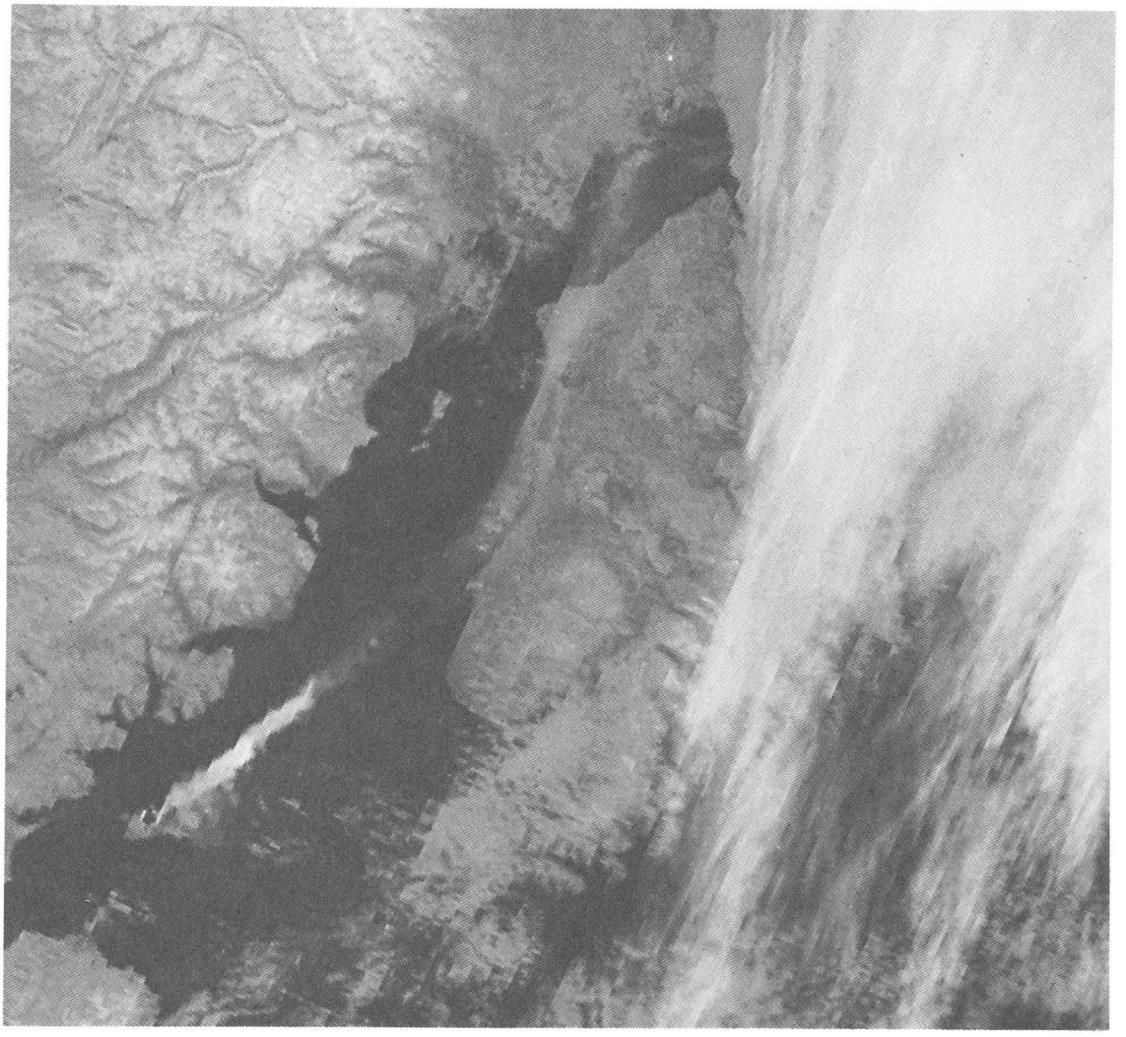

Figure 9.--Satellite image of eruption plume taken 5:18 A.M. AST, March 28, showing narrow ash plume extending from Augustine across Kenai and Tyonek toward Skwentna. Westward bend in plume resulted in less ashfall in Anchorage than would otherwise have occurred.

fluorine, and sulfur which vented both during and following the eruptive episodes were dispersed and diluted downwind, posing no significant health threat except perhaps on Augustine Island. Heavy rainfall during the August episode was probably highly acidic in the immediate vicinity of the mountain, accounting for the marked destruction of brush on the volcano's slopes noted in early September.

Effects of the eruptions on south-central Alaska

Because Augustine is a remote, uninhabited island, effects of its 1986 eruptions on the population centers of Cook Inlet are limited to two main categories: those resulting from ash and those resulting from the threat of a tsunami. Airborne ash disrupted air traffic in south-central Alaska, especially in the upper Cook Inlet basin from March 27 to 30. The Federal Aviation Administration issued Notices To Airmen (NOTAMS) warning of the hazard and restricting flights around the volcano. Most commercial and general aviation flights were either canceled or diverted to airports away from the affected area as ash stagnated in the atmosphere over Cook Inlet. On March 28, when Anchorage International Airport would ordinarily have handled 300 flights, 16 flights were served (The Anchorage Times, March 29, 1986). Military aircraft stationed at Elmendorf Air Force Base were deployed to other bases during the period March 27-30. By March 31, as the atmosphere around Anchorage cleared, aircraft schedules were resumed. Despite these precautions, slight damage to aircraft was reported. For example, on March 29, a DC-10 on

Figure 10.--Ash cloud over Anchor Point on March 31, 1986. This remarkable ash plume, resulting from final large explosive event at 10:00 A.M. AST, dropped approximately 2-3 mm of ash on Anchor Point and Homer (analyses 5 and 6, table 1). Similar billowing clouds of ash were seen over eastern Washington following 1980 eruption of Mount St. Helens (see Findley, 1981). Use of photograph by permission of photographer Linda Sandlin is gratefully acknowledged.

descent into Anchorage flew through a cloud of disseminated ash, causing minor damage to engine parts and light frosting of its windshield.

During the first few days of eruption, radio stations and newspapers advised residents of potential ashfall hazards and how to mitigate them. Early predictions of significant ashfall in Anchorage prompted concern about electrical generating capabilities because generator turbines sustained minor abrasion and loss of power during the 1976 eruption. Chugach Electric Company requested the public to curtail unnecessary electrical use on March 27 in anticipation of a possible shortfall in power supply due to shutdown of the turbines. Employers responded by sending workers home early and shutting down computers and other machines sensitive to ash abrasion; a 13 percent drop in electrical consumption resulted (The Anchorage Times, March 29, 1986). On March 28, Anchorage municipal health officials measured airborne particulates in concentrations of up to 862 micrograms per cubic meter, 13 $\mu g/m^3$ short of a health emergency if sustained for 24 hours (The Anchorage Times, March 29, 1986).

Because of the potential for a tsunami in lower Cook Inlet, State and local emergency management personnel reviewed and revised

Table 1.--Chemical composition of airborne ash samples from Augustine Volcano, Alaska
[Analyses do not represent magma chemical composition because larger and denser particles drop out of an ash cloud first due to eolian sorting and ash samples include rock particles from previous eruptions from the vent walls. Major element analyses by XRF; analysts: Tom Frost, Stuart MacPherson, L.F. Espos, B.W. King, Sarah Neil, Lois Schlocker; Rb and Sr analyses by Kevex XRF, analyst: Bruce Gamble]

	1	2	3	4	5	6	7	8	9
	weight percent								
Si_2O	65.8	66.8	64.0	67.9	64.9	64.6	64.3	63.6	63.1
Al_2O_3	15.5	15.5	16.2	15.2	16.1	16.0	16.2	16.4	16.7
Fe_2O_3	2.08	1.74	1.91	1.75	1.60	1.66	1.50	2.31	2.58
FeO	2.09	1.96	2.44	1.74	2.61	2.58	2.88	2.48	2.61
MgO	1.8	1.7	2.3	1.30	2.0	2.1	2.1	2.27	2.65
CaO	5.14	4.90	5.25	4.14	5.55	5.50	5.60	5.84	6.41
Na_2O	3.9	3.6	3.5	3.8	3.5	3.7	3.6	3.82	3.51
K_2O	1.50	1.50	1.30	1.62	1.30	1.30	1.25	1.23	1.04
H_2O+	.35	.24	.71	.26	.14	.16	.19	.18	.16
H_2O-	.06	.08	.05	< .01	.12	.09	.14	.12	.06
TiO_2	.53	.50	.56	.49	.53	.54	.55	.59	.62
P_2O_5	.20	.20	.25	.18	.23	.23	.23	.15	.15
MnO	.09	.09	.09	.08	.09	.09	.09	.09	.10
CO_2	.70	.39	1.79	.21	< .01	< .01	< .01	.06	.08
Cl	.095	.15	.091	.16	.12	.11	.10	.14	.07
F	.02	.02	.02	.02	.02	.02	.02	--	--
Total S	.03	.06	.06	< .01	.12	.12	.12	.16	.04
	Parts per million								
Rb	31	29	30	33	29	29	28	--	--
Sr	260	257	282	239	296	306	296	--	--
Rb/Sr	.119	.113	.106	.138	.098	.095	.094	--	--

Notes: date and place collected, collector, comments:
1--March 28, 1986, Anchorage, John Decker
2--March 29, 1986, Drift River, from deck of oil loading platform
3--March 29, 1986, A.M., Seward, R. Folger, overnight airfall on cars
4--March 31, 1986, 8 A.M. AST, Anchorage, Bruce Gamble
5--March 31, 1986 A.M., Homer, Joe Gallegar
6--March 31, 1986, A.M., Homer, Deena Benson
7--April 3, 1986, Homer airport, FAA-FSS personnel from porch railing
8--January 25, 1976, Anchorage, Tom Miller
9--1976, Knutson Bay (Iliamna quadrangle), Bruce Reed

evacuation plans for residents of low-lying areas. This was particularly important because the April eruptive episode occurred on a weekend during one of the lowest spring tides of the year, when several thousand people would normally be digging clams on the beaches along the eastern side of Cook Inlet. Although no attempt was made to restrain public access to the beaches, the Alaska Division of Emergency Services and the Kenai Peninsula Borough Emergency Management Office broadcast radio and television warnings advising people of the potential hazard. Other effects due to the threat of a tsunami included delay of a liquid-natural-gas tanker scheduled for loading at Kenai until after the eruption was over.

The April eruptive episode coincided with local fishing season in the shallow waters immediately surrounding Augustine Island. Since some of the larger pyroclastic flows generated during the March eruptive episode reached the ocean, mariners were kept advised of the progress of the eruption through broadcast messages from the U.S. Coast Guard. Alaska Fish and Game personnel were prepared to close the fishing season should the hazard become high, but this was not deemed necessary.

Conclusion

The 1986 eruptions of Augustine Volcano have tested and strengthened the volcanic eruption monitoring and response capabilities of federal and State officials in Alaska. Although damage due to airborne ash was minimized by its distribution pattern and the response of airline and charter aircraft operators, effects of future ashfalls may be quite different. Based on ash deposits from Cook Inlet volcanoes preserved in sediments over the last 10,000 years (Riehle, 1985), inhabitants of the Cook Inlet region can expect to be confronted with a measureable ash eruption on the average of every 30 years. Although no tsunami resulted from its 1986 eruptions, tsunamis are a major potential hazard during future eruptions of Augustine Volcano.

REFERENCES CITED

Beget, James, 1986, Prehistoric tephra eruptions, debris avalanches, and tsunamis at Mt. St. Augustine--The geologic record (abs.): Eos (American Geophysical Union Transactions), v. 67, no. 44, p. 1260.

Blong, R.J., 1984, Volcanic hazards, a sourcebook on the effects of eruptions: Sydney, Academic Press, 424 p.

Casadevall, T.J., Johnston, D.A., Harris, D.M., Rose, W.I., Jr., Malinconico, L.L., Stoiber, R.E., Bornhorst, T.J., Williams, S.N., Woodruff, Laurel, and Thompson, J.M., 1981, SO_2 emission rates at Mount St. Helens from March 29 through December, 1980: U.S. Geological Survey Professional Paper 1250, p. 193-200.

Casadevall, T.J., Rose, W.I., Jr., Gerlach, T.M., Greenland, L.P., Ewart, J., Wunderman, R., and Symonds, R.B., 1983, Gas emissions and the eruptions of Mount St. Helens through 1982: Science, v. 221, p. 1383-1385.

Davidson, George, 1884, Notes on the volcanic eruption of Mount St. Augustin, Alaska, Oct. 6, 1883: Science, v. 3, no. 51, p. 186-189.

Findley, Rowe, 1981, St. Helens: National Geographic, v. 159, no. 1, p. 3-65.

Harris, D.M., Sato, Motoaki, Casadevall, T.J., Rose, W.I., Jr., and Bornhorst, T.J., 1981, Emission rates of CO_2 from plume measurements: U.S. Geological Survey Professional Paper 1250, p. 201-207.

Kienle, Juergen, Davies, J.N., Miller, T.P., and Yount, M.E., 1986, 1986 eruption of Augustine Volcano: Public safety response by Alaskan volcanologists: Eos (American Geophysical Union Transactions), v. 67, no. 29, p. 580-582.

Kienle, Juergen, and Swanson, S.E., 1983, The hazards of Augustine: The Northern Engineer, v. 15, no. 3, p. 10-14 and 30-37.

----- 1985, Volcanic hazards from future eruptions of Augustine Volcano, Alaska: Fairbanks, University of Alaska, Geophysical Institute Report UAG R-275, 122 p.

Miller, T.P., Yount, M.E., and Nelson, S.W., 1987, Pyroclastic flow characteristics during the initial phase of the 1986 eruption of Augustine Volcano, Alaska (abs.): Hilo, Hawaii, Abstracts of the Hawaiian Volcano Observatory Diamond Jubilee, p. 175.

Riehle, J.R., 1985, A reconnaissance of the major Holocene tephra deposits in the upper Cook Inlet region, Alaska: Journal of Volcanology and Geothermal Research, v. 26, p. 37-74.

Rose, W.I., Jr., Heiken, G.H., Wohletz, K.H., Eppler, D., Barr, S., Miller, T., Chuan, R.L., and Symonds, R.B., 1987, Direct rate measurements of Mt. St. Augustine eruption plumes: A problem of scaling up and uncontrolled variables (abs.): Hilo, Hawaii, Abstracts of the Hawaiian Volcano Observatory Diamond Jubilee, p. 212.

Siebert, Lee, Glicken, Harry, and Kienle, Juergen, 1986, Debris avalanches and lateral blast at Mount St. Augustine Volcano, Alaska (abs.): Eos (American Geophysical Union Transactions), v. 67, no. 44, p. 1259.

Symonds, R.B., Rose, W.I., Jr., Reed, M.H., Briggs, Paul, and Gerlach, T.M., 1987, The speciation and fluxes of gases from Augustine Volcano, Alaska: A system rich in halides and transition metals (abs.): Hilo, Hawaii, Abstracts of the Hawaiian Volcano Observatory Diamond Jubilee, p. 247.

Yount, M.E., and Miller, T.P., 1987, The April 1986 eruptive phase of Augustine Volcano and associated hazards (abs.): Hilo, Hawaii, Abstracts of the Hawaiian Volcano Observatory Diamond Jubilee, p. 276.

Reviewers: S.W. Nelson and J.R. Riehle

STATEWIDE

Abandoned gold dredge on Harris Creek, Seward Peninsula.
Photo by Warren Yeend.

Alaska Gold Company dredge mining gold from a buried beach deposit near Nome.
Photo by Warren Yeend.

STATUS OF ALASKA MINERAL RESOURCES DATA SYSTEM

Kenneth R. Leonard and Donald F. Huber

The Mineral Resources Data System (MRDS) is a computerized file of information pertaining to metallic- and nonmetallic-mineral deposits and occurrences in the United States and worldwide. MRDS stores information about the location and economic geology of each deposit or occurrence in a record consisting of about 140 individual parameters. Data may be searched using any selected parameter stored in a given record and retrieved using interactive access. Highly selective searches allow the user to filter out unwanted data in order to focus on specific information.

The Alaska portion of MRDS is composed of two separate data sets: (1) an older set of more than 4,000 records containing limited commodity and location information, and (2) a newer set of records intended to expand and replace the older records. The current phase of Alaska MRDS work has generated 2,051 new records covering 40 1:250,000-scale quadrangles, mainly in south-central and southeastern Alaska (fig. 1). The records contain available data on location, commodities, ore minerals, analytical results, exploration and development history, deposit type, deposit size and description, geology, production, reserves, and pertinent literature. Records vary in the amount of information they contain, mainly due to variations in the availability of data. Much more detailed information is generally available for a major mine than for a small prospect or mineral occurrence. Alaska MRDS records focus on metallic-mineral commodities. Nonmetallic-mineral commodities, except for asbestos, barite, and important radioactive minerals, are generally excluded. New additions are made on the basis of 1:250,000-scale quadrangle areas with the objective of expanding the data base to cover the entire State by the end of fiscal year 1987. Funding for current Alaska MRDS work is provided through the Federal Land Information System program managed by the National Mapping Division of the U.S. Geological Survey.

To provide a preliminary overview of the important mineral deposits of Alaska, a separate file containing only those records for major mines and prospects was created. There are currently 111 records distributed in 50 quadrangles in this Major Deposit File.

Data for the Alaska MRDS records have been integrated from a variety of sources, including published and unpublished geologic literature. Most of the data are derived from a series of bibliographies compiled by E.H. Cobb and others and published as USGS open-file reports (see Cobb, 1978). Each bibliography contains data summaries and lists of references for discrete mineral localities within a specific area of Alaska, generally a 1:250,000-scale quadrangle or group of quadrangles. The compilations primarily cover historically important mining districts, with less emphasis on recently active prospects, and are drawn mainly from publications of the U.S. Geological Survey, U.S. Bureau of Mines, and Alaska Division of Geological and Geophysical Surveys (now called the Alaska Division of Mining and Geology). These data have been expanded and updated with information from resource assessments prepared for the Regional Alaska Mineral Resource Assessment Program (RAMRAP) and the Alaska Mineral Resource Assessment Program (AMRAP). The AMRAP data sets are incorporated into MRDS as they become available. Other sources for Alaska MRDS include 1) unpublished information and non-confidential private reports residing in USGS files, 2) M.S. and Ph.D. theses, 3) news items culled from mining industry journals, and 4) personal communications with USGS geologists familiar with specific areas of Alaska.

Locations are recorded in latitude and longitude and, in some instances, also in township and range coordinates. Recorded locations are as accurate as possible within the constraints of the available information. No records have been made for sites that cannot be located to within a 1-mile (1.6-km) radius. A location is designated as "accurate" if its position is known to within 500 ft (150 m). Generally, this requires that the site has been plotted on a large-scale topographic map, preferably a USGS base map, or that an unambiguous location is corroborated by more than one reference source. Most locations are recorded as "estimated" and a distance of accuracy is given. In some cases, site locations may be available only on small-scale maps in which the symbol used for the site covers a large area. These sites are taken as the center of the symbol used to represent them and are given large distances of accuracy. Placer deposits, which often cover a large area or considerable length along a stream, are given an "estimated" location with coordinates for a reference point reported in the record.

Consistency in quality and detail is one of the principal problems found in any data compilation. This is attributable to variations in the original data, as well as to differences between individual contributors. Alaska MRDS records have been compiled by a small number of reporters compared to data sets for many of the other states, and all new entries are consistent with the revised format for MRDS as outlined by Huber (1981) and Koch (1984). Individual entries for the Alaska MRDS are based on compilations of information gathered from various sources and presented in summary form. MRDS records are

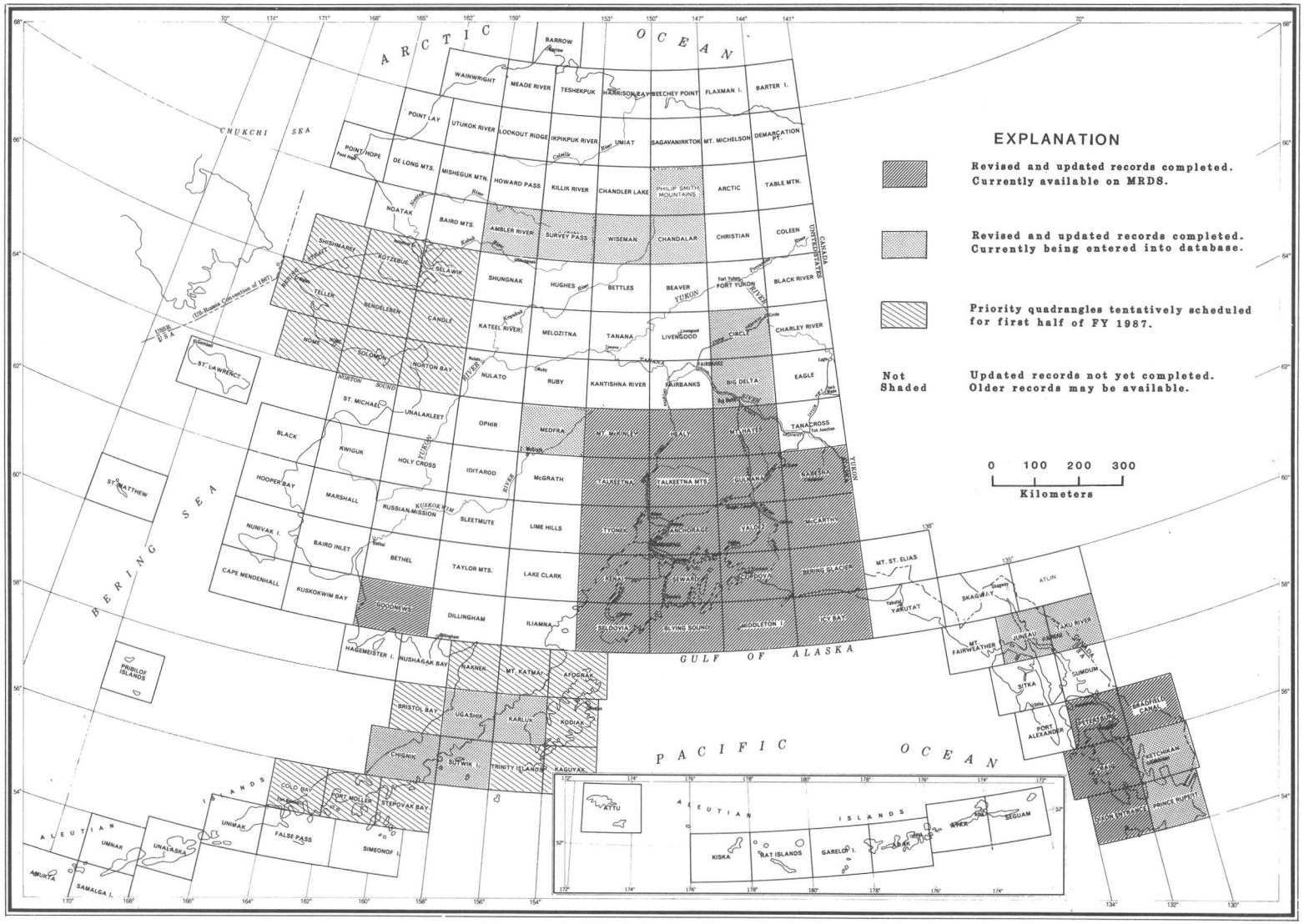

Figure 1.--Status of Alaska Mineral Resources Data System by quadrangle as of the end of fiscal year 1986.

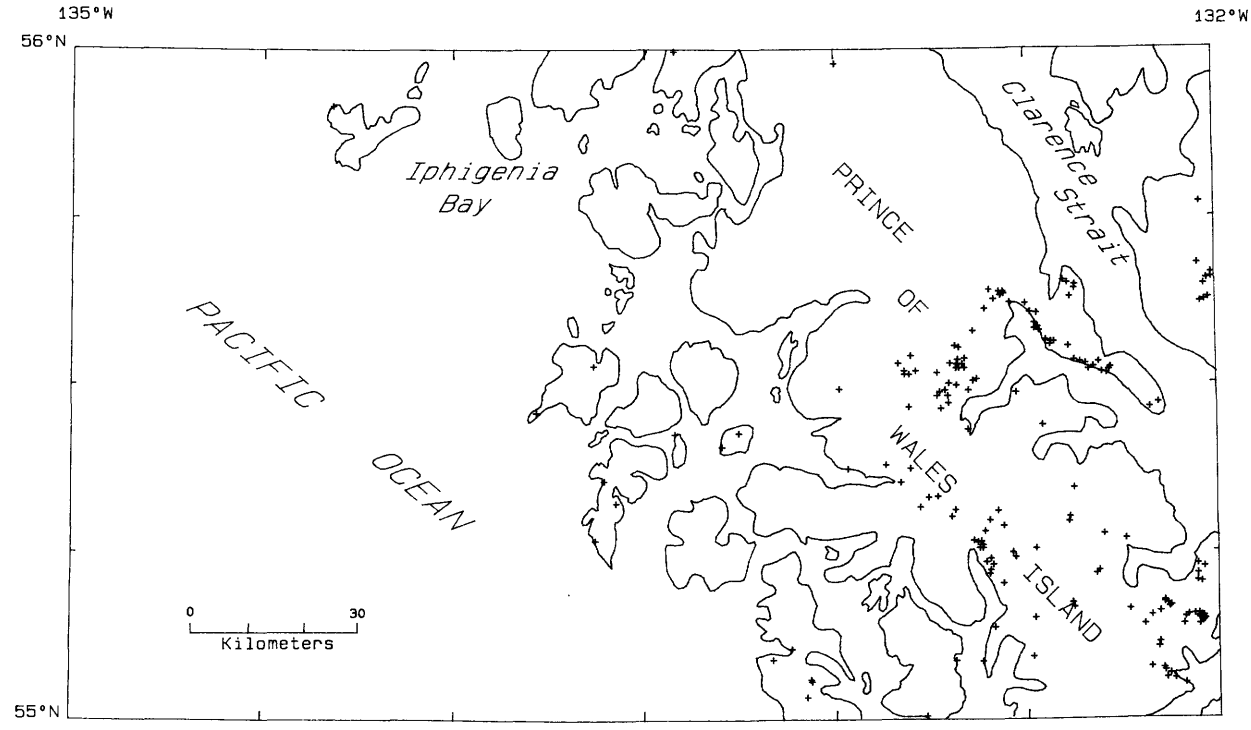

Figure 2.--Computer-generated map of Craig, Alaska 1 x 3 degree quadrangle showing MRDS record locations. Coastline boundaries are approximate.

not meant to supplant the geological literature, but are primarily a means of storing, manipulating, and retrieving site-specific information. Researchers interested in more detailed geological information are directed to consult the references documented in the database.

MRDS records provide Federal, State, and mineral industry geologists with a readily accessible reference source of known or potentially locatable mineral resources. MRDS also serves as a research tool in the development of regional mineral resource assessments, grade-tonnage and descriptive deposit models, and regional metallogenic studies. MRDS data can be easily integrated with other digital data using a geographic information system to produce map plots showing various relationships, such as the number of gold deposits associated with a particular rock unit within an area of mineral potential. The data base is particularly well suited to the rapid production of mineral deposit/occurrence spot maps for use in exploration or as a means of providing researchers with background information on known mineral deposits within unfamiliar study areas.

MRDS resides on the USGS Branch of Resource Analysis' PRIME minicomputer which uses a modern relational database management system called INFORMATION. A compatible version of MRDS known as MRDS-REV has been developed for use on microcomputers using a data base management system called REVELATION (Schruben, 1985). Retrieval output is available in the form of computer text for entire records or sections of records, tabulations of data, or map plots for selected areas (fig. 2).

The Alaska MRDS data set is intended to complement other computerized resource files that contain information on water and geothermal resources, organic fuels, industrial minerals, and construction materials (Office of the Data Administrator, 1983). Information on the economic parameters of mineral resource production is available in the U.S. Bureau of Mines' Mineral Availability System (MAS), which contains fairly detailed data on well-known deposits (U.S. Bureau of Mines, 1974). The Mineral Industry Location System (MILS), a location subsystem of MAS, is similar to MRDS in coverage but contains limited geologic data (Berg and Carillo, 1980). MAS and MILS data on Alaska are available through the U.S. Bureau of Mines, Alaska Field Operations Center, P.O. Box 550, Juneau, Alaska 99802. Mining claims information is available in the Alaska Division of Geological and Geophysical Surveys' KARDEX file, maintained on cards at the

Division's Fairbanks Office, 794 University Avenue, Fairbanks, Alaska 99701. The KARDEX file is the basis for the University of Alaska's MINFILE, a computer-processable storage and retrieval system developed by the Mineral Industry Research Laboratory at the University of Alaska, Fairbanks (Heiner and Porter, 1972).

Information regarding public access to MRDS files can be obtained by contacting one of the following regional MRDS representatives:

Antoinette A. Medlin
Eastern Region Representative
U.S. Geological Survey, MS 920
12201 Sunrise Valley Drive
Reston, VA 22092
703-648-6136

Donald F. Huber
Central and Western Region Representative
U.S. Geological Survey, MS 984
345 Middlefield Road
Menlo Park, CA 94025
415-329-5358

REFERENCES CITED

Berg, A.W., and Carillo, F.V., 1980, MILS: The mineral industry location system of the Federal Bureau of Mines: U.S. Bureau of Mines Information Circular 8815, 24 p.

Cobb, E.H., compiler, 1978, Summary of references to mineral occurrences (other than fuels and construction minerals) in the Juneau quadrangle, Alaska: U.S. Geological Survey Open-File Report 78-374, 156 p.

Heiner, L.E., and Porter, E., 1972, A computer processable storage and retrieval program for Alaska mineral information: Fairbanks, University of Alaska, Mineral Industry Research Laboratory Report 24, v. 1, 145 p.

Huber, D.F., 1981, Mineral data system, computerized resources information bank, U.S. CRIB-site form, instructions for reporters: U.S. Geological Survey unpublished instruction manual.

Koch, R.D., 1984, Guidelines for compilation of Alaska mineral deposit data for entry into MRDS: U.S. Geological Survey unpublished instruction manual.

Office of the Data Administrator, compiler, 1983, Scientific and technical, spatial, and bibliographic data bases and systems of the U.S. Geological Survey, 1983, including other Federal agencies (revised ed.): U.S. Geological Survey Circular 817.

Schruben, P.G., 1985, MRDS-REV, A mineral occurrence/deposit data base for microcomputer: U.S. Geological Survey Open-File Report 86-34, 57 p.

U.S. Bureau of Mines, 1974, The Bureau of Mines minerals availability system and resource classification manual: U.S. Bureau of Mines Information Circular 8654, 199 p.

Reviewers: D.A. Brew and W.D. Menzie

THE ANIAKCHAK TEPHRA DEPOSIT, A LATE HOLOCENE MARKER HORIZON IN WESTERN ALASKA

James R. Riehle, Charles E. Meyer, Thomas A. Ager, Darrell S. Kaufman, and Robert E. Ackerman

We describe here a Holocene tephra (volcanic ash) deposit that, because of its widespread occurrence, ready identification, and approximately known absolute age, should prove to be a useful stratigraphic marker throughout western Alaska from the Alaska Peninsula north to at least the Seward Peninsula. Moreover, the deposit is of interest because we have identified its source in the caldera-forming eruption of Aniakchak Crater, in the Aleutian volcanic arc on the Alaska Peninsula (fig. 1).

Our analyzed tephra samples are from four distal sites--three around Norton Sound and one in southwestern Alaska --and three proximal sites on the Alaska Peninsula near the source at Aniakchak Crater (fig. 1). The distal samples are uniformly fine-grained and, where not contaminated, consist almost entirely of glass (table 1). Megascopically, the glass fragments are clear to pale gray to solid or streaked brown. Particles composing the distal samples have variable shapes that include bubble-wall platelets, fibrous pumice, and equant blocks (fig. 2). In most tephra deposits, the ratio of glass (nonporous density 2.3-2.5 g cm^{-3}) to minerals (density >2.56 g cm^{-3}) normally increases with increasing distance of transport, as for example in the May 18, 1980 eruption of Mount St. Helens (Sarna-Wojcicki and others, 1981). Thus, the ratios of glass to the phenocryst phases are not a quantitative basis for correlation among samples. However, all of our proximal and distal samples are remarkably similar to one another, and are distinguishable from other tephra samples from the Alaska Peninsula (J.R. Riehle, unpub. data) except for the rhyolitic ash of the 1912 Katmai eruption (Hildreth, 1983), on the basis of their large proportion of glass. The mineral content of the samples (plagioclase > orthopyroxene > clinopyroxene = amphibole > opaques = apatite = zircon [?]) is not unique among tephra deposits of the Alaska Peninsula.

Glass separates have been analyzed by microprobe for nine major elements (table 2). To compare the degree of similarity of different pairs of samples we use a similarity coefficient, s.c. (Borchardt and others, 1972), which is the averaged ratio of all pairs of oxides (normalized to 100 percent) where the lesser oxide is the numerator. Because analytical uncertainty is inversely proportional to concentration, we exclude from calculation of the s.c. any oxide occurring in concentrations less than an arbitrary 0.40 percent (MnO, occasionally MgO and TiO_2). A perfect match of 1.00 is not expected even where comparing duplicate analyses of the same sample because the average standard deviation of the oxides is about 5 percent. Riehle (1985) concluded that tephra samples from elsewhere in the Aleutian arc are provisionally the same deposit, that is, the same fall of tephra, if their similarity coefficient exceeds 0.95. He interpreted an s.c. of 0.94 or 0.95 to indicate that sample pairs are either of different falls of coincidentally similar tephra, or may be the same tephra fall where analysis of one or more oxides was less reliable than usual. Similarity coefficients less than 0.94 were interpreted to preclude correlation as the same tephra fall. We adopt the same interpretations here.

Samples of the ash-flow tuff produced during formation of Aniakchak Crater, and of the antecedent proximal airfall deposits (fig. 3), are highly similar (each s.c. >0.95) to one another and to each of our distal samples except for the sample from site 4 (table 3). The lower similarity coefficients for sample 4 are mainly due to a single oxide, TiO_2 (table 2), which is only marginally significant due to its low abundance. Because the approximate age and petrographic character of sample 4 are similar to those of the other distal samples, we still consider it a

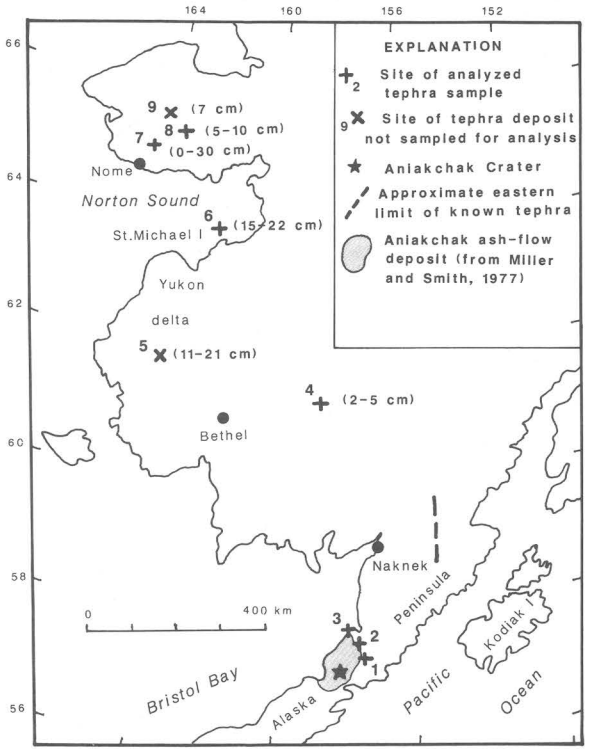

Figure 1.--Sites in western Alaska where late Holocene tephra deposit of Aniakchak Crater has been sampled. Thickness of deposit is given at distal sites in parentheses and is known to include some reworked tephra at sites 5 and 6.

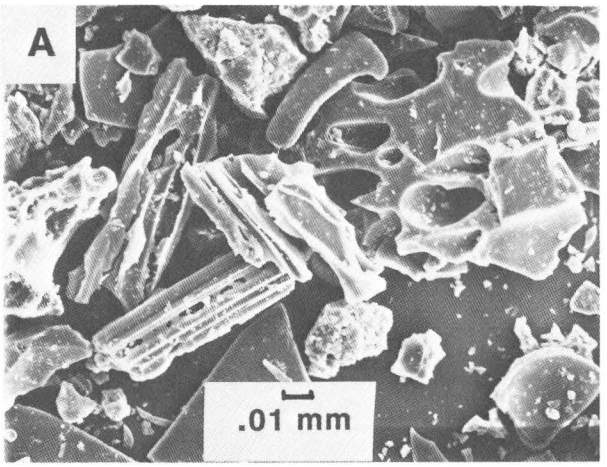

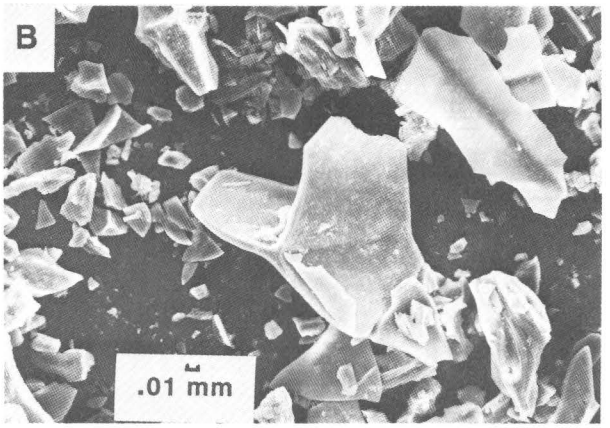

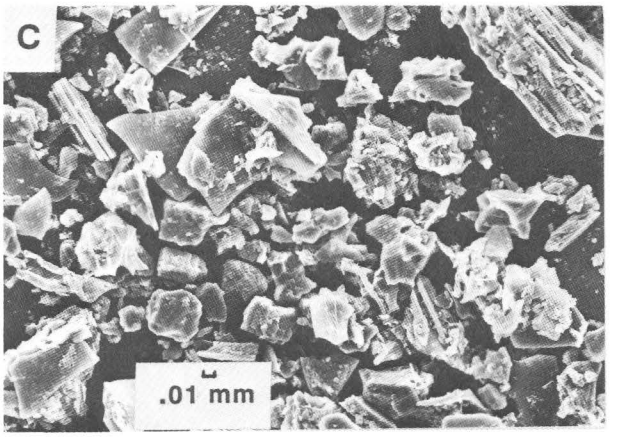

Figure 2.--Representative scanning electron micrograph of distal tephra samples of Aniakchak Crater. A, Blocky equant clast with a few coarse vesicles (upper right), curving platelets (lower right and upper left), and fibrous pumice (center); site 6. B, Bubble-wall junction (center) from which curving platelets in all samples are derived; site 7. C, Fibrous pumice (top right), equant blocks (center), and curving platelets (center of left margin); site 4. Occurrence of equant clasts with a few coarse vesicles and with adhering microparticles may indicate phreatic component of eruption (see Heiken and Wohletz, 1985). Photographs taken by Effie Shaw.

correlative. Of 130 samples of other tephra deposits from the Alaska Peninsula (J.R. Riehle and C.E. Meyer, unpub. data), none have a similarity coefficient that is greater than 0.94 with any of these distal samples. Because two to four tephra deposits (beds) can be recognized at the proximal sites (see fig. 3), the distal samples may be a composite of the deposits of two or more tephra falls.

Black glass shards handpicked from the sample at site 6 for microanalysis have a composition similar to lithic clasts of black vitrophyre in tephra deposits that immediately overlie and underlie Aniakchak deposits at site 1 (fig. 3; table 3, "vitrophyre"). The vitrophyre may be accessory to the Aniakchak eruptions or it may be contamination from nearly contemporaneous eruptions. Black glass in rare amounts was tentatively identified in the other distal samples and provides another criterion for recognition.

Radiocarbon ages indicate that the Aniakchak tephra deposit is of late Holocene age. The age of the Aniakchak ash-flow deposit that overlies the tephra deposits at proximal sites 2 and 3 (fig. 3) was originally estimated as 3,300-3,700 yr (Miller and Smith, 1977). Three samples of wood contained in the ash-flow deposit now yield a

Table 1.--Petrographic descriptions of proximal and distal tephra samples, Aniakchak caldera-forming eruption

Proximal deposits	
1C:	white to tan pumice and scoriaceous dark glass; mineral abundances not determined
1E:	fibrous, clear to tan pumice; trace of brown microvesicular glass and dense gray vitrophyre; 96% glass, 2% plagioclase, 2% mafics by weight
2M:	like sample 1E
3F:	like sample 1E; 97% glass, 1.5% plagioclase, 1.5% mafics by weight
3G:	like sample 1E
3I:	dominantly white pumice; rare scoriaceous glass and dense black vitrophyre; mineral abundances not determined
Distal deposits	
4:	clear to pale gray glass and fibrous white pumice; trace pale grey to medium brown scoriaceous glass; rare fine black fragments may be black glass shards; estimated 98% glass, remainder is plagioclase and pyroxene>amphibole>opaques=apatite=zircon(?)
6:	like sample 4
8:	like sample 4
7B:	dominantly clear to pale gray glass with some brown streaks; clast shapes range from fibrous pumice to curving platelets; estimated 99% glass, remainder is plagioclase and pyroxene>amphibole>opaque=apatite=zircon(?)

weighted mean age of 3,430 yr (T.P. Miller, USGS, written commun., 1986).

A maximum limiting age for our distal sample 8 is 4,000 ± 100 yr B.P. (I-13,990); an unanalyzed sample from site 9 petrographically resembles the other Aniakchak samples and is bounded by ages of 2,400 ± 80 yr B.P. (Beta 7760) and 3,340 ± 90 yr B.P. (Beta 7761) (Kaufman and Hopkins, 1985). Our analyzed sample 6 is from lake sediments cored on St. Michael Island; lacustrine sediments in the interval from 0 to 11 cm above the tephra deposit yielded a date of 4,830 ± 80 yr B.P. (W 4929) and the interval from 0 to 10 cm below yielded a date of 6,430 ± 90 yr B.P. (W 4625) (Ager, 1983). A similar tephra deposit at site 5 (Tungak Lake) has not been chemically analyzed but is correlated with the Aniakchak deposit on the basis of petrographic similarity; the 12-cm interval immediately overlying the tephra deposit yielded a date of 3,400 ± 750 yr B.P. (W 3776) and the interval from 13 to 44 cm below the tephra deposit yielded a date of 5,645 ± 250 yr B.P. (W 3934) (Ager, 1982). The sample from site 4 contains partially to completely charred wood, which may have been mixed by cryoturbation from an overlying horizon; it yielded a date of 3,684 ± 98 yr B.P. (WSU 2759).

If the available radiocarbon data are taken at face value, then the distal tephra deposits must span 3,000 years. The apparent lack of soils or erosional contacts between the proximal airfall deposits, however, weighs against such a hypothesis (see fig. 3). Moreover, tephra deposited on the Seward Peninsula must be a major component of the deposits on St. Michael Island because these sites are in line with Aniakchak Crater; thus, the ages of the Seward Peninsula and St. Michael deposits may differ from the age of the ash-flow deposit, but they should themselves be identical or at least overlap. Clearly the ages do not overlap, and consequently we cannot accept

Table 2.--Composition of glass separates
[Analyses by electron microprobe; analysts, C.E. Meyer and J.R. Riehle. FeO* is total iron reported as FeO. One standard deviation as percentage of reported abundance is given in parentheses. For brevity, compositions of proximal samples are not reported here but are available from the authors]

Oxide	7B		8		6 pumice		6 black glass		4	
SiO_2	69.9	(0.9)	69.9	(0.9)	70.1	(0.9)	57.1	(0.9)	69.7	(2.1)
Al_2O_3	14.92	(3.1)	15.03	(3.1)	14.58	(3.1)	15.97	(3.1)	14.81	(3.5)
FeO*	2.34	(3.5)	2.34	(3.5)	2.39	(3.4)	7.16	(2.4)	2.49	(4.8)
MgO	.49	(6.9)	.51	(6.7)	.50	(6.7)	2.92	(2.9)	.47	(5.0)
CaO	1.71	(2.0)	1.72	(2.0)	1.72	(2.0)	6.00	(1.3)	1.69	(6.4)
Na_2O	5.19	(3.4)	5.13	(3.4)	5.38	(3.0)	4.49	(3.1)	5.04	(3.2)
K_2O	2.91	(1.8)	2.95	(1.8)	2.91	(1.8)	1.50	(2.2)	2.97	(5.1)
TiO_2	.46	(12)	.45	(13)	.46	(13)	1.34	(6.6)	.58	(10)
MnO	.14	(20)	.15	(19)	.13	(22)	.20	(16)	.13	(25)
Total	98.1		98.1		98.2		96.7		98.2	

Table 3.--Similarity coefficients among distal and proximal samples, Aniakchak tephra deposits
[-- , no data]

Distal samples	Proximal samples 1C	1E	2M	3F	3G	3I	(vitrophyre) 1E	1J
7B	0.97	0.97	0.98	0.96	0.97	0.98	--	--
8	.96	.96	.98	.96	.97	.98	--	--
6, pumice	.96	.97	.97	.96	.97	.97	--	--
4	.95	.95	.95	.93	.96	.95	--	--
6, black glass	--	--	--	--	--	--	0.98	0.96

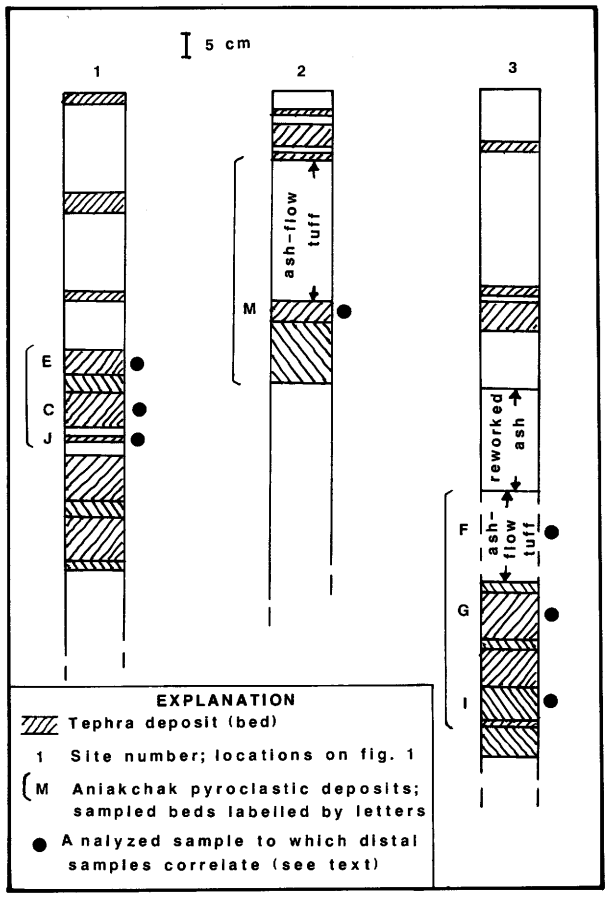

Figure 3.--Geologic sections at proximal sites where Aniakchak ash-flow deposit and underlying tephra deposits have been sampled. Non-pyroclastic deposits are loess or peat.

the radiocarbon ages from the distal sites at face value. One of several possible sources of error is that the lacustrine sediments at site 6 contain older reworked organic material. If the ages from site 6 are deleted, then the remaining ages limit the tephra deposit to between 3,400 yr B.P. and about 4,000 yr B.P. In conclusion, the lack of evidence for any hiatus between the proximal airfall deposits suggests that the age range is no more than a few hundred years, from about 3,400 yr to perhaps 4,000 yr. We cannot rule out an age range of as much as 3,000 years for these tephra deposits, however, and additional dating of samples from western Alaska would help to confirm this provisional age assignment.

In summary, the Aniakchak tephra deposit is sufficiently thick to be readily identified where preserved in late Holocene deposits that extend from its source at Aniakchak Crater north to the Seward Peninsula. The deposit may be recognizable even north of the Seward Peninsula by a high ratio of glass to phenocrysts (>98:2) and by the presence in rare amounts of (accessory?) black glass shards, but beyond the Seward Peninsula its fine grain size will probably make chemical analysis intractable. North of the Alaska Peninsula, the deposit is probably a mixture of the compositionally similar deposits of two or more tephra falls. The inferred age of the distal deposits ranges from a minimum of 3,400 yr, the age of the ash-flow deposit, to probably no more than 4,000 yr.

REFERENCES CITED

Ager, T.A., 1982, Vegetational history of western Alaska during the Wisconsin glacial interval and the Holocene, in Hopkins, D.M., Matthews, J.V. Jr., Schweger, C.E., and Young, S.B., eds., Paleoecology of Beringia: New York, Academic Press, p. 75-93.

___ 1983, Holocene vegetational history of Alaska, in Wright, H.E. Jr., ed., Late Quaternary environments of the United States, v. 2, The Holocene: Minneapolis, University of Minnesota Press, p. 128-141.

Borchardt, G.A., Aruscavage, P.J., and Millard, H.T., Jr., 1972, Correlation of the Bishop ash, a Pleistocene marker bed, using instrumental neutron activation analysis: Journal of Sedimentary Petrology, v. 42, p. 301-306.

Heiken, Grant, and Wohletz, Kenneth, 1985, Volcanic ash: Berkeley, University of California Press, 246 p.

Hildreth, Wes, 1983, The compositionally zoned eruption of 1912 in the Valley of Ten Thousand Smokes, Katmai National Park, Alaska: Journal of Volcanology and Geothermal Research, v. 18, p. 1-56.

Kaufman, D.S., and Hopkins, D.M., 1985, Late Cenozoic radiometric dates, Seward and Baldwin Peninsulas, and adjacent continental shelf, Alaska: U.S. Geological Survey Open-File Report 85-374, 27 p.

Miller, T.P., and Smith, R.L., 1977, Spectacular mobility of ash flows around Aniakchak and Fisher calderas, Alaska: Geology, v. 5, p. 173-176.

Riehle, J.R., 1985, A reconnaissance of the major Holocene tephra deposits in the upper Cook Inlet region, Alaska: Journal of Volcanology and Geothermal Research, v. 26, p. 37-74.

Sarna-Wojcicki, A.M., Shipley, Susan, Waitt, R.B., Jr., Dzurisin, Daniel, and Wood, S.H., 1981, Areal distribution, thickness, mass, volume, and grain size of air-fall ash from the six major eruptions of 1980, in Lipman, P.W., and Mullineaux, D.R., eds., The 1980 eruptions of Mount St. Helens, Washington: U.S. Geological Survey Professional Paper 1250, p. 577-600.

Reviewers: J.E. Beget and M.E. Yount

NORTHERN ALASKA

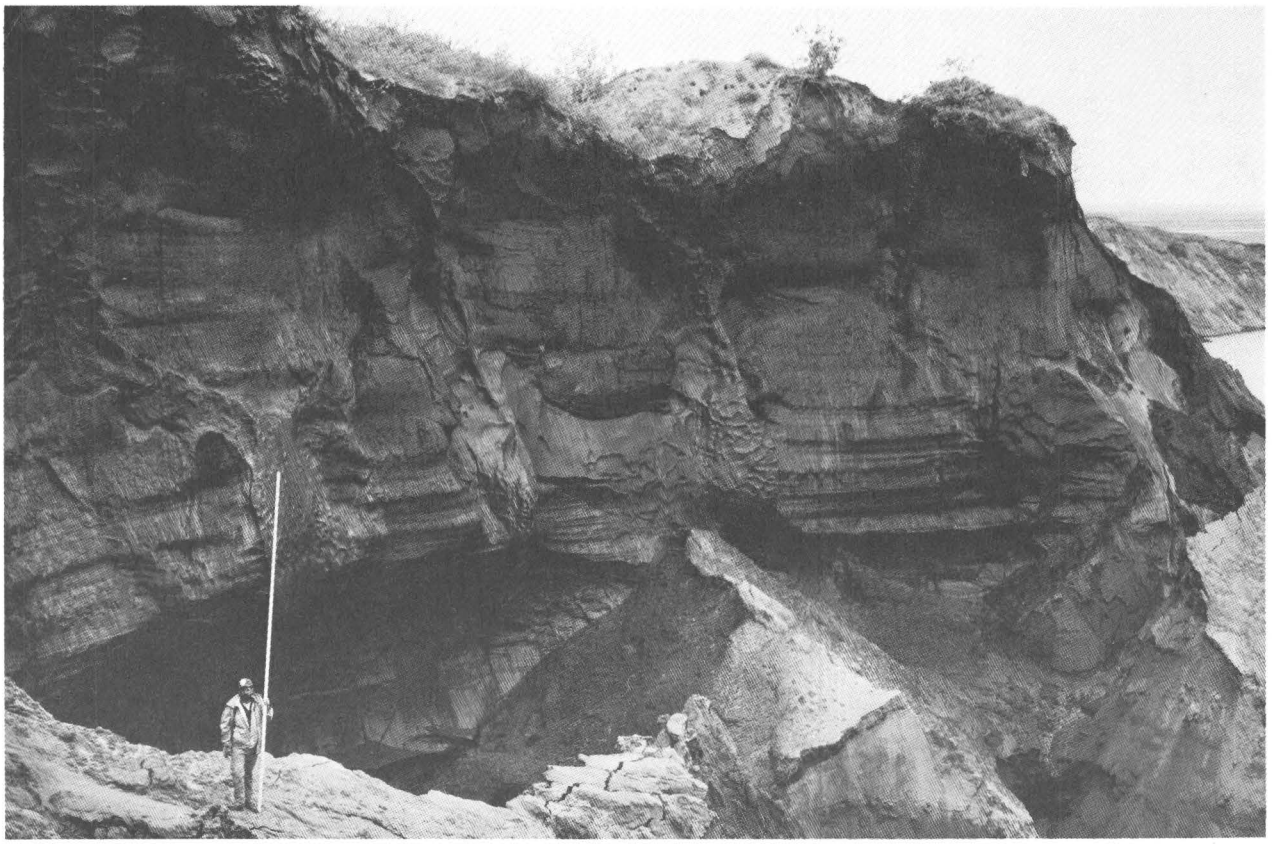

Syngenetic ice-wedges, Titaluk River, Arctic Coastal Plain. These long, narrow wedges grew upward during aggradation of the silt in which they occur. Photo by L.D. Carter, 1986.

GEOCHEMICAL AND GEOLOGIC CONTROLS ON THE INFERRED OCCURRENCE OF NATURAL GAS HYDRATE IN THE KUPARUK 2D-15 WELL, NORTH SLOPE, ALASKA

Timothy S. Collett, Keith A. Kvenvolden, Leslie B. Magoon, and Kenneth J. Bird

Gas hydrates are crystalline substances composed of water and gas in which the solid-water lattice accommodates the gas molecules in a cage-like structure. Significant quantities of naturally occurring gas hydrates have been detected in many regions of the Arctic, including western Siberia, the Mackenzie Delta of Canada, and the North Slope of Alaska; they may represent an unconventional source of natural gas (Kvenvolden and McMenamin, 1980). However, little is known about the physical nature of gas hydrates. Direct evidence for gas hydrates on the North Slope (fig. 1) comes from a core in the Northwest Eileen State 2 well. Indirect evidence is provided by drilling information and open-hole geophysical logs, which suggest the presence of numerous gas-hydrate layers in the area of the Kuparuk River Oil Field (Collett, 1983).

Gas hydrates exist under a limited range of pressure and temperature conditions with depth, known as the gas hydrate stability field (fig. 2). The gas hydrate stability diagram in figure 2 has been generated from laboratory data and field evaluations. The intersection of the methane hydrate stability curve with the projected geothermal gradient denotes the top and base of the methane hydrate stability field. In figure 2, "HT" is the top of the methane hydrate stability field, and "HB" is its base. Five reservoir and fluid properties may affect the stability of in-situ gas hydrates: geothermal gradient, gas chemistry, pore-fluid salinities, pore pressures, and reservoir-rock grain size. Subsurface-temperature data on the North Slope come from 46 high-resolution, equilibrated wellbore surveys (Lachenbruch and others, in press) and from estimates based on identification of the base of ice-bearing permafrost in 98 other wells (Collett and others, in press). Gas chemistry data are from analysis of mud logs and well cuttings. Subsurface pressure and pore-fluid salinity data have been obtained from well-log calculations and formation testing. Our North Slope studies suggest that the gas hydrate stability field is controlled primarily by subsurface temperatures and gas chemistry, and that other factors, such as pore-fluid salinity, pore-pressure variations, and reservoir-rock grain size, appear to have little effect.

In the Kuparuk 2D-15 well, the estimated geothermal gradient ranges from 2.14 °C/100 m in the ice-bearing permafrost sequence to 3.42 °C/100 m below the base of ice-bearing permafrost. A 30-m-thick interval is inferred to contain gas hydrates in the Kuparuk 2D-15 well (fig. 3). The occurrence of gas hydrates is

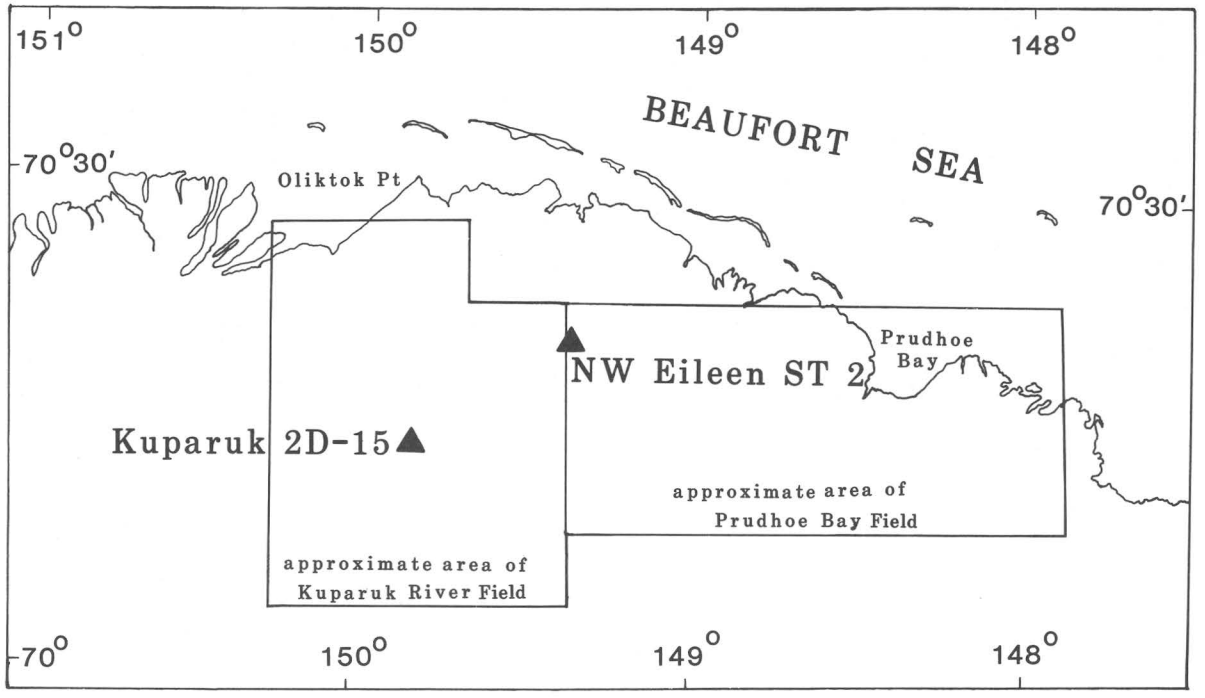

Figure 1.--Location of Kuparuk 2D-15 and Northwest Eileen State 2 wells.

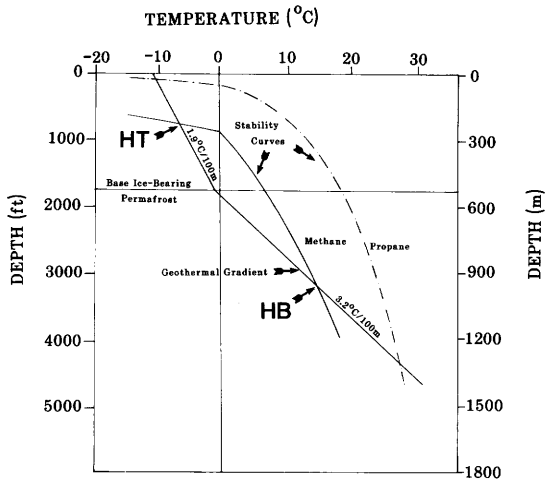

Figure 2.--Gas hydrate stability diagram for Northwest Eileen State 2 well. "HT" is top of methane hydrate stability field; "HB" is its base (pore-pressure gradient: 9.795 kPa/m or [0.433 $lb/in^2/ft$]).

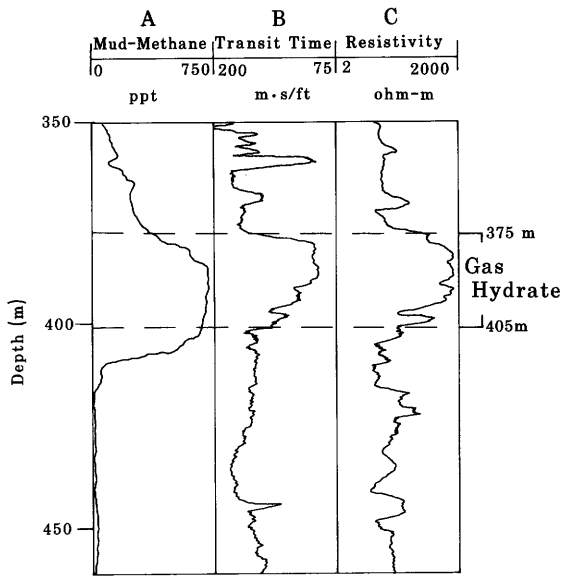

Figure 3.--Well logs from Kuparuk 2D-15 well, showing response considered to indicate gas hydrate occurrence.

suggested by the release of unusually large (up to 750 ppt) amounts of methane as indicated on the mud log (fig. 3, column A), and an increase in transit-time velocity (fig. 3, column B) and electrical resistivity (fig. 3, column C) on the open-hole well logs. Canned drill-cutting samples from the Kuparuk 2D-15 well have been analyzed to determine the origin and composition of the gases from this interval. Headspace-gas analysis of the cuttings reveal methane to propane-plus-ethane ratios $[C_1/(C_2+C_3)]$ typical of biogenic gas, with values ranging from 3,300 to 14,500. In contrast, the isotopic composition of the methane indicates the presence of thermogenic gas, with C^{13}/C^{12} isotope values from -49.13 to -38.64 o/oo. Vitrinite reflectance measurements (0.4 percent Ro) show that the near-surface, potentially gas-hydrate-bearing sediment has never been subjected to high enough temperatures to generate thermogenic methane. Thus, the thermogenic gas must have migrated from greater depths, and the gas hydrates may contain a mixture of biogenic and thermogenic gases. Formation-water samples and well-log calculations from the 2D-15 well and nearby wells indicate low pore-fluid salinities, ranging from 0.5 to 18.1 ppt. The maximum recorded salinity would suppress methane hydrate stability temperatures by approximately 1.0 °C, thus moving the methane hydrate stability curve to the left in figure 2.

Pressure data, obtained from drill-stem testing and well-log calculations in nearby wells, indicate a hydrostatic pore-pressure gradient (9.795 kPa/m or 0.433 $lb/in^2/ft$) within the uppermost 2,000 m of sediments, which has no abnormal effect on gas hydrate stability. The effect of sediment grain size on gas hydrate stability is very difficult to evaluate in the absence of laboratory studies. However, it is believed that coarse-grained sediments do not affect gas hydrate stability. Therefore, in the near-surface coarse sand and gravel sediment in the Kuparuk River area, grain size should have little or no effect on gas hydrate stability.

In summary, the evaluation of geochemical and geologic data from the Kuparuk 2D-15 and nearby wells indicate that gas hydrates occur in the Kuparuk River area, and their stability is controlled primarily by subsurface temperatures and gas chemistry. This work was partially funded by the Morgantown Energy Technology Center under the U.S. Geological Survey-U.S. Department of Energy Agreement No. DE-AI21-83MC20422.

REFERENCES CITED

Collett, T.S., 1983, Detection and evaluation of natural gas hydrates from well logs, Prudhoe Bay, Alaska, in Proceedings of the Fourth International Conference on Permafrost, Fairbanks, Alaska: Washington, D.C., National Academy of Sciences, p. 169-174.

Collett, T.S., Bird, K.J., Kvenvolden, K.A., and Magoon, L.B., in press, Subsurface temperatures and geothermal gradients on the North Slope of Alaska: U.S. Geological Survey Oil and Gas Map.

Kvenvolden, K.A., and McMenamin, M.A., 1980, Hydrates of natural gas: A review of their geologic occurrence: U.S. Geological Survey Circular 825, 11 p.

Lachenbruch, A.H., Sass, J.H., Lawver, L.A., Brewer, M.C., Marshall, B.V., Munroe, R.J., Kennelly, J.P., Jr., Galanis, S.P., Jr., and Moses, T.H., Jr., in press, Temperature and depth of permafrost on the Alaskan Arctic Slope, in Gryc, George, ed., National Petroleum Reserve in Alaska: U.S. Geological Survey Professional Paper 1399, 38 p.

Reviewers: L.A. Beyer and R.G. Stanley

USE OF FACTOR ANALYSIS IN LOCATING BASE METAL MINERALIZATION IN THE KILLIK RIVER QUADRANGLE, ALASKA

Karen A. Duttweiler

A reconnaissance geochemical survey of the Killik River quadrangle has been under way since 1981 as part of the Alaska Mineral Resource Assessment Program. Analyses of stream-sediment and nonmagnetic heavy-mineral concentrate samples were published by Barton and others (1982) and Sutley and others (1984). My subsequent application of factor analysis to the log-transformed emission spectrographic data for the concentrate samples was highly successful in characterizing the dominant geochemical associations in the southern part of the quadrangle (fig. 1). Major lithologic differences were discerned, and previously unrecognized areas favorable for hosting base-metal sulfide deposits were clearly defined.

R-mode factor analysis with varimax rotation (Koch and Link, 1971) was used to define the geochemical associations in the concentrate data. This type of factor analysis groups the elements that tend to behave similarly into multielement associations, or factors, based on their mutual linear correlation coefficients. In this way, a large number of variables is reduced to only a few variables that best characterize the original data. The factors produced from R-mode factor analysis reflect geological features and geochemical processes.

I selected a five-factor model as the geologically most meaningful solution for the reconnaissance geochemical data (table 1). These five factors explain 73 percent of the variance within the original data set. Factor loadings represent the contribution of each element onto each factor. Factor scores measure the "effect" of a factor on each individual sample.

Factors 1, 2, and 4 (table 1), accounting for about 57 percent of the total data variability, represent lithogeochemical associations. Elements that load heavily onto factor 1 include Ca, Ti, B, Cr, La, Ni, Sc, V, Y, and Zr. Most heavy-mineral-concentrate samples with high scores for this factor contain various amounts of rutile, zircon, apatite, and sphene. These samples are from drainages underlain primarily by the Upper Devonian and Lower Mississippian(?) Kanayut Conglomerate (Nilsen and Moore, 1984), a rock unit composed of conglomerate, sandstone, siltstone, and minor shale (Brosgé, and others, 1979).

Factor 2 (Ca-Ba-Sr) defines concentrates containing abundant barite. Samples with high scores for factor 2 are spatially related to exposures of limestone and dolomite of the Mississippian and Pennsylvanian Lisburne Group, and shale and siltstone of the Pennsylvanian to Lower Triassic Siksikpuk Formation (Mull and others, 1982), which locally contain barite nodules.

Factor 4 is associated mainly with concentrates derived from local mafic rocks in the vicinity of Kikiktat Mountain. Magnesiochromite, a Mg-rich end member of the chromite solid-solution series, was identified in a few concentrates northeast of Kikiktat Mountain. The strong Mg-Mn-Cr-V-Sc association characterized by factor 4 may be a result of magnesiochromite in the concentrates.

Factors 3 and 5 represent mineralization suites. The Fe-Co-Cu-Ni-Zn association that characterizes factor 5 defines areas with the greatest concentration of pyrite (±chalcopyrite) in the heavy-mineral concentrates. The Ag-Pb-Zn-Cu association (factor 3) indicates the presence of galena and sphalerite (±chalcopyrite). Distribution of scores for these factors provides a means of distinguishing between areas hosting pyrite mineralization and those hosting pyrite plus base-metal sulfides. Figure 1 shows the distribution of scores for factor 3 (base-metal sulfide factor) and factor 5 (pyrite factor). The scores were divided into three groups on the basis of percentiles; the 99th, 95th, and 90th percentiles were chosen to represent anomalously high scores for each factor.

Anomalous scores for both the pyrite and base-metal sulfide factors are concentrated in two distinct areas (fig. 1), both of which are underlain by the Devonian Hunt Fork Shale and relatively younger Kanayut Conglomerate (Brosgé, and others, 1979). The easternmost area is characterized by a central zone of samples with high scores for the base-metal sulfide factor surrounded by zones of high scores for the pyrite factor. Concentrates from the central zone

Table 1.--Factor loadings for the first five factors of heavy-mineral-concentrate data
[Total variance explained by the five factors equals 73 percent. For simplification, all loadings less than 0.30 have been omitted]

Factors	1	2	3	4	5
Fe	--	-0.33	--	--	0.76
Mg	--	--	--	0.82	--
Ca	0.52	.61	--	--	--
Ti	.88	--	--	--	--
Mn	--	-.48	--	.59	--
Ag	--	--	0.88	--	--
B	.60	-.37	--	--	--
Ba	-.33	.67	--	--	--
Co	--	--	--	--	.75
Cr	.77	--	--	.41	--
Cu	--	--	.35	--	.73
La	.87	--	--	--	--
Ni	.31	--	--	--	.80
Pb	--	--	.84	--	--
Sc	.39	--	--	.58	--
Sr	--	.78	--	--	--
V	.75	--	--	.37	--
Y	.86	--	--	--	--
Zn	--	--	.62	--	.38
Zr	.85	--	--	--	--
Percent of total data variance explained by factor	36.0	13.9	12.1	6.5	5.1

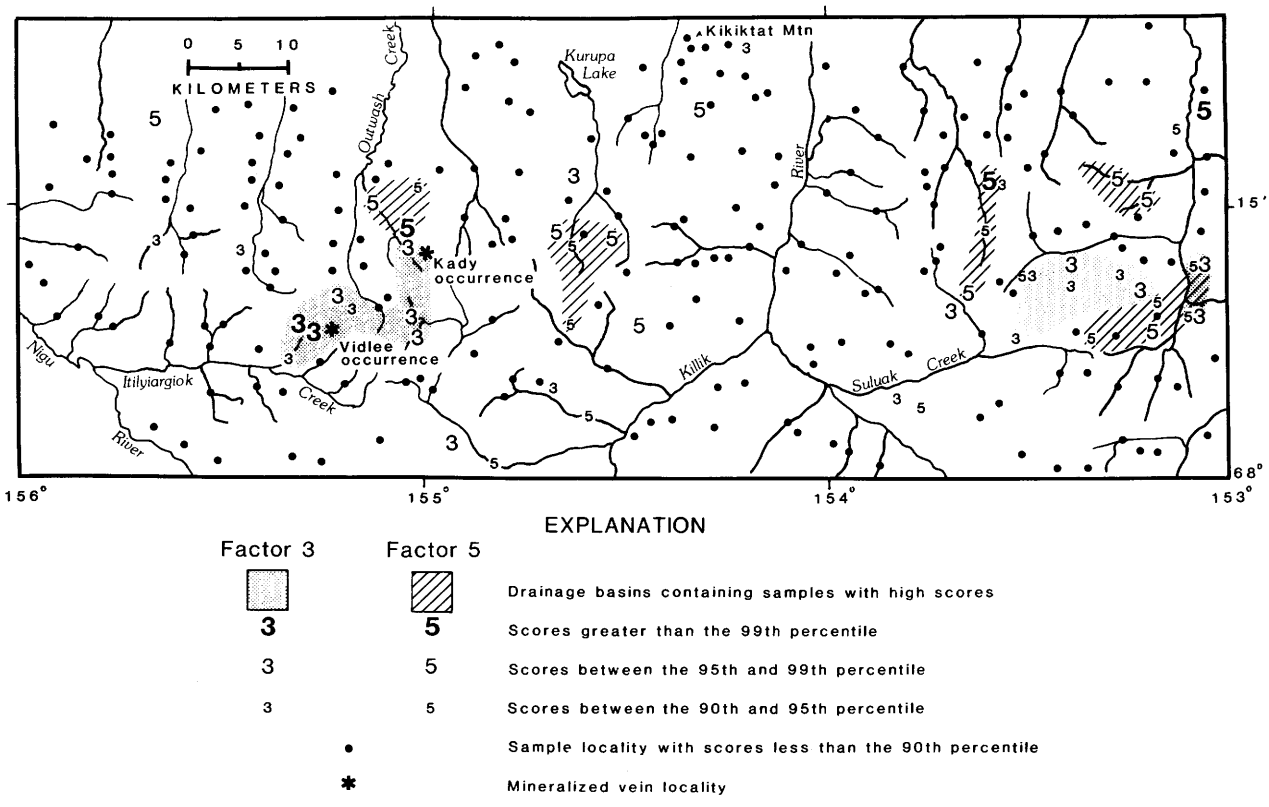

Figure 1.--Southern part of Killik River quadrangle, showing distribution of samples with high scores for factor 3 and factor 5.

contain abundant sphalerite, galena, pyrite, and chalcopyrite; a few samples contain traces of arsenopyrite, and one sample contains realgar. Although an extensive area of possible mineralization is delineated by the two factors in this area, the only identified source of the sulfides was found to be veins hosted by the Hunt Fork Shale. The veins, averaging 1-2 cm wide, consist primarily of quartz with a few scattered occurrences of galena, pyrite, and sphalerite.

Samples with the highest scores for the base-metal sulfide factor (factor 3) occur in the western part of the quadrangle, where they occupy a total drainage basin area of about 80 km^2. Follow-up studies to locate the source of the sulfides was conducted on the basis of the anomalous scores for factor 3. Highly mineralized veins were found in two areas in the western part of the quadrangle. The northernmost area, informally named the Kady occurrence, is located at the headwaters of a tributary of Outwash Creek (fig. 1); the other vein system, the Vidlee occurrence, is located at the headwaters of Itilyiargiok Creek.

The Kady occurrence is about 2 km north of a major east-west-trending thrust fault that separates rocks of the Hunt Fork Shale from the underlying but relatively younger Kanayut Conglomerate (C.G. Mull and others, unpub. mapping). The veins, which are exposed on a hillside south of a small east-west-trending tributary, are hosted by clastic rocks of the Kanayut Conglomerate. The veins trend approximately N. 35° W. and can be traced along strike for at least 300 m. They range in width from 2-cm stockwork veinlets to massive veins 3 m wide. One zone, consisting of rubble of oxidized vein material in a small saddle, was estimated to be about 10 m wide. Mineralization consists of sphalerite, pyrite, chalcopyrite, and galena in stockwork quartz veins. The most highly mineralized rocks consist of massive sulfide-bearing vein-breccias, in which sphalerite and pyrite are the most abundant minerals. Much of the mineralized vein material has been weathered to form boxwork silica textures; locally, oxidation of Fe-sulfides to limonite has resulted in extensive bright red- to orange-weathering zones.

Veins at the Vidlee occurrence (fig. 1) are exposed at stream level on the north side of a first-order tributary of Itilyiargiok Creek near the contact between the Hunt Fork Shale and the Kanayut Conglomerate. The vein outcrop, which cannot be traced either laterally or vertically from this single exposure, is about 5 m wide. Compared to those at the Kady location, the veins

Table 2.--Analytical data for mineralized rocks from the Killik River quadrangle
[All analyses by semi-quantitative emission spectrography and reported in parts per million. N, not detected at the lower limit of determination. Note: gold was not detected by emission spectrographic methods and gold data from atomic absorption methods are not yet available]

Sample No.	Pb	Zn	Cd	Ag	As	Sb	Co	Cu	Ni	Sn
KADY OCCURRENCE										
605C	30	>10,000	100	3	N	N	50	1,000	20	N
605D	500	<200	N	.7	N	N	10	500	15	N
605E	50	>10,000	>500	5	700	N	200	2,000	150	200
605F	N	>10,000	150	2	N	N	20	1,000	10	N
606A	15	10,000	100	1.5	N	N	7	70	5	30
606C	20	>10,000	>500	1.5	N	<100	50	1,000	20	20
606D	50	>10,000	>500	7	N	N	70	200	<10	N
607C	100	<200	N	150	500	N	30	>20,000	100	200
607D	10	<200	N	10	N	N	15	7,000	20	N
VIDLEE OCCURRENCE										
608	20,000	>10,000	150	20	>10,000	500	500	1,500	50	100
609A	150	500	N	7	200	<100	50	10,000	20	70
609B	70	2,000	<20	2	200	N	50	50	10	N
609C	2,000	>10,000	>500	20	N	<100	50	500	10	30
609D	1,000	>10,000	>500	50	N	200	50	500	7	70
610A	2,000	3,000	20	20	<200	<100	70	1,000	20	20
610B	>20,000	>10,000	>500	300	200	2,000	70	7,000	20	300
610C	15,000	>10,000	>500	150	N	500	50	300	5	70

at this locality are more massive, less brecciated, and less oxidized. Three zones, based on dominant sulfide mineralogy, are distinguished within the vein system: (1) the pyrite zone, which contains little or no galena or sphalerite, (2) the sphalerite zone, containing minor galena, and (3) the galena-dominant zone, which locally contains chalcopyrite. All three are typified by bands of sulfides in quartz gangue.

Mineralized rocks from the Kady area contain high concentrations of Zn, Cd, and Cu with lesser amounts of Pb, Ag, and As (table 2). Mineralized rocks from the Vidlee area contain high Pb, Ag, Zn, Cd, Cu, As, and Sb concentrations. In addition to the anomalous concentrations of these elements, a few rocks from the Kady and Vidlee areas contain high amounts of Co and Ni, which reflects the abundance of pyrite in the veins. Also of interest is the high tin content of many of the mineralized rocks. For example, two samples from each area contain Sn concentrations of 100 ppm or more. Each sample containing anomalous Sn also contains high concentrations of Cu. Based on this Cu-Sn association, I suggest that stannite (Cu_2FeSnS_4) may be present as an accessory mineral in addition to pyrite, galena, and sphalerite, although detailed petrographic work is needed to confirm this inference.

In conclusion, factor analysis applied to the concentrate data from the southern part of the Killik River quadrangle was highly successful in outlining those areas most favorable for hosting base-metal sulfide deposits and in locating two specific areas of previously unknown mineralization. The Pb-Zn-Ag-Cu association characteristic of the mineralized areas was well represented by the base-metal sulfide factor obtained from the factor analysis.

REFERENCES CITED

Barton, H.N., Odland, S.K., O'Leary, R.M., and Day, G.W., 1982, Geochemical data for the Killik River and Chandler Lake quadrangles, Alaska: U.S. Geological Survey Open-File Report 82-1026, 52 p.

Brosgé, W.P., Reiser, H.N., Dutro, J.T., Jr., and Nilsen, T.H., 1979, Geologic map of Devonian rocks in parts of the Chandler Lake and Killik River quadrangles, Alaska: U.S. Geological Survey Open-File Report 79-1224, 1 sheet, scale 1:200,000.

Koch, G.S., Jr., and Link, R.F., 1971, Statistical analysis of geological data: New York, Dover, 438 p.

Mull, C.G., Tailleur, I.L., Mayfield, C.F., Ellersieck, Inyo, and Curtis, S., 1982, New upper Paleozoic and Lower Mesozoic stratigraphic units, central and western Brooks Range, Alaska: AAPG Bulletin, v. 66, no. 3, p. 348.

Nilsen, T.H., and Moore, T.E., 1984, Stratigraphic nomenclature for the Upper Devonian and Lower Mississippian(?) Kanayut Conglomerate, Brooks Range, Alaska: U.S. Geological Survey Bulletin 1529-A, 64 p.

Sutley, S.J., Duttweiler, K.A., and Hopkins, R.T., 1984, Analytical results and sample locality map of stream-sediment and panned-concentrate samples from the Killik River 1 x 3° quadrangle, Alaska: U.S. Geological Survey Open-File Report 84-406, 18 p.

Reviewers: P.F. Folger and R.J. Goldfarb

PRELIMINARY EVALUATION OF GEOCHEMICAL ANOMALIES IN THE BAIRD MOUNTAINS QUADRANGLE, ALASKA

Peter F. Folger,
Richard J. Goldfarb, and
Jeanine M. Schmidt

The Baird Mountains quadrangle is underlain mainly by low-grade metamorphosed Paleozoic marine carbonate, pelitic, and clastic rocks with minor amounts of terrigenous clastic rocks (Karl and others, 1985). Minor mafic volcanic and volcaniclastic rocks and rare felsic volcanic rocks occur within the Paleozoic sedimentary sequences. Mesozoic marine volcanic rocks and minor chert crop out in the extreme northwestern part of the quadrangle, and Cretaceous and (or) Tertiary conglomerates occur in the southeastern corner. Amphibolite-grade Precambrian schist and minor metaplutonic rocks of intermediate composition are structurally juxtaposed with greenschist-grade Paleozoic rocks in the northeastern corner of the quadrangle (A. B. Till, USGS, written commun., 1986). Pelitic schist and phyllite of uncertain age occur in the southern and eastern parts of the quadrangle. Folding and thrust faulting during the Jurassic(?) to Cretaceous Brooks Range orogeny have added further complexity to regional stratigraphic and structural relationships.

Known mineralization in the Baird Mountains quadrangle (fig. 1) includes the carbonate-hosted Omar copper prospect (Folger, 1987), the Frost barite-lead-zinc occurrence (Degenhart and others, 1978), the Powdermilk zinc - lead - silver occurrence (Schmidt and Folger, 1986), and the Klery Creek and Timber Creek gold placers (Degenhart and others, 1978). With the exception of the Klery Creek-Timber Creek area, mineral resources have not been commercially exploited in the Baird Mountains quadrangle.

In order to identify additional mineralized areas in the Baird Mountains quadrangle, we conducted a geochemical reconnaissance survey between 1983 and 1985 as part of the Alaska Mineral Resource Assessment Program (AMRAP). Both stream sediments and heavy-mineral concentrate samples were collected at an average density of 1 per 10 km^2 from low-order drainage basins. The minus-80-mesh fraction of stream sediments and the nonmagnetic heavy-mineral concentrate fraction were analyzed by semiquantitative emission spectrography for 31 elements. The resulting geochemical data for 1,493 stream-sediment samples and 1,185 heavy-mineral concentrate samples are tabulated in Bailey and others (1987).

Both data sets were first log-transformed, and elements for which the majority of values were "greater than" or "less than" the detection limits (highly censored elements) were removed. Then, R-mode factor analysis with varimax rotation was used to identify intercorrelated variables within each data set. This analysis places similarly behaving experimental variables, in this case elemental concentrations, into groups termed **factors.** The number of factors chosen from each data matrix, and discussed here, were based on the breaks in slope for the plots of factor number versus total variance. The stream-sediment and nonmagnetic heavy-mineral concentrate data were interpreted in terms of mineral potential by using both plots of factor scores (the "effect" of a factor on each sample) and plots of individual concentration values for highly censored elements.

Four factors explain 76 percent of the total variance in the stream-sediment data (table 1). Factors 1, 2, and 4 apparently represent lithogeochemical associations within the Baird Mountains quadrangle. Samples with the highest scores onto factor 1 are mainly from watersheds containing mafic rocks. High factor 2 scores identify drainages underlain by relatively pure carbonate rocks, mainly in the southwestern and west-central part of the quadrangle. The highest factor 4 scores occur more irregularly within areas of pelitic schist, black shale, and mixed carbonate and clastic rocks.

Factor 3, with high lead and copper, is the only association within the stream-sediment data that clearly identifies areas of mineral potential. Five areas of high factor 3 scores occur within the quadrangle (fig. 1).

Table 1.--Factor loadings for 1,493 stream sediment samples
[Loadings depict the influence of each factor on each variable and may be interpreted similarly to correlation coefficients. Loadings less than 0.3 have been omitted]

Element	Factor 1	Factor 2	Factor 3	Factor 4
Fe	0.81	---	---	0.37
Mg	---	0.52	---	-.47
Ca	-.32	.80	---	-.36
Ti	.71	---	---	.55
Mn	.72	---	---	.38
B	.67	---	---	.56
Ba	.69	---	---	.51
Be	.41	---	---	.66
Co	.79	---	---	.30
Cr	.80	-.30	---	---
Cu	.70	---	0.42	---
La	---	---	---	.73
Ni	.78	---	---	.31
Pb	---	---	.88	---
Sc	.73	---	---	.47
Sr	---	.87	---	---
V	.81	---	---	.38
Y	.49	---	---	.65
Zr	.62	---	---	.57
Percent total variance	38	12	6	20

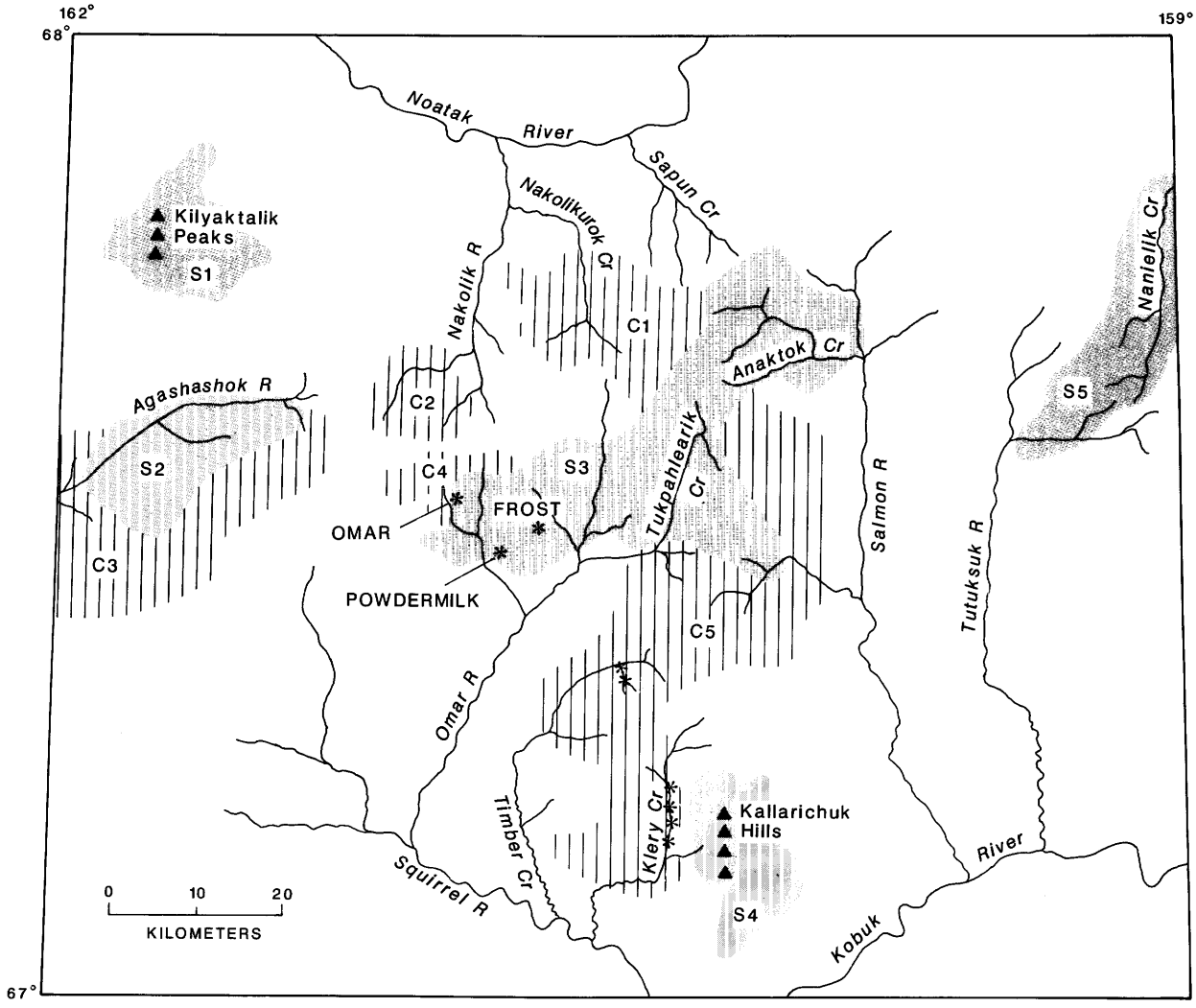

Figure 1.--Areas containing geochemical anomalies in Baird Mountains quadrangle. Shaded areas indicate anomalous stream sediment values; vertical lines indicate anomalous heavy-mineral concentrate values. Labels for anomalous areas are discussed in text. Areas of known mineralization shown by asterisks.

1. Anomalous amounts of lead with local Cu, Ag, Ba, Mo, and Zn, occur within the Kilyaktalik Peaks area (S1 on fig. 1). The spatial association of these samples with black to dark-gray shale, and the local occurrence of disseminated and massive pyrite, suggest high favorability for silver-rich base-metal mineralization within fine-grained sediments. (These and all other mineral occurrences mentioned here are from unpublished field observations of this study.)
2. A strong copper and lead anomaly, locally with anomalous zinc, occurs within the Agashashok River drainage (S2 on fig. 1). This area is geochemically favorable for carbonate-hosted Omar- or Frost-type mineralization, for pyrite and base-metal mineralization in quartz veins, and for disseminated-stratabound base metals within the mixed carbonate-clastic sequences.
3. The most extensive area with high factor 3 stream-sediment scores is area S3 in the center of the quadrangle (fig. 1). This area is better delineated by the distribution of anomalously high molybdenum, and to a lesser extent by high silver, barium, and zinc. The S3 area includes the Omar, Frost, and Powdermilk mineral occurrences, and the headwaters of the Omar River, Tukpahlearik Creek,

and Anaktok Creek. The S3 region has geochemical favorability for base-metal mineralization with variable silver and barite in carbonate rocks as well as in black and mixed pelitic schists.

4. In the Kallarichuk Hills (S4; fig. 1), samples anomalous in Ba, Cu, Mo, and Pb occur within drainages underlain by mixed schists, and pelitic rocks of phyllitic to garnet grade. Because few sulfide occurrences have been noted, and because corresponding concentrate samples contain only minor amounts of sulfide minerals, these stream-sediment geochemical anomalies probably reflect high lithogeochemical background values.
5. Samples from the headwaters of the Tutuksuk River and Naneilik Creek in the northeast corner of the quadrangle (area S5) are enriched in Ag, Ba, Cu, Mo, Pb, and Zn. This area is underlain by a complexly faulted mixture of Paleozoic carbonate and mafic rocks; black shale, sandstone, and conglomerate of unknown Paleozoic age; and minor Proterozoic schist of amphibolite grade. Scattered minor pyrite, Fe-oxides, and Cu-oxides are known from this area, and parts of the Naneilik creekbed are intensely iron-stained, but the types of mineralization possible here are unknown and presently unconstrained by the geology.

Six factors explain 70 percent of the total variance in the heavy-mineral concentrate data (table 2). Factors 1, 5 and 6 are geochemical associations which probably reflect lithologic variations of heavy minerals such as Fe- and Ti-oxides and spinels, because they have no obviously related sulfide mineral suite. The elements occurring in factor 1, however, are those which are common in metal-enriched marine black shales (Desborough and Poole, 1983), and may still indicate nonsulfide resource potential. Some samples with high factor 6 scores in the Kallarichuk Hills just north of area S4 contain visible cassiterite (G. Bennett, USGS, written commun., 1986). The source of cassiterite and the factor 6 geochemical association is presently unknown.

Factor 3 loadings are highest for barium and zinc. Samples with high factor 3 scores are scattered throughout the northwest quarter of the quadrangle. Most of these samples have low lead and silver values, and may indicate disseminated sphalerite and barite in shale and sandstone.

Two factor associations in the concentrate data delineate areas of possible mineral potential. Factor 2 loadings are strongest for Co, Cu, Fe, and Ni, and high scores identify concentrate samples containing pyrite and lesser amounts of chalcopyrite. Samples with high factor 4 scores outline areas with high silver, lead and zinc; galena and (or) cerussite and sphalerite are visible in some of these samples (G. Bennett, USGS, written commun., 1986).

Factor 2 and 4 scores outline four geochemically favorable areas not identified by anomalous stream-sediment samples:

1. Samples with anomalous Co, Cu, Fe, and Ni (±Mn) cluster in the headwaters of Nakolik and Nakolikurok Creeks (areas C1 and C2 on fig. 1), and probably reflect disseminated pyrite and chalcopyrite mineralization noted in some sandstones.
2. High Ag, Pb, and Zn in samples from area C3 (overlapping part of S2) may be derived from sandstone-hosted, disseminated and vein base-metal mineralization with high silver values.
3. Samples with anomalous Pb, Zn, and Ag in area C4 apparently reflect carbonate-hosted mineralization, possibly similar to the Powdermilk occurrence. Samples anomalous in zinc with lesser lead and silver are scattered between area C4 and the southern part of area C2, and may reflect the lithologic transition from carbonate-hosted to sandstone-hosted mineralization.

An individual element concentration plot for tungsten indicates anomalous values across a broad area (C5) including the Klery Creek/Timber Creek placer gold area. Many of the anomalous samples contain visible scheelite (G. Bennett, USGS, written commun., 1986). Three concentrate samples containing visible gold also have high tungsten values, suggesting that area C5 has potential for vein-related gold-tungsten mineralization.

Table 2.--Factor loadings for 1,185 heavy-mineral concentrate samples
[Loadings less than 0.3 have been omitted]

Element	Factor 1	Factor 2	Factor 3	Factor 4	Factor 5	Factor 6
Fe	---	.88	---	---	---	---
Mg	---	---	---	---	-.88	---
Ca	---	---	-.56	---	-.33	-.49
Ti	.65	---	---	---	.56	---
Mn	.41	.33	---	---	---	---
Ag	---	---	---	.80	---	---
B	.72	---	---	---	---	---
Ba	---	---	.74	---	---	---
Be	.32	---	---	---	---	.61
Co	---	.85	---	---	---	---
Cr	.80	---	---	---	---	---
Cu	---	.83	---	---	---	---
La	.46	.42	.36	---	---	---
Nb	.45	---	---	---	.46	.32
Ni	---	.88	---	---	---	---
Pb	---	---	---	.81	---	---
Sc	.73	---	---	---	---	---
Sn	---	---	---	---	---	.70
V	.81	---	---	---	---	---
Y	.46	---	---	---	.74	---
Zn	---	---	.57	.44	---	---
Zr	.37	---	.36	---	.65	---
Percent of total variance	18	17	9	8	12	6

The reconnaissance data indicate that at least 25 percent of the Baird Mountains quadrangle is geochemically favorable for the occurrence of additional mineral deposits. The most likely deposit types are stratabound and stratiform, and occur within continental margin sedimentary rocks, that are unrelated to igneous activity.

REFERENCES CITED

Bailey, E.A., Folger, P.F., Thompson, W.B., Sutley, S.J., Schmidt, J.M., and Karl, S.M., 1987, Analytical results and sample locality map of stream-sediment and heavy-mineral concentrate samples from the Baird Mountains quadrangle, Alaska: U.S. Geological Survey Open-File Report 87-65.

Degenhart, C.E., Griffis, R.J., McQuat, J.F., and Bigelow, C.G., 1978, Mineral studies of certain ANCSA 17(d)(2) lands in Alaska, performed under contract J0155089: U.S. Bureau of Mines Open File Report 103-78, p. 250-279.

Desborough, G.A., and Poole, F.G., 1983, Metal concentrations in some marine black shales of the United States, in Shanks, W.C., ed., Cameron Volume on unconventional mineral deposits: New York, Society of Mining Engineers, p. 99-110.

Folger, P.F., in press, Geology and mineralization at the Omar Copper prospect, Baird Mountains quadrangle Alaska: U.S. Geological Survey Open-File Report, 99 p.

Karl, S.M., Schmidt, J.M., and Folger, P.F., 1985, Selected anomalous rock and sediment samples from central and northwestern Baird Mountains quadrangle, in Bartsch-Winkler, Susan, ed., The Unites States Geological Survey in Alaska--Accomplishments during 1984: U.S. Geological Survey Circular 967, p. 8-13.

Schmidt, J.M., and Folger, P.F., 1986, Pb-Zn-Ag mineralization in Paleozoic dolostones, Powdermilk prospect, Baird Mountains B-4 quadrangle, in Bartsch-Winkler, Susan and Reed, K.M., eds., Geologic studies in Alaska by the U.S. Geological Survey during 1985: U.S. Geological Survey Circular 978, p. 19-21.

Reviewers: K.A. Duttweiler and Harley King

GLACIAL ADVANCE OF LATE WISCONSIN (ITKILLIK II) AGE IN THE UPPER NOATAK RIVER VALLEY—A RADIOCARBON-DATED STRATIGRAPHIC RECORD

Thomas D. Hamilton, George A. Lancaster, and Deborah A. Trimble

The last major glaciation of the central Brooks Range, the Itkillik II advance of Hamilton and Porter (1975), has been dated at between about 24 and 11.5 ka (thousand years before present) based on indirect evidence such as periglacial mass wastage, river alluviation, and eolian activity (Hamilton, 1982; Ashley and others, 1984). We report here seven new radiocarbon dates on three measured stratigraphic sections along the Noatak River that provide a direct age bracket for the advance and retreat of the glacier that filled its upper valley during Itkillik II time.

Detailed field mapping (Hamilton, 1981, 1984a, b) shows that late Pleistocene valley glaciers flowed north and west from highland source areas and extended as far as 140 km down the Noatak valley from its head. Three principal advances of probable late Pleistocene age are recognized. These have been assigned to the Itkillik glaciation of Detterman and others (1958) and informally designated as phases IA, IB, and II (Hamilton and Porter, 1975; Hamilton, 1984a, b, 1986a, b). Our radiocarbon dates bracket the advance of Itkillik II age and provide an age limit on the next-older (Itkillik IB) glacial expansion.

Three prominent river bluffs along the Noatak River near Douglas Creek (fig. 1) intersect the end-moraine belt of Itkillik II age, the outwash apron that formed in front of it, and a lake basin that formed as the glacier retreated upvalley. The three bluffs, which range in height from 18 to 70 m, expose diamict, alluvium, outwash, and lacustrine sediments, capped by about a meter of sod, peat, and frost-churned stony silt.

Exposure A (fig. 2A), a south-facing, 70-m bluff within the end moraine of Itkillik II age, is situated 5.5 km below Douglas Creek. The bluff intersects an irregular surface that contains numerous kettles and several river-terrace remnants that formed as drainage became reestablished during retreat of the glacier from its end moraine. The lowest stratigraphic unit (unit 1), which forms vertical buttresses near the base of the section, consists of compact pebble-small-cobble gravel with a silty sand matrix. The upper part of the deposit is structureless, but overturned folds and one near-vertical, 30-cm bed of deformed peaty silt are present at greater depth. The peaty silt bed has an apparent radiocarbon age of 34,990 ± 230 yr B.P.

Overlying alluvium (unit 2) consists of packages of parallel-bedded to crossbedded sand, pebbly sand, and pebble-small-cobble gravel about 50 cm thick. Beds of oxidized organic silt with in situ rootlets 4 m and 2 m below the top of the alluvium are dated at 34,840 ± 950 yr B.P. and 30,070 ± 470 yr B.P., respectively. Gravel beds at greater depth dip upvalley at angles of 12-34° then level out and fine laterally to form a paleobasin floor composed of muddy sand. This closed depression within the gravel may have resulted from continued melt of buried glacier ice during deposition of unit 2.

The upper diamict (unit 3) is interpreted as massive till in its upper part and redeposited river gravel in its lower part. Unsorted, rounded to subrounded, striated clasts up to boulder size dispersed in a compact, gray, silty matrix grade downward at about 3.5 m depth into compact rounded pebbles and small cobbles that resemble the diamict of unit 1. Like unit 1, this deposit exhibits faint, highly deformed size stratification. Clasts of peaty silt incorporated in the diamict 70 cm above its base are dated at 34,010 ± 350 yr B.P., and clearly were redeposited from unit 2.

Unit 4 consists of rounded to subrounded alluvial pebbles and cobbles in a poorly sorted matrix of sand with phyllite chips. The alluvium contains several near-horizontal sand beds 10-30 cm thick that are continuous laterally for at least 20 m. A lag concentration of boulders up to 60 cm diameter occurs at the base of the alluvium and on the upper surface of the underlying diamict.

Exposure B (fig. 2B), 13 km downvalley from Douglas Creek, intersects an outwash terrace that originates at the end moraine of Itkillik II age. The terrace surface is planar for about 1 km upvalley from the exposure, then it degenerates into kame-and-kettle topography that may represent the downvalley limit of glacier ice of Itkillik II age. Other kettle fields downvalley from the exposure (hachured areas on fig. 1) probably developed from melting of older glacial ice of Itkillik IB age. The outwash at exposure B consists of alluvium which coarsens progressively upward and lacks obvious erosion surfaces or unconformities. In the basal part of the exposure, beds of medium to coarse sand up to 25 cm thick alternate with beds of sandy pebble-small-cobble gravel about 50 cm thick. The central part of the section consists of faintly bedded rounded pebbles, small cobbles, and sparse medium cobbles with some 10-cm interbeds of pebbles, of well-sorted coarse sand, or of muddy gravel. Pebbles, small to medium cobbles, and sparse larger cobbles in a matrix of nonoxidized medium to coarse sand and granules predominate in the upper part of the deposit. Progressive changes in clast lithology show increasing dominance of upvalley sources as sediment size increases. Locally derived carbonate rocks decrease upward from 30 percent of all clasts near the base of the section to about 10 percent near the top. Granitic rocks from

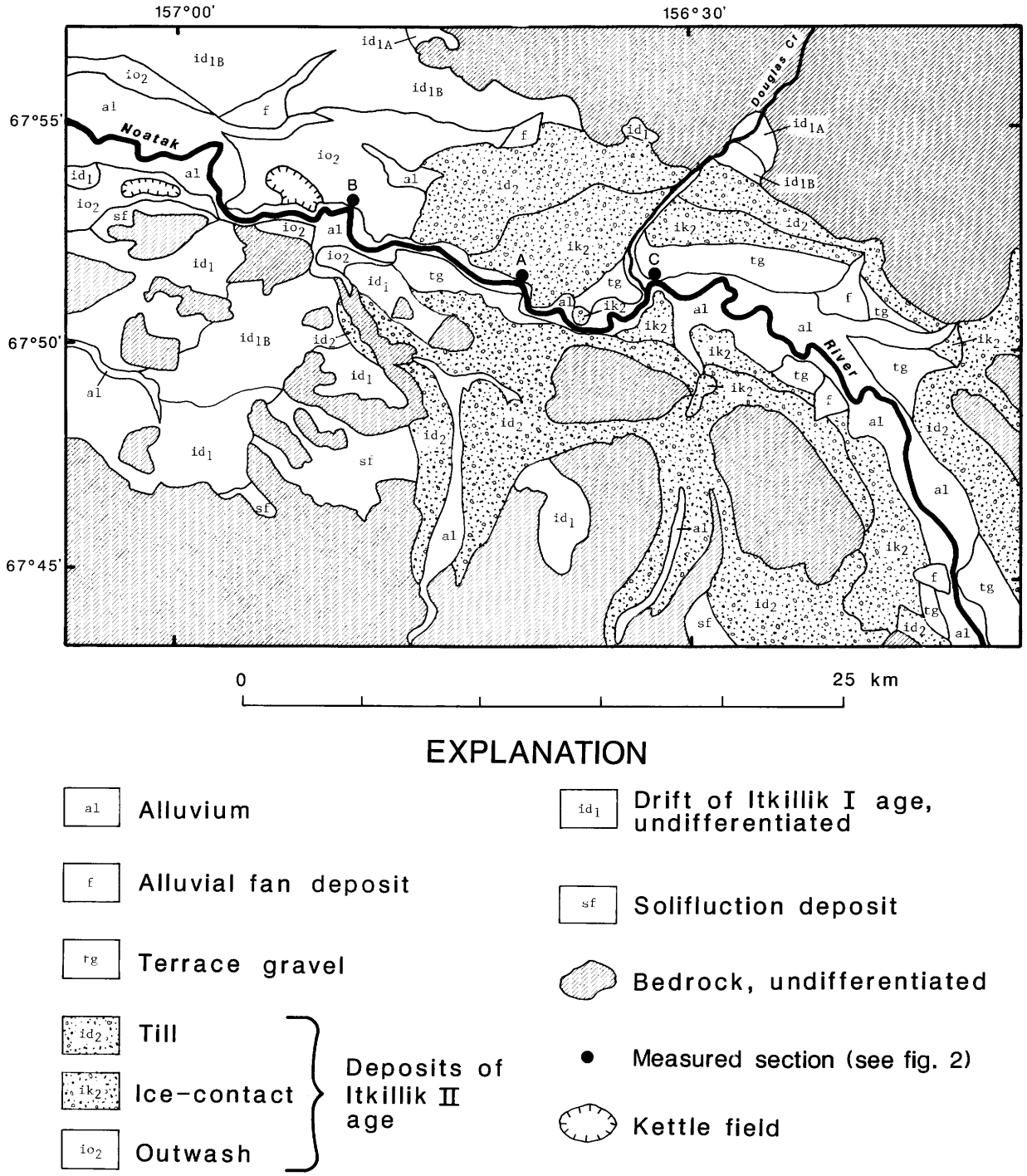

Figure 1.--Geologic map of Douglas Creek area, upper Noatak valley, showing location of measured stratigraphic sections. Note that drift of Itkillik I age (unit id_1) is locally divisible into older (id_{1A}) and younger (id_{1B}) components. Geology from Hamilton (1984a).

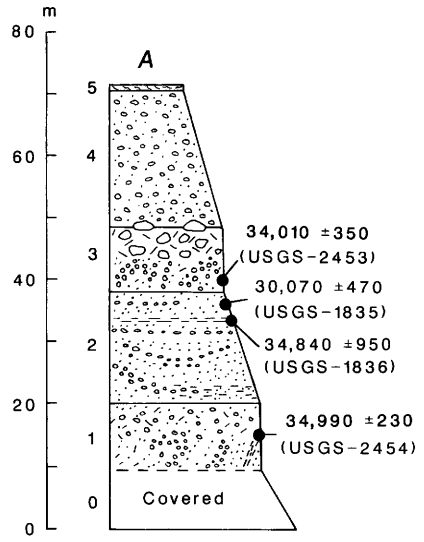

SECTION A

UNIT	THICKNESS (m)	DESCRIPTION
5	0.7	BLUFF CAP. Peat above frost-mixed silty peat that grades downward into silty gravel.
4	22	COARSE ALLUVIUM. Pebbles and cobbles in matrix of poorly sorted sand with phyllite chips. Contains some sand interbeds.
3	10.1	UPPER DIAMICT. Clasts up to boulder size dispersed in compact gray silt. Grades downward into compact, deformed, pebbles and small cobbles in silty matrix.
2	18	FINE ALLUVIUM. Fine to medium sand, pebbly sand, and pebble-small-cobble gravel. Contains 20-cm bed of oxidized organic silt 4 m below upper contact.
1	10.5	LOWER DIAMICT. Rounded pebbles and small cobbles in matrix of compact silty sand to sandy silt. Structureless near top; faintly bedded and deformed near base.
0	9.7	DEBRIS APRON.

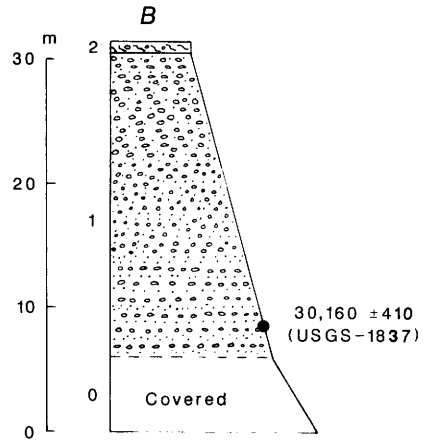

SECTION B

UNIT	THICKNESS (m)	DESCRIPTION
2	1.1	BLUFF CAP. Sod (0.3 m) above frost-churned stony silt (0.8 m).
1	24.5	OUTWASH AND ALLUVIUM. Weakly stratified pebbles and cobbles in matrix of medium to coarse sand and granules (upper 8 m of deposit). Grades downward into pebble-small-cobble gravel with some sand and pebble interbeds (middle 8 m), then into interbedded sand and pebble-small-cobble gravel (basal 8 m).
0	6.0	DEBRIS APRON.

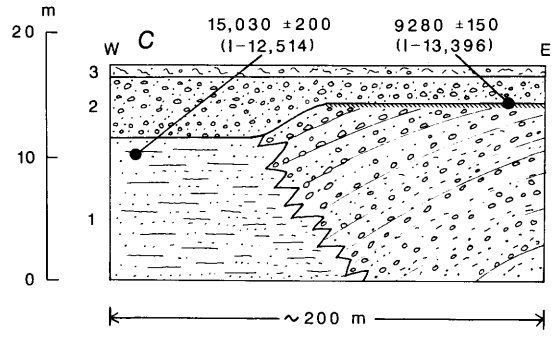

SECTION C

UNIT	THICKNESS (m)	DESCRIPTION
3	0.7	BLUFF CAP. Surface sod above peaty to stony silt.
2	4.8-2.5	GRAVEL. Pebbles and small cobbles, with some larger cobbles. Sand interbeds occur in W part of unit.
1	12.0-14.3	LACUSTRINE BEDS. Steeply dipping deltaic sand and fine gravel; grades westward (downvalley) into horizontally bedded fine sand, silty fine sand, and clayey silt.

Figure 2.--Measured stratigraphic sections with radiocarbon dates, Noatak River near Douglas Creek. USGS, U.S. Geological Survey radiocarbon laboratory, Menlo Park, Calif.; I, Teledyne Isotopes, Westwood, N.J. Locations on figure 1.

glacial source areas near the valley head show an inverse gradation from less than 1 percent of all clasts near the base of the section to about 10 percent near the top. A bed of dark-gray (5Y 4/1) clayey silt and gray (5Y 5/1) silty fine sand 8.5 m above river level contains sparse rootlets and organic detritus that are dated at 30,160 ± 410 yr B.P.

Exposure C (fig. 2C), on the north side of the Noatak River near the mouth of Douglas Creek, intersects an 18-m alluvial terrace that is inset within the end-moraine belt. Separate sections were measured at the eastern and western ends of the exposure, and one radiocarbon sample was taken from each section. The eastern (upvalley) section consists dominantly of deltaic foreset beds that dip downvalley at angles as steep as 26°. Fine to medium sand, stony sand, and fine gravel alternate in beds 10-50 cm thick. Near the center of the exposure, the deltaic sediments grade downward and westward into gray (5Y 5/1), horizontally bedded, well sorted fine sand with some 20-cm interbeds of clayey silt to silty fine sand. Near the west end of the bluff, dark gray organic silt grades upward into sandy fine gravel. Small wood fragments and rootlets from along bedding planes 1.4 m below the base of the gravel are dated at 15,030 ± 200 yr B.P. Unit 2 is fluvial gravel that consists of pebbles, small cobbles, and some larger cobbles in a sparse sandy matrix. The gravel thickens downvalley, where an inactive fan of Douglas Creek is graded to the gravel terrace. A bed of black (5Y 2.5/1) autochthonous peat 2-8 cm thick at the contact between the gravel and the underlying deltaic beds is dated at 9,280 ± 150 yr B.P. The peat extends through the eastern part of the bluff, indicating that deltaic sediments were exposed subaerially for some time before the Noatak River overran the site.

Radiocarbon dates and stratigraphic relations in the Douglas Creek area demonstrate that the associated end moraine (id_2 on fig. 1) is of Itkillik II age as defined by Hamilton and Porter (1975) and as dated by Hamilton (1982). Deposition of fine alluvium prior to the ice advance began some time before 35 ka and continued until some time after 30 ka. Subsequent expansion of the Itkillik II glacier is recorded by coarsening-upward sediments with increasing upvalley lithologies at site B and by the upper diamict at site A. The glacier initially deformed and redeposited preexisting alluvium from the valley center, but it later deposited massive, bouldery, silt-rich till at the site. A minimum age for deglaciation is provided by the date of about 15 ka on lake sediments that formed as the glacier retreated from its end moraine.

The lower diamict at site A was originally interpreted as glacial drift on the basis of (1) its generally unsorted character, (2) high degree of compaction, and (3) incorporation of overturned and evidently ice-thrust sediments near its base. However, our radiocarbon date of 34,990 ± 230 yr B.P. on this unit suggests the alternative possibility that the diamict may have been deposited as a component of a rapidly aggrading alluvial sequence. If the date is correct, then the deformation features in the lower diamict may have resulted from melting of underlying stagnant glacier ice rather than from later thrusting beneath an advancing glacier. We cannot ascertain at present whether the radiocarbon date or the original field interpretation is correct.

Regardless of how the lower diamict is interpreted, our radiocarbon dates place a minimum age limit of about 35 ka on the Itkillik IB glacial advance, which formed the prominent lateral moraine near the northern valley wall (unit id_{1B} on fig. 1). We believe that the Itkillik IB event probably is of early Wisconsin age (isotope stage 4 of the marine record) because (1) its drift is only slightly more subdued and weathered than drift of the Itkillik II advance, (2) the alluvium that separates the lower and upper diamicts at site A lacks identifiable paleosols, weathering horizons, or unconformities, and (3) kettle fields downvalley from site B (fig. 1) indicate that stagnant glacier ice from the older advance still was present on the valley floor when the outwash train of Itkillik II age was being deposited.

REFERENCES CITED

Ashley, G.M., Hamilton, T.D., and Reed, K.M., 1984, Epiguruk bluff--Chronology and regional correlations (abs.): Geological Society of America Abstracts with Programs, v. 16, no. 5, p. 267.

Detterman, R.L., Bowsher, A.L., and Dutro, J.T., Jr., 1958, Glaciation on the Arctic Slope of the Brooks Range, northern Alaska: Arctic, v. 11, p. 43-61.

Hamilton, T.D., 1981, Surficial geologic map of the Survey Pass quadrangle, Alaska: U.S. Geological Survey Miscellaneous Field Studies Map MF-1320, scale 1:250,000.

___ 1982, A late Pleistocene glacial chronology for the southern Brooks Range--Stratigraphic record and regional significance: Geological Society of America Bulletin, v. 93, p. 700-716.

____ 1984a, Surficial geologic map of the Ambler River quadrangle, Alaska: U.S. Geological Survey Miscellaneous Field Studies Map MF-1678, scale 1:250,000.

____ 1984b, Surficial geologic map of the Howard Pass quadrangle, Alaska: U.S. Geological Survey Miscellaneous Field Studies Map MF-1677, scale 1:250,000.

___ 1986a, Late Cenozoic glaciation of the central Brooks Range, in Hamilton, T.D., Reed, K.M., and Thorson, R.M., eds., Glaciation in Alaska--The geologic record: Anchorage, Alaska Geological Society, p. 9-49.

_____ 1986b, Glaciation of the Brooks Range, in Heginbottom, J.A., and Vincent, J.-S., eds., Correlation of Quaternary deposits and events around the margin of the Beaufort Sea: Geological Survey of Canada Open-File Report 1237, p. 27-29.

Hamilton, T.D., and Porter, S.C., 1975, Itkillik glaciation in the Brooks Range, northern Alaska: Quaternary Research, v. 5, p. 471-497.

Reviewers: L.D. Carter and J.S. Kelley

ORDOVICIAN AND SILURIAN FOSSILS FROM THE DOONERAK ANTICLINORIUM, CENTRAL BROOKS RANGE, ALASKA

John E. Repetski, Claire Carter, Anita G. Harris, and J. Thomas Dutro, Jr.

The Doonerak anticlinorium, a structural high in the central Brooks Range, Alaska, exposes lower Paleozoic stratified rocks and mafic intrusive rocks that lie unconformably beneath Devonian and Carboniferous beds (fig. 1). Until recently, no fossils had been found in this dominantly argillite and volcaniclastic sequence. In 1981, Middle Cambrian trilobites were collected from calcareous beds in the dark pelitic sequence that stratigraphically underlies a siliceous volcaniclastic sequence (Dutro and others, 1984a, 1984b).

Conodonts identified as *Periodon* sp. (fig. 2), collected by D.L. Jones from the siliceous volcaniclastic rocks (cherts) on the north flank of the Doonerak anticlinorium (locality 1 in fig. 1 and table 1), indicate an Ordovician age range from Arenigian through Caradocian. Current taxonomic practice divides the conodont genus *Periodon* into three species. These occur in phylogenetic sequence from the late Early through the early Late Ordovician. Because the few specimens from the Doonerak area are limited to ramiform elements, a relatively conservative element in the conodont apparatus, assignment to species is not currently possible.

In the past two years, Ordovician conodonts have also been identified by A.G. Harris (Dillon and others, in press) from rocks near Snowden Mountain in the Chandalar quadrangle. These collections, from carbonaceous phyllite and metacarbonate, occur in the Hammond subterrane (of the Arctic Alaska terrane) southeast of the Doonerak anticlinorium. Representatives of *Periodon aculeatus* Hadding are the most common elements in the collections. This species and other more biostratigraphically diagnostic taxa indicate an approximate Llandeilan to earliest Caradocian (middle Ordovician) age for these rocks. We tentatively correlate these two areas and suggest that they both represent the same lower Paleozoic basement in the south-central Brooks Range.

In 1983, Michael Churkin, Jr. made two collections of graptolites from dark-gray, calcareous, chloritic phyllite and argillite just west of Fish Creek and north of Kachwona Creek. This locality is about 5 km west of the Ordovician conodont locality, in rocks overlying the Ordovician cherts (loc. 2, fig. 1, and table 1). The graptolites include *Orthograptus*? sp., *Pristiograptus*? sp., *Monograptus* sp. (with lobed thecae), *Monograptus*? sp., and indeterminate biserial forms (perhaps diplograptids). Carter suggests that this assemblage is middle to late Early Silurian (Llandoverian). In 1984, Dutro collected, from the graptolite locality, a sample that yielded conodonts. According to Harris, these consist chiefly of representatives of *Dapsilodus* and a few digyrate and dolabrate ramiform elements of post-Ordovician morphotype. Taken together, these conodonts indicate a Silurian age.

Dikes of two ages (470 and 350 Ma) intrude the lower Paleozoic terrane of the anticlinorium (Dutro and others, 1976). According to radiometric calibrations of the early Paleozoic (Harland and others, 1982; Odin, 1982), the older of these dike systems approximately corresponds either to the Arenigian-Llanvirnian boundary (Odin, 1982) or to the upper Llanvirnian (Harland and others, 1982). However, Ross and others (1982) placed the 470 Ma level in the lower Caradocian. In any case, the strata that are mapped stratigraphically high in the Doonerak structure (Dillon and others, in press) are also reasonably interpreted as middle Ordovician in age.

Because the dated intrusive rocks do not directly cut the rocks that yielded the Ordovician conodonts, but instead intrude the older pelitic sequence, it can be argued that these dikes might have been feeders for the volcanic activity that is recorded in the siliceous volcaniclastic suite. Consequently, the 470 Ma radiometric age might date the fossiliferous Ordovician beds rather closely. The stratigraphic range reported for these conodonts spans about the same time interval as do the three interpretations of the radiometric date described above.

Table 1.--Fossil localities in Doonerak anticlinorium (see fig. 1)

North of Frigid Crags on the west side of North Fork of Koyukuk River, Wiseman 1:250,000 quadrangle, Alaska.

1. Ordovician: USGS loc. 9473-CO. Wiseman B-2 quadrangle; 67°51.5' N., 150°56' W.; greenish-gray to red chert (siliceous volcaniclastics); approximately 30-m-thick cliff. Collector: D.L. Jones, 1982.

2. Silurian: Field Number 83BR 781MC and 84 ADu 5 (USGS loc. 11447-SD). Wiseman B-3 quadrangle; 67°51.2' N., 151°03' W.; small stream valley north of Kachwona Creek and west of Fish Creek; elev. approx. 1050 m (3500 ft); black to dark-gray, calcareous, chloritic phyllite and argillite. Collectors: Michael Churkin, Jr., 1983; J.T. Dutro, Jr., 1984.

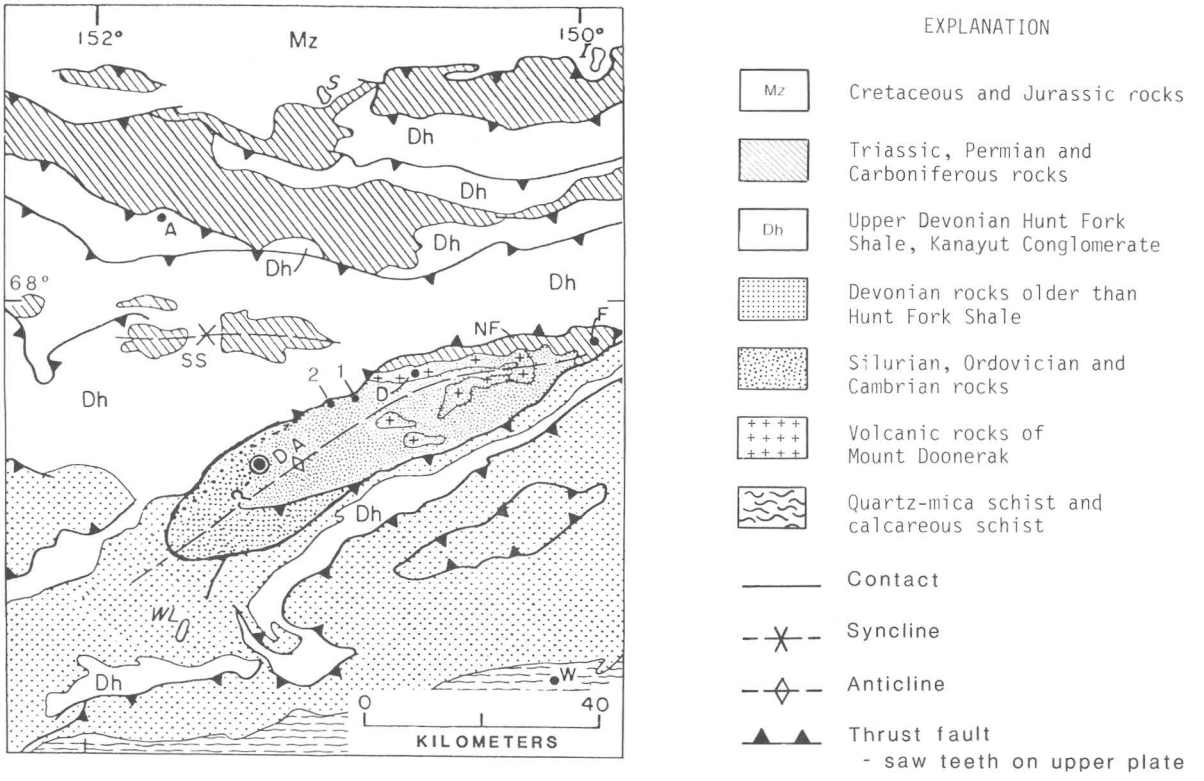

Figure 1.--Index map and generalized structural map of Doonerak anticlinorium and adjacent areas. Circled dot, Cambrian locality; 1, Ordovician locality; 2, Silurian locality; A, Anaktuvuk Pass; DA, axis of Doonerak anticlinorium; D, Mount Doonerak; F, Falsoola Mountain; I, Itkillik Lake; NF, North Fork Koyukuk River; S, Shainin Lake; SS, Savioyuk synclinorium; W, Wiseman; WL, Wild Lake. Geology modified from Dutro and others (1976).

Consequently, we now know that the layered rocks of the Doonerak anticlinorium include Middle Cambrian, middle Ordovician, and Lower Silurian fossiliferous strata, that they were intruded by dikes about 470 Ma and 350 Ma, and that they have been folded, cleaved, faulted, and subsequently overstepped unconformably by shallow-water marine sequences in both late Middle Devonian and Early Mississippian times.

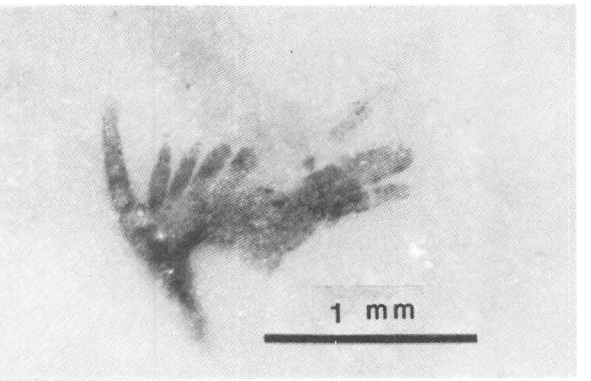

Figure 2.--*Periodon* sp. from Ordovician siliceous volcaniclastic rocks, locality 1, north flank of Doonerak anticlinorium, USGS loc. 9473-CO; ramiform element on bedding surface, photographed under glycerine: USNM 414609. Specimen reposited in collections of the Department of Paleobiology, U.S. National Museum of Natural History, Washington, D.C.

REFERENCES CITED

Dillon, J.T., Brosgé, W.P., and Dutro, J.T., Jr., 1986, Generalized geologic map of the Wiseman quadrangle, Alaska: U.S. Geological Survey Open-file Report 86-219, 1 sheet, scale 1:250,000.

Dillon, J.T., Harris, A.G., and Dutro, J.T., Jr., in press, Preliminary description and correlation of lower Paleozoic fossil-bearing strata in the Snowden Mountain area of the south-central Brooks Range, Alaska, in Tailleur, I. L. and

Weimer, Paul, eds.: Alaska North Slope geology: Pacific Section Society of Economic Paleontologists and Mineralogists and Alaska Geological Society.

Dutro, J.T., Jr., Brosge, W.P., Lanphere, M.A., and Reiser, H.N., 1976, Geologic significance of Doonerak structural high, central Brooks Range, Alaska: American Association of Petroleum Geologists Bulletin, v. 60, no. 6, p. 952-961.

Dutro, J.T., Jr., Palmer, A.R., Repetski, J.E., and Brosge, W.P., 1984a, The Doonerak anticlinorium revisited, in Coonrad, W.L and Elliott, R.L., eds., The United States Geological Survey in Alaska: Accomplishments during 1981: U.S. Geological Survey Circular 668, p. 17-19.

_____ 1984b, Middle Cambrian fossils from the Doonerak anticlinorium, central Brooks Range, Alaska: Journal of Paleontology, v. 58, no. 6, p. 1364-1371.

Harland, W.B. and others, 1982, A geologic time scale: Cambridge, U.K., Cambridge University Press, 131 p.

Odin, G.S., 1982, The Phanerozoic time scale revisited: Episodes, v. 5, no. 3, p. 3-9.

Ross, R.J., Jr., and others, 1982, The Ordovician System in the United States: International Union of Geological Sciences Publication 12, 73 p.

Reviewers: J.M. Berdan and John Pojeta, Jr.

ORGANIC CARBON OCCURRENCE AND CONTENT IN CARBONATE ROCKS FROM THE OMAR COPPER PROSPECT, BAIRD MOUNTAINS, ALASKA

Jeanine M. Schmidt and Peter F. Folger

Complexly faulted carbonate rocks of Ordovician through Devonian age underlie most of the Squirrel River basin in the southwestern Baird Mountains (Dumoulin and Harris, 1985 and in press). The Omar copper prospect (fig. 1) covers an area of approximately 8 km^2 along a tributary of the Omar River, 45 km north of the Squirrel River. At the prospect, irregularly distributed copper sulfides and tetrahedrite form disseminations and occur within vein-breccias that crosscut Lower and Middle Devonian dolostones (Degenhart and others, 1978; Folger and Schmidt, 1986). After mineralization, these rocks underwent syndeformational greenschist to glaucophane-schist facies metamorphism during the Jurassic-Cretaceous Brooks Range orogeny (Snelson and Tailleur, 1969).

White to dark-gray dolostone and limestone at the prospect contain varying amounts of organic matter. Organic material also occurs as discrete millmeter- to centimeter-sized blebs and fillings within Cu-bearing veins. In order to determine the variability, type, and thermal history of organic material at Omar, 14 samples were submitted to ExLog Laboratories for total organic carbon (TOC) analyses and Rock-Eval pyrolysis (Tissot and Welte, 1978). Such information from the organic material would ideally reflect its source, the conditions under which it was deposited with sulfide minerals, and the subsequent history of the rocks. Twelve rock samples submitted (table 1) are representative of all types of carbonate rocks exposed in the prospect area: unmineralized Ordovician and Devonian (Emsian and Eifelian) dolostones, unmineralized Ordovician(?) argillaceous limestone, and mineralized Devonian dolostone. Two samples of organic blebs from within the mineralized breccia were also analyzed.

All samples were washed, dried, split and crushed. For TOC analysis, 1 g of crushed sample was used, and carbonate minerals were dissolved by heating for 3 hr at 60 °C in 50 mL of 3 M HCl. The residue, vacuum filtered onto a glass-fiber mat, was washed and then dried at 80 °C for 1 hr in preparation for analysis. A Rock-Eval II pyrolysis instrument was used, with helium gas and a temperature ramp of 25 °C per minute. Analyses were calibrated with standards and blanks every 10 samples.

The total organic carbon content of some lithologic units within the Omar prospect area is distinct. Unmineralized Ordovician dolostone and argillaceous limestone contain 0.07-0.15 weight-percent carbon and unmineralized Emsian dolostone 0.19-0.22 weight-percent carbon. Three other samples of carbonate rocks of probable Ordovician age (J.A. Dumoulin, USGS, oral commun., 1986), from approximately 8 km southeast of Omar, have TOC contents (0.06-0.14 weight percent) similar to those at Omar. These values suggest that the organic content of carbonate rock units may be distinctive and internally homogeneous over areas as large as 20 km^2. Mineralized Devonian dolostones have both the lowest and highest (0.05 and 0.73 weight percent) carbon contents. This difference in TOC is probably accounted for by the presence of organic blebs in some of these samples.

S_1 and S_2 peak values produced during pyrolysis are measures of the hydrocarbon yield of a rock. S_1 measures the free hydrocarbons distilled at low temperatures (below 300 °C); S_2 measures the additional hydrocarbons produced by heating of the remaining kerogen in the rock (Bustin and others, 1985). An X-ray diffraction peak at 26° 2Θ indicates that the organic blebs have structures that approach crystalline graphite (Joel Leventhal, USGS, oral commun., 1986). S_2 peak values were below detection limits for 4 of 5 Devonian samples, therefore productivity ratios (S_1/ S_1+S_2) for these rocks cannot be determined. Productivity ratios for the Ordovician rocks are relatively high (0.62-0.94, avg. 0.84), indicating that all rock types at Omar contain mainly free hydrocarbons and have been heated well beyond the thermal windows necessary for production of oil (100-200 °C) and gas (150-250 °C; Tissot and Welte, 1978).

Table 1.--Total organic carbon contents, conodont alteration indices and selected Rock-Eval pyrolysis data from the Omar Cu prospect and nearby
[na, not applicable; *, values greater than 1,000 are due to low total organic carbon or presence of carbonate in sample. See text for explanation of symbols]

		Rock-Eval pyrolysis						Conodonts	
Sample type	Sample No.	TOC (wt pct.)	S_1 (mg/g)	S_2 (mg/g)	S_3 (mg/g)	S_2/TOC (HI)	S_3/TOC (OI)	CAI	Tmin °C
Omar prospect									
Hydrocarbon blebs	159A	na	0.50	0.60	12.33	--	--	--	--
	159B	na	1.52	.54	10.40	--	--	--	--
Mineralized (Emsian) dolostone	9	0.05	.19	--	6.32	--	(12,640)*	--	--
	74A	.05	.46	--	2.49	--	(4,980)*	--	--
	74B	.69	.56	--	2.89	--	419	--	--
	77	.73	.09	--	.37	--	51	--	--
Emsian dolostone	55	.22	.49	.05	.17	23	77	5-5.5	300-350
	83	.19	.02	--	.16	--	84	5.5	350
Ordovician(?) limestone	8	.11	.97	.08	.10	73	91	--	--
	11	.10	.64	.11	.19	110	190	--	--
Ordovician dolostone	52	.09	.59	.04	.10	44	111	--	--
	57	.07	.33	.03	.08	43	114	5.5-6	350-400
	86	.08	.28	.08	.73	100	912	6-7	400-450
	112	.15	.24	.15	.34	100	227	5.5	350
8 km south of Omar									
Ordovician(?) limestone	5JS59A	0.14	0.37	--	0.19	7	136		
Mineralized Ordovician(?) dolostone	5JS39	.06	.08	--	4.42	17	(7,367)*		
	5JS62B	.12	1.20	0.27	3.35	225	(2,792)*		

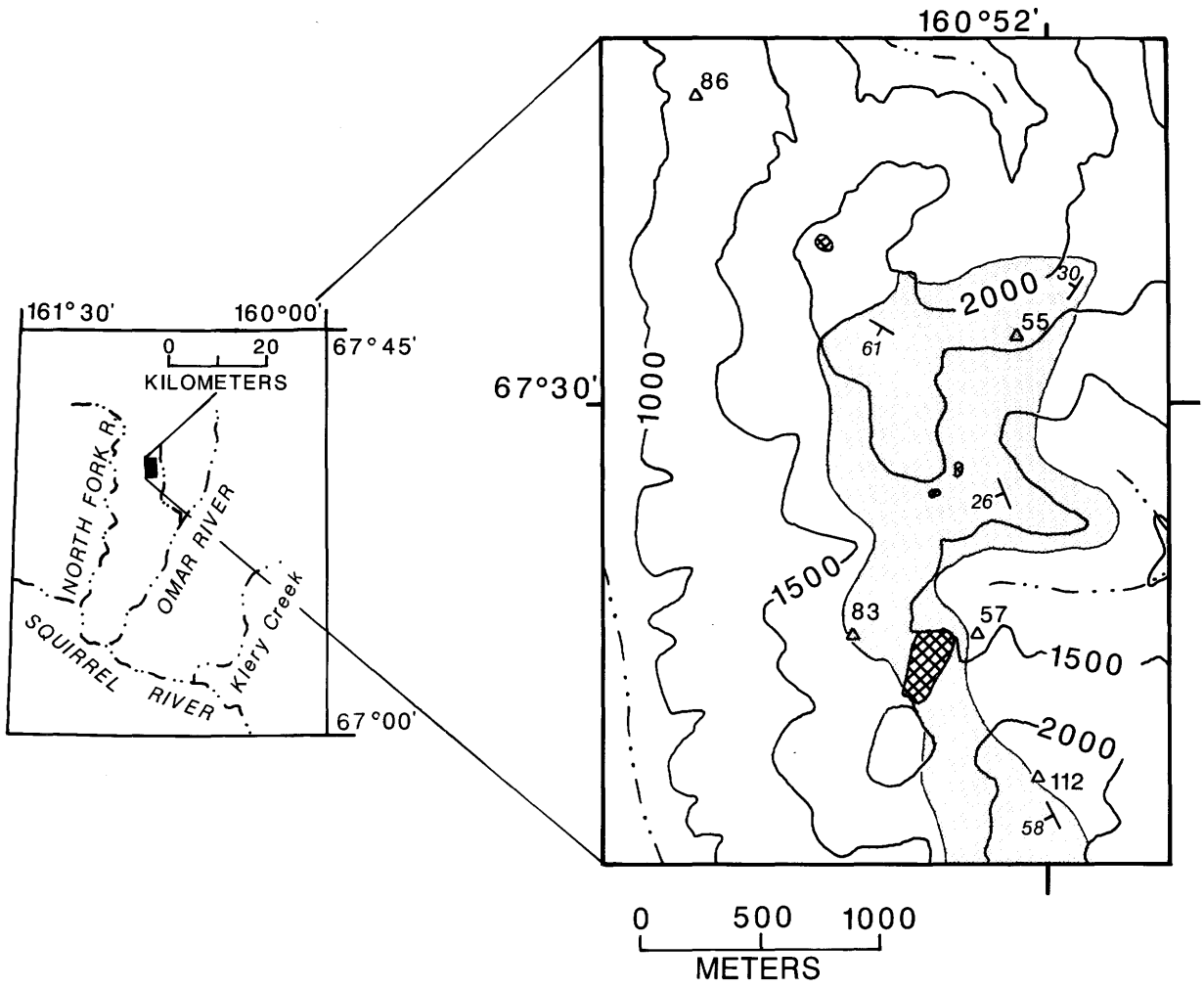

Figure 1.--Map of Omar copper prospect. Shaded pattern shows areas underlain by Devonian dolostones. Cross-hatches indicate areas of sulfide mineralization. Triangles indicate sample locations (table 1). All mineralized samples and hydrocarbon blebs are from within largest cross-hatched area. Contour intervals in feet.

The organic clots are paragenetically late in the mineralization sequence and fill interstices within the dolostone breccia (fig. 2). Approximately 20 percent of these blebs are spherical, suggesting transport as an immiscible phase, probably a hydrocarbon, in an aqueous solution. The spheres occur only within mineralized rocks at Omar, and are always enclosed by vein-filling, hydrothermal dolomite or calcite. Similar spherical carbon blebs with hydrothermal carbonate occur in mineralized breccias and vugs in some unmetamorphosed Pb-Zn deposits of the Viburnum trend in southeastern Missouri (Marikos, 1984). Hydrothermal fluids associated with mineralization transported the clots in both the Viburnum trend and Omar, but later metamorphism heated the organic material at Omar to its present near-graphite composition. Lower productivity ratios (0.45 and 0.74) of the blebs relative to the whole rocks may reflect their isolated and homogeneous habit, in which they may have been less affected by metamorphic heating than disseminated organic material in the whole rocks.

Of the 14 samples, 7 yielded Tmax values (334-416 °C) from the S_2 pyrolysis peak. However, Tmax values are difficult to interpret in rocks that have been metamorphosed and undergone possible surface weathering (Joel Leventhal, USGS, oral commun., 1986). These pyrolysis-derived Tmax values are compatible with low greenschist to glaucophane-schist facies, which are the conditions suggested for the Omar area by the mineralogy of noncarbonate rocks

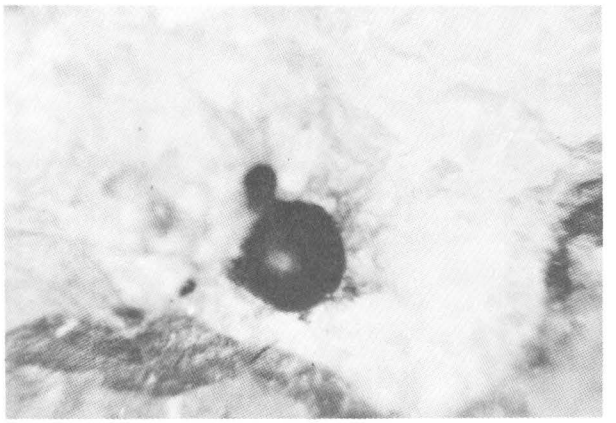

Figure 2.--Organic, carbon-rich sphere in hydrothermal dolomite (white) within Devonian dolostone breccia. Sphere is 5 mm in diameter. Photograph by Joel Leventhal (USGS).

(Armstrong and others, 1986). A temperature range of 300-450 °C is indicated by the color alteration indices (CAI's) of conodont microfossils from the same samples (Anita Harris, USGS, written commun., 1985, 1986; table 1). These temperature ranges suggest that metamorphic heating consistently overprinted any mineral-related paleothermal anomaly in rocks of the Omar area.

The S_3 value is a measure of the pyrolysis-derived organic oxygen in the rock. Mineralized samples and organic globules at Omar have organic CO_2 values an order of magnitude higher than unmineralized samples (5.80 mg/g versus 0.23 mg/g average). This suggests that the solutions that transported and deposited sulfide minerals with dolomite and hydrocarbons were oxidizing, or caused oxidation of organic matter by reaction with SO_4. Alternatively, the mineralized rocks may have become more fractured and permeable, and localized later oxidizing fluids unrelated to the mineralizing event. Variation in organic CO_2 content between unmineralized samples is small.

Plots of oxygen index (OI) versus hydrogen index (HI) are used to indicate the type of organic material originally present in fresh rock samples and the degree of maturation of that material (Bustin and others, 1985). HI values of samples from Omar are low (23-110) and indicate that the organic matter is highly evolved in terms of its hydrogen content relative to carbon. The OI values are widely scattered, and some are much higher than those characteristic of overmature hydrocarbon source rocks (typically <100). The anomalously high OI values of these rocks result from exposure to oxidizing conditions independent of the normal burial-maturation process, and therefore are not useful for interpreting the type of organic source material or the path of its evolution. The source is presumed to be marine algal matter, since these are platform carbonate rocks. Oxidizing conditions may have occurred during mineralization, primary dolomitization, or surface weathering. Anomalously high CAI values of 7-8 versus a regional 5-6 average indicate that oxidation also occurred during local bleaching of dolostone (J.A. Dumoulin, USGS, oral commun., 1985).

Comparison of organic material at Omar with that from Ruby Creek, a similar copper deposit hosted in Devonian carbonate rocks 200 km to the east in the Ambler River quadrangle (Hitzman, 1983), shows that the TOC contents of both host and mineralized rocks at Omar are lower than those at Ruby Creek, where both black and carbonaceous carbonates occur, and where hydrocarbon seams, disseminations, and blebs are common. The oxygen content of hydrocarbons in mineralized rocks at Ruby Creek is consistently low. Their position on a H/C versus O/C plot reflects maturation to a point beyond both the oil and gas windows. Temperatures of sulfide deposition at Ruby Creek are 120-217 °C (from fluid-inclusion studies), much lower than the CAI temperatures indicated at Omar. CAI's from Silurian and Devonian carbonate rocks in the Ruby Creek area are 5-6 (Anita Harris, USGS, written commun., 1985, 1986), indicating minimum temperatures of 300-350 °C, which also represents the later metamorphic overprint.

Unmineralized Ordovician and Devonian carbonate rock units have distinct TOC contents within a spatially restricted area (8 km^2) around the Omar prospect. All rocks in this area have been heated well beyond the windows necessary for production of oil and gas; all hydrocarbons in the rocks are overmature. Oxidizing conditions during mineralization, bleaching, dolomitization(?), or surface weathering apparently altered the oxygen content of the hydrocarbons. However, organic matter in all mineralized rocks contains much higher CO_2 than that in unmineralized samples. Temperatures suggested for metamorphism by conodont CAI's are consistent with mineral assemblages within the rocks. No conclusions can be drawn regarding the type of organic material originally present, or its maturation path, although a marine algal source is most likely for these platform carbonate rocks.

REFERENCES CITED

Armstrong, R.L., Harakal, J.E., Forbes, R.B., Evans, B.W., and Thurston, S.P., 1986, Rb-Sr and K-Ar study of metamorphic rocks of the Seward Peninsula and southwestern Brooks Range, Alaska: Geological Society of America Memoir 164, p. 185-203.

Bustin, R.M., Barnes, M.A., and Barnes, W.C., 1985, Diagenesis 10: Quantification and

modelling of organic diagenesis: Geoscience Canada, v. 12, no. 1, p. 1-21.

Degenhart, C.E., Griffis, R.J., McOuat, J.F. and Bigelow, C.G., 1978, Mineral studies of certain ANSCA 17(d)(2) lands in Alaska: U.S. Bureau of Mines Open File Report 103-78, 529 p.

Dumoulin, J.A., and Harris, A.G., 1985, Lower Paleozoic carbonate rocks of Baird Mountains quadrangle, Alaska (abs.): Tulsa, American Association of Petroleum Geologists, Program and Abstracts, 60th Annual meeting, Pacific section, p. 55.

Dumoulin, J.A., and Harris, A.G., in press, Lower Paleozoic carbonate rocks of the Baird Mountains, Western Brooks Range, Alaska, in American Association of Petroleum Geologists Memoir, Tailleur, Irv and Weimer, P., eds.

Folger, P.F., and Schmidt, J.M., 1986, Geology of the carbonate-hosted Omar copper prospect, Baird Mountains, Alaska: Economic Geology, v. 81, p. 1690-1695.

Hitzman, M.W., 1983, Geology of the Cosmos Hills and its relationship to the Ruby Creek copper-cobalt deposit: Stanford, Calif., Stanford University, Ph.D. dissertation, 266 p.

Marikos, M. A., 1984, Relation of bitumen to ore in the Magmont West orebody, southeast Missouri: Rolla, Mo., University of Missouri, M.S. thesis, 122 p.

Snelson, S., and Tailleur, I.L., 1969, Large scale thrusting and migrating Cretaceous foredeeps in the western Brooks Range and adjacent regions of northwest Alaska, (abs.): American Association of Petroleum Geologists Bulletin, v. 523, no. 3, p. 567.

Tissot, B.P., and Welte, D.H., 1978, Petroleum formation and occurrence: Berlin, Springer Verlag, 538 p.

Reviewers: J.A. Dumoulin and J. Leventhal

PLANT MEGAFOSSILS, VERTEBRATE REMAINS, AND PALEOCLIMATE OF THE KOGOSUKRUK TONGUE (LATE CRETACEOUS), NORTH SLOPE, ALASKA

Robert A. Spicer and Judith Totman Parrish

The upper part of the nonmarine Kogosukruk Tongue of the Prince Creek Formation is well exposed along 80 km of the Colville River between Uluksrak Bluff and Ocean Point (fig. 1). In the summer of 1986, palynological and megafossil collections were made at 48 localities as part of a study that has the aim of reconstructing the vegetation and, subsequently, the paleoclimate of the North Slope during the Late Cretaceous. The Kogosukruk Tongue is of particular importance to paleoclimatic studies because at the time of deposition, northern Alaska was at 80° to 85° N. paleolatitude (Smith and others, 1981; Ziegler and others, 1983). Paleoclimatic information derived from the study of the Kogosukruk Tongue is vital to the reconstruction of the global latitudinal temperature gradient near the close of the Late Cretaceous.

The Kogosukruk Tongue is Campanian and Maestrichtian in age, based on marine fossils in rocks above and below (Brosgé and Whittington, 1966; Marincovich and others, 1985; McDougall, 1986) and on pollen (Frederiksen and others, 1986). A variety of sedimentary facies is present within the unit. Fluvial and floodplain deposits, especially channel-fill and overbank deposits, compose the bulk of the sediments, but lacustrine and bog deposits also are represented. Coal beds composed of autochthonous or allochthonous material occur throughout the Kogosukruk. Those near the base of the unit tend to be bituminous, rich in resin, and thicker than those near the top, which also are of lower rank; the coal beds typically are 0.5 m, but rarely more than 1.0 m, thick. Paleosols and bentonites occur throughout the unit.

We recovered a maximum of 10 megafossil taxa from the Kogosukruk Tongue. These consist of two conifer forms, *Parataxodium wigginsii* Arnold and Lowther and a cupressaceous form; one terrestrial angiosperm leaf, *Hollickia quercifolia* (Hollick) Krassilov; one aquatic angiosperm, *Quereuxia angulata* (Lesquereux) Kryshtofovich (also referred to "*Trapa*"); one angiosperm fruit; two ferns; the sphenophyte *Equisetites* sp.; and two types of small, ovoid seeds. The preservation of intact deciduous conifer shoots, the lack of hydraulic size-sorting, and evidence of minimal selective mechanical and biogenic degradation in most assemblages all suggest rapid deposition near the site of growth. The ubiquitous preservation of *Equisetites* rhizome systems in growth position and the three-dimensional preservation of a fern in growth position within an ash horizon provide important data on early colonizers and ground

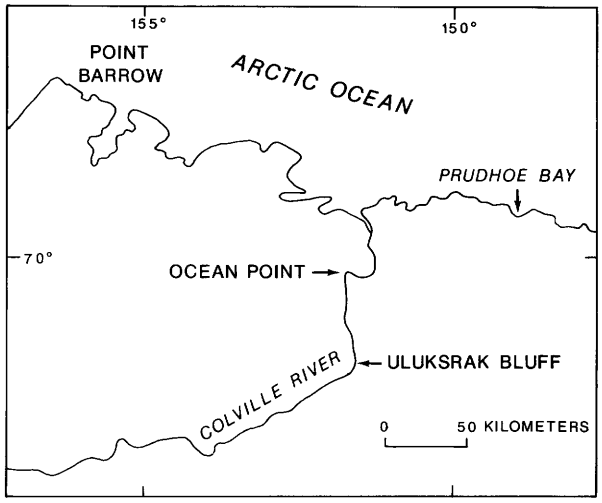

Figure 1.--North-central Alaska. The Kogosukruk Tongue of the Prince Creek Formation crops out along the Colville River between Uluksrak Bluff and Ocean Point.

cover within the floodplain environment. The *Equisetites* rhizome systems penetrate sediments below paleosols and autochthonous coal beds, and this suggests that the plant was an early colonizer of floodplain environments, much as *Equisetum* is today in the Yukon River Valley. *Equisetites*, together with ferns, probably composed the ground cover over much of the region.

The plant megafossils show no evidence of major vegetational change throughout the period of deposition of the Kogosukruk Tongue. However, the later coal beds appear to contain less woody material than do the earlier ones, which may reflect a diminution of the forest ecosystem leading to a more open vegetation. The forest community was dominated by the deciduous conifer *Parataxodium wigginsii*, which, because of the close association of the leafy shoots with branches and logs, we interpret to have reached small-tree stature. Structurally preserved (calcified and silicified to minimally altered) coniferous logs rarely exceed 20 cm in diameter, and the maximum diameter observed was 50 cm. No angiosperm wood has been identified, and it is likely that the angiosperms formed only a minor understory or lake-margin component. No angiosperms were recovered from channel-fill sediments, suggesting that the riparian, large-leaved angiosperm communities of the Cenomanian (Spicer and Parrish, 1986a) had ceased to exist. Angiosperm pollen diversity increased in latest Maestrichtian time (T.A. Ager, USGS, written commun., 1986), but the absence of complementary leaf fossils suggests to us that the increase may reflect diversification of herbaceous elements.

In 1985, we made a similar study of the mid-Cretaceous Niakogon Tongue of the Chandler Formation along the Colville River (Spicer and Parrish, 1986a), and recovered 80 to 90 plant megafossil taxa from those units. We estimated that the mean annual temperature at that time was 10 ± 3 °C, based on leaf-margin analysis of the angiosperms (67 forms; Wolfe, 1979). Although the Kogosukruk Tongue contains too few angiosperm leaf forms to permit similar quantitative estimates of mean annual temperature, the drop in diversity from the mid-Cretaceous strongly suggests a lower mean annual temperature in the Campanian and Maestrichtian than earlier. We estimate the mean annual temperature in the Campanian and Maestrichtian to have been at least 5 °C lower than in the mid-Cretaceous. The marked drop in diversity during the Late Cretaceous probably cannot be attributed to sampling bias because the same sedimentary and diagenetic facies occur throughout.

Analysis of growth-ring characteristics in fossil wood from the Niakogon Tongue (Spicer and Parrish, 1986b) led us to conclude that the Cretaceous light regime was similar to that at high latitudes today. At latitude 80° N., summer and winter consist of four months of continuous daylight and darkness, respectively, and the photoperiod during the short spring and autumn changes very rapidly. Field examination of the fossil wood from the Kogosukruk Tongue suggests a similar light regime for the Campanian and Maestrichtian interval. However, rings from wood of the Kogosukruk Tongue seem to be narrower overall and contain more late wood than those from the Niakogon Tongue. Thus, growing conditions apparently deteriorated during the Late Cretaceous.

The predominance of fluvial sediments and the existence of coal beds in the Kogosukruk Tongue are indicative of abundant supply of water to the regional environment. However, the angiosperm leaf is small compared to the leaves from the Chandler Formation, and fossil charcoal is much more abundant, whereas it is practically unknown in the Chandler Formation. These lines of evidence suggest drier conditions, under which wildfires became much more common.

In addition to the plant megafossils, we recovered remains of ceratopsian (horned) dinosaurs from the Kogosukruk Tongue. These were a horn core, an occipital condyle (the part of the skull that articulates with the spinal column), and the distal part of a femur (thigh bone); the horn core is from a group of ceratopsians that lived during middle Campanian to early Maestrichtian time (J.M. Parrish, Univ. of Colorado Museum, written commun., 1986). Skeletal remains of hadrosaurian (duck-billed) dinosaurs and teeth of carnivorous dinosaurs have been reported from near the top of the Kogosukruk Tongue near Ocean Point (W.A. Clemens, written commun., 1985) and, with the discovery of ceratopsians, it would appear that a moderately diverse dinosaurian fauna occupied the North Slope during the Campanian and Maestrichtian.

In conclusion, plant megafossil evidence from the Kogosukruk Tongue of the Prince Creek Formation, particularly in comparison with evidence from the Chandler Formation, indicates that the climate on the North Slope during deposition of the Kogosukruk Tongue was cold temperate and at least periodically dry. The presence of dinosaurs so close to the Cretaceous North Pole has important implications for dinosaurian ecology.

REFERENCES CITED

Brosgé, W.P., and Whittington, C.L., 1966, Geology of the Umiat-Maybe Creek region, Alaska: U.S. Geological Survey Professional Paper 303-H, p. 501-638.

Frederiksen, N.O., Ager, T.A., and Edwards, L., 1986, Comment and reply on "Early Tertiary marine fossils from northern Alaska: Implications for Arctic Ocean paleogeography and faunal evolution: Geology, v. 14, p. 802-803.

McDougall, Kristin, 1986, Maestrichtian benthic foraminifers from Ocean Point, Alaska (abs.): Geological Society of America Abstracts with Program, v. 18, p. 688.

Marincovich, Louis, Jr., Brouwers, E.M., and Carter, L.D., 1985, Early Tertiary marine fossils from northern Alaska: implications for Arctic Ocean paleogeography and faunal evolution: Geology, v. 13, p. 770-773.

Smith, A.G., Hurley, A.M., and Briden, J.C., 1981, Phanerozoic paleocontinental world maps. Cambridge, U.K., Cambridge University Press, 102 p.

Spicer, R.A., and Parrish, J.T., 1986a, Paleobotanical evidence for cool north polar climates in middle Cretaceous (Albian-Cenomanian) time: Geology, v. 14, p. 703-706.

____ 1986b, Fossil woods from northern Alaska and climate near the middle Cretaceous north pole (abs.): Geological Society of America 99th Annual Meeting and Exposition Abstracts with Programs, p. 759.

Wolfe, J.A., 1979, Temperature parameters of humid to mesic forests of eastern Asia and relation to forests of other regions of the northern hemisphere and Australasia: U.S. Geological Survey Professional Paper 1106, 37 p.

Ziegler, A.M., Scotese, C.R., and Barrett, S.F., 1983, Mesozoic and Cenozoic paleogeographic maps, in Brosche, P., and Sündermann, J., eds., Tidal friction and the earth's rotation II: Berlin, Springer-Verlag, p. 240-252.

Reviewers: J.P.Galloway and C.M. Molenaar

PETROGRAPHY OF THE BAIRD MOUNTAINS SCHISTOSE LITHOLOGIES, NORTHWESTERN ALASKA

Mark R. Zayatz

Metamorphic rocks from the southeast corner of the Baird Mountains 1:250,000 quadrangle consist of two distinct rock units: a homogeneous pelitic schist and a mixed schist (fig. 1). Petrographic criteria, from approximately 600 thin sections of metamorphic rocks, were used to determine 13 stable mineral assemblages indicating blueschist- and greenschist-facies conditions. K-Ar cooling ages of 90-110 m.y. from micas within the schistose lithologies indicate that regional metamorphism and deformation associated with the Brooks Range orogeny came to an end within the middle Cretaceous (Wilson and Turner, 1975).

The pelitic schist unit consists of dark-green to greenish-gray, well-foliated and lineated, fine- to medium-grained, polydeformed schist characterized by five stable mineral assemblages (listed in order of decreasing mineral abundance):

(1) quartz-albite-white mica-chlorite
(2) quartz-albite-white mica
(3) quartz-albite-chlorite
(4) quartz-albite-white mica-chlorite-chloritoid
(5) quartz-albite-white mica-chlorite-garnet

Rare quartz and albite porphyroblasts commonly preserve the S_1 foliation. Primary chlorite forms hypidioblastic to xenoblastic laths and aggregates which define primary (S_2) foliation. Secondary chlorite occurs as crystal clots that replace primary minerals along fractures. Chloritoid occurs as pleochroic slate-blue to green, idioblastic to hypidioblastic, elongate crystals which tend to be retrograded to white mica + chlorite (fig. 2A). Chloritoid is generally oriented subparallel to the pervasive (S_2) foliation direction. Garnets, which occur rarely and only in assemblage 5, are inclusion-free, unaltered, idioblastic to hypidioblastic grains partially enveloped by a sheath of primary chlorite parallel to S_2 foliation. Petrographic evidence of zoning within garnets was not noted.

The mixed schist unit consists of quartz-mica schist, black carbonaceous schist, marble, calcareous-mica schist, micaceous calc-schist, chlorite schist, metabasite, and two blue-amphibole-bearing lithologies. The micaceous and calcareous rocks are characterized by assemblages 1-5 and four additional assemblages:

(6) quartz-albite-graphite-white mica-chlorite
(7) quartz-albite-carbonate-white mica-chlorite
(8) quartz-feldspar-white mica-chlorite-stilpnomelane
(9) quartz-albite-white mica-chlorite-biotite

Prograde development of biotite from chlorite is common along grain boundaries (fig. 2B). Petrographic evidence of zoning within garnets is rarely noted. Shattered garnet grains are commonly altered to chlorite + quartz + magnetite or white mica + quartz + chlorite (fig. 2C).

Metabasite within the mixed schist unit is a very dark green, massive rock with variable grain size and an outcrop extent of less than 2 km. This lithology is characterized by two stable low-grade metamorphic mineral assemblages:

(10) albite-actinolite-chlorite-epidote
(11) albite-actinolite-epidote-stilpnomelane

Two distinct blue-amphibole-bearing lithologies, which also occur within the mixed schist unit, are a massive, glaucophane-bearing metabasite (assemblage 12) and a well-foliated and well-lineated glaucophane schist (assemblage 13) identical to assemblage 1 except for the occurrence of amphibole.

(12) albite-chlorite-epidote-actinolite-glaucophane-garnet
(13) quartz-albite-white mica-chlorite-actinolite-glaucophane

The occurrence of glaucophane-bearing metabasite and schist, observed locally in distinct layers throughout the mixed schist unit, is probably compositionally controlled. Partial to near-complete retrograde replacement of glaucophane by chlorite + albite (fig. 2D) and of garnet by chlorite is common along grain boundaries, fractures, and cleavage planes.

Microfabrics in the various lithologies of the pelitic schist and mixed schist units (with the exception of the metabasite, which has a "directionless fabric") suggest at least three pervasive, ductile deformation events. The earliest deformation recognized (F_1) is characterized by a poorly preserved schistosity

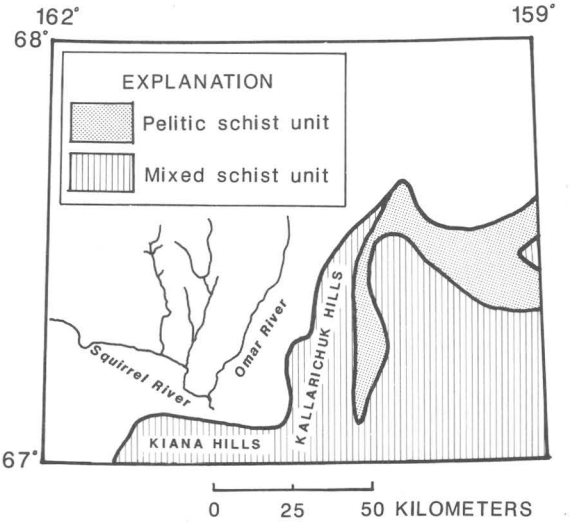

Figure 1.--Location of pelitic schist and mixed schist units within Baird Mountains 1:250,000 quadrangle.

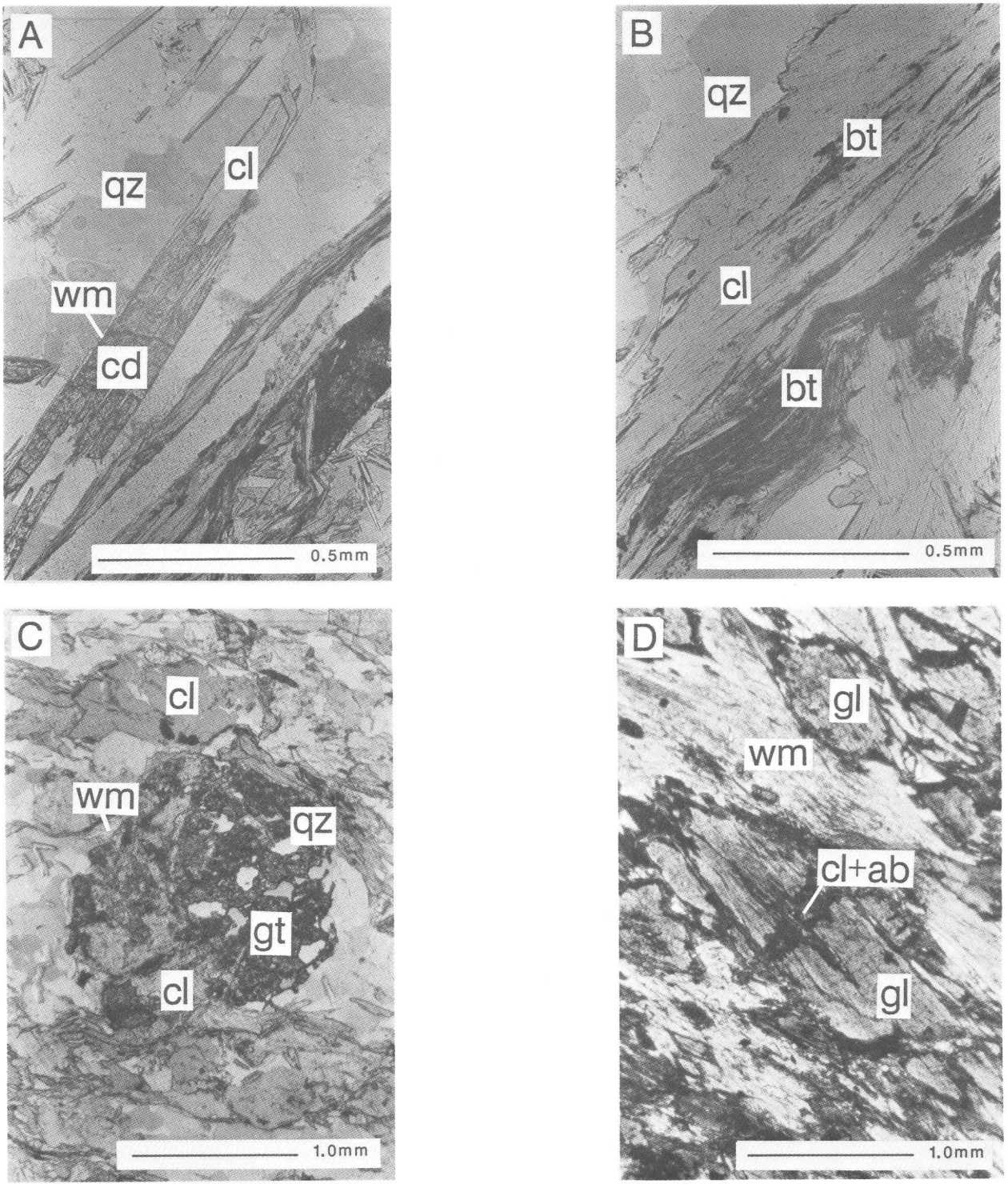

Figure 2.--Photomicrographs of selected samples from schistose lithologies of Baird Mountains quadrangle taken in plane-polarized light: ab, albite; bt, biotite; cd, chloritoid; cl, chlorite; gl, glaucophane; gt, garnet; qz, quartz; wm, white mica. A, Retrograde alteration of chloritoid to white mica and chlorite. B, Prograde development of biotite from chlorite. C, Retrograde alteration of garnet to chlorite and white mica. D, Retrograde alteration of glaucophane to chlorite and albite.

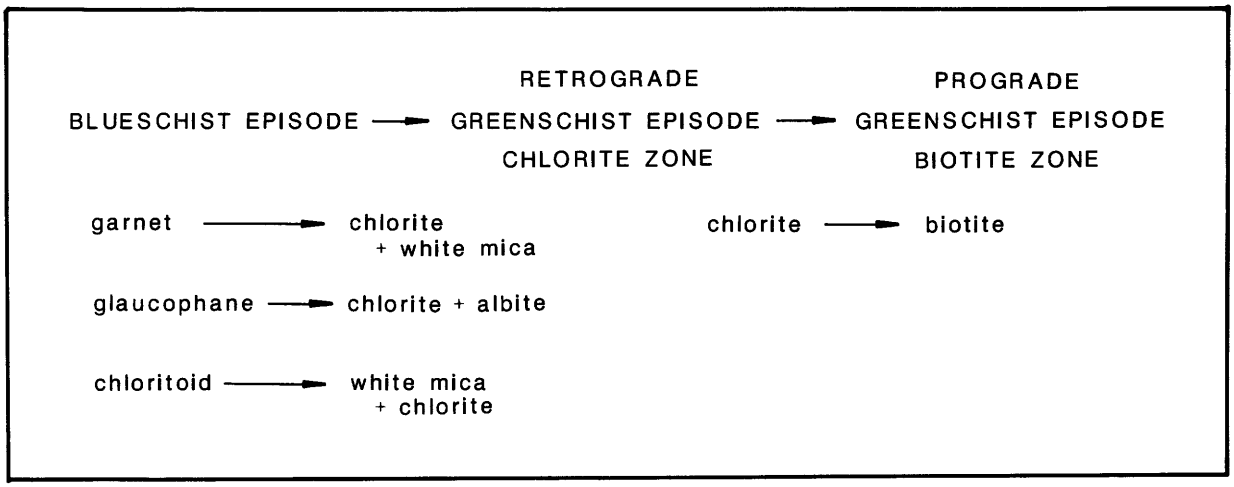

Figure 3.--Progression of metamorphic episodes and characteristic mineral reactions preserved within Baird Mountains schistose rock units.

(S_1) observed within some large helicitic quartz and albite porphyroblasts. F_1 folds appear to have been obliterated by the tightly crenulated, dominant folds of subsequent folding events.

The prominent folding event (F_2) is characterized by tight asymmetric crenulations and a dominant schistosity (S_2). F_2 folds are in turn refolded into gentler, broader folds (F_3) of variable style without significantly altering F_2 morphology. Petrofabric analyses of three measurements on each of 100 thin sections shows that S_2 is cut at an angle of 100° to 120° by the axial plane cleavage (S_3) created during the F_3 event. A fourth (F_4), more brittle deformation is developed locally along the western margin of the Kallarichuk Hills.

Both blueschist-facies and greenschist-facies metamorphic assemblages are preserved within the study area. Blueschist-facies assemblages are characterized by glaucophane-bearing metabasite (assemblage 12) and metapelite (assemblage 13). Petrographic evidence suggests that the blueschist-facies rocks may represent the oldest regional metamorphic episode preserved within the schistose lithologies studied in the southeast corner of the Baird Mountains quadrangle.

Following blueschist-facies metamorphism, these rocks were subjected to a retrogressive greenschist-facies metamorphism characterized by chlorite-zone mineral assemblages. Greenschist-facies chlorite-zone rocks contain retrograded glaucophane, garnet, and chloritoid (fig. 3), suggesting a lowering of pressure. The mineralogies of equilibrium assemblages (1-8, 10, 11) are representative of the chlorite zone of the greenschist facies. Stilpnomelane (assemblage 8) suggests that moderate pressures characterized the event (Miyashiro, 1973). Since many of the same minerals are stable within both the blueschist- and greenschist-facies assemblages, these minerals probably formed during the blueschist episode and remained stable throughout the greenschist episode.

Prograde development of biotite from chlorite, observed within the fabric of some metapelites of the mixed schist unit, suggests an increase in temperature at some time during the greenschist-facies episode. This reaction characterizes a change within the greenschist facies from the lower temperature chlorite zone to the higher temperature biotite zone (fig. 3). This reaction may not be found within the pelitic schist unit due to unfavorable whole-rock chemistry.

The pelitic schist and mixed schist units from the southeast corner of the Baird Mountains quadrangle are characterized by both blueschist-facies and greenschist-facies metamorphic assemblages. Microfabrics suggest that these rocks have been involved in at least three deformational events. These preliminary findings seem to agree with that observed for similar polymetamorphosed and polydeformed metasedimentary rocks that trend along strike of the south flank of the Brooks Range (Dillon and others, 1980; Hitzman, 1982).

REFERENCES CITED

Dillon, J.T., Pessel, G.H., Chen, J.H., and Veach, N.C., 1980, Middle Paleozoic magmatism and orogenesis in the Brooks Range, Alaska: Geology, v. 7, p. 338-343.

Hitzman, M.W., 1982, Metamorphic petrology of the Ambler district, southwestern Brooks Range, Alaska (abs.): Geological Society of America Abstracts with Programs, v. 14, p. 173.

Miyashiro, A., 1973, Metamorphism and metamorphic belts: London, George Allen and Unwin, 492 p.

Wilson, F.H., and Turner, D.L., 1975, Radiometric age map of Alaska--Northern Alaska: Alaska Division of Geological and Geophysical Surveys Open-File Report AOF-86, 11 p., 1 sheet, scale 1:1,000,000.

Reviewers: Cynthia Dusel-Bacon, S.W. Nelson, and J.M. Schmidt

EAST-CENTRAL ALASKA

Hydraulic mining for gold on the North Fork of Harrison Creek, Circle Mining Distict. Photo by Warren Yeend.

A LATE ORDOVICIAN AGE REAPPRAISAL FOR THE UPPER FOSSIL CREEK VOLCANICS, AND POSSIBLE SIGNIFICANCE FOR GLACIO-EUSTASY

Robert B. Blodgett, Karen L. Wheeler, David M. Rohr, Anita G. Harris, and Florence R. Weber

The Fossil Creek Volcanics of Ordovician age is exposed in the White Mountains of east-central Alaska. This rock unit, which is used here as defined by Mertie (1937), consists of more than 610 m of basalt, agglomerate, and intrusive and sedimentary rocks. The Fossil Creek Volcanics was divided into two components by Chapman and others (1971). The lower component is primarily sedimentary, consisting of slate, chert, limestone, and a minor amount of mafic intrusive rocks. This component grades laterally and vertically into an upper component of basalt, tuff, and agglomerate that is generally capped by a thin layer of volcanic-rich sediments. The Fossil Creek Volcanics unconformably overlies the Wickersham grit unit of Proterozoic and Cambrian age (Weber and others, 1985) and disconformably underlies the Tolovana Limestone, a peloid- and ooid-rich platform carbonate succession more than 1,200 m thick. The Tolovana is of Silurian age in the White Mountains proper, but elsewhere its age ranges from Silurian to Middle Devonian.

Fossil collections by R.W. Stone, L.M. Prindle, B.L. Johnson, and Eliot Blackwelder from the uppermost part of the Fossil Creek Volcanics were examined by Edwin Kirk and assigned a Middle Ordovician (Mohawkian) age (Mertie, 1937). Kirk originally favored a Late Ordovician (Richmondian) age, but changed his mind later. W.A. Oliver, Jr., U.S. National Museum (in Oliver and others, 1975, p. 24), considered several species of tabulate and rugose corals from the uppermost limestone of the formation to be of "undoubted Late Ordovician age." He, however, called this a tuffaceous limestone and excluded it from the Fossil Creek.

We have collected fossil assemblages from four localities (fig. 1) in the upper volcanic-rich sedimentary part of the Fossil Creek Volcanics and the overlying Tolovana Limestone. These faunas refine previous age determinations on the two rock units and allow us to document the magnitude of the unconformity that separates them.

Locality A (65°37'16" N., 147°21'11" W.) is situated in a saddle on a north-south-trending ridge spur 0.5 km east-southeast of VABM 4153 (fig. 1). The contact between the Fossil Creek Volcanics and Tolovana Limestone is well exposed at this locality, and lithostratigraphy of the uppermost Fossil Creek Volcanics was measured in detail (see Wheeler and others, this volume). Abundant megafossils occur in the uppermost beds of sandy clastic and carbonate rocks of the Fossil Creek. Fossils were recovered from three intervals (fig. 2). Sample "a" was taken from 4.3 m of green sandstone and minor pebble conglomerate containing an abundant and diverse fauna, sample "b" was from a 0.76-m-thick coral biostrome composed chiefly of the tabulate coral *Chaetetipora* that grades laterally into bioclastic limestone, and sample "c" was from 1.2 m of interbedded sandstone, limestone, and minor conglomerate. Finally, at the top of the Fossil Creek, above the latter unit, is 0.3 m of iron-stained calcareous sandstone, with minor limy lenses interpreted as having a paleokarst surface. Light-yellow, buff- or ochre-weathering argillaceous lime mudstone beds of the Tolovana Limestone disconformably overlie the Fossil Creek Volcanics in this section.

Brachiopods (determined by R.B. Blodgett) from the uppermost beds of the Fossil Creek Volcanics at locality A are represented by at least seven species that include both inarticulates (lingulids and trimerellids) and articulates (orthids, strophomenids, and pentamerids). Generic identification of most of the brachiopod fauna is precluded by the lack of well-preserved interiors.

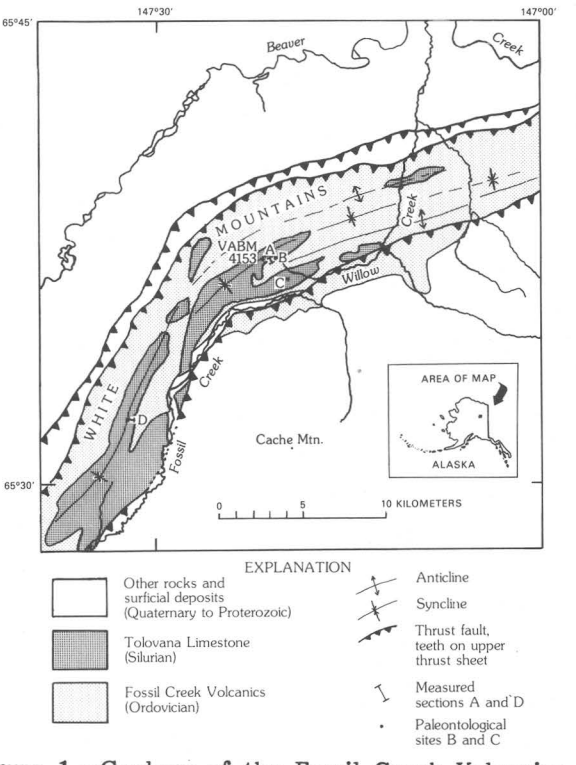

Figure 1.--Geology of the Fossil Creek Volcanics and Tolovana Limestone in White Mountains, Livengood C-1 and C-2 quadrangles generalized from Chapman and others (1971). Map shows localities A, B, C, and D.

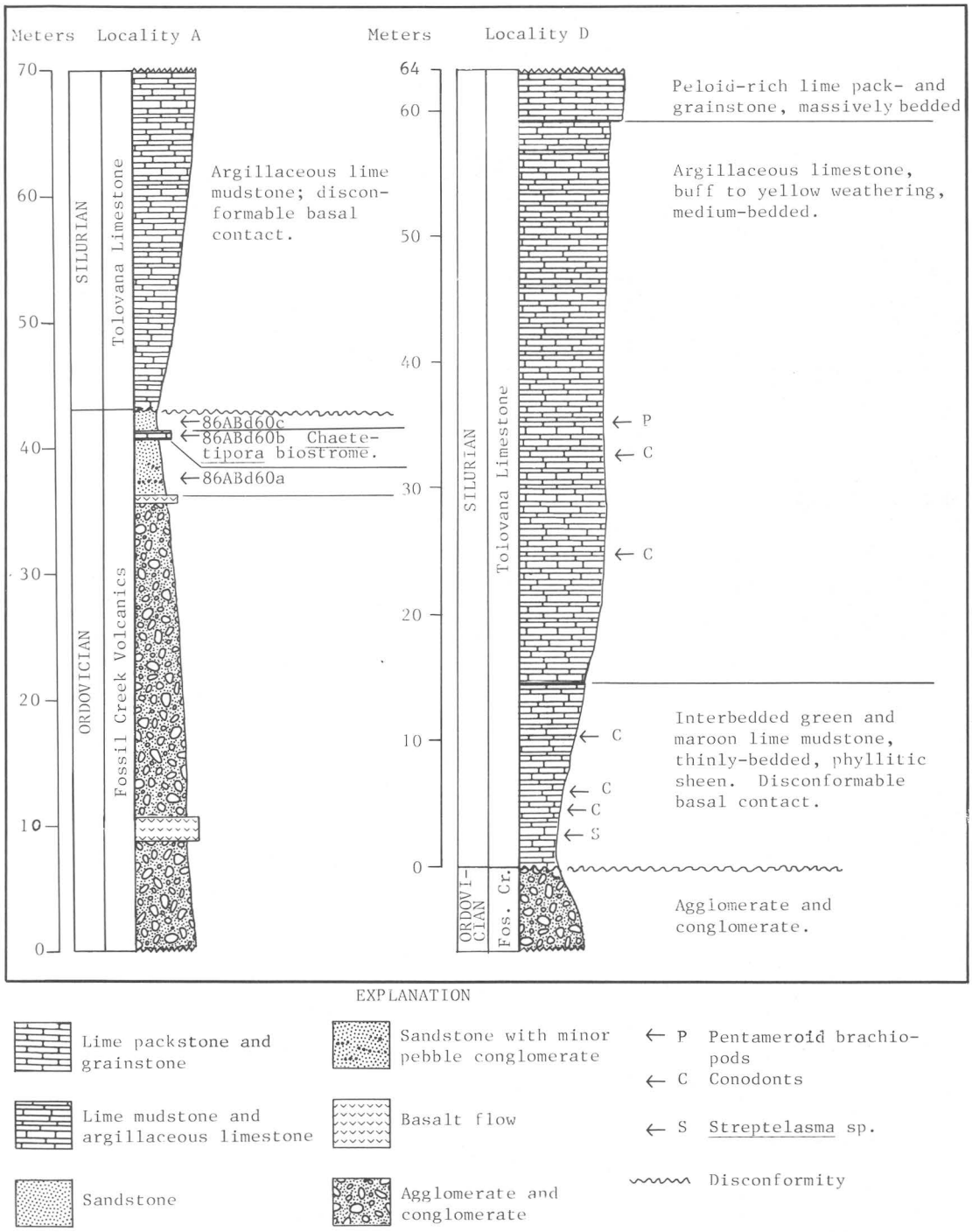

Figure 2.--Measured stratigraphic sections at localities A and D (fig. 1) of uppermost part of the Fossil Creek Volcanics and Tolovana Limestone in White Mountains of Livengood C-1 and C-2 quadrangles. See Wheeler and others, this volume for detailed lithostratigraphy of Fossil Creek Volcanics at locality A.

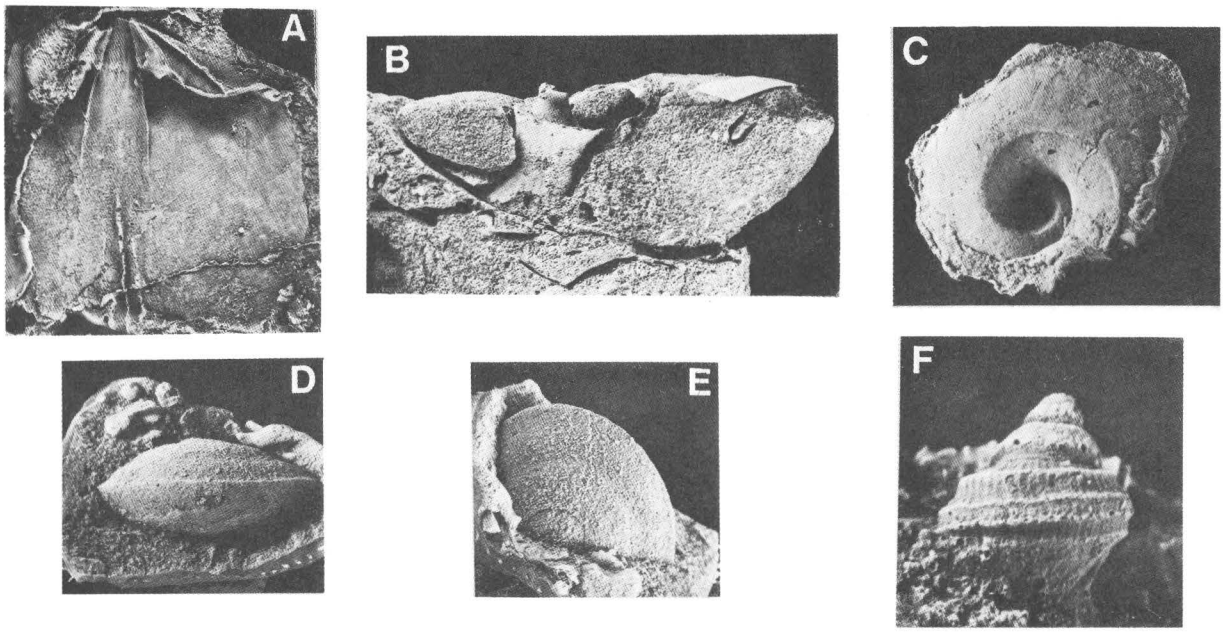

Figure 3.--Significant Ashgillian (Late Ordovician) age fossils from uppermost beds (all from interval 86ABd60a) of the Fossil Creek Volcanics. A, *Holorhynchus* n. sp., USNM 414983, latex replica of dorsal interior, x3.0. B, C, *Maclurites* sp., USNM 414984, B, side view of specimen before acid etching, x1.0, C, latex replica of upper surface of shell (made after acid etching) showing a distinct crestal angulation, x1.0. Whorl shape is similar to *M. manitobensis* but does not display spiral ornamentation of that species. D, E, *Liospira* sp., USNM 414985, latex replica of external mold, D, side view, x2.0. E, apical view x2.0. F, *Trochonemella* sp., USNM 414986, side view of latex replica of external mold, x10.0.

The pentamerids, however, are represented by *Holorhynchus* n. sp. (fig. 3A). This large, smooth pentamerid genus was previously known only from Ashgillian (Upper Ordovician) rocks of Eurasia (Sapelnikov, 1985). Its presence in the uppermost Fossil Creek Volcanics affirms the Late Ordovician age suggested by Oliver and others (1975), and also extends the geographical range of the genus to North America. Gastropods (identified by D.M. Rohr) from these beds include *Maclurites* sp. (fig. 3B and 3C), *Liospira* sp. (fig. 3D and 3E), and *Trochonemella* sp. (fig. 3F). *Maclurites* and *Liospira* are widespread genera in the Middle and Upper Ordovician. *Trochonemella* is known from the Middle and Upper Ordovician of eastern North America, California, west-central Alaska, and Seward Peninsula, Alaska. A bioclastic limestone laterally equivalent to the *Chaetetipora* interval (fig. 2) yielded one conodont element, *Belodina* sp. indet., indicating a Middle to Late Ordovician age.

Locality B (65°37'23" N., 147°20'40" W.) is a poorly exposed outcrop of the uppermost part of the Fossil Creek Volcanics 0.5 km east-northeast of locality A (fig. 1). No section was measured at this locality. The rocks at locality B consist of pebble to cobble conglomerate with clasts of rounded to subangular mafic volcanic rocks, green chert, and gritty quartzite (2.5-15.2 cm in diameter) in a matrix of maroon and green silty to limy mudstone. Abundant megafossils were recovered from the more lime-rich beds. Trilobites (determined by A.R. Ormiston, AMOCO Production Co.), the most common faunal element, include *Anataphrus*? sp. and a rare pteryogemetopid, *Denella* n. sp., both genera known only from Middle and Upper Ordovician rocks. Significantly, the genus *Denella* Ludvigsen

and Chatterton, is previously known only from western Canada, so our discovery significantly extends its known geographic range. The brachiopod *Holorhynchus* n. sp. also occurs here and indicates an Ashgillian age for this horizon. Conodonts from this locality (identified by A.G. Harris) include 34 small fragments of *Belodina* sp. indet. of Late Ordovician morphotype; their color alteration index (CAI) is 6 to 6½ , indicating that the host rock reached at least 400 °C. The contact with the overlying Tolovana Limestone is covered at this locality. However, above the uppermost exposure of the Fossil Creek Volcanics are rubbly yellow- to ochre-weathering argillaceous limestone beds about 30-60 m thick of the Tolovana Limestone. The basal beds are overlain by the more resistant, light-gray-weathering outcrops of the peloid- and ooid-rich lime packstone and grainstone beds, more typical of the upper part of the Tolovana Limestone.

Locality C (65°36'34" N., 147°19'57" W.), in a prominent saddle along a northwest-southeast-trending ridge spur near VABM 4153 (fig. 1), exhibits the contact between the Fossil Creek Volcanics and overlying Tolovana Limestone. The uppermost part of the Fossil Creek Volcanics at this locality consists mostly of basalt flows. A very thin, dark-gray limestone lens approximately 1-2 m below the top of the Fossil Creek Volcanics yielded conodonts of Middle or Late Ordovician age. Conodonts recovered from the basal beds of the Tolovana Limestone here indicate a Middle Ordovician to Middle Devonian, though probably Silurian, age. Their CAI is 5 to 5½, indicating that the host rock reached at least 300-350 °C. The Silurian age suggested by the conodonts is confirmed by the associated megafauna, which includes pentamerid brachiopods of Silurian aspect.

At locality D (65°32'06" N., 147°31'52" W.), the lower part of the Tolovana Limestone rests disconformably upon volcanic and agglomeratic rocks of the Fossil Creek Volcanics (fig. 2). The lowermost 14.6 m of the Tolovana Limestone is made up of thin- to medium-bedded, alternating green and maroon lime mudstone with a phyllitic sheen. The only megafossils were found 2.3-3.0 m above the base of this interval and are representatives of *Streptelasma* sp., a solitary rugose coral that indicates a Middle Ordovician to Early Silurian age (R.J. Elias, written commun., 1986). Poorly preserved conodonts from the lowermost beds are representatives of long-ranging genera (Middle Ordovician to Early Silurian); however, collections taken at 4.6 m, 6.1 m, and 10.7 m above the base were more age specific (early to middle Llandoverian). Because the Fossil Creek Volcanics disconformably underlie the Tolovana Limestone and because the lower part of the Tolovana is lithologically consistent, the lowermost Tolovana Limestone is considered early or middle Llandoverian (Early Silurian) in age.

The overlying beds (about 30-45 m thick) consist of yellowish-brown-weathering, silty, argillaceous lime mudstone and wackestone. Conodonts recovered at 25.0 m [(*Ozarkodina hassi* (Pollock, Rexroad, and Nicol)] and at 32.8 m [*Ozarkodina* cf. *O. oldhamensis* (Rexroad)] also indicate an early or middle Llandoverian age. Poorly preserved, partly silicified pentameroid brachiopods were recovered at 35.4 m above the base. The beds above the argillaceous limestone interval are peloid- and ooid-rich lime packstone and grainstone typical of the upper Tolovana Limestone.

The disconformity between the uppermost Fossil Creek Volcanics (Ashgillian) and the overlying basal beds of the Tolovana Limestone (early or middle Llandoverian) coincides with the widespread hiatus recognized at the Ordovician-Silurian boundary in shallow water settings of western and Arctic Canada (Lenz, 1976) and elsewhere in the world (Berry and Boucot, 1973; Sheehan, 1973). This widely recognized stratigraphic gap, usually represented by an unconformity separating Upper Ordovician and Lower Silurian strata, is thought to have been caused by a major sea-level drop accompanying the Late Ordovician glaciation in Gondwanaland (Beuf and others, 1966; Bennacef and others, 1971). The stratigraphic hiatus in the White Mountains fits this pattern, because the faunas and sedimentary features indicate extremely shallow water marine conditions on both sides of the contact. This is the first time that this globally widespread stratigraphic hiatus has been recognized in Alaska.

REFERENCES CITED

Bennacef, A., Beuf, S., Biju-Duval, B., Decharpal, O., Gariel, O., and Rognon, P., 1971, Examples of cratonic sedimentation: Lower Paleozoic of Algerian Sahara: American Association of Petroleum Geologists Bulletin, v. 55, p. 2225-2245.

Berry, W.B.N., and Boucot, A.J., 1973, Glacio-eustatic control of Late Ordovician-Early Silurian platform sedimentation and faunal changes: Geological Society of America Bulletin, v. 84, p. 275-284.

Beuf, S., Biju-Duval, B., Stevaux, J., and Kulbicki, G., 1966, Ampleur des glaciations "Siluriennes" au Sahara: Leurs influences et leurs consequences sur la sedimentation: Institut Francais du Petrole, Revue, v. 21, p. 363-381.

Chapman, R.M., Weber, F.R., and Taber, Bond, 1971, Preliminary geologic map of the

Livengood quadrangle, Alaska: U.S. Geological Survey Open-File Report 71-66, 2 pl.

Lenz, A.C., 1976, Late Ordovician-Early Silurian glaciation and the Ordovician-Silurian boundary in the northern Canadian Cordillera: Geology, v. 4, p. 313-317.

Mertie, J.B., Jr., 1937, The Yukon-Tanana region, Alaska: U.S. Geological Survey Bulletin 872, 276 p.

Oliver, W.A., Jr., Merriam, C.W., and Churkin, M.C., Jr., 1975, Ordovician, Silurian, and Devonian corals of Alaska: U.S. Geological Survey Professional Paper 823-B, p. 13-44.

Sapelnikov, V.P., 1985, Sistema i stratigraficheskoe znachenie brakhiopod podotryada pentameridin: Moscow, Nauka, 205 p.

Sheehan, P.M., 1973, The relation of Late Ordovician glaciation to the Ordovician-Silurian changeover in North American brachiopod faunas: Lethaia, v. 6, p. 147-154.

Weber, F.R., Smith, T.E., Hall, M.H., and Forbes, R.B., 1985, Geologic guide to the Fairbanks-Livengood area, east-central Alaska: Anchorage, Alaska Geological Society, 44 p.

Reviewers: R.M. Chapman and J.E. Repetski

PRELIMINARY GEOLOGY, INCLUDING THE TINTINA FAULT SYSTEM, OF PART OF THE SOUTHWESTERN CHARLEY RIVER QUADRANGLE, ALASKA

Helen L. Foster and Terry E.C. Keith

The geology of the southwestern part of the Charley River quadrangle is poorly known because of the remoteness and generally heavy vegetation cover of that area. However, this important area includes parts of both the Yukon-Tanana and Seventymile terranes (Jones and others, 1984) and is bounded by strands of the Tintina fault system. In addition, it is cut by a northeast-southwest-trending high-angle fault, and it also exhibits evidence for thrust faults. Knowledge of the geology of this area is critical for interpretation of the geologic structure and history of east-central Alaska.

Brabb and Churkin (1969) mapped the area included in this report in reconnaissance in 1962. Further reconnaissance work was done primarily in the Charley River A-5 and A-6 quadrangles by H.L. Foster, F.R. Weber, and others in 1982. Some additional geologic information was obtained in the summers of 1985 and 1986 by the present authors with personnel of the National Park Service from boat traverses of the northern part of the Charley River, and in 1985 from four days of helicopter-supported work. Although geologic work is far from complete, we are presenting here a preliminary map (fig. 1) to demonstrate the complexity and importance of the area as well as the need for further studies.

More than half of the area of this report is underlain by the northern Yukon-Tanana terrane, which is segmented and bounded on the north by strands of the Tintina fault system. A major strand of the Tintina fault system, the Seventymile fault (Foster, 1976), separates the metamorphic rocks of the Yukon-Tanana terrane from black argillite of uncertain age and affinities. The argillite resembles the Glenn Shale (Brabb and Churkin, 1969), but other similar black argillites are known in the southwestern part of the Charley River quadrangle north of the Tintina fault zone. Prior to their displacement along the Tintina fault system, the greenschist- to amphibolite-facies metamorphic rocks of the Yukon-Tanana terrane were overthrust by greenstone, gabbro, chert and other sedimentary rocks, altered hypabyssal intrusive and volcanic rocks, and ultramafic rocks of the Seventymile terrane (fig. 1; Foster and others, in press).

The Yukon-Tanana terrane within the map area consists primarily of three units: (1) amphibolite-facies gneiss, (2) amphibolite-facies schist, and (3) greenschist-facies schist. The gneiss unit borders the granitic pluton of Twin Mountain on the north and occurs as screens and roof pendants within the pluton. The gneiss is characteristically composed of quartz + biotite + feldspar + white mica + garnet ± sillimanite. Zircon and opaque minerals occur as accessory minerals, and locally biotite has altered to chlorite. In some places the crystals of the gneiss are shattered and crushed and some recrystallization has followed mylonitization.

The most extensive unit is a pelitic schist with interlayered amphibolite of epidote-amphibolite to amphibolite facies. A common mineralogy of the pelitic schist is quartz + biotite + white mica + garnet + staurolite ± feldspar. Locally, biotite has gone to chlorite and opaque minerals may be present. The contact between the pelitic schist unit and the gneiss unit north of the Twin Mountain pluton is generally sharp, suggesting a fault contact, possibly that of a thrust fault.

The greenschist-facies rocks are mostly quartz + chlorite + white mica schists which are commonly calcareous. The carbonate occurs as thin stringers and lenses or as layers up to a few centimeters thick. Large orange-brown crystals of biotite commonly lie across the foliation. The greenschist-facies rocks are in contact with the amphibolite-facies pelitic schist unit. This contact is also sharp and is probably a thrust fault.

The Seventymile terrane includes the Mount Sorenson ophiolite (Foster and Keith, 1974; Keith and others, 1981), composed largely of serpentinized peridotite cut by diabase dikes with cumulate gabbro, greenstone amphibolite, and plagiogranite. Chert, dolomite, limestone, argillite, and graywacke, recrystallized in varying degrees, are associated with the mafic rocks. These rocks are all believed to have been thrust over the Yukon-Tanana terrane prior to intrusion of the Early Cretaceous Twin Mountain pluton, in early Jurassic(?) time (Cushing and others, 1984; Foster and others, 1985).

Fieldwork and study of aerial photographs indicate that the Tintina fault system has many splays of several different ages, but none of the splays have been observed to cut the Twin Mountain pluton. The movement along the splays is probably right-lateral, as has been previously postulated (Roddick, 1967). Total displacement along the splays south of the Seventymile strand in the southwestern Charley River quadrangle appears to have been about 20 km. Cushing and others (1986) postulated that displacement along what they interpreted to be the most recently active main strand, which lies north of this area, was less than 100 km. Although more detailed study is needed, total displacement in the Tintina fault zone in this area does not appear to have been as great as that previously postulated for the Tintina fault system in Alaska and Canada. A highly altered felsic hypabyssal intrusion (map unit fph, fig. 1) has been displaced along several

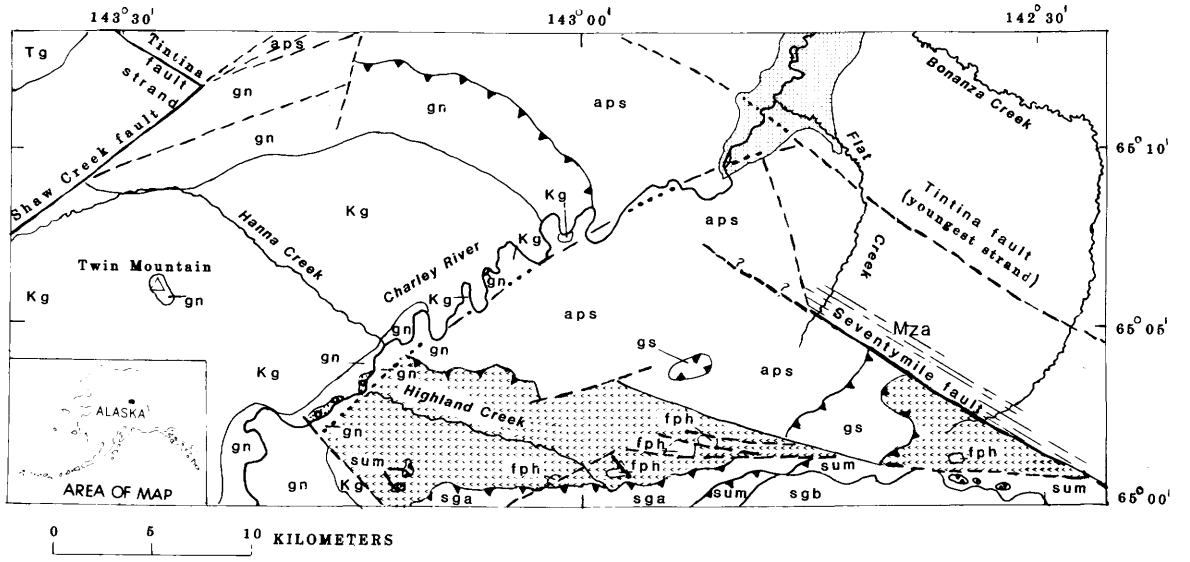

EXPLANATION

Qa — Alluvium (Holocene)

TKc — Conglomerate (Tertiary and (or) Cretaceous)

Mza — Argillite; may be equivalent to Glenn Shale (Mesozoic(?))

Yukon-Tanana terrane

Tg — Granite (Tertiary(?))

Kg — Granite of Twin Mountain (Early Cretaceous)

gn — Gneiss (age uncertain)

aps — Amphibolite-facies pelitic schist (age uncertain)

gs — Greenschist-facies schist (age uncertain)

Seventymile terrane

fph — Felsic porphyritic hypabyssal breccia (age uncertain)

gc — Greenstone, chert, argillite, dolomite, limestone, quartzite, and amphibolite (age uncertain)

Mount Sorenson ophiolite (age uncertain)

Consists of:

sgb — Gabbro

sga — Greenstone, argillite, and chert

sum — Ultramafic rocks

Geology north of the Tintina fault system

Contact or inferred contact

Fault, dotted where concealed

Probable fault

Thrust fault, sawteeth on upper plate

Figure 1.--Preliminary geologic map of part of southwestern Charley River quadrangle, east-central Alaska.

different strands of the Tintina, but its maximum single displacement appears to be about 13 km. This distinctive felsic rock is mostly coarsely porphyritic with phenocrysts of potassium feldspar and embayed quartz as long as 2 cm. It displays a complex history of brecciation followed by intense hydrothermal alteration. Fractures formed after hydrothermal alteration were filled by quartz. Its displacement along strike-slip faults was still later.

A northeast-southwest-trending high-angle fault is postulated to lie approximately along the course of the Charley River as the rocks there are much fractured, shattered, and locally brecciated. Rock units that intersect the inferred fault are abruptly terminated and apparently displaced. Such a fault (or possibly several en echelon faults) would approximately parallel the Shaw Creek fault to the west (fig. 1).

The rocks of the Yukon-Tanana terrane are generally considered to be of continental origin. Although most of the rocks are of unknown age, sparse fossils indicate that some protoliths were Paleozoic in age, but other protoliths may have been of Proterozoic age or included Proterozoic material (Aleinikoff and others, 1986).

The rocks of the Seventymile terrane are of oceanic and mantle origin and range in age from middle Paleozoic to Triassic. The Seventymile terrane is postulated to have been thrust upon the Yukon-Tanana terrane in early Jurassic time with the closing of the ocean in which its components accumulated (Foster and others, 1985). Some of the thrusting of the rocks of the Yukon-Tanana terrane in the southwestern Charley River quadrangle may have also taken place at this time. The Tintina fault system appears to have become active some time thereafter, but before

the intrusion in Early Cretaceous time of the granite of Twin Mountain, because early strands of the Tintina system that show minor strike-slip movement do not appear to cut the granite. In response to this tectonism, local conglomerates were deposited in several places in the area. After granitic intrusion, high-angle faulting along northeasterly trends followed. Additional faulting in the Tintina system also probably occurred after intrusion of the granite, and more conglomerates were then deposited.

REFERENCES CITED

Aleinikoff, J.N., Dusel-Bacon, Cynthia, and Foster, H.L., 1986, Geochronology of augen gneiss and related rocks, Yukon-Tanana terrane, east-central Alaska: Geological Society of America Bulletin, v. 97, p. 626-637.

Brabb, E.E., and Churkin, Michael, Jr., 1969, Geologic map of the Charley River quadrangle, east-central Alaska: U.S. Geological Survey Miscellaneous Geologic Investigations Map I-573, scale 1:250,000.

Cushing, G.W., Foster, H.L., Harrison, T.M., and Laird, Jo, 1984, Possible Mesozoic accretion in the eastern Yukon-Tanana Upland (abs.): Geological Society of America Abstracts with Programs, v. 16, no. 6, p. 481.

Cushing, G.W., Meisling, K.E., Christopher, R.H., and Carr, T.R., 1986, The Cretaceous to Tertiary evolution of the Tintina fault zone, east-central Alaska: Geological Society of America Abstracts with Programs, v. 18, no. 2, p. 98.

Foster, H.L., 1976, Geologic map of the Eagle quadrangle, Alaska: U.S. Geological Survey Miscellaneous Geologic Investigations Series Map I-922, scale 1:250,000.

Foster, H.L, Cushing, G.W., Keith, T.E.C., and Laird, Jo, 1985, Early Mesozoic tectonic history of the Boundary area, east-central Alaska: Geophysical Research Letters, v. 12, no. 9, p. 553-556.

Foster, H.L., and Keith, T.E.C., 1974, Ultramafic rocks of the Eagle quadrangle, east-central Alaska: U.S. Geological Survey Journal of Research, v. 2, no. 6, p. 657-669.

Foster, H.L., Keith, T.E.C., and Menzie, W.D., in press, Geology of east-central Alaska, in Plafker, George, and Jones, D.L., eds., The Cordilleran Orogen: Alaska: Geological Society of America Decade of North American Geology v. G-1.

Jones, D.L., Silberling, N.J., Coney, P.J., and Plafker, George, 1984, Lithotectonic terrane map of Alaska (west of the 141st meridian), Part A, in Silberling, N.J., and Jones, D.L., eds., Lithotectonic terrane maps of the North American Cordillera: U.S. Geological Survey Open-File Report 84-523, p. A1-A12.

Keith, T.E.C., Foster, H.L., Foster, R.L., Post, E.V., and Lehmbeck, W.L., 1981, Geology of an alpine-type peridotite in the Mount Sorenson area, east-central Alaska, in Shorter contributions to general geology: U.S. Geological Survey Professional Paper 1170-A, p. A1-A9.

Roddick, J.A., 1967, Tintina Trench: Journal of Geology, v. 75, no. 1, p. 23-33.

Reviewers: Béla Csejtey and W.D. Menzie

PLATINUM-GROUP ELEMENT CONCENTRATIONS IN A BIOTITE-RICH CLINOPYROXENITE SUITE, EAGLE C-3 QUADRANGLE, ALASKA

Terry E. C. Keith, Norman J Page, Robert L. Oscarson, and Helen L. Foster

Platinum-group elements (PGE) are not common in east-central Alaska (Cobb, 1975). Occurrences of PGE consisting of alloyed Pt in placer gold nuggets were reported by Mertie (1942) from three widely separated localities approximately 40 to 100 km north of the Eagle C-3 quadrangle. Anomalous PGE concentrations later were reported by Keith and Foster (1973) and Foster (1975) in biotite clinopyroxenite of the Eagle C-3 quadrangle (fig. 1). Additional samples of the ultramafic and associated rocks were collected in the summer of 1975 to study the mineralogy of the rocks and the possible origin of the PGE concentrations.

The regional geologic framework of the area that includes the PGE anomalies consists of a complex metamorphic terrane that was extensively intruded by granitic rocks of Mesozoic age and is part of the Yukon-Tanana terrane (Foster, 1976; Foster and others, in press). The major portion of an overthrust sheet of dismembered ophiolite, known as the Seventymile terrane (Foster and others, in press), is exposed approximately 45 km to the northwest of the study area along the north-central edge of the Eagle quadrangle, and small remnants irregularly crop out as klippen throughout the area included in this report (Foster and Keith, 1974).

The anomalous PGE values occur in two lenses of coarse-grained biotite clinopyroxenite and minor biotitite which appear to be pendants, along with biotite schist country rock, on a small hornblende granodiorite pluton of probable Mesozoic age (Foster, 1976). Both ultramafic lenses cover an area of approximately 0.5 km^2 and are of unknown thickness. A third lens of similar size crops out 2 km to the west, but rocks from it have not been analyzed. Coarse-grained felsic dikes of irregular size and shape cut the biotite clinopyroxenites, parts of which are brecciated and included in the dike rock. Hydrothermal alteration accompanied intrusion of felsic dikes into fractured parts of the ultramafic rocks. Although the ultramafic rocks have some outcrop characteristics which are similar to concentric zoned intrusions, the outcrops here are too discontinuous and the vegetative cover too heavy to determine a pattern in the course of reconnaissance mapping.

The biotite clinopyroxenite consists of anhedral grains of clinopyroxene ranging in grain size from approximately 0.25 to 2 cm in diameter, and biotite of the same size range which usually appears to be codepositional. Locally biotite composes as much as 90 percent of the rock and poikilitically includes small clinopyroxene grains. The ratio of biotite to clinopyroxene throughout the outcrops varies irregularly from 10 to 90. Large grains of primary green amphibole locally make up less than 5 percent of the rock; orthopyroxene, olivine, and plagioclase were not found. Anhedral magnetite occurs as small inclusions in clinopyroxene; chromite does not appear to be present.

Felsic dikes intruded the biotite clinopyroxenites and formed actinolite, chlorite, scarce muscovite, and scarce pyrite locally by reaction. The felsic rock textures show evidence of extensive hydrothermal alteration in the form of exsolution in the plagioclase and alkali feldspars and recrystallization along grain boundaries. The felsic dikes may be specifically associated with the ultramafic rocks and thus unrelated to the underlying pluton; they may be a differentiate at the top of the hornblende granodiorite pluton, or they may be later felsic dikes which cut the entire sequence (field relations were not conclusive).

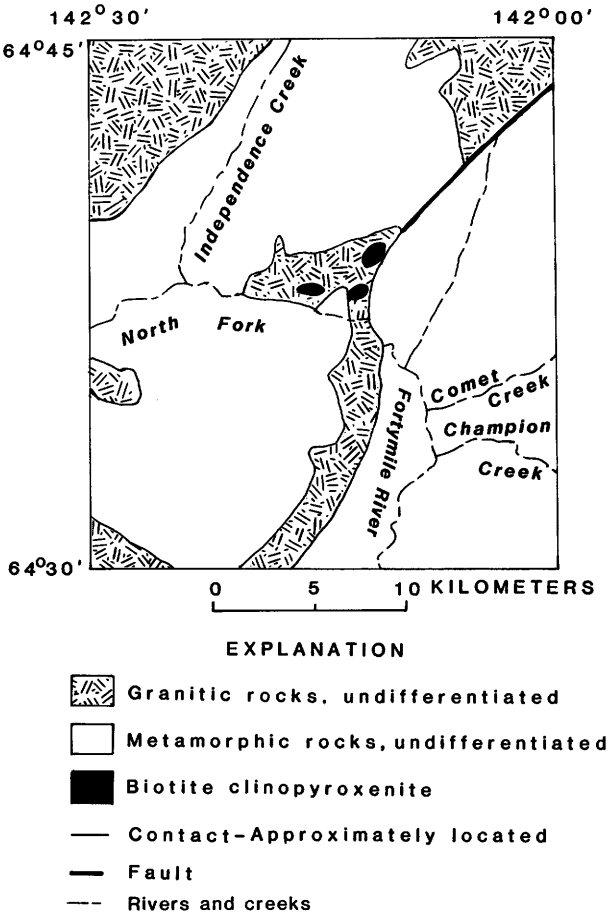

Figure 1.--Generalized geology of Eagle C-3 quadrangle (after Foster, 1976) showing location of biotite clinopyroxenite and associated rocks.

Random sampling of rocks for background geochemical data was done during the course of reconnaissance geologic mapping of the Eagle quadrangle, and anomalous PGE were discovered in samples of the biotite clinopyroxenite and in felsic rocks with biotite clinopyroxenite inclusions or contact zones (table 1, samples prefixed 1969 and 1974). For the present study, 20 samples (table 1, prefixed 1975) were collected in sequence across the northeastern-most of the 3 ultramafic rock lenses for the purpose of determining, if possible, where in the rocks the PGE were concentrated. The 1969 and 1974 samples were analyzed for PGE by the fire-assay emission-spectrographic method of Haffty and Riley (1968); the 1975 samples were analyzed using fire-assay-atomic absorption (AAS) methods (Simon and others, 1978). Associated Au (table 1) was determined by AAS fire-assay method.

Table 1.--Platinum group element and gold analyses (in parts per million) of rock samples from the Eagle C-3 quadrangle

[Analysts for 1969 and 1974 samples: R.R. Carlson and E.F. Cooley; analysts for 1975 samples: A. Love, C. Gent, S.G. Crock. N, not detected; na, not analyzed; *, average of 4 runs]

Sample No.	Rock description (BC = biotite clinopyroxenite)	Pt	Pd	Rh	Au	Pt/Pt+Pd
1969-748B	BC	0.3*	0.2*	0.002*	na	0.6
1974-8A	BC	N	.005	N	N	
8A1	BC	.007	.003	N	N	.7
8B1	Actinolite with felsic dike	N	N	N	N	
8B2	Actinolite with felsic dike	.007	.005	N	N	.6
8C1	BC	.015	.015	N	.001	.5
8C3	BC	.100	.150	.020	.005	.7
8C4	BC with felsic dike	.070	.030	.007	.001	.7
8D1	BC with felsic dike	.030	.030	N	.003	.5
8D2	BC with felsic dike	3.0	1.5	.030	.020	.7
8D3	BC with felsic dike	.003	.005	.002	.003	.4
8D4	BC with felsic dike	.100	.050	.030	N	.7
8D5	BC with felsic dike	.200	.050	.005	.002	.8
Detection limits		<.002	<.001	<.002	<.001	
1975-95-1	BC	.048	.014	N	N	.8
95-3	Clinopyroxenite	.021	.012	N	.08	.6
95-6A	Felsic dike	N	N	N	N	
95-7	BC	.036	.009	N	N	.8
95-7A	Felsic dike	N	.002	N	N	
95-8	Pyroxene biotitite	N	.004	N	N	
95-10	BC	.032	.017	N	N	.7
95-11	BC	.027	.012	N	N	.7
95-12	BC with felsic dike[a]	.850	.210	.036	N	.8
95-12A	Felsic dike with clinopyroxenite inclusions	1.9	.330	N	N	.9
95-13	Biotite gneiss with clinopyroxenite	.160	.065	N	N	.7
95-14	BC	.037	.012	N	N	.8
95-15	BC with felsic dike	.017	.008	N	N	.7
95-16	BC with felsic dike, sulfide	.038	.013	N	N	.8
95-18	Biotite gneiss	N	.002	N	N	
95-18A	Felsic dike	N	.007	N	N	
95-19	BC with felsic dike	.036	.013	N	N	.7
95-19A	Felsic dike	N	N	N	N	
95-6	Biotite gneiss	N	N	N	N	
Detection limits		<.010	<.001	<.001	<.05	

[a] Ru = .036 ppm; Ir = 0.038 ppm.

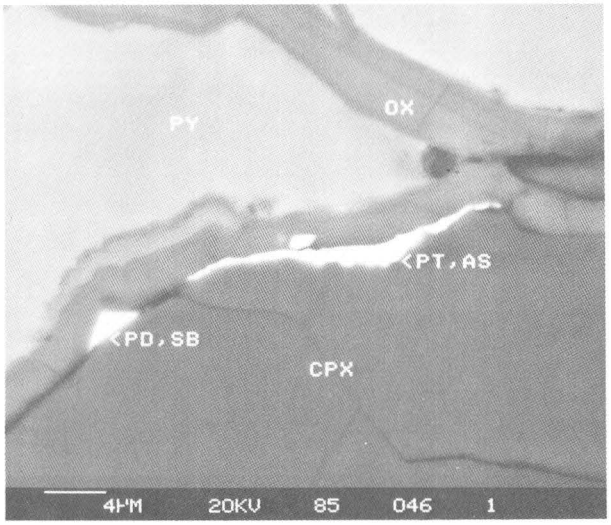

Figure 2.--Scanning electron micrograph of backscattered electrons showing a Pt, As mineral (sperrylite?) and a Pd, Sb mineral (stibiopalladinite?) at contact between a clinopyroxene (cpx) grain and oxidized edge (ox) of pyrite (py) grain.

PGE enrichment was determined to be associated with the rocks of the contact reaction zone which included fragments of biotite clinopyroxenite within felsic dike rock. Biotite clinopyroxenite away from the intrusive rocks contains lower, but still anomalous, concentrations of PGE; the felsic dikes are essentially barren. Ru is as high as 0.036 ppm in the few rocks in which it was detected (table 1). The Pt/Pt+Pd average is 0.7 and 0.8 for the 1969-1974 and 1975 groups of samples, respectively (table 1).

Splits of selected samples with anomalous PGE content and with pyrite were analyzed for 44 minor elements by R. Lerner, U.S. Geological Survey, using semiquantitative emission spectrographic methods. No anomalous trace-element values were found; Cu varied from 9.4 to 16 ppm, Ni from 9.5 to 83 ppm, Cr from 70 to 700 ppm, Co from 9.6 to 54 ppm, and V from 65 to 280 ppm. The low Cu and Ni contents reflect the scarcity of Cu and Ni sulfide minerals, suggesting that at least some of the PGE are present as alloys.

PGE-bearing minerals typically are extremely small and difficult to find under the best of conditions (Page and others, 1972; Gray and others, 1986). However, polished sections of selected rocks for this study were examined under the scanning electron microscope (SEM). Scans at high magnification using backscattered electrons provided extreme visual contrast of PGE minerals, because of their high atomic number, with other minerals in the rock (fig. 2). This technique resulted in locating scarce tiny (usually less than 4 µm diameter, but as large as 25 µm x 1 µm) grains of PGE-bearing minerals along cracks in clinopyroxene and associated magnetite grains, and at grain contacts of clinopyroxene with magnetite or pyrite. The energy dispersive X-ray spectrographic capability for chemical analysis with the SEM permitted chemical verification of the PGE-bearing minerals. Several grains, including the largest ones, are composed of Pt and As and likely are sperrylite. Several grains of less than 3 µm diameter are composed of Pd and Sb (stibiopalladinite?). One grain less than 1 µm across consists of Fe, Pt, As, Rh, Ir, Cu, and S indicating a complex PGE-bearing sulfide. In addition, scarce 5-20 µm-diameter grains of pyrite, galena, and sphalerite were found in biotite clinopyroxenite, and similar-sized grains of barite were found in the felsic rock.

Several interpretations for the origin of the biotite clinopyroxenite and concentration of associated PGE anomalies must be considered:

1. The biotite clinopyroxenite may be part of a dismembered ophiolite sequence that was thrust over metamorphic rocks of the Yukon-Tanana terrane (Foster and others, in press), and therefore it constitutes a thrust remnant of the ophiolite of the Seventymile terrane. Because the Pt and especially the Pd contents appear to be too high for normal ultramafic rocks from ophiolites as compared to other types of occurrences (Page and others, 1979, 1984, 1985; Oshin and Crocket, 1982; Carlson and others, 1986), we do not consider this explanation likely.
2. Pt, Pd, and Au may have been concentrated by hydrothermal reactions associated with the hornblende granodiorite pluton or by hydrothermal reactions generated by the felsic dikes. However, chemical characteristics of the rocks of this study are different from those of hydrothermal Pt-rich deposits, such as the New Rambler mine, Wyoming, where Pd is much higher than Pt, and other metals, Au, Ag, and Cu, make up ore-grade deposits (McCallum and others, 1976).
3. The biotite clinopyroxenite may be a portion of a concentrically zoned intrusion of the Alaska type. The Pt/Pt+Pd ratios of 0.7 and 0.8 are acceptable for this type of complex, as indicated by examples from southwestern Oregon (Gray and others, 1986), the Tulameen Complex of British Columbia (St. Louis and others, 1986), and numerous localities in southeastern Alaska (Clark and Greenwood, 1972; Page and others, 1977). Associated low Au values are also characteristic of this type (St. Louis and others, 1986).

The PGE contents and Pt/Pt+Pd of the Eagle C-3 quadrangle biotite clinopyroxenite and the PGE minerals found best fit the Alaska-type zoned ultramafic deposits. However, the major biotite and trace amphibole mineral composition of these clinopyroxenites, as well as the lack of major magnetite and chromite, are significant differences from other reported PGE-bearing ultramafic rocks. Except for biotite-bearing clinopyroxenites at the Pd-bearing ultramafic body near Salt Chuck in southeastern Alaska (see Loney and others, this volume), biotite is accessory or not present in other reported Alaska-type ultramafic rocks.

Other coarse-grained clinopyroxenites and associated rocks of the Yukon-Tanana terrane, and especially known outcrops in the Eagle quadrangle (Foster and Keith, 1974), should be explored for the occurrence of anomalous PGE concentrations.

REFERENCES CITED

Carlson, C.A., Page, N.J, and Carlson, R.R., 1986, The distribution of the platinum-group elements and gold in rocks from the western half of the Medford 1 x 2 degree quadrangle and adjacent areas, Oregon: U.S. Geological Survey Miscellaneous Investigations Map MF-1832, scale 1:250,000.

Clark, A.L., and Greenwood, W.R., 1972, Geochemistry and distribution of platinum-group metals in mafic to ultramafic complexes of southern and southeastern Alaska: U.S. Geological Survey Professional Paper 800-C, p. C157-C160.

Cobb, E.H., 1975, Occurrences of platinum-group metals in Alaska: U.S. Geological Survey Mineral Investigations Resources Map MR-64, scale 1:2,500,000.

Foster, H.L., 1975, Significant platinum values confirmed in ultramafic rock of the Eagle C-3 quadrangle, in Yount, M.E., ed., U.S. Geological Survey Alaska Program, 1975: U.S. Geological Survey Circular 722, p. 42-43.

____ 1976, Geologic map of the Eagle quadrangle, Alaska: U.S. Geological Survey Miscellaneous Investigations Map I-922, Scale 1:250,000.

Foster, H.L., and Keith, T.E.C., 1974, Ultramafic rocks of the Eagle quadrangle, east-central Alaska: U.S. Geological Survey Journal of Research, v. 2, p. 657-669.

Foster, H.L., Keith, T.E.C., and Menzie, W.D., in press, Geology of east-central Alaska, in Plafker, George, and Jones, D. L., eds., The Cordilleran Orogen: Alaska: Geological Society of America Decade of North American Geology, v. G-1.

Gray, Floyd, Page, N.J, Carlson, C.A., Wilson, S.A., and Carlson, R.R., 1986, Platinum-group element geochemistry of zoned ultramafic intrusive suites, Klamath Mountains, California and Oregon: Economic Geology, v. 81, p. 1252-1260.

Haffty, Joseph, and Riley, L.B., 1968, Determination of palladium, platinum, and rhodium in geologic materials by fire-assay and emission spectrography: Talanta, v. 15, p. 111-117.

Keith, T.E.C., and Foster, H.L., 1973, Basic data on the ultramafic rocks of the Eagle quadrangle, east-central Alaska: U.S. Geological Survey Open-file Report 73-140, 4 sheets.

McCallum, M.E., Loucks, R.R., Carlson, R.R., Cooley, E.F., and Doerge, T.A., 1976, Platinum metals associated with hydrothermal copper ores of the New Rambler mine, Medicine Bow Mountains, Wyoming: Economic Geology, v. 71, p. 1429-1450.

Mertie, J.B., 1942, Tertiary deposits of the Eagle-Circle district, Alaska: U.S. Geological Survey Bulletin 917-D, p. 213-264.

Oshin, I.O., and Crocket, J.H., 1982, Noble metals in Thetford Mines ophiolites, Quebec, Canada. Part I. Distribution of gold, iridium, platinum and palladium in the ultramafic and gabbroic rocks: Economic Geology, v. 77, p. 1556-1570.

Page, N.J, Berg, H.C., and Haffty, Joseph, 1977, Platinum, palladium, and rhodium in volcanic and plutonic rocks from the Gravina-Nutzotin belt, Alaska: U. S. Geological Survey Journal of Research, v. 5, p. 629-636.

Page, N.J, Carlson, C.A., Gray, Floyd, Carlson, R.R., Briggs, P.H., Haffty, Joseph, and Cooley, E.F., 1985, Map showing geochemical characteristics of the North Fork Smith Roadless Areas, Del Norte County, California, Curry and Josephine Counties, Oregon: U.S. Geological Survey Miscellaneous Field Studies Map MF-1423-C, scale 1:62,500.

Page, N.J, Carlson, R.R., Miller, M.S., Gray, Floyd, and Carlson, C.A., 1984, Map showing geochemical characteristics of platinum group elements and gold in rock samples from the Kalmiopsis Wilderness, southwestern Oregon: U.S. Geological Survey Miscellaneous Field Studies Map MF-1240-F, scale 1:62,000.

Page, N.J, Haffty, Joseph, and Ahmad, Zaki, 1979, Palladium, platinum, and rhodium concentrations in mafic and ultramafic rocks from the Zhob Valley and Dargai complexes, Pakistan: U.S. Geological Survey Professional Paper 1124-F, 6 p.

Page, N.J, Riley, L.B., and Haffty, Joseph, 1972, Vertical and lateral variation of platinum, palladium, and rhodium in the Stillwater Complex, Montana: Economic Geology, v. 67, p. 915-924.

St. Louis, R.M., Nesbitt, B.E., and Morton, R.D., 1986, Geochemistry of platinum-group elements in the Tulameen ultramafic

complex, southern British Columbia: Economic Geology, v. 81, p. 961-973.

Simon, R.O., Aruscavage, P.J., and Moore, R., 1978, Determination of platinum, palladium, and rhodium in geologic material by fire-assay and atomic absorption spectroscopy using electrothermal atomization (abs.): American Chemical Society National Meeting, 176th, Paper 19.

Reviewers: Floyd Gray, R.A. Loney, and W.D. Menzie

SOURCES OF PLACER GOLD IN THE SOUTHERN PART OF THE WHITE MOUNTAINS RECREATION AREA, EAST-CENTRAL ALASKA

Thomas D. Light, John W. Cady, Florence R. Weber, Richard B. McCammon, and C. Dean Rinehart

The White Mountains National Recreation Area (NRA), in the northwestern part of the Yukon-Tanana Upland, comprises an area of about 3,100 km^2 in the eastern Livengood and western Circle quadrangles. The area is underlain by a northeasterly trending sequence of Precambrian, Paleozoic, and Mesozoic metasedimentary and sedimentary rocks, locally intruded by Cretaceous and (or) Tertiary granitic rocks that presently form topographic highs. Placer gold has been recovered from creeks draining the metamorphic rocks in the southern part of the White Mountains NRA for many years, and we have observed flakes of gold in 34 heavy-mineral-concentrate samples from Nome, Trail, Ophir, O'Brien, and Bear Creeks (fig. 1) during the U.S. Geological Survey's investigations of the resource potential of the NRA.

The metamorphic rocks of the southern part of the White Mountains NRA consist of the Precambrian Fairbanks schist unit of Robinson and others (1982), which grades up into the Precambrian and Cambrian Wickersham unit of Weber and others (1985). The Fairbanks schist unit consists chiefly of quartzite and quartz-mica schist, whereas the Wickersham unit consists of bimodal quartzite (commonly called "grit"), quartzite, phyllite, limestone, and a distinctive maroon and green slate or argillite (Chapman and others, 1971). Although both units are metamorphosed to greenschist facies, the Wickersham unit is slightly lower grade than the Fairbanks schist unit. Quaternary loess, probably a by-product of glaciation in the local mountains, buries much of the terrain in the southern third of the area, and perennially frozen organic-rich silt fills the valleys, so that there are very few bedrock exposures south of Nome and Beaver Creeks. Two periods of tectonism and associated metamorphism produced sub-isoclinal, northeast-vergent, northwest-trending folds and a later generation of northeast-trending folds and northwest-vergent thrust faults that control the distribution of rock types that are presently exposed. The rocks generally strike northeast-southwest and dip northwest (Weber and others, 1985).

Placer gold was reported in the upper tributaries of Beaver Creek (fig. 1) prior to the turn of the century; the first substantial gold discovery in the area was in 1910 when mineable deposits were found on Ophir Creek (Ellsworth and Parker, 1911). Subsequently, gold was discovered on Nome Creek and Trail Creek. The deposits along both Ophir and Trail Creeks proved to be limited in extent, and although it is not known how much gold was produced, the amount probably was small. Dredges were operated on Nome Creek for many years, beginning in 1926 (Cobb, 1973), and gold was recovered from an 11-km stretch upstream from the confluence with Moose Creek. The upstream extent of placer mining coincides with the maximum extent of Pleistocene glacial ice from Mount Prindle (Weber and Hamilton, 1984) that scoured the creek bed and served to concentrate gold below the terminus of the glacier. A nominal figure for the cumulative production from Nome Creek has been estimated at between 10,000 and 20,000 oz (300 and 600 kg) of gold (W.D. Menzie, written commun., 1986). Dragline operations have continued along Nome Creek intermittently to the present time.

We believe that the source of the gold in Nome Creek may be the Cleary sequence, a distinctive 120-m-thick section of probable volcanogenic beds that occurs in the Fairbanks schist unit and consists of "interlensing felsic schist, laminated white micaceous quartzite, actinolitic greenschist, graphitic schist, metabasite, metarhyolite, and calcsilicate beds" (Robinson and others, 1982, p. 228). This sequence is believed to be the source for most of the gold in placer deposits in the Fairbanks Mining District (Smith and others, 1981). Similar and possibly correlative rocks were recognized near Mount Prindle (T.E. Smith, oral commun., 1986). Based on the regional northeast-southwest strike, these rocks project southwestward roughly parallel to Nome Creek. Remobilization of the gold in the inferred Cleary sequence at the head of Nome Creek as a result of the intrusion of the Mount Prindle pluton, followed by fluvial concentration, provides a reasonable hypothesis for the origin of the Nome Creek placers. The gold in Bear Creek (fig. 1), which also heads near Mount Prindle, is probably of the same origin.

Trail Creek, Ophir Creek, and an unnamed creek east of Ophir Creek (fig. 1) do not originate in the Mount Prindle area, therefore the gold in these drainages must be derived from some other source. Southeast of the Chatanika River in the Circle quadrangle, Cady and Weber (1983) determined that linear magnetic highs reflected magnetic chloritic schists within the Fairbanks schist unit (probably in the Cleary sequence itself). These highs were inferred to overlie the crests of antiforms that bring magnetic schist close to the surface. Such linear magnetic highs, labeled H1 and H2 on figure 1, extend southwestward from Mount Prindle toward the heads of Trail and Ophir Creeks and are coincident with a known antiform. It is very likely that the Cleary sequence is present in this structure, but is not recognized in the meager outcrops.

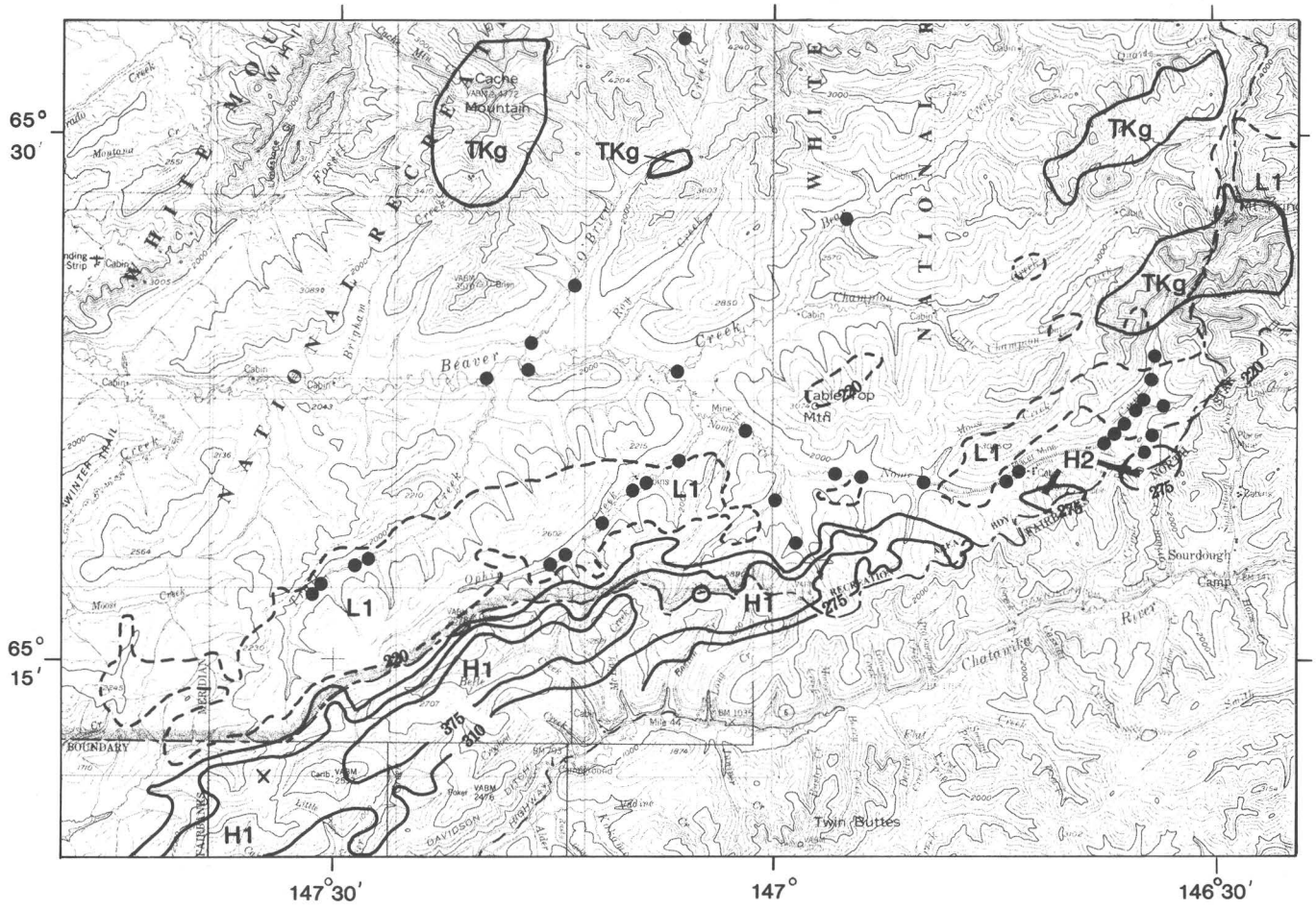

Figure 1.--Aeromagnetic sketch map of portions of southeast Livengood and southwest Circle quadrangle. Solid lines are selected magnetic contours outlining magnetic highs (H1 and H2). Dashed lines outline magnetic lows (L1). Total magnetic field in nanoteslas on arbitrary datum. TKg indicates approximate outcrop area of Tertiary-Cretaceous granite. Black dots show heavy-mineral-concentrate samples containing visible gold. The sample locality of schist containing randomly oriented biotite is shown by "X". The alternating short and long dashed line is the approximate boundary of the White Mountains National Recreation Area.

The Mount Prindle granite is nonmagnetic, as are felsic hypabyssal intrusions near Mount Prindle in the axis of a magnetic low. A belt of magnetic lows extends southwestward from Mount Prindle toward a strong low (L1 in fig. 1) that also occurs near the headwaters of Ophir and Trail Creeks. Cady and Weber (1983) suggested that magnetic lows indicate continuity of nonmagnetic plutons at depth, therefore it is possible that buried plutons are present at the heads of these gold-bearing creeks. Further evidence that buried plutonic rocks may underlie the Ophir and Trail Creek drainages was found in a sample of schist collected just south of the head of Trail Creek (fig. 1). The schist, normally of greenschist facies, was found to contain randomly oriented biotite, indicating that the metamorphic grade had been locally raised sufficiently to crystallize biotite in random orientation similar to the fabric in contact-metamorphosed rocks.

It seems likely, therefore, that the intrusion of Cretaceous and (or) Tertiary pluton(s), inferred from the aeromagnetic low (L1 in fig. 1), caused hydrothermal remobilization of gold from the Cleary sequence buried along the northwestern flank of an antiform. Hydrothermal fluids migrating through dilatant fractures caused by warping associated with the intrusion formed gold-bearing veins and stringers. Because of the lesser degree of erosion as compared to the head of Nome Creek, gold-bearing veins may still be in place along the ridge south of Trail and Ophir Creeks.

Finally, visible gold found in samples from O'Brien Creek (fig. 4) cannot have been derived from the Cleary sequence in the Mount Prindle area. Cache Mountain, from which part of O'Brien Creek originates, represents the upper part of a highly evolved granitic pluton with associated tin-greisen mineralization. This pluton is similar in age, style, and mineralization to the Rocky Mountain (Lime Peak) pluton 30 km to the northeast (Menzie and others, 1986). Hydrothermal mineralization associated with the intrusion of the Cache Mountain pluton is likely to be the source of the gold in O'Brien Creek.

REFERENCES CITED

Cady, J.W., and Weber, F.R., 1983, Aeromagnetic map and interpretation of magnetic and gravity data, Circle quadrangle, Alaska: U.S. Geological Survey Open-File Report 83-170-C, scale 1:250,000.

Chapman, R.M., Weber, F.R., and Taber, Bond, 1971, Preliminary geologic map of the Livengood quadrangle, Alaska: U.S. Geological Survey Open-File Report 71-66, 2 sheets, scale 1:250,000.

Cobb, E.H., 1973, Placer deposits of Alaska: U.S. Geological Survey Bulletin 1374, 213 p.

Ellsworth, C.E., and Parker, G.L., 1911, Placer mining in the Yukon-Tanana region: U.S. Geological Survey Bulletin 480, p. 153-172.

Menzie, W.D., Reed, B.L., and Keith, T.E.C., 1986, Lime Peak--An evolved granite with tin-enriched alteration, in Bartsch-Winkler, Susan, and Reed, K.M., eds., Geologic studies in Alaska by the United States Geological Survey during 1985: U.S. Geological Survey Circular 978, p. 25-27.

Robinson, M.S., Smith, T.E., and Bundtzen, T.K., 1982, Cleary sequence of the Fairbanks mining district--Primary stratigraphic control of lode gold/antimony mineralization (abs.): Geological Society of America Abstracts with Programs, v. 14, no. 4, p. 228.

Smith, T.E., Robinson, M.S., Bundtzen, T.K., and Metz, P.A., 1981, Fairbanks mining district in 1981: New look at an old mineral province: The Alaska Miner, The Journal of the Alaska Miners Association, v. 9, no. 11, p. 8, 28.

Weber, F.R., and Hamilton, T.D., 1984, Glacial geology of the Mt. Prindle area, Yukon-Tanana Upland, in Short notes on Alaskan geology 1982: Alaska Division of Geological and Geophysical Surveys, Professional Report 86, p. 42-48.

Weber, F.R., Smith, T.E., Hall, M.H., and Forbes, R.B., 1985, Geologic guide to the Fairbanks-Livengood area, east-central Alaska: Anchorage, Alaska Geological Society Guidebook, 44 p.

Reviewers: John Antweiler and E.L. Mosier

LITHOSTRATIGRAPHY, PETROLOGY, AND GEOCHEMISTRY OF THE ORDOVICIAN FOSSIL CREEK VOLCANICS, WHITE MOUNTAINS, EAST-CENTRAL ALASKA

Karen L. Wheeler, Robert B. Forbes, Florence R. Weber, and C. Dean Rinehart

The White Mountains and surrounding area are composed of Proterozoic to Mesozoic sedimentary and volcanic rocks deformed by southeast-dipping, northwest-verging folds and imbricate thrust faults (fig. 1). The core of the White Mountains is composed of the Late Proterozoic and Cambrian Wickersham grit unit, overlain by the Ordovician Fossil Creek Volcanics and by the Silurian Tolovana Limestone.

The Fossil Creek Volcanics, as defined by Mertie (1937), includes more than 610 m of mafic volcanic flows and pyroclastic deposits and a few small bodies of mafic intrusive rocks, agglomerate, conglomerate, and bedded sedimentary rocks. Chapman and others (1971) divided the Fossil Creek into a lower, predominantly sedimentary part that interfingers with an upper, predominantly volcanic part. Thicknesses vary considerably as the facies change from volcanic to sedimentary toward the east. The Fossil Creek Volcanics unconformably overlies the Wickersham grit unit. Its contact with the overlying Tolovana Limestone, which is of Silurian age within the White Mountains, is interpreted as an erosional disconformity.

The lower sedimentary part of the Fossil Creek Volcanics, approximately half of its thickness, is composed of (1) thinly interbedded calcareous dark-gray slate to light-gray slaty phyllite and black tuffaceous shale, (2) gray to black calcareous and siliceous siltstone, (3) medium-gray sandy platy limestone, (4) black and gray banded silty chert, and (5) minor intercalations of basalt flows, pillow lavas, and gabbroic sills. Early Ordovician (Arenigian) conodonts (J.W. Huddle, USGS, written commun., 1972), and trilobites (M.E. Taylor, USGS, written commun., 1972) occur in medium- to dark-gray limestone lenses in the light-gray calcareous phyllitic slate interpreted to be near the base of this unit on Willow Creek. Conodont-trilobite faunas suggest that the earliest Fossil Creek sedimentary beds were deposited in relatively shallow water; but lithology indicates that the bulk of the lower section was probably of deep water origin with turbiditic characteristics (R.B. Blodgett, Oregon State University, oral commun., 1986).

The upper volcanic part of the Fossil Creek Volcanics consists of abundant thick flows of basalt, olive-green agglomerate, and volcaniclastic conglomerate. The basalt described by Church and Durfee (1961) contains phenocrysts and microphenocrysts of clinopyroxene and plagioclase in a groundmass of plagioclase, clinopyroxene, opaque minerals, and devitrified glass. Aggregates of magnesian chlorite and (or) iddingsite are believed to replace olivine. Plagioclase is typically decalcified and partially replaced by saussuritic aggregates of epidote, albite, sericite, and carbonate. Carbonate commonly fills fissures and vesicles, and the groundmass of most of the basalt contains variable amounts of secondary chlorite, sericite, prehnite, leucoxene, and iddingsite. Although clinopyroxene has been partially replaced by aggregates of chlorite and opaque minerals in some of the basalt, it persists as relatively unaltered relict phenocrysts and microphenocrysts in other variants.

Four basalt samples were selected for whole-rock chemical analysis following the completion of Church and Durfee's work in 1961. Unfortunately, the analyses were not completed in time to be included in their theses, and, until this report, the data have not been published. The rocks analyzed were the most representative and least altered of the basalt units that were collected during the 1960 field investigations. The analyses (table 1) were made by T. Katsura and H. Haramura under the auspices of the U.S.-Japan Cooperative

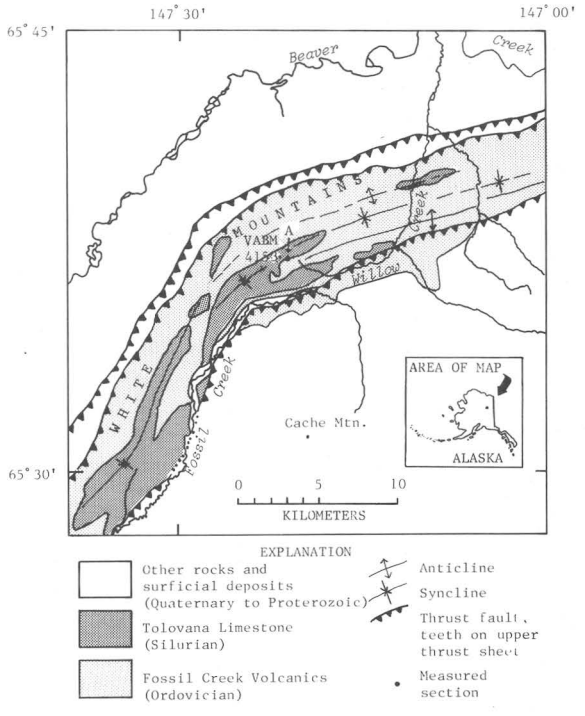

Figure 1.--Geology of the Fossil Creek Volcanics and Tolovana Limestone in White Mountains, Livengood C-1 and C-2 quadrangles, Alaska. Generalized from Chapman and others (1971).

Science Program in 1964. All of the basalt samples meet the chemical criteria for alkali basalt as established by Chayes (1964)--TiO_2 greater than 1.75 weight percent, and nepheline in the norm. The basalt also qualifies as alkali-olivine basalt as discussed by Macdonald and Katsura (1964), with nepheline, olivine, and diopside in the norm, and compositions that plot in the alkaline field of the $Na_2O + K_2O / SiO_2$ diagram.

Although TiO_2 and P_2O_5 are considered to be among the least mobile species (along with Cr, Ni, Zr, Nb, and Y) during low-grade metamorphism of basaltic rocks, the analyzed P_2O_5 values are anomalously low when compared with the coexisting TiO_2 concentrations in typical alkali basalts. Some P_2O_5 may have been lost during hydration reactions which occurred at temperatures of 300° C or greater.

Overlying or interlayered with the basalt flows are agglomerate beds with fine-grained basalt matrices that contain both volcanic and sedimentary clasts. Volcaniclastic conglomerates have sedimentary or tuffaceous matrices. Locally the conglomerate is overlain by olive-green conglomeratic sandstone and medium- to fine-grained calcareous sandstone containing a few thin lenses of coralline limestone. Conodonts from a gray limestone lens in the uppermost part of the Fossil Creek Volcanics are of Middle to Late Ordovician age and of Late Ordovician age (A.G. Harris, USGS, written commun., 1986). The color alteration index (CAI) of these conodonts is 5 1/2, indicating temperatures of 300 to 350° C; these temperatures are compatible with the low-grade metamorphic mineral assemblages characteristic of the basalts. Petrographic descriptions provided by Church and Durfee (1961) indicate that the basalt has undergone zeolite- to lower greenschist-facies metamorphism.

The upper part of the Fossil Creek Volcanics is lithologically variable due to facies changes and subsequent erosion. Section A, 0.5 km east-southeast of VABM 4153, includes 108.5 m of fining-upward sedimentary rocks that locally comprise the upper part of the Fossil Creek Volcanics (fig. 2). Unsorted boulder-to-granule conglomerate and agglomerate are most abundant in the lower 100 m of section A. Bedding in the lower 58 m is massive with relic large-scale, trough-shaped scours. Sorting increases, grain size decreases, and bedding thins upsection. Two basalt beds occur 93.5 m and 68.6 m above the base of the measured section. The lower basalt is 1.8 m thick and the upper is 0.6 m thick. The upper basalt is overlain by 4.3 m of very thinly bedded poorly sorted medium- to fine-grained greenish-gray calcareous feldspatholithic sandstone with lenses of granule conglomerate and coquina. Late Ordovician megafossils are abundant in this interval (see Blodgett and others, this volume). Coralline limestone, 0.76 m thick, occurs within the upper 2 m and is overlain by a thin zone of highly weathered, iron-stained, slightly calcareous, feldspathic sandstone. This limestone was originally called a tuffaceous limestone and included at the very top of the Fossil Creek Volcanics by Mertie (1937). Chapman and others (1971) and Churkin (1973) had some reservations about its inclusion in the Fossil Creek, and Oliver and others (1975, p. 25, fig. 16) excluded it from the Fossil Creek. Careful sampling shows it to be entirely Ordovician in age and part of the Fossil Creek Volcanics (see Blodgett and others, this volume). Only the lower 27 m of the Tolovana Limestone, a light-gray sparsely fossiliferous argillaceous lime mudstone, was measured at section A.

The clasts within the upper part of the Fossil Creek Volcanics are well-rounded maroon and green mafic volcanic rocks, pink granite, bimodal quartzite, light-gray limestone, and phyllite. Most

Table 1.--Whole-rock analyses and CIPW norms for basaltic rocks from the Ordovician Fossil Creek Volcanics, White Mountains, Alaska

	MCD82	MCD56	MCD59	MCD96
	Whole-rock analyses (weight percent)			
SiO_2	48.84	47.00	46.63	43.30
TiO_2	2.13	2.43	1.87	1.87
Al_2O_3	18.18	15.68	15.42	14.04
FeO	9.11	6.22	9.80	9.51
Fe_2O_3	1.63	6.60	1.79	3.34
MnO	.13	.11	.19	.17
MgO	4.37	5.29	7.37	8.96
CaO	8.16	6.42	9.54	11.34
Na_2O	4.83	3.21	2.69	2.66
K_2O	.75	3.19	1.50	1.58
P_2O_5	.06	.06	.03	.07
H_2O+	1.72	3.82	3.22	3.45
H_2O-	.17	.23	.21	.23
Total	100.08	100.24	100.26	100.45
Cr	.0020	.0049	.014	.015
Ni	.0039	.0055	.0081	.010
	CIPW norms			
Orthoclase	4.43	18.85	8.86	9.34
Albite	32.35	25.95	19.66	4.97
Anorthite	25.71	18.96	25.57	21.70
Nepheline	4.61	.66	1.68	9.50
Diopside	11.94	9.89	17.67	27.66
Olivine	12.59	7.58	17.16	15.11
Magnetite	2.36	9.57	2.60	4.84
Ilmenite	4.05	4.62	3.55	3.55
Apatite	.14	.14	.07	.16
Percent An in Plagioclase	An44	An42	An57	An81

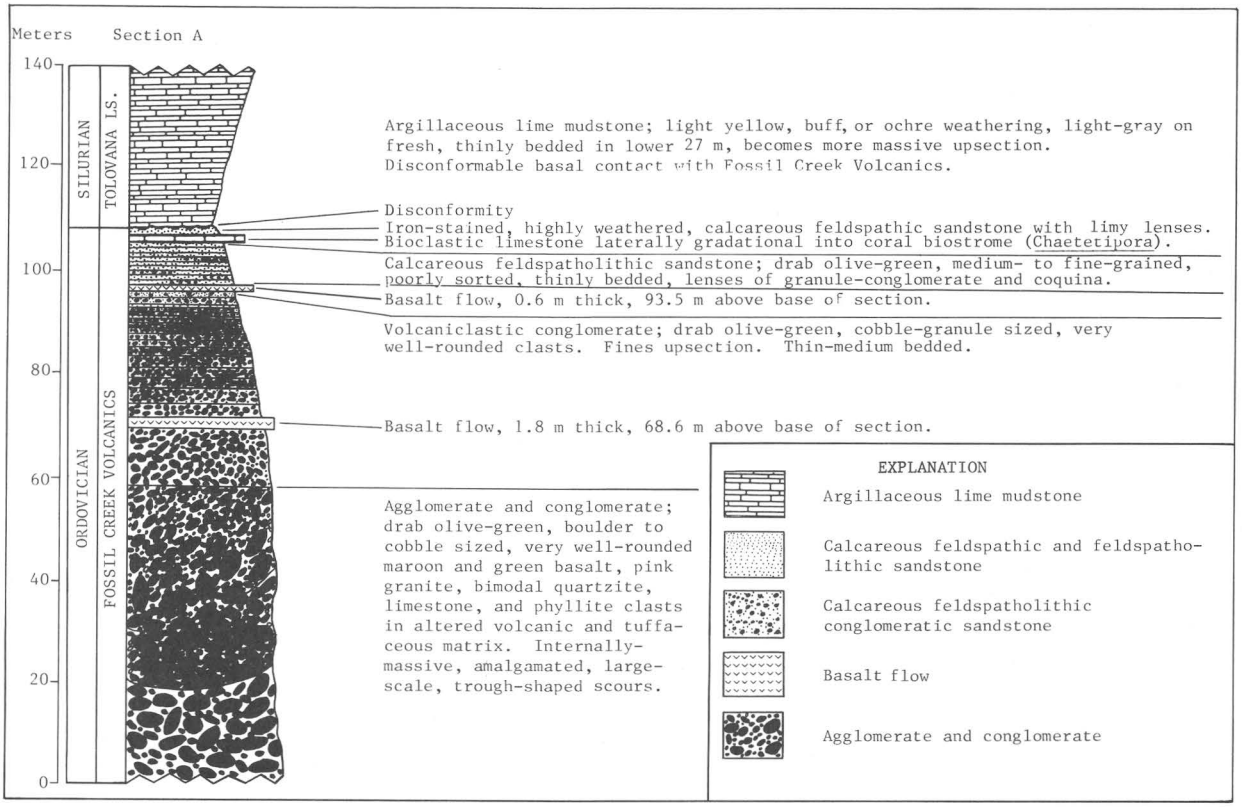

Figure 2.--Measured stratigraphic section A in upper part of the Fossil Creek Volcanics and Tolovana Limestone. Located at 65°37'16" N., 147°21'11" W. in Livengood C-1 quadrangle.

of these clasts display local source affinities. However, the pink granite clasts are unlike any known pre-Late Ordovician rocks in the Yukon-Tanana Upland. This granite is composed of massive, medium-grained chlorite-quartz-orthoclase-albite and has xenomorphic- to hypautomorphic-granular texture, modified only by mild protoclasis. Crude zonal distribution of alteration products in the albite crystals indicate that the original plagioclase was probably more calcic--perhaps oligoclase or andesine. The chlorite is partly pseudomorphous after biotite, indicating that the original unaltered rock may have been a common biotite granite or granodiorite that was subsequently metamorphosed to greenschist facies.

Because of its well-defined, alkalic composition, the basalt of the Fossil Creek Volcanics is unlikely to be island arc, mid-ocean-ridge, or continental tholeiitic basalt. The question, therefore, is whether or not the parental basalts erupted in an oceanic or a continental setting. A few pillow lavas were found in the flows associated with the lower, predominantly sedimentary section. The clasts in the conglomerate and agglomerate of the upper part of the Fossil Creek Volcanics are suggestive of lahar and debris-flow deposits near a continental source area. The coral biostromes and marine fossil hash in the upper part of the Fossil Creek Volcanics indicate a warm, shallow-marine environment. The fining upward of grain size, and increasingly mature sandstone compositions and textures in the upper part of the Fossil Creek Volcanics, are characteristic of nearshore shallowing-upward marine deposits. Based on the Ordovician faunal assemblages and depositional environments, a strong case can be presented for the eruption of the alkali-basalt flows in the continental margin and (or) shallow-marine (shelf) environment. The Silurian Tolovana limy deposits prograded over the erosional surface on the Upper Ordovician part of the Fossil Creek Volcanics.

The Fossil Creek Volcanics and the Tolovana Limestone are the major formations constituting the White Mountains terrane (Churkin and others, 1982; Jones and others, 1984). We interpret the contact between the White Mountains terrane and the Wickersham terrane of Jones and others (1984) to be simply an unconformity and not a tectonic

feature. This unconformity is similar to that found between rocks of similar types and ages in Yukon Territory, Canada, in which Cambrian strata have been removed (Thompson and Roots, 1982, p. 410).

REFERENCES CITED

Chapman, R.M., Weber, F.R., and Taber, Bond, 1971, Preliminary geologic map of the Livengood quadrangle, Alaska: U.S. Geological Survey Open-File Report 71-66, scale 1:250,000, 2 sheets.

Chayes, F., 1964, A petrographic distinction between Cenozoic volcanics in and around the open oceans: Journal of Geophysical Research, v. 69, p. 1573-1588.

Church, R.E., and Durfee, M.C., 1961, Geology of the Fossil Creek area, White Mountains, Alaska: Fairbanks, University of Alaska, M.S. thesis, 96 p.

Churkin, M.C., Jr., 1973, Paleozoic and Precambrian rocks of Alaska and their role in its structural evolution: U.S. Geological Survey Professional Paper 740, 64 p.

Churkin, M.C., Jr., Foster, H.L., Chapman, R.M., and Weber, F.R., 1982, Terranes and suture zones in east-central Alaska: Journal of Geophysical Research, v. 87, no. 85, p. 3718-3730.

Jones, D.L., Silberling, N.J., Coney, P.J., and Plafker, George, 1984, Part A--Lithotectonic terrane map of Alaska (west of the 141st meridian), in Silberling, N.J., and Jones, D.L., eds., Lithotectonic terrane maps of the North American Cordillera: U.S. Geological Survey Open-File Report 84-523, p. A1-12A.

Macdonald, G.A., and Katsura, T., 1964, Chemical composition of Hawaiian lavas: Journal of Petrology, v. 5, no. 1, p. 82-133.

Mertie, J.B., 1937, The Yukon-Tanana Region, Alaska: U.S. Geological Survey Bulletin 872, 276 p.

Oliver, W.A., Jr., Merriam, C.W., and Churkin, M.C., Jr., 1975, Ordovician, Silurian, and Devonian corals of Alaska: U.S. Geological Survey Professional Paper 823-B, p. 13-44.

Thompson, R.I., and Roots, C.F., 1982, Ogilvie Mountains Project, Yukon, Part A: A new regional mapping program: Geological Survey of Canada, Current Research, Part A, Paper 82-1A, p. 403-411.

Reviewers: R.M. Chapman and J.H. Dover

PLACER GOLD RELATED TO MAFIC SCHIST(?) IN THE CIRCLE DISTRICT, ALASKA

Warren Yeend

The Circle District is one of the major placer gold mining districts within Alaska, with estimated total production of 1 million oz (31,000 kg) (Bundtzen and others, 1984). Placer operations continue in many of the same creeks that have been mined since the original gold discovery in 1893. Despite many decades of search by prospectors and geologists, a lode source for the gold placers has eluded discovery.

The placers occur in the Yukon-Tanana Upland (Wahrhaftig, 1965) south of the Tintina fault zone where the rocks are dominated by widespread, rarely mineralized quartzites and quartzitic and mafic schists (Foster and others, 1983). Early reports refer to the occurrence of placer gold fragments with attached quartz (Mertie, 1938), and a gold-rich quartz vein in a block of quartz schist was described by Spurr (1898). In a more recent work, Menzie and others (1983) concluded that the distribution of gold by rock type and by its location suggests that gold occurs in small fracture zones, in veins and in association with felsic dikes that developed and were emplaced above the granite in the Circle Mining District. Thinly laminated muscovite schists with traces of gold and sulfides, inferred to be a volcanogenic rock, have also been suggested as the source for much of the gold in the placers (Mining and Minerals, 1985).

The accordant summits in the upland areas drained by the gold-producing creeks might suggest an old erosion surface--the location of, perhaps, a fossil placer river system. Although it would be possible to reconstruct such a drainage that could have provided a gold source for the existing creek placers, evidence for the existence of such a fossil placer is absent. No remnants of high-level gravel are present in the summit areas, a highland bedrock source for the fossil placer is missing, and surrounding areas lack gold placers and lodes through which an old river system would have flowed.

It is reasonable therefore to look for a local bedrock gold source. Recent mapping in the Circle quadrangle (Foster and others, 1983) delineates a mafic schist unit within the monotonous quartzitic schists (fig. 1) that should be seriously considered as a possible gold source or, at least, a control on the source. The mafic schist crops out within the Circle quadrangle in the headwaters of many of the most productive gold placer creeks, implying a possible genetic relationship. Furthermore, gold production from each creek is correlated with the amount of its drainage within the outcrop limits of the mafic schist. Mastodon Creek, one of the most productive creeks in the district, has at least 75 percent of its drainage basin within the mafic schist (fig. 1). Similarly, the very productive North Fork of Harrison Creek has almost 100 percent of its drainage basin within the mafic schist. Other very productive creeks, Deadwood, Bottom Dollar, Harrison, and Gold Dust, drain substantial areas within the mafic schist. Bedrock, Boulder, Butte, Ketchem, and Portage Creeks, which drain small areas of the mafic schist, have been less important gold producers. The granites which crop out in several places within the Circle quadrangle do not appear to be spatially related to the presence of placer gold. The granites of the Circle Mining District, mainly present within a portion of the drainages of Deadwood, Ketchem, and Portage Creeks, were determined to be high in tin, however (Menzie and others, 1983).

As described by Foster and others (1983), the mafic schist is a green, chlorite-quartz-carbonate schist with abundant plagioclase porphyroblasts. It is associated with amphibolitic schist, minor marble, quartzite, and pelitic schist. Locally it is interlayered in the quartzitic schist unit. The surrounding rock types, and those most commonly present south of the Tintina fault zone, are gray or greenish-gray quartzite and quartzitic schist with minor pelitic schist, calcsilicate rock, mafic schist, and rare interlayered marble (Foster and others, 1983).

The contact of the mafic schist unit with the quartzite and quartzitic schist is generally gradational. Thin units of mafic schist too small to map at 1:250,000 scale are locally present interlayered in the quartzite and quartzitic schist unit. Assuming that the mafic schist is, in fact, a gold source or host rock for gold, these unmapped scattered occurrences could explain the presence of minor amounts of gold in some creeks where no mafic schist has been mapped. The upper portions of Loper and Porcupine Creeks would seem to be such an area where there could be some small exposures of mafic schist.

The uppermost parts of some gold-producing creeks and those creeks with little or no gold production which drain areas of mafic schist generally possess such steep gradients that they transported gravel but allowed little deposition. Although incapable of supporting a large placer mining operation, they might contain sufficient gold to attract small-scale mining. The south-flowing Traverse and Portage Creeks, which empty into Birch Creek, and several of the southward-flowing tributaries of Harrison Creek, are examples of such creeks.

The contact relationships of the mafic schist unit with surrounding rock units are not sufficiently well understood to be able to identify their structural setting, thus it is unclear whether more or less area of mafic schist was available for

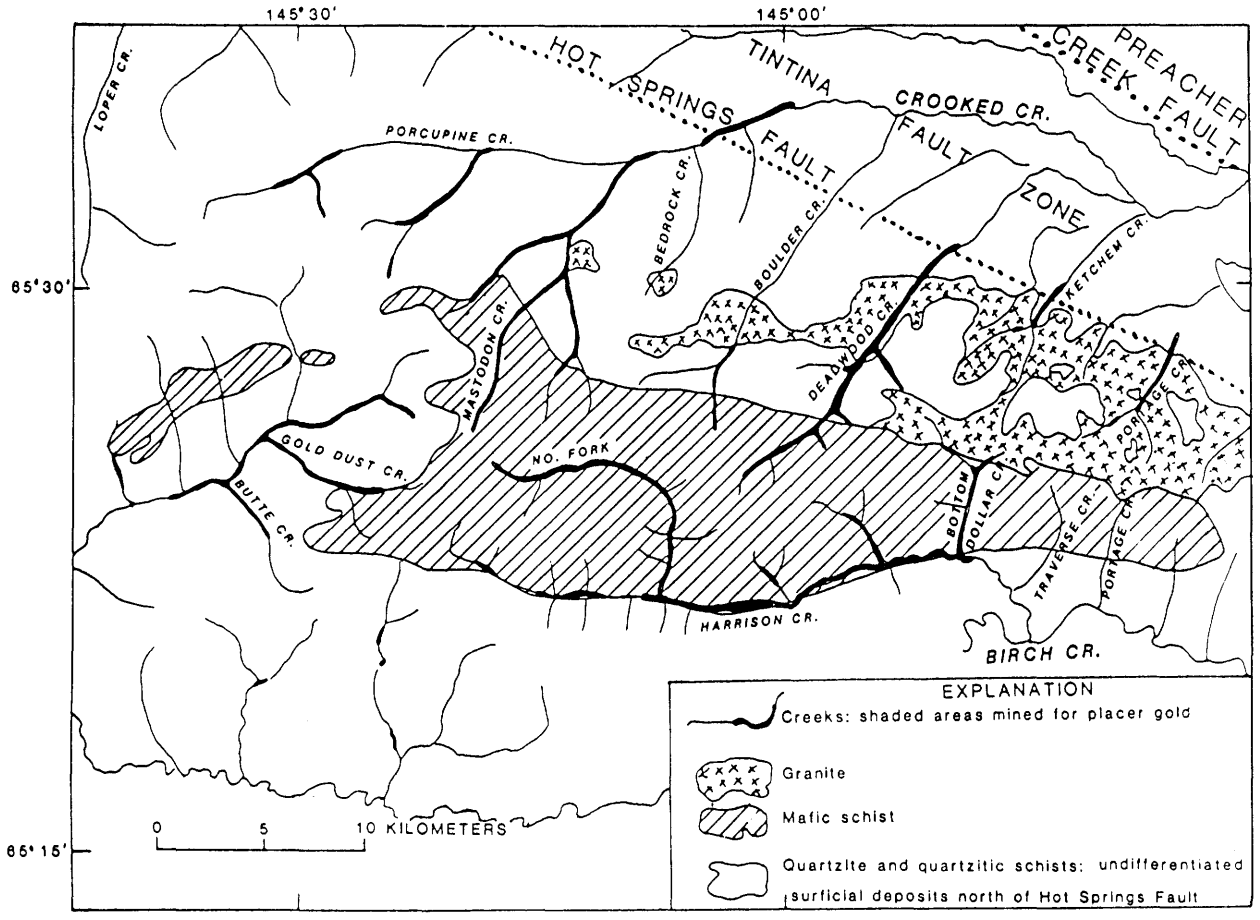

Figure 1.--Simplified geologic map of Circle mining district showing relation of gold placers and mafic schist (geology from Foster and others, 1983).

erosion in earlier geologic time. Likewise, it is not known what happens to the mafic schist unit at depth. More detailed mapping of these contacts might reveal this information and allow a better understanding of the magnitude and size of the original gold source area.

Although the Circle District has no reported production of lode gold, the adjacent Fairbanks mining district has produced 245,000 oz (7,600 kg) of gold from lode sources. The lode gold, present within quartz-sulfide veins with associated lead-antimony sulfosalts, is hosted by the Cleary sequence, a mafic and felsic schist of probable volcanic origin (Mining and Minerals, 1985). The very productive placers of the Fairbanks District, from which 7,555,000 oz (235,000 kg) of gold has been taken since 1902, exist in close spatial association with the rocks of the Cleary Sequence and most probably were derived from them (Mining and Minerals, 1985). Placer gold within the Circle quadrangle, when analyzed for trace elements, was found to be anomalously high in antimony as compared to placer gold from other areas in Alaska (Yeend, 1985), and might suggest a lode association similar to the Fairbanks Mining District.

If the mafic schist is the primary lode gold source in the Circle District, the nature of gold occurrence within the schist remains to be determined. The fact that only one of 44 rock samples collected within the mafic schist unit contained detectable gold (Menzie and others, 1983) implies that the gold, if present in significant amounts, is not uniformly distributed throughout the schist.

REFERENCES CITED

Bundtzen, T.K., Eakins, G.R., Clough, J.G., Lueck, L.L., Green, C.B., Robinson, M.S., and Coleman, D.A., 1984, Alaska's mineral industry 1983: Alaska Division of Geological and Geophysical Surveys Special Report 33, 56 p.

Foster, H.L., Laird, Jo, Keith, T.E.C., Cushing, G., and Menzie, W.D., 1983, Preliminary geological map of the Circle quadrangle, Alaska: U.S. Geological Survey Open-File Report 83-170-A, 30 p.

Menzie, W.D., Foster, H.L., Tripp, R.B., and Yeend, W.E., 1983, Mineral resource assessment of the Circle quadrangle, Alaska: U.S. Geological Survey Open-File Report 83-170-B, 57 p.

Mertie, J.B., Jr., 1938, Gold placers of the Fortymile, Eagle, and Circle districts, Alaska: U.S. Geological Survey Bulletin 897-C, p. 133-261.

Mining and Minerals, 1985, In the golden heart of Alaska: Fairbanks, North Star Borough, 80 p.

Spurr, J.E., 1898, Geology of the Yukon gold district, Alaska: U.S. Geological Survey 18th Annual Report, pt. 3, p. 87-392.

Wahrhaftig, Clyde, 1965, Physiographic divisions of Alaska: U.S. Geological Survey Professional Paper 482, 52 p.

Yeend, Warren, 1985, Trace elements of placer gold, in Bartsch-Winkler, Susan, and Reed, K.M., eds., The United States Geological Survey in Alaska: Accomplishments during 1983: U.S. Geological Survey Circular 945, p. 4-7.

Reviewers: R.M. Chapman and Helen Foster

SOUTHWESTERN ALASKA

Kisaralik Lake, Bethel quadrangle. Photo by S.E. Box, 1986.

LATE MESOZOIC STRUCTURAL AND STRATIGRAPHIC FRAMEWORK, EASTERN BETHEL QUADRANGLE, SOUTHWESTERN ALASKA

Stephen E. Box and John M. Murphy

In July of 1986 we made a boat traverse along the Kisaralik River in the eastern Bethel quadrangle (fig. 1) in order to study the initiation, evolution, and deformation of the depositional basin of the Albian to Coniacian (late Early and early Late Cretaceous) Kuskokwim Group in the context of the tectonic evolution of the region. This report presents our initial field results augmented by preliminary petrographic study of our samples, and includes a geologic map and cross section along the Kisaralik River (fig. 1).

Pre-mid-Cretaceous rocks of the Togiak and Goodnews terranes are exposed along the Kisaralik River. The Togiak terrane is a Mesozoic andesitic volcanic and volcaniclastic terrane with a Late Triassic through Early Cretaceous history (Box, 1985). The eastern third of the Kisaralik River traverse exposes a generally west-dipping section of the Togiak terrane divisible into three unfoliated stratigraphic units (fig. 1). Fossils of Valanginian (early Early Cretaceous) age occur about 25 km to the southwest along strike in strata apparently correlative with the middle or upper unit of the Togiak terrane along the Kisaralik River (Hoare and Coonrad, 1978). The Goodnews terrane is exposed beneath Kuskokwim conglomerates in the core of the Kisaralik anticline and at Greenstone Ridge. The Goodnews terrane in the Kisaralik anticline is similar to the lower unit of the Togiak terrane, but differs in that it is overprinted by slaty to phyllitic cleavage. The Goodnews terrane at Greenstone Ridge consists of greenschist-facies metabasite with a southeast-dipping foliation and northeast-trending plagioclase lineation. Actinolite separated from a Greenstone Ridge metabasite sample yielded a K/Ar age of 146 ± 15 Ma (fig. 1). The structural relationship between the rocks at Greenstone Ridge and those of the Kisaralik anticline is uncertain, but both apparently record an earliest Cretaceous low-grade metamorphic event.

Two other terranes underlie the region of the Kisaralik traverse, but they are not exposed near the Kisaralik River. The Kilbuck terrane occurs west of the Goodnews terrane in the southern Bethel and northern Goodnews quadrangles (fig. 1, inset), and consists of regionally metamorphosed Precambrian quartzofeldspathic amphibolite-facies schist (Hoare and Coonrad, 1979), which underwent a greenschist-facies overprint about 150-130 Ma (Late Jurassic and Early Cretaceous time) (Turner, 1983). The Nyac terrane crops out west of the westernmost part of the Kuskokwim Group on the Kisaralik River and consists of Middle and Upper Jurassic andesitic volcanic and volcaniclastic strata intruded by an Early Cretaceous granitic pluton (Hoare and Coonrad, 1959b; Wilson, 1977). It is uncertain whether the Nyac terrane is anywhere overlapped by the Kuskokwim Group.

The Kuskokwim Group covers the contact between the Goodnews and Togiak terranes. Basal conglomerates overlie foliated metamorphic rocks of the Goodnews terrane at Greenstone Ridge and along the Kisaralik anticline (fig. 2). Both sections exhibit a lower conglomeratic section of local provenance and near-sea-level depositional setting, and an upper conglomeratic section of deep-water origin derived from a terrane of quartz-mica schist and granite gneiss, presumably the Kilbuck terrane. Basal conglomerates are absent on the east side of the Kuskokwim depositional basin.

The basal Kuskokwim conglomerates at Greenstone Ridge and the Kisaralik anticline are overlain by several kilometers of thin-bedded, fine sandstone and shale. This shaly facies of the Kuskokwim Group conformably overlaps and possibly interfingers with volcanogenic strata of the Togiak terrane along the eastside of the basin without an intervening basal conglomerate. Coarse sandstone beds occur only at Upper Falls, where two 30-m-thick turbidite channel-fill sequences are separated by 50 m of thin-bedded fine sandstone and shale. Flute marks indicate northeast-directed flow within these channels. Stratigraphically above the basal conglomerate, the depositional environment of the Kuskokwim Group along the Kisaralik River is interpreted as a deepwater basin dominated by channel and overbank deposition along northeasterly directed submarine channels.

Fossils recovered from the Kuskokwim Group in the vicinity of the Kisaralik River range from Albian to Coniacian in age (Hoare and Coonrad, 1959a). A middle Albian fossil was recovered from the fine-grained turbidite strata just above the basal conglomerate flanking the Eek Mountains anticline about 40 km to the south-southwest along strike from the Kisaralik anticline (see Murphy, this volume). The depositional onlap of the fine-grained facies onto the Togiak terrane just south of the Kisaralik River above Upper Falls (fig. 1) is Cenomanian(?) in age (D.L. Jones and J.W. Miller, written commun. to W.L. Coonrad, USGS, 1979). The younger age of its depositional base, its predominantly quartzose composition, and its lack of a basal conglomerate indicate that the eastern flank of the Kuskokwim depositional basin in the Bethel quadrangle was passively onlapped by turbidite basin-fill derived predominantly from highlands along the western basin margin.

Strata of the Kuskokwim Group west of Golden Gate Falls have subtle lithologic and compositional differences from the Kuskokwim strata exposed east of the falls. The western

strata display (1) a much greater proportion of sandstone in most outcrops, (2) south-directed paleocurrents, and (3) argillites which lack a slaty cleavage. The sandstones are superficially similar in composition to those from the eastern area, except for a much higher percentage of chert clasts (5 percent versus a trace amount in the eastern sandstones). The compositional and paleoflow data imply that the western strata were not part of the same depositional system as the eastern strata. As age relationships are uncertain, these western strata either may be of a different age than the eastern strata or were deposited in a different depositional basin and subsequently faulted against the eastern strata.

The predominant structural fabric of the Bethel quadrangle is a result of Late Cretaceous deformation. In the northeastern Bethel quadrangle, highly deformed Kuskokwim strata as young as Coniacian (87.5-88.5 Ma) are unconformably overlain by volcanic rocks (Hoare and Coonrad, 1959a) that have yielded a whole-rock K-Ar age of 71.4 ± 2.1 Ma (Robinson and Decker, 1986). Along the Kisaralik River this Late Cretaceous deformation resulted in the development of northeast-southwest-trending tight folds, often overturned to the northwest. Shaly Kuskokwim strata east of Golden Gate Falls generally preserve a moderately to steeply southeast-dipping axial planar slaty cleavage. Preexisting mineral foliation in the older units at Greenstone Ridge and the Kisaralik anticline is also folded by the northeast-southwest-trending folds. The Kuskokwim Group downstream from Golden Gate Falls is also deformed into northeast-southwest-trending folds, often overturned to the northwest, but lacks a slaty cleavage.

The western flank of Greenstone Ridge is marked by a southeast-dipping thrust fault that places metabasite over undated Kuskokwim strata (fig. 1). As the Kisaralik anticline is asymmetric with a steeper western limb, it is suspected that this feature also overlies a southeast-dipping thrust fault at depth. On our cross section the Kisaralik anticline, as well as northwest-vergent overturned folds within the Kuskokwim Group, are interpreted to continue downward into southeast-dipping thrust faults.

The late Mesozoic history of the northern Bristol Bay region has been interpreted by Box (1985) to record the partial underthrusting of continental crust (Kilbuck terrane) beneath the accretionary forearc (Goodnews terrane) of an active intraoceanic volcanic arc (Togiak terrane) in Early Cretaceous time. Early Cretaceous metamorphism of the Kilbuck and Goodnews terranes along the crustal suture, as well as Early Cretaceous explosive andesitic volcanism evidenced in the Togiak terrane, are manifestations of this collisional event. Subsequent uplift of the metamorphosed Kilbuck terrane and the western part of the Goodnews terrane in late Early and early Late Cretaceous time provided detritus for the deep Kuskokwim basin between the uplifted collisional suture and the quiescent volcanic-arc terrane. Renewed compressional deformation in middle Late Cretaceous time resulted in shortening of the mid-Cretaceous basinal strata by northwest-vergent thrust faults and associated folds, reactivating the structural grain inherited from earlier subduction and collision episodes (see Murphy, this volume). Late Late Cretaceous volcanism records the northward underthrusting of Pacific seafloor under the newly consolidated continental mass of accreted terranes in western Alaska (Wallace and Engebretson, 1984; Moll-Stalcup, in press). Whether strike-slip faulting played a significant role in the late Mesozoic evolution of this area of southwestern Alaska is uncertain.

REFERENCES CITED

Box, S.E., 1985, Terrane analysis, northern Bristol Bay region, southwestern Alaska, in Bartsch-Winkler, Susan, ed., The United States Geological Survey in Alaska: Accomplishments during 1984: U.S. Geological Survey Circular 967, p. 32-37.

Hoare, J.M., and Coonrad, W.L., 1959a, Geology of the Bethel quadrangle, Alaska: U.S. Geological Survey Miscellaneous Investigations Map I-285, scale 1:250,000.

_____1959b, Geology of the Russian Mission quadrangle, Alaska: U.S. Geological Survey Miscellaneous Investigations Map I-292, scale 1:250,000.

_____1978, Geologic map of the Goodnews and Hagemeister Island quadrangles region: U.S. Geological Survey Open-File Report 78-9-B, scale 1:250,000.

_____1979, The Kanektok metamorphic complex, a rootless belt of Precambrian rocks in southwestern Alaska, in Johnson, K.M., and Williams, J.R., eds., The United States Geological Survey in Alaska: Accomplishments during 1978: U.S. Geological Survey Circular 804-B, p. 72-74.

Jones, D.L., Silberling, N.J., Coney, P.J., and Plafker, George, 1984, Lithotectonic terrane map of Alaska, in Silberling, N.J., and Jones, D.L., eds., Lithotectonic terrane maps of the North American Cordillera: U.S. Geological Survey Open-File Report 84-523, p. A1-A12, scale 1:2,500,000, 4 sheets.

Moll-Stalcup, E.J., in press, Latest Cretaceous and Cenozoic magnetism in mainland Alaska, in Plafker, George, and Jones, D.L., eds., The Cordilleran orogen: Decade of North American Geology Special Publication, Geological Society of America, Boulder, Colo.

Robinson, M.S., and Decker, John, 1986, Preliminary age dates and analytical data for selected igneous rocks from the Sleetmute,

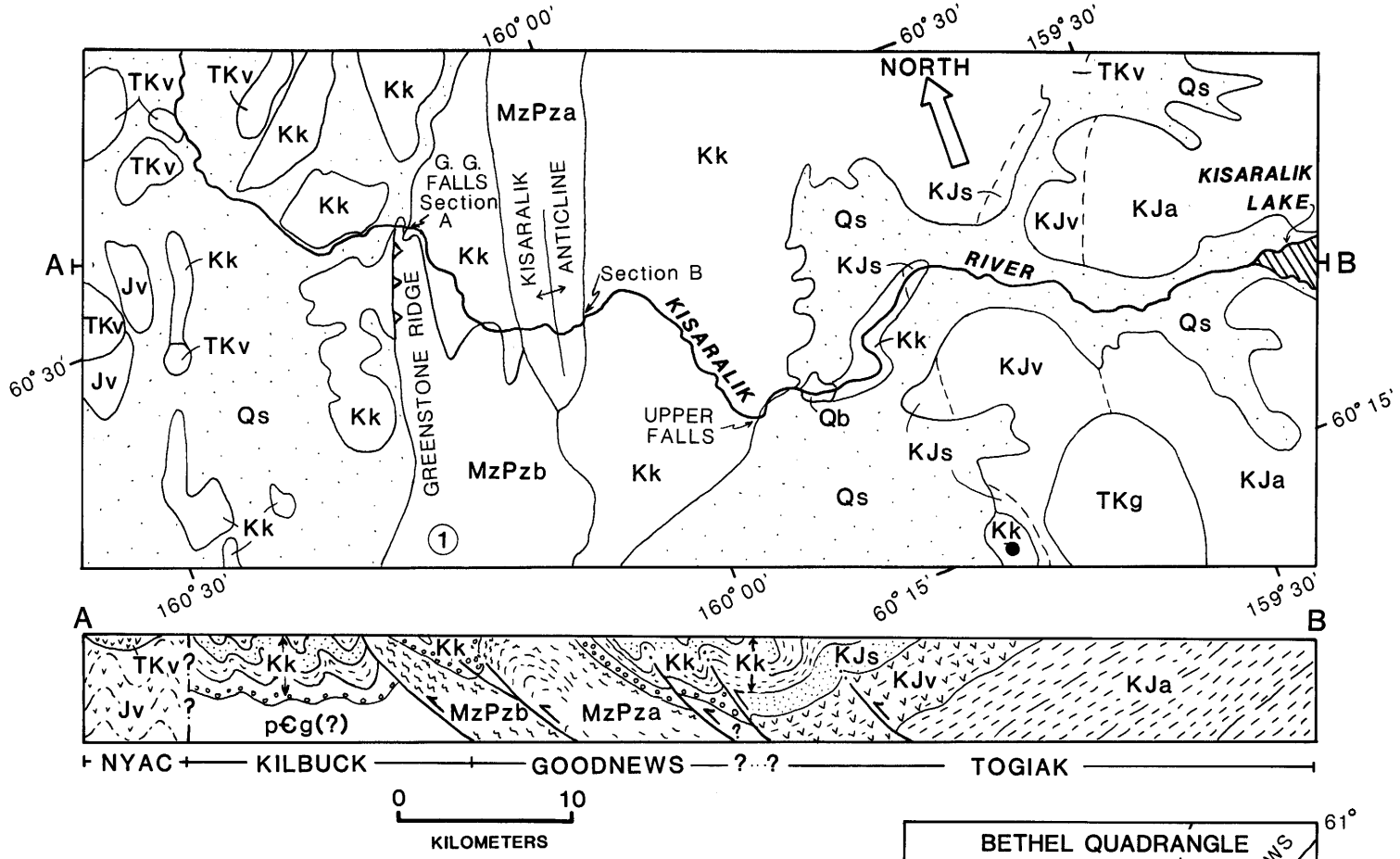

K-Ar analytical data: (sample 1 – 60° 20.5' N, 160° 18.8' W)

Rock type (Map-unit symbol)	Material analyzed	K_2O pct. (wt. pct.)	^{40}Ar (moles/gx10^{11})	$\frac{^{40}Ar\ rad}{^{40}Ar\ total}$	Calculated age (Ma)
Metabasite (MzPzb)	Amphibole	0.0679	1.81	0.169	146 ± 15

Constants used in calculation of age: $\lambda_\beta = 4.96 \times 10^{10}$/yr.; $\lambda_\varepsilon = 0.581 \times 10^{-10}$/yr.; $k^{40}/K = 1.167 \times 10^{-4}$g/g

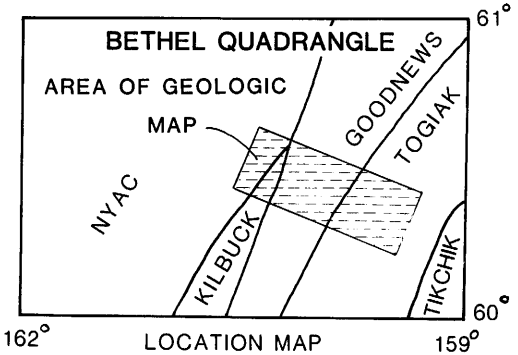

EXPLANATION

OVERLAP SEQUENCES

Qs	Surficial deposits (Quaternary)	TKg	Granitic pluton (early Tertiary and Late Cretaceous)
Qb	Olivine basalt (Quaternary)	TKv	Volcanic rocks (early Tertiary and Late Cretaceous)
		Kk	Kuskokwim Group (late Early Cretaceous and early Late Cretaceous)

PRE-MID-CRETACEOUS TERRANES

TOGIAK TERRANE

KJs	Volcaniclastic sedimentary rocks (Early Cretaceous and (or) Jurassic)
KJv	Andesitic volcanic rocks (Early Cretaceous and (or) Jurassic)
KJa	Tuffaceous argillite and chert (Early Cretaceous and (or) Jurassic)

NYAC TERRANE

Jv	Andesitic volcanic rocks (Jurassic)

GOODNEWS TERRANE

MzPza	Tuffaceous argillite and chert (Mesozoic or Paleozoic)--Slaty to phyllitic cleavage
MzPzb	Foliated metabasite and minor marble and metachert (Mesozoic or Paleozoic)

KILBUCK(?) TERRANE

p€g(?)	Granitic gneiss and quartz-mica schist (Precambrian)--Only in cross section

SYMBOLS

MAP

- Contact--Approximately located. Dashed when inferred
- Thrust fault--Teeth on upper plate
- (1) Location of K-Ar dated sample
- ● Location of Cenomanian(?) fossil (discussed in text)
- A⊢ ⊣B Location of cross-section line A-B

CROSS SECTION

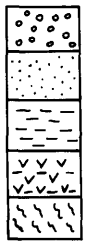

- Conglomerate
- Sandstone turbidite
- Argillaceous rocks
- Volcanic rocks
- Schistosity or phyllitic cleavage

Figure 1.--Geologic map and cross section of part of eastern Bethel quadrangle along Kisaralik River (map adapted from Hoare and Coonrad, 1959a). Inset location map shows terranes of Bethel quadrangle (Jones and others, 1984). Stratigraphic sections A and B are shown in figure 1. K-Ar analysis by Krueger Enterprise Inc. for W. Connelly, AMOCO (written commun., 1978).

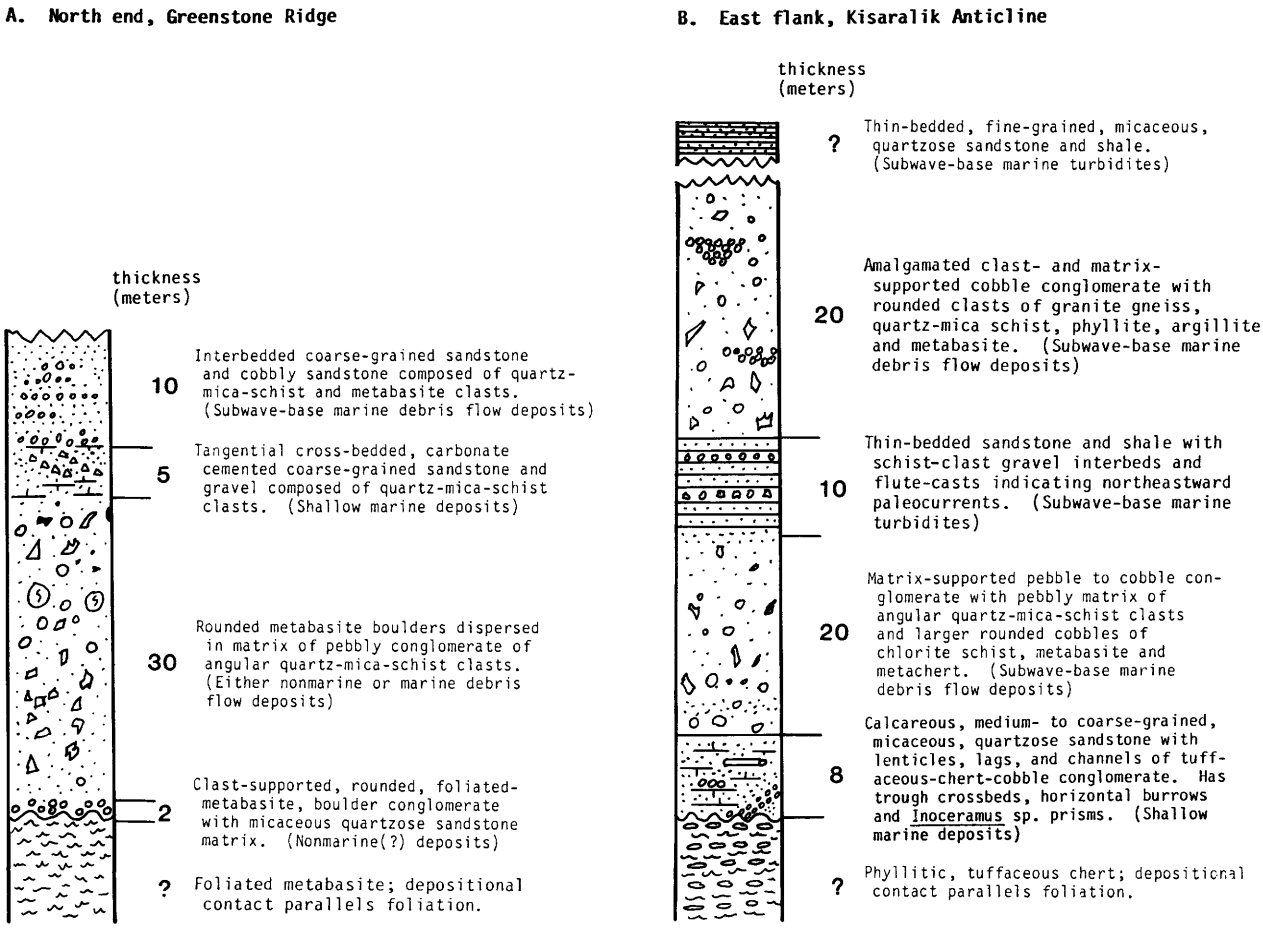

Figure 2.-- Stratigraphic sections of basal part of the Kuskokwin Group along Kisaralik River (located in figure 1).

Russian Mission, Taylor Mountains and Bethel quadrangles, southwestern Alaskan: Alaska Division of Mining and Geological and Geophysical Surveys, Public-Data File 86-99, 9 p.

Turner, D.L., 1983, Geochronology of the Kilbuck terrane of southwestern Alaska: Geological Society of America Abstracts with Programs, v. 15, no. 5, p. 407.

Wallace, W.K., and Engebretson, D.C., 1985, Relationships between plate motions and Late Cretaceous to Paleocene magmatism in southwestern Alaska: Tectonics, v. 3, p. 295-315.

Wilson, F.H., 1977, Some plutonic rocks of southwestern Alaska, a data compilation: U.S. Geological Survey Open-File Report 77-501, 7 p.

Reviewers: W.L. Coonrad and T.E. Moore

EARLY CRETACEOUS CESSATION OF TERRANE ACCRETION, NORTHERN EEK MOUNTAINS, SOUTHWESTERN ALASKA

John M. Murphy

The Eek Mountains form the northwestern-most boundary of the oceanic Goodnews terrane and lie adjacent to the eastern margin of Precambrian quartzofeldspathic metamorphic rocks of the Kilbuck terrane (Jones and Silberling, 1979) (fig. 1). Hoare and Coonrad (1979) considered the informally named Kanektok metamorphic complex (Kilbuck terrane) a rootless belt of Precambrian rocks. Box (1985) interpreted the Goodnews terrane as a composite subduction complex whose subterranes record progressive addition of two oceanic terranes and a single continental (Kilbuck) crustal terrane to the northwest side of the Togiak terrane of Jones and Silberling (1982) during late Mesozoic time. Both the Goodnews and Kilbuck terranes are overlapped unconformably by Lower Cretaceous clastic rocks of the Kuskokwim Group (Hoare and Coonrad, 1959). The northern end of the Eek Mountains, Bethel A-4 quadrangle, was mapped at 1:40,000 scale as part of my M.S. thesis research undertaken at the University of Alaska, Fairbanks (Murphy, in review). This paper summarizes the constraints on timing of accretion of the Goodnews and Kilbuk terranes using Lower Cretaceous sedimentary overlap assemblages mapped in the northern Eek Mountains.

Two Early Cretaceous proximal turbidite units, the Eek Mountains belt and Kuskokwim Group, occur in the northern Eek Mountains. These units have common sediment sources, but they are separated by an angular unconformity interpreted as a submarine canyon cut-and-fill sequence (Murphy and Decker, 1985a, b). The two units differ in age and deformation intensity, and they serve to bracket cessation of a collision event which placed oceanic components of the Goodnews terrane against the continental Kilbuck terrane.

The oldest dated rocks in the Goodnews terrane of the northern Eek Mountains consist of pillow basalt flows and associated volcanogenic sedimentary rocks intercalated with bioclastic limestone composed of fragments of the Permian surf-zone bivalve *Atomodesma* sp. (Hoare and Coonrad, 1978; Kauffman and Runneger, 1975) (table 1, No. 1; unit Pbl, fig. 1.). The basalt and limestone association indicates a Permian ocean-island setting (Murphy and Decker, 1985a, b). Pumpellyite, quartz, and carbonate fill vesicles and fractures in basalt. Plagioclase consists of albite or has been replaced by prehnite. Structurally overlying the basalt and limestone unit are interbedded and interfoliated volcanogenic deposits including flows, debris flows, turbidites, argillite, and tuff of Late Jurassic or Early Cretaceous age (table 1, Nos. 2, 3; unit KJv, fig. 1) and late Paleozoic and (or) early Mesozoic age (unit MzPzu, fig. 1). The Upper Jurassic or Lower Cretaceous volcaniclastic rocks are interpreted as elements of the Togiak terrane which were either tectonically emplaced or stratigraphically overlapped onto the Goodnews terrane prior to their shared deformation during the late Early Cretaceous. They have predominantly southeast-dipping bedding and foliation and are cut by veins of prehnite and pumpellyite.

The Valanginian (table 1, nos. 4, 5; unit Ke, fig. 1) Eek Mountains belt (Hoare and Coonrad, 1983), here composed of interbedded grain-flow, turbidite, and argillite deposits that comprise an inner-fan channel and channel-levee complex, shares the southeast-dipping bedding and foliation orientations with both the Permian and the Upper Jurassic or Lower Cretaceous units; however, the Eek Mountains belt contains only detrital metamorphic minerals. The absence of metamorphic mineral foliation in the Eek Mountains belt, coupled with sharing of structural fabrics with older rocks, suggests that prehnite-pumpellyite-facies metamorphism in the northern Eek Mountains predates Valanginian time, but that reactivation of structural deformation occurred during or soon after deposition of the Eek Mountains belt.

Conglomerates of the Eek Mountains belt consist of amalgamated, bimodal, matrix-supported, and poorly sorted beds composed of subangular to well-rounded clasts floating in fine- to medium-pebble or sand-size matrix. Clast types, in decreasing abundance, include green and gray chert and tuff, massive porphyritic and amygdaloidal greenstone, quartzofeldspathic schist and gneiss, white quartz, fine-grained sandstone, and siltstone. The chert, tuff, and greenstone are diagnostic rock types of the Goodnews terrane; however, the quartzose schist and gneiss must have been derived from the Kilbuck terrane. This is the earliest quartzose metamorphic detritus known locally and marks the arrival of the Kilbuck terrane into sedimentary proximity of the Eek Mountains belt and, therefore, the Goodnews terrane during Valanginian time. This provenance tie also marks the imminent collision of the Kilbuck and Goodnews terranes.

The Kuskokwim Group unconformably overlies the structurally dismembered Goodnews terrane, including the Eek Mountains belt, with a basal submarine conglomerate at least 550 m thick (Hoare and Coonrad, 1959). Conformably overlying the conglomerate are thin-bedded sandstone turbidites and shale that contain a middle Albian (late Early Cretaceous) ammonite (table 1, No. 6; W.K. Wallace, University of Alaska, written commun., 1985).

Kuskokwim conglomerates consist of laterally extensive, amalgamated, matrix-

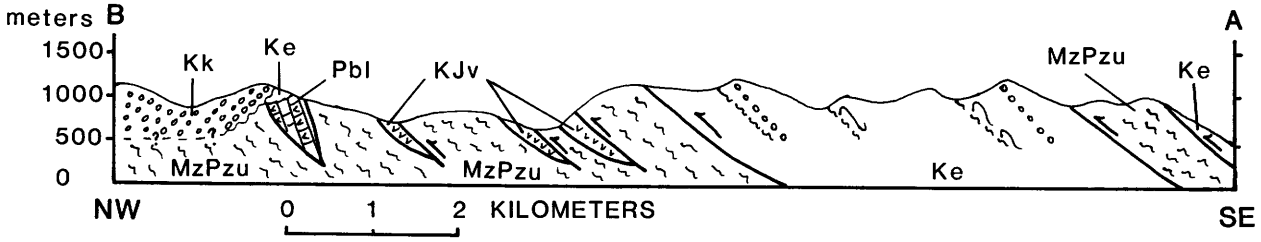

EXPLANATION

Kk	Kuskokwim Group (Lower Cretaceous)--Conglomerate; age is middle Albian
Ke	Eek Mountains belt (Lower Cretaceous)--Conglomerate, sandstone, and shale; age is Valanginian
KJv	Volcanogenic flows, debris flows, and turbidites (Lower Cretaceous or Upper Jurassic)
MzPzu	Undivided basalt, chert, and argillite (lower Mesozoic and (or) upper Paleozoic)
Pbl	Pillow basalt flows and bioclastic limestone (Permian)

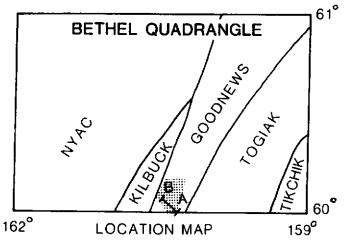

Figure 1.--Geologic cross section and location map of northern Eek Mountains study area. Terranes of Jones and Silberling (1979) outlined on location map. Cross section simplified from Murphy (in review).

supported, poorly sorted pebble- to cobble-conglomerate beds composed of subangular to well-rounded clasts in a matrix of sandstone and fine pebbles. Basic clast types include varicolored chert and tuff, limy siltstone, argillite, quartzofeldspathic schist and gneiss, massive and foliated greenstone, white quartz, and sandstone. As in the Eek Mountains belt, the chert, tuff, and greenstone are derived from the Goodnews terrane, while the schist and gneiss are derived from the Kilbuck terrane. Some clasts of limy siltstone contain fragments of *Atomodesma*, thus providing firm linkage to the Goodnews source terrane (table 1, No. 7). Basal Kuskokwim conglomerates at Greenstone Ridge and Kisaralik anticline may record an unconformable shallow to deep-marine transition (Hoare, 1961; see also Box and Murphy, this volume); however, the Kuskokwim conglomerates of the Eek Mountains are interpreted as deep marine deposits, where submarine canyon-facies conglomerate laps onto foliated rocks of the Goodnews terrane (Murphy and Decker, 1985a, b).

In summary, cessation of Early Cretaceous deformation in the northern Eek Mountains is interpreted to correspond with final emplacement of the Kilbuck terrane and Goodnews terrane. Cessation of this deformation event is constrained by the basal submarine unconformity beneath conglomerate of the Kuskokwim Group (Hoare and Coonrad, 1959). The middle Albian ammonite from stratigraphically above the basal Kuskokwim conglomerate, and the underlying foliated Valanginian Eek Mountains belt deposits bracket the time when deformation ceased. The Kuskokwim Group was itself folded in the Late Cretaceous at a time bracketed by deformed deposits of Turonian age at Great Ridge (Hoare and Coonrad, 1959) and by undeformed crosscutting dikes correlated with the 71 Ma (Shew and Wilson, 1981) Mount Oratia pluton.

REFERENCES CITED

Box, S.E., 1985, Terrane analysis, northern Bristol Bay Region, southwestern Alaska, in Bartsch-Winkler, Susan, ed., The United States Geological Survey in Alaska: Accomplishments during 1984: U.S. Geological Survey Circular 967, p. 32-37.

Hoare, J.M., 1961, Geology and tectonic setting of the lower Kuskokwim-Bristol Bay region, Alaska: American Association of Petroleum Geologists Bulletin, v. 45, no. 5, p. 594-611.

Hoare, J.M., and Coonrad, W.L., 1959, Geology of the Bethel quadrangle, Alaska: U.S. Geological Survey Miscellaneous Geologic Investigations Map I-285, scale 1:250,000.

_____1978, Geologic map of the Goodnews and Hagemeister Island quadrangles region, southwestern Alaska: U.S. Geological Survey Open-File Report 78-9-B, scale 1:250,000.

Table 1.--Age diagnostic fossils from northrn Eek Mountains
[Ages reported by J.W. Miller, U.S. Geological Survey]

USGS collection No.	Latitude Longitude	Fossils	Age	Stratigraphic unit (fig. 1)
1. M7975	60°04.38' N. 160°26.25' W.	Pelecypod *Atomodesma* sp. clastic limestone	Permian	Pbl
2. M7970	60°04.79' N. 160°23.38' W.	Pelecypod *Buchia* sp.	Late Jurassic or Early Cretaceous	KJv
3. M7969	60°04.75' N. 160°23.32' W.	Pelecypod *Buchia* sp.	Late Jurassic or Early Cretaceous	KJv
4. M7972	60°05.82' N. 160°22.45' W.	Pelecypod probably *Buchia sublaevis* Keyserling	probably Valanginian	Ke
5. M7963	60°03.02' N. 160°24.50' W.	Pelecypod *Buchia* sp., probably *B. Keyserlingi* (Lahusen) or *B. Sublaevis* Keyserling	probably Valanginian	Ke
6. M7772	60°05.09' N. 160°27.02' W.	Cephalopod *Paragastroplites flexicostasis* Imlay	middle Albian	Kk
7. M7973	60°07.52' N. 160°21.19' W.	Pelecypod *Atomodesma* sp. fragments in clast	Permian	Kk

_____1979, The Kanektok metamorphic complex, a rootless belt of Precambrian rocks in southwestern Alaska, in Johnson, K.M., and Williams, J.R., eds., The United States Geological Survey in Alaska: Accomplishments during 1978: U.S. Geological Survey Circular 804-B, p. B72-B74.

_____1983, Graywacke of Buchia Ridge and correlative Lower Cretaceous rocks in the Goodnews Bay and Bethel quadrangles, southwestern Alaska: U.S. Geological Survey Bulletin 1529-C, 17 p.

Jones, D.L., and Silberling, N.J., 1979, Mesozoic stratigraphy--The key to tectonic analysis of southern and central Alaska: U.S. Geological Survey Open-File Report 79-1200, 41 p.

_____ 1982, Mesozoic stratigraphy--the key to tectonic analysis of southern and central Alaska in Leviton, A.E., and others eds., Frontiers of geological exploration of western North America: Pacific Section, American Association for the Advancement of Science, p. 139-153.

Kauffman, E.G., and Runnegar, B., 1975, *Atomodesma* (Bivalvia), and Permian species of the United States: Journal of Paleontology, v. 49, no. 1, p. 23-41.

Murphy, J.M., 1987, Geology, sedimentary petrology and tectonic synthesis of Early Cretaceous submarine fan deposits, northern Eek Mountains, southwest Alaska: Fairbanks, University of Alaska, M.S. thesis (in review).

Murphy, J.M., and Decker, John, 1985a, The Goodnews terrane and Kuskokwim Group in the Eek Mountains, southwest Alaska: Open marine to trench-slope transition: American Association of Petroleum Geologists Bulletin, v. 69, no. 4, p. 672.

_____1985b, The Goodnews terrane and Kuskokwim Group in the Eek Mountains, southwest Alaska: Deep marine to trench-slope transition, in Rosel, J., Remacha, E., and Zamorano, M., eds., Abstracts and poster abstracts: International Association of Sedimentologists, European Regional Meeting, 6th, p. 622-623.

Shew, Nora, and Wilson, F.H., 1981, Map and table showing radiometric ages of rocks in southwestern Alaska: U.S. Geological Survey Open-File Report 82-866, 26 p.

Reviewers: S.E. Box and W.L. Coonrad

PETROLOGY AND PROVENANCE OF SANDSTONES OF THE NAKNEK FORMATION, ALASKA PENINSULA

Michael W. Mullen

The Upper Jurassic Naknek Formation crops out in an extensive belt throughout much of the Alaska Peninsula from Kamishak Bay to Black Hill. In the study area (fig. 1), it reaches a maximum thickness of more than 3,000 m, but its thickness averages between 1,700 and 2,000 m (R.L. Detterman, USGS, unpub. data). The formation was deposited in a series of arc-trench gap basins in depositional environments ranging from nonmarine fluvial to outer shelf (Detterman and others, 1981a, 1985). During recent investigations on the Alaska Peninsula as part of the Alaska Mineral Resource Assessment Program, R. L. Detterman collected sandstone samples from several measured sections. Samples from four sections have been analyzed for composition in order to determine the source rocks and the depositional history of this formation. This information in turn will be of value in determining regional tectonic uplift and the duration of magmatic arc activity.

Sandstone samples from measured sections at Indecision Creek, Wandering Ridge, Northeast Creek, and Clark River (fig. 1) were analyzed by standard thin-section techniques, scanning electron microscope (SEM), and X-ray probe microanalyzer. The Indecision Creek and Wandering Ridge sections represent the upper sandstone member of the Naknek Formation; the Northeast Creek and Clark River sections represent the Snug Harbor Siltstone Member and the lower sandstone member of the Naknek Formation (fig. 2). The four sections therefore represent almost the entire formation.

Modal analyses of 40 thin sections indicate that samples from Indecision Creek and Wandering Ridge (upper sandstone member) are generally richer in quartz and lithic fragments than samples from Northeast Creek and Clark River (Snug Harbor Siltstone Member and lower sandstone member), with the exception of one fine grained, quartz-rich wacke from the Clark River locality (fig. 3). The sandstones from the Indecision Creek and Wandering Ridge sections range from fine-grained, moderately sorted, subangular lithic arkoses and litharenites to very fine grained, very poorly sorted, angular feldspathic and lithic wackes (sandstone terminology of Dott, 1964, and Folk, 1974). The samples from the Northeast Creek and Clark River sections, in contrast, are medium-grained, well-sorted, subangular to subrounded arkoses to very fine grained, poorly sorted, angular feldspathic wackes.

Light-mineral suites in the Naknek sandstones (table 1) are mainly monocrystalline, slightly undulose quartz, minor polycrystalline quartz (ranging from polygonal to straight borders), plagioclase (mainly oligoclase, but varying in amounts of albite and andesine), minor orthoclase, rare microcline and perthite, and very rare chalcedony. The major heavy minerals are biotite, hornblende, epidote, clinozoisite, muscovite, chlorite, and magnetite. These components vary in abundance from sample to sample, but together they compose from 6 to 20 percent of the total grains. Minor heavy minerals generally compose less than 1 percent individually, but up to 1 percent when summed; these are zircon, apatite, garnet of almandine-spessartine composition (fig. 4), sphene, augite, and rare allanite, tremolite, and pumpellyite.

Lithic fragments within the Naknek sandstones are primarily plutonic and metamorphic grains, although volcanic fragments also are abundant in a few samples from the Clark River section (fig. 3). The plutonic rock fragments are mainly quartz-plagioclase, quartz-plagioclase-biotite, and quartz-hornblende composites, and include graphic intergrowths of quartz and plagioclase. The metamorphic rock fragments are chiefly metaquartzite, micaceous metaquartzite, quartz mica schist, mica schist, and rare phyllite, metalimestone, and epidote-quartz-hornfels. Volcanic rock fragments are present in about 60 percent of the samples, but are usually very rare and of the altered silicified type. They are most abundant in two samples from the Northeast Creek section near its top and from three samples from the Clark River section. The weakly altered andesitic to basaltic grains from medium-grained arkoses of the Clark River section commonly exhibit pilotaxitic structure, and the larger grains contain zoned phenocrysts of plagioclase. Sedimentary rock fragments are absent or uncommon in most samples except for soft-sediment rip-up clasts, which were excluded from the calculations in order not to confuse the provenance determinations. The chief sedimentary rock fragments are chert, mudstone, argillite, and limestone. All framework grains are summarized in table 1.

The components of the sandstones from the Naknek Formation indicate a largely magmatic arc provenance with associated metamorphosed country rock. The granitic rock fragments, especially the graphic grains, and monocrystalline grains such as microcline and perthite, point to an igneous plutonic source. Also, minor heavy minerals, namely allanite (determined by X-ray microanalysis, fig. 4), occur almost exclusively in granitic rocks (Deer, Howie, and Zussman, 1962). The volcanic rock components may be associated with the plutons or may be part of older country rock, since many grains are highly silicified. The metamorphic grains, including epidote, clinozoisite, garnet, tremolite, and pumpellyite, were probably eroded from country rock which the plutons intruded, as indicated by the presence of

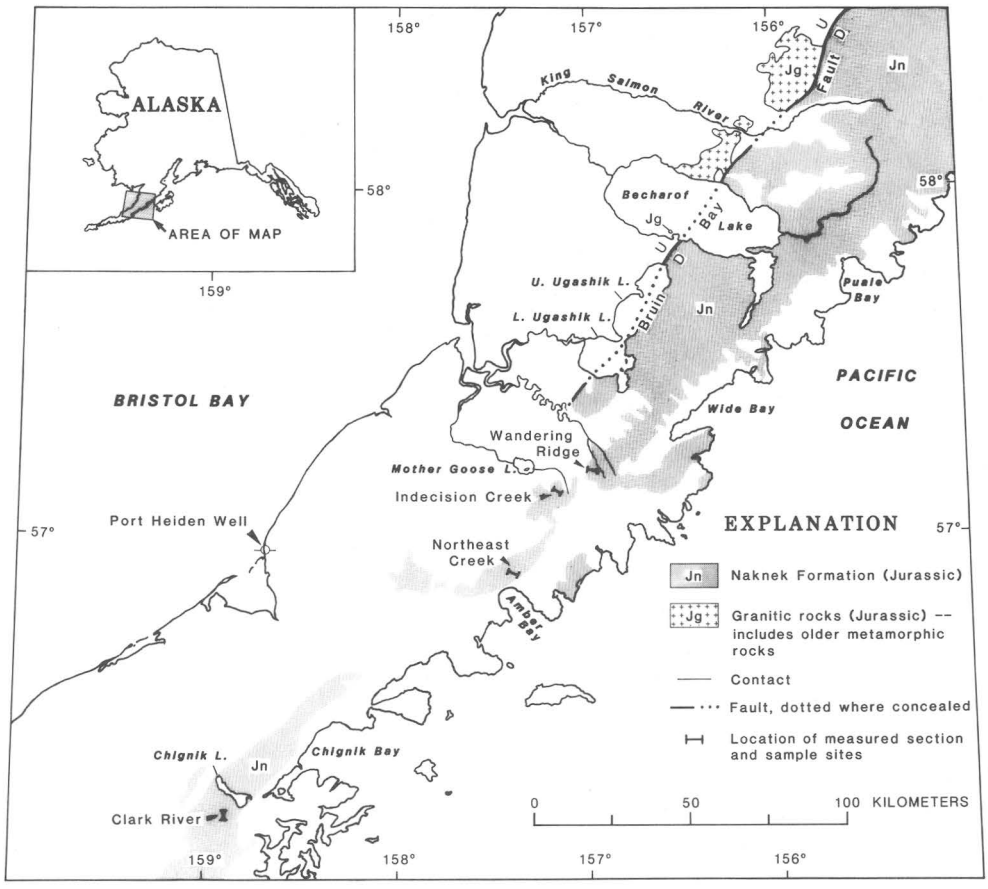

Figure 1.--Index map of study area showing distribution of the Naknek Formation, location of measured sections, and exposed granitic source rocks. Geology from Detterman and others (1981b, 1985) and unpub. data.

hornfels grains. The sedimentary rock fragments may be from several sources. The mudstone and argillite probably were derived from the underlying Middle Jurassic Shelikof and Kialagvik Formations and possibly older rocks; the limestone and chert probably originated from the Upper Triassic Kamishak Formation. Also, the presence in a few samples (mainly the Clark River and Northeast Creek sections) of well-rounded, nonundulose to slightly undulose, monocrystalline quartz grains, some with silica overgrowths, indicate reworking from older sandstones.

The closest outcrops of possible plutonic source rocks are located on an island near the south shore of Lake Becharof and north along the drainage of the King Salmon River (fig. 1). These rocks are the southernmost outcrops of the Alaska-Aleutian Range batholith. They probably underlie much of the study area, as indicated by well data from the Gulf Oil Corporation Port Heiden well, which bottomed in granite of Jurassic age, and by gravity and aeromagnetic anomalies (Andreasen and others, 1963, Case and others, 1981). Metamorphic rocks, including metaquartzite, phyllite, schist, and gneiss, occur as roof pendants in the plutons and are correlated with the Kakhonak Complex of Permian(?) through Jurassic age in the Iliamna quadrangle to the north (Detterman and Reed, 1980).

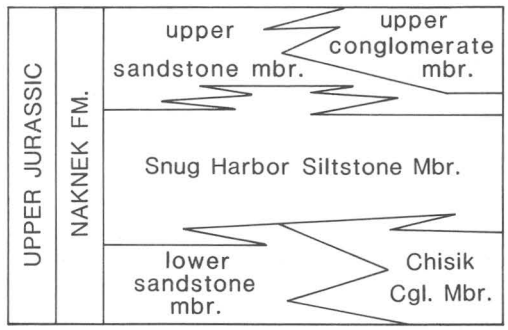

Figure 2.-Schematic diagram showing members of the Naknek Formation on Alaska Peninsula (R.L. Detterman, written commun., 1986).

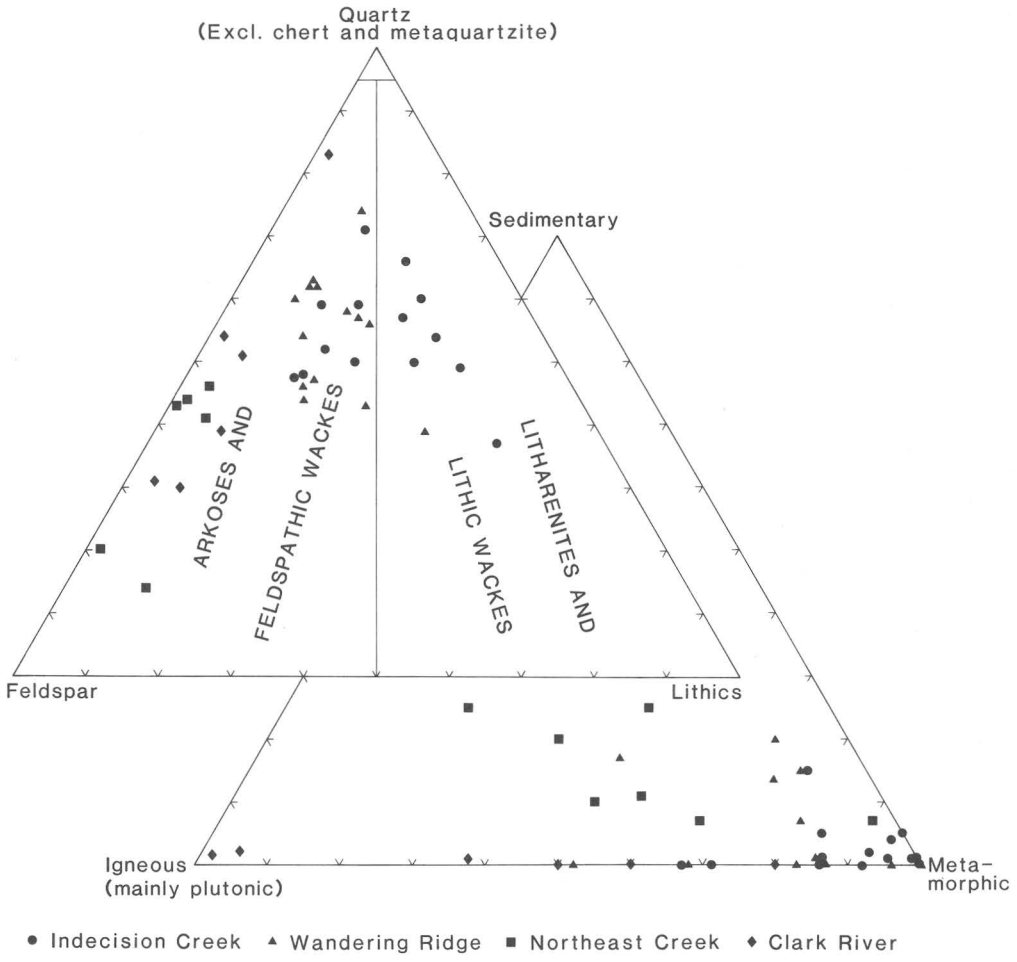

Figure 3.--Triangular Q-F-L and Lithic fragment plots for 40 sandstone thin sections from the Naknek Formation. Classification modified from Dott (1964) and Folk (1974).

The persistence of granitic grains in all the members indicates the presence of a plutonic rock source throughout the depositional history of the Naknek Formation on the Alaska Peninsula. Sandstones of the Snug Harbor Siltstone Member and lower sandstone member at the Northeast Creek and Clark River sections are more arkosic (fig. 3), and they may have been proximal to the granitic source. In addition, the two conglomerate members contain up to 30 percent granitic clasts, which may indicate two major regional uplifts (Detterman and Reed, 1980). The upper sandstone member at the Indecision Creek and Wandering Ridge sections contains more lithic fragments, mainly metamorphic types, and where volcanic rock fragments are present, they are mostly the resistant silicified type. This may represent reworking of sedimentary rocks and the destruction of unstable grains, or increasing exposure of a metamorphic rock source. The

Table 1.--Summary of framework grains from the Naknek Formation on the Alaska Peninsula

Light minerals	Major heavy minerals	Minor heavy minerals	Rock fragments
Quartz	Biotite	Zircon	Metaquartzite
Plagioclase	Hornblende	Apatite	Mica schist
Orthoclase	Epidote	Garnet	Plutonic
Perthite	Clinozoisite	Sphene	Metavolcanic
Microcline	Muscovite	Augite	Volcanic
Chalcedony	Chlorite	Allanite	Epidote-quartz hornfels
	Magnetite	Tremolite	Mudstone
		Pumpellyite	Argillite
			Limestone
			Phyllite
			Chert
			Metalimestone

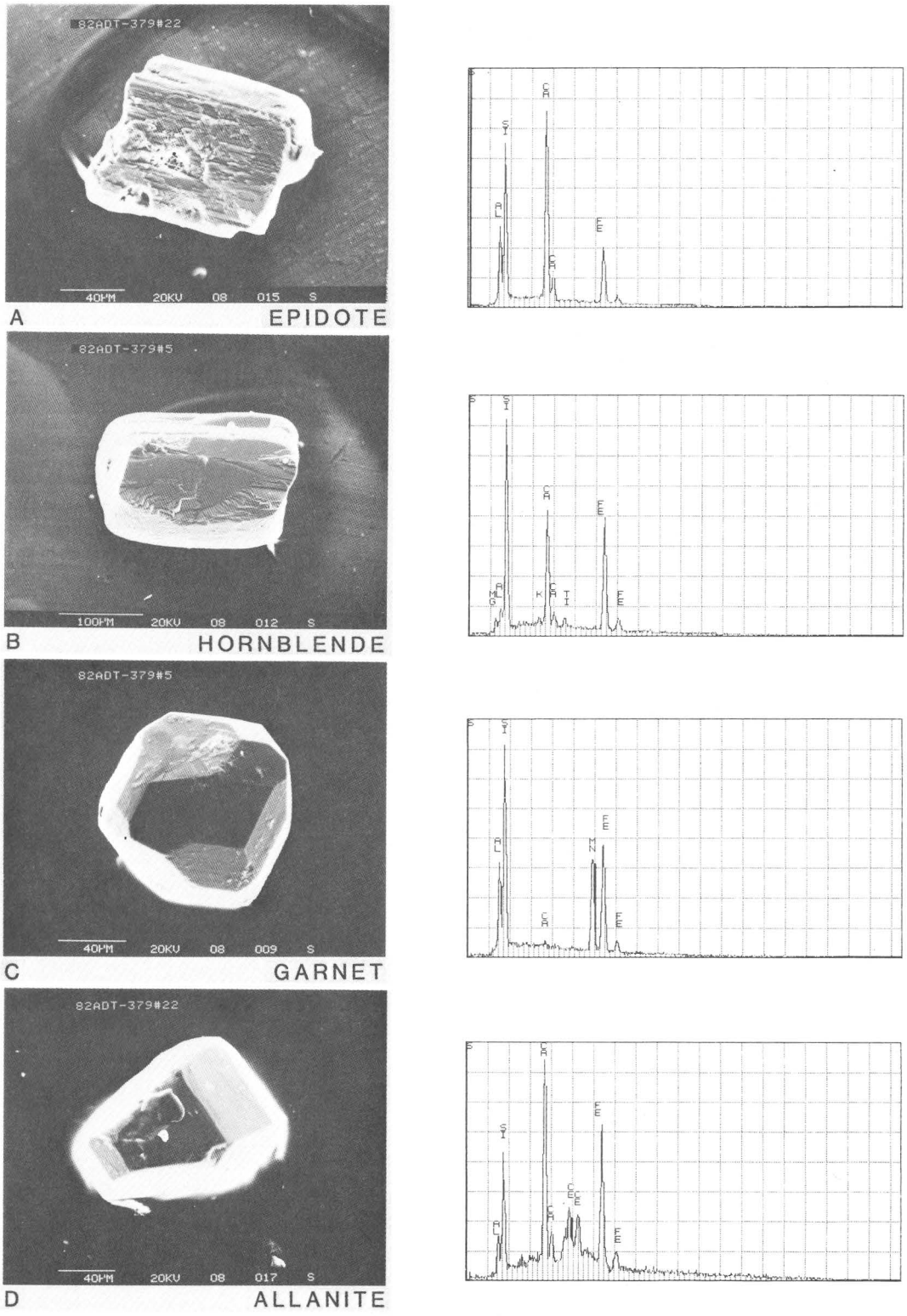

Figure 4.--Scanning electron micrographs and X-ray probe analyses of selected heavy minerals from sandstones of the Naknek Formation. X-ray probe analyses are semiquantitative and show relative amounts of elements present.

presence of large (2.5 mm), weakly altered volcanic fragments in some parts of the Snug Harbor Siltstone Member and the lower sandstone member at the Clark River section may indicate active volcanism near the time of deposition. The recording of a widespead catastrophic event marked by a volcanic graywacke in the Snug Harbor Siltstone Member indicates active volcanism during the time of deposition (Detterman and Miller, 1986). Also, newly examined thin sections from Black Hill, farther south in the northern Cold Bay quadrangle, are from volcanic arenites, which indicate volcanic activity during the deposition of the upper sandstone member.

In summary, compositional analyses of sandstone samples of the Naknek Formation from measured sections shows a largely granitic and subordinate metamorphic source, but volcanic detritus dominates in a few samples from the Snug Harbor Siltstone and lower sandstone members. These compositional data indicate that tectonic uplift of the Alaska-Aleutian Range batholith was nearly continuous throughout the deposition of the Naknek Formation, and that volcanic activity, though sporadic, also continued through Naknek time.

REFERENCES CITED

Andreasen, G.E., Dempsey, W.J., and Vargo, J.L., 1963, Aeromagnetic map of parts of Ugashik and Karluk quadrangles, Alaska: U. S. Geological Survey Geophysical Investigations Map GP-353, scale 1:250,000.

Case, J.E., Barnes, D.F., Detterman, R.L., Morin, R.L., and Sikora, R.F., 1981, Gravity anomaly and interpretation map of the Chignik and Sutwik Island quadrangles, Alaska: U.S. Geological Survey Miscellaneous Field Studies Map MF-1053-J, scale 1:250,000.

Deer, W.A., Howie, R.A., and Zussman, J., 1962, Rock-forming minerals v., 1, ortho- and ring-silicates: London, Longman, 333 p.

Detterman, R.L., Case, J.E., Cox, D.P., Detra, D.E., Miller, T.P., and Wilson, F.H., 1981a, The Alaska Mineral Resource Assessment Program: Background information to accompany folio of geologic and resource maps of the Chignik and Sutwik Island quadrangles, Alaska: U.S. Geological Survey Circular 802, 16 p.

Detterman R.L., and Miller, J.W., 1986, A widespread catastrophic event in the Naknek Formation, Alaska Peninsula, in Bartsch-Winkler, Susan, and Reed, K.M., eds., The United States Geological Survey in Alaska -- Accomplishments during 1985: U.S. Geological Survey Circular 978, p. 27-29.

Detterman, R.L., Miller J.W., and Case, J.E., 1985, Megafossil locality map checklists, and pre-Quaternary stratigraphic sections of Ugashik, Bristol Bay, and part of the Karluk quadrangles, Alaska: U.S. Geological Survey Miscellaneous Field Studies Map MF-1053-A, scale 1:250;000.

Detterman, R.L., Miller, T.P., Yount, M.E., and Wilson, F.H., 1981b, Geologic map of the Chignik and Sutwik Island quadrangles, Alaska: U.S. Geological Survey Miscellaneous Investigation Map I-1229, scale 1:250,000.

Detterman, R.L., and Reed, B.L., 1980, Stratigraphy, structure, and economic geology of the Iliamna quadrangle, Alaska: U.S. Geological Survey Bulletin 1368-B, p. B1-B86.

Dott, R.H., 1964, Wacke, graywacke, and matrix -- What approach to immature sandstone classification?: Journal of Sedimentary Petrology, v. 34, p. 625-632.

Folk, R.L., 1974, Petrology of sedimentary rocks: Austin, Tex., Hemphill, 182 p.

Reviewers: R.L. Detterman and Inyo Ellersieck

SOUTHERN ALASKA

Alaska Range.

EARTHQUAKE-CAUSED SEDIMENTARY COUPLETS IN THE UPPER COOK INLET REGION

Susan Bartsch-Winkler and Henry R. Schmoll

The Cook Inlet region experiences frequent earthquakes as a result of subduction near the Aleutian arc. Earthquakes originate beneath and north of Cook Inlet on the steeply dipping Wadati-Benioff zone, which marks the descent of the Pacific plate into the mantle (Stephens and others, 1986). Although many earthquakes of generally low to moderate magnitude are associated with the Wadati-Benioff zone, only the large magnitude earthquakes that occur closer to the Aleutian trench south and east of Cook Inlet are likely to be capable of significantly affecting intertidal sedimentation in the region. In particular, during the 1964 earthquake (moment magnitude 9.2; Kanamori, 1977), two areas of regional uplift and subsidence were produced in two nearly parallel zones trending southwest-northeast above the gently dipping Aleutian megathrust (Plafker, 1969, fig. 15, p. I-22). Upper Cook Inlet, and especially upper Turnagain Arm, lies within the subsidence zone, which is centered over the Kenai-Chugach Mountains (Plafker, 1969).

Regional uplift and regional and localized subsidence produced by the 1964 earthquake affected intertidal and near-intertidal sediments in south-central Alaska (Plafker and Rubin, 1967; Plafker, 1969; Ovenshine and others, 1976; Bartsch-Winkler and Schmoll, 1984a). Relative sea-level changes along the coast are recorded in sedimentary sequences at the affected sites (figs. 1 and 2). Areas of accumulating organic sediments, particularly marsh areas that have undergone earthquake-induced subsidence and are preserved beneath subsequently deposited sediments, can be dated by the radiocarbon method and the age of the earthquake event thus determined (Plafker and Rubin, 1967; Plafker, 1972; Ovenshine, 1976; Bartsch-Winkler and others, 1983; Bartsch-Winkler and Schmoll, 1984b; Atwater and Grant, 1986).

In the Portage area at the head of Turnagain Arm (fig. 1), upper intertidal or freshwater marshlands subsided into the lower intertidal zone and were covered with deeper-water (tidal) sediment at the time of the 1964 earthquake (Ovenshine and others, 1976). The postearthquake intertidal deposit, the Placer River Silt of Ovenshine and others (1976), and the underlying unnamed 1964 marsh deposit were described. The subsidence-induced deposition at Portage, which totals as much as 2.5 m in thickness in some locations, has been subsequently monitored; the sedimentation rate has declined to nearly nil and the surrounding area has attained a state of equilibrium only 20 years after the earthquake (Bartsch-Winkler and Garrow, 1982). That is, a new marsh and forest have become established in an area where marsh and forest were destroyed by subsidence into the intertidal zone at the time of the 1964 earthquake.

Our data from Upper Cook Inlet support the suppositions of Plafker (1972) and of Ovenshine and others (1976) that older submerged marsh and forest layers would be found in intertidal zones of regions experiencing earthquakes. Such organic horizons beneath intertidal silt form depositional packages termed "earthquake couplets" by A.T. Ovenshine (U.S.G.S., written commun., 1976). When dated by radiocarbon methods, these couplets provide information on the late Holocene earthquake history of the region surrounding Anchorage.

Seventeen sections have been measured in the intertidal zone of the Susitna Lowland, Knik Arm, and Turnagain Arm (figs. 1 and 2). Two sections in the Placer River Silt at Portage (secs. 16, 17) have been described previously (Ovenshine and others, 1976), as have two sections (secs. 5,6) in convoluted and hummocky beds of the lower intertidal zone at Anchorage and within Knik Arm (Bartsch-Winkler and Schmoll, 1984b). Section 10 was measured in a drainage channel constructed after the earthquake in June 1983, and the remaining 13 sections (secs. 1-4, 7-9, and 11-15) were measured in July 1986.

The bases of most of the sections are at the lower-low tide level or at river level. Tops of the sections vary with the availability of exposure at each site, but most are within the upper intertidal zone. The elevations of the upper, middle, and lower intertidal zones vary throughout Upper Cook Inlet region; maximum tide range is about 11.4 m (35 ft) at the official tide station at Anchorage. Records from the unofficial tide station midway in Turnagain Arm near Hope indicate a larger mean tide range there than at Anchorage. The tide range at the mouth of the Little Susitna River is not documented. Because the tide range is large in this estuary, an effort was made to observe the deposits that had bases at tide level when the tide range was the greatest for the month (spring tide) and at lower-low tide; this enabled measurement during maximum exposure at the base of the sections.

Sections 3 and sections 8-11, located within the upper intertidal zone, contain the most abundant organic material (fig. 2) because of their position near the continuous marsh zone. Conversely, sections 4-6, located within the lower intertidal zone, contain the largest proportion of inorganic silt and sand and are the only sections that contain shell debris. Sections 1-2, 7, 12-15, and 17 are located in a narrow zone in the middle of the intertidal region, here called the middle intertidal zone. Section 16 was measured within the Twentymile River channel, a major fluvial and

estuarine channel that drains extensive glacial and estuarine areas of the Portage flats. With the exception of section 16, which contains a large amount of sediment carried by this river, the sections measured in the middle intertidal zone have the greatest number of distinct organic layers separated by intertidal silt deposits.

The middle intertidal zone is the most useful region for locating earthquake-induced sedimentary couplets. This zone has numerous distinct peat and wood layers intercalated with silt, a deposit that results from the burial of marsh and forest by intertidal sediment after earthquake-induced subsidence (fig. 3). Earthquake events can be identified by dating radiocarbon samples collected from the top of the organic layers and correlating them with other such radiocarbon-dated layers in the Upper Cook Inlet region (table 1). By dating organic material from the base of organic layers and measuring their thickness, the rate of accretion of the marsh might also be determined.

Table 1.--Radiocarbon dates and laboratory numbers of samples collected from Upper Cook Inlet as of 1983

Radiocarbon date (yr B.P.)	Laboratory No.	Section No.	Reference
180 ± 45	USGS-332	17	Ovenshine and others (1976)
350 ± 80	I-12,027	5	Bartsch-Winkler and Schmoll (1984b)
635 ± 40	USGS-1780	10	This paper
1,000 ± 70	USGS-1781	10	This paper
1,480 ± 50	USGS-1782	10	This paper
1,595 ± 75	I-11,767	5	Bartsch-Winkler and Schmoll (1984b)
1,825 ± 45	USGS-1570	6	Bartsch-Winkler and Schmoll (1984b)
1,840 ± 50	USGS-1117	15	This paper
2,350 ± 125	I-12,008	6	Bartsch-Winkler and Schmoll (1984b)
3,040 ± 50	USGS-1573	6	Bartsch-Winkler and Schmoll (1984b)
3,205 ± 110	I-11,718	6	Bartsch-Winkler and Schmoll (1984b)
3,270 ± 90	I-11,717	5	Bartsch-Winkler and Schmoll (1984b)
3,280 ± 90	I-11,706	6	Bartsch-Winkler and Schmoll (1984b)

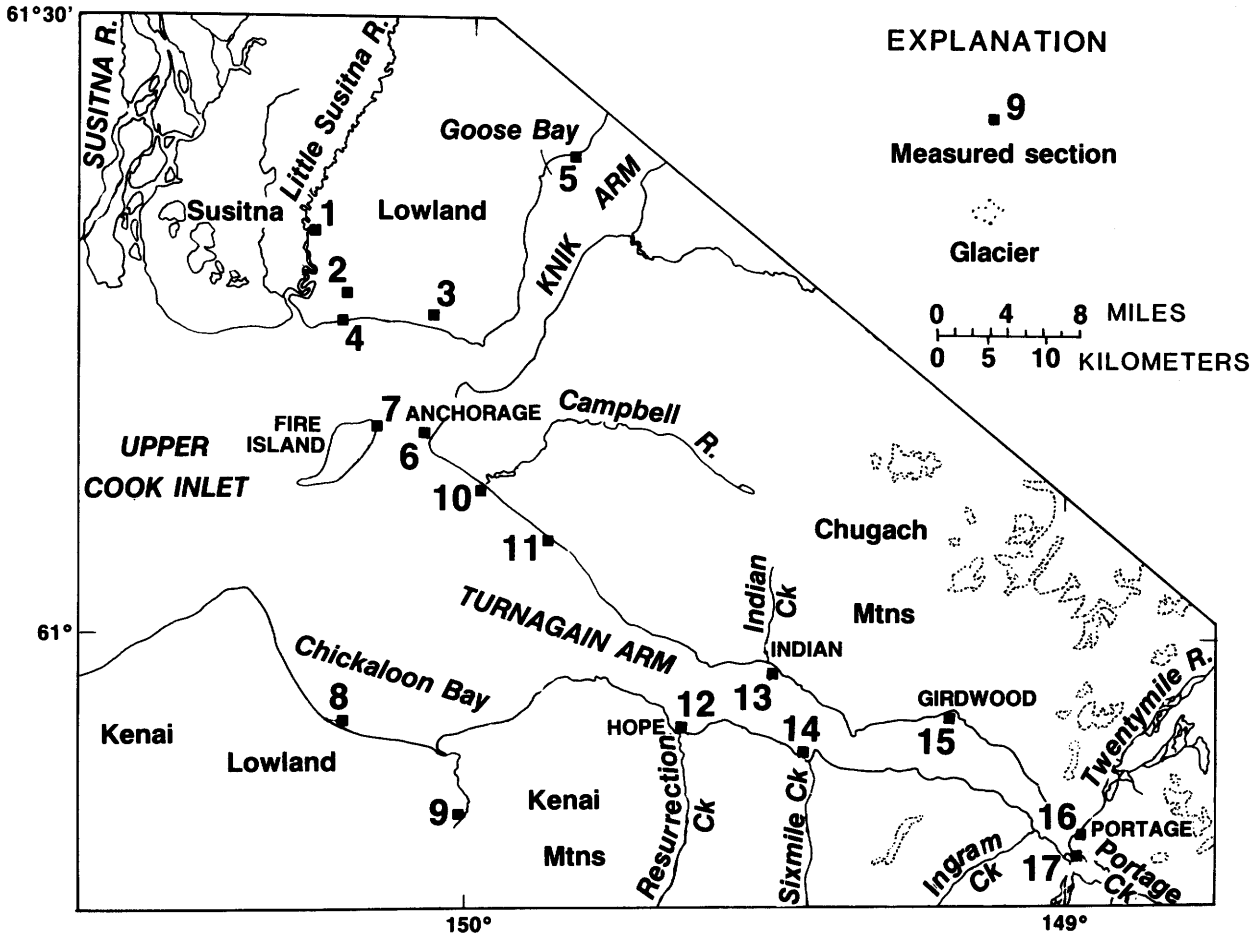

Figure 1.--Upper Cook Inlet showing locations of measured stratigraphic sections in intertidal deposits.

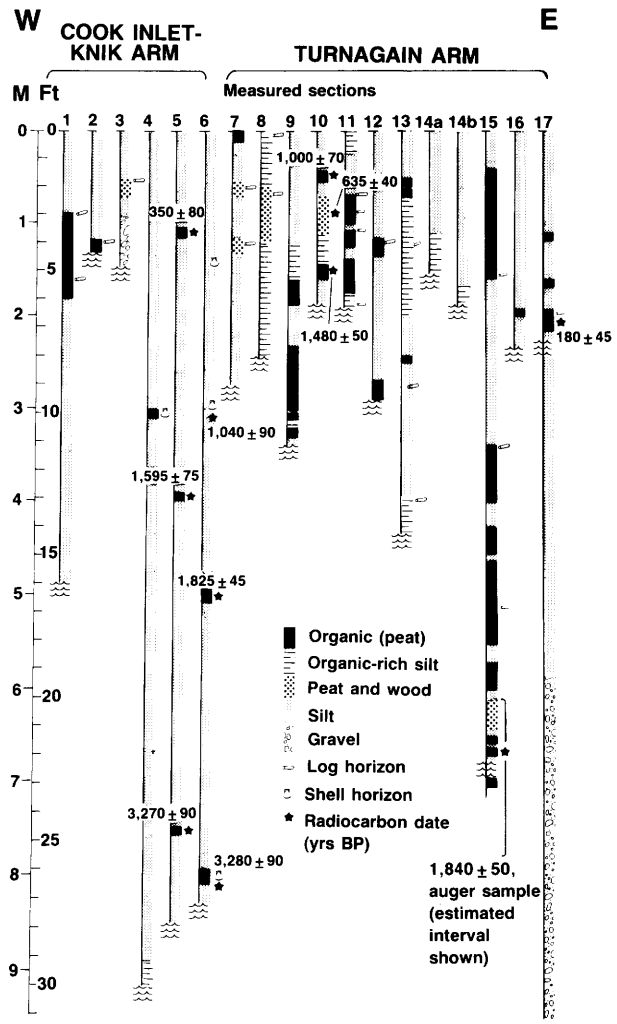

Figure 2.--Stratigraphic sections showing organic layers and lithologies, wood and shell horizons, and radiocarbon-dated samples at 17 sites in Upper Cook Inlet. The tide or stream level is indicated by wave symbol. Table 1 lists pertinent information on radiocarbon dates.

Earthquake recurrence is more difficult to determine from sediment and organic layers deposited above or below the middle intertidal zone. In the upper intertidal zone, pre- and post-earthquake organic layers commonly are deposited directly above each other without intervening intertidal silt layers (fig. 3.). Discrete log layers enclosed in peat are the most likely indicators of an earthquake in this zone, because subsidence of the coastal forest immediately following an earthquake would result in forest kill by saltwater incursion (as occurred in 1964 at Portage). In the lower intertidal zone, in contrast, the absence of in situ organic-rich layers complicates the analysis. In this zone, bedding discontinuities, such as planar beds that truncate underlying contorted beds, are the best criteria for distinguishing earthquakes (Bartsch-Winkler and Schmoll, 1984b). Because such discontinuities might be caused by sedimentary processes other than those induced by earthquakes (see Bartsch-Winkler and Schmoll, 1984b, p. 1246-1248), they cannot be used alone to date earthquake events in these areas.

As indicated by the sedimentary sequences measured in our 17 sections from the intertidal zone of Upper Cook Inlet, the most reliable area for obtaining earthquake-caused sedimentary couplets from the Upper Cook Inlet intertidal zone is the narrow, middle intertidal region. The 11 radiocarbon dates presently available from 4 of our 17 sections (table 1) suggest that earthquake-related events may have occurred repeatedly throughout Cook Inlet during late Holocene time. This hypothesis is currently being tested by radiocarbon dating that is now in progress on over 50 additional organic samples that we collected from our measured sections in 1986.

REFERENCES CITED

Atwater, B.F., and Grant, W.C., 1986, Holocene subduction earthquakes in coastal Washington (abs.): Eos (Transactions, American Geophysical Union), v. 67, no. 44, p. 906.

Bartsch-Winkler, Susan and Garrow, H.C., 1982, Depositional system approaching maturity at Portage Flats, in Coonrad, W.L., ed., The United States Geological Survey in Alaska--Accomplishments during 1980: U.S. Geological Survey Circular 844, p. 115-117.

Bartsch-Winkler, Susan, Ovenshine, A.T., and Kachadoorian, Reuben, 1983, Holocene history of the estuarine area surrounding Portage, Alaska, as recorded in a 93-m core: Canadian Journal of Earth Science, v. 20, no. 5, p. 802-820.

Bartsch-Winkler, Susan, and Schmoll, H.R., 1984a, Guide to Late Pleistocene and Holocene deposits of Turnagain Arm, Alaska: Anchorage, Alaska Geological Society, 70 p., 2 maps (Fieldtrip guide for the 80th Cordilleran Section Meeting, Geological Society of America).

___ 1984b, Bedding types in Holocene tidal channel sequences, Knik Arm, Upper Cook Inlet, Alaska: Journal of Sedimentary Petrology, v. 54, no. 4, p. 1239-1250.

Kanamori, Hiroo, 1977, The energy release in great earthquakes: Journal of Geophysical Research, v. 82, p. 2981-2987.

Ovenshine, A.T., Lawson, D.E., and Bartsch, S.R., 1976, The Placer River Silt--Intertidal sedimentation caused by the Alaska earthquake of March 27, 1964: U.S. Geological Survey Journal of Research, v. 4, no. 2, Mar-Apr 1976, p. 151-162.

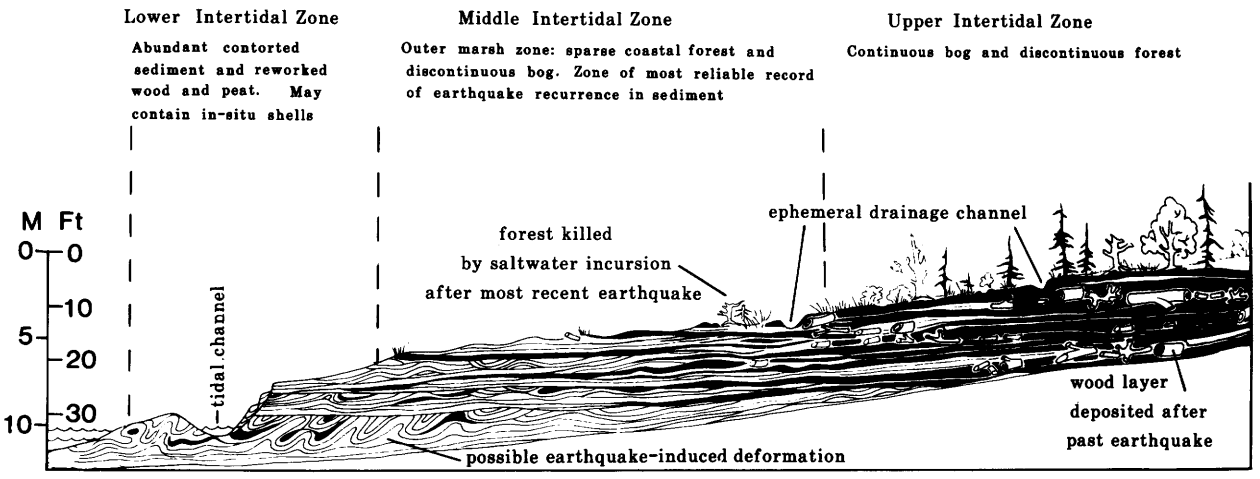

Figure 3.--Diagrammatic section showing characteristics of upper, middle, and lower intertidal zones and sedimentary features indicative of earthquake deformation. Model assumes a constant shoreline position not subject to progradation or regression.

Plafker, George, 1969, Tectonics of the March 27, 1964 Alaska earthquake, in The Alaska Earthquake, March 27, 1964: Regional effects: U.S. Geological Survey Professional Paper 543-I, p. I1-I74.

Plafker, George, 1972, Alaskan earthquake of 1964 and Chilean earthquake of 1960--Implications for arc tectonics: Journal of Geophysical Research, v. 77, no. 5, p. 901-925.

Plafker, George, and Rubin, Meyer, 1967, Vertical tectonic displacements in south-central Alaska during and prior to the Great 1964 Earthquake: Journal of Geosciences, Osaka City University, v. 10, p. 53-66.

Stephens, C.D., Fogleman, K.A., Lahr, J.C., and Page, R.A., 1986, Seismicity in southern Alaska, October 1984-September 1985; in Bartsch-Winkler, Susan, and Reed, K.M., eds., Geologic studies in Alaska by the U.S. Geological Survey during 1985: U.S. Geological Survey Circular 978, p. 81-85.

Reviewers: A.F. Espinosa and J.R. Riehle

LATE TRIASSIC AND EARLY CRETACEOUS FOSSIL AGES FROM THE McHUGH COMPLEX, SOUTHERN ALASKA

Steven W. Nelson, Charles D. Blome, and Susan M. Karl

The McHugh Complex of southern Alaska was recognized and named by Clark (1972, 1973) and was considered to be of Late Jurassic and (or) Cretaceous age. Plafker and others (1976) included the McHugh Complex in the melange facies of the accretionary Chugach terrane. In general, the McHugh Complex is considered to be a melange of low-grade metamorphosed sedimentary and volcanic rocks that includes irregular sized blocks and clasts of chert, marble, plutonic, volcanic, and ultramafic rocks. Clark (1973) recognized two chaotically juxtaposed lithologic associations within the type locality --a metasedimentary association and a metavolcanic association. The metasedimentary association, which makes up most of the complex, includes weakly metamorphosed siltstone, graywacke, arkose, and conglomerate. The metavolcanic association includes blocks of mafic greenstone, ultramafic rocks, and marble associated with lenses and blocks of radiolarian chert in siliceous argillite, and argillite. The previously reported range of paleontologic ages for the McHugh Complex in the Anchorage area, summarized by Nelson and others (1986), was Pennsylvanian(?) to Early Cretaceous. Nelson and others (1986) reported new fossil ages of Late Mississippian through Early Pennsylvanian and Early Jurassic and suggested possible source terranes for rock units found in the melange. This report discusses new radiolarian fossil ages (Late Triassic and Early Cretaceous) determined by Blome from the type locality of the McHugh Complex. The Late Triassic radiolarians are the first reported from this area. The Early Cretaceous radiolarian faunas have a similar age range, but somewhat different fauna than that reported by Karl and others (1979).

Two Early Cretaceous sites are located on the north side of the Seward Highway in sec. 15, T. 11 N., R. 3 W., Anchorage A-8 quadrangle, 3.25 km and 3.4 km northwest of VABM Isle (fig. 1). The more southerly site (#1 on fig. 1) consists of red-weathering ribbon chert in layers averaging 4 cm in thickness. Radiolarians present include *Archaeodictyomitra excellens* (Tan Sin Hok), *Mirifusus baileyi* Pessagno, *Parvicingula citae* Pessagno, *Pseudodictyomitra carpatica* (Loznyak), *Pseudodictyomitra depressa* Baumgartner, *Sethocapsa cetia* Foreman, and *Thanarla conica* (Aliev). These fauna are considered to be Berriasian to Hauterivian in age. This collection was made approximately 4 m south of a chert locality containing Early Jurassic radiolarians (Nelson and others, 1986).

The more northerly of the two Cretaceous sites (#2 on fig. 1) is along a 150-m-long road cut that is predominantly massive greenstone with subordinate dark-gray argillite and gray chert. Radiolarians present include *Archaeodictyomitra apiara* (Rust), *Archaeodictyomitra excellens* (Tan Sin Hok), *Parvicingula citae* Pessagno, *Pseudodictyomitra* sp. cf. *carpatica* (Loznyak), *Sethocapsa* sp., and *Ristola cretacea* Baumgartner. The age of the fauna is considered to be Berriasian to late Valanginian.

The Triassic site (#3 on fig. 1) is located in sec. 23, T. 11 N., R. 3 W. of the Anchorage A-8 quadrangle, 2.9 km northwest of VABM Isle. Here, gray chert occurs as centimeter-sized lenses or boudins in a sheared, black argillaceous matrix. Approximately 50 percent of the outcrop area is composed of the argillite with approximately 30 percent gray chert lenses and 20 percent green metavolcanic (tuff?) in centimeter-scale layers. Radiolarians present include *Betraccium*(?) sp. cf. *incohatum* Blome, *Canoptum* sp aff. *farawayense* Blome, *Canoptum* sp., *Pseudostylosphaera* sp., and *Triassocampe* sp. The age of this fauna is considered to be late Carnian or early Norian. It is noteworthy that the Triassic chert occurs as thin layers alternating with tuff and argillite, whereas the younger cherts commonly occur as monolithologic blocks of ribbon chert associated with greenstone or as independent blocks in an argillite matrix.

Triassic fossil ages from the McHugh Complex have not been reported previously from the type locality. Triassic fossil ages have, however, been recognized from some correlative units elsewhere in Alaska that also contain younger fossils (fig. 2). Units stratigraphically correlative, at least in part, with the McHugh Complex are the Kelp Bay Group in southeastern Alaska (Decker, 1980; Johnson and Karl, 1985), the

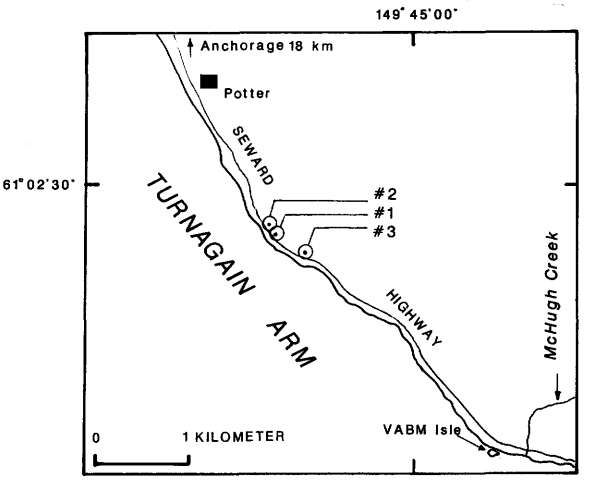

Figure 1.--Locality map for microfossil collections from the McHugh Complex.

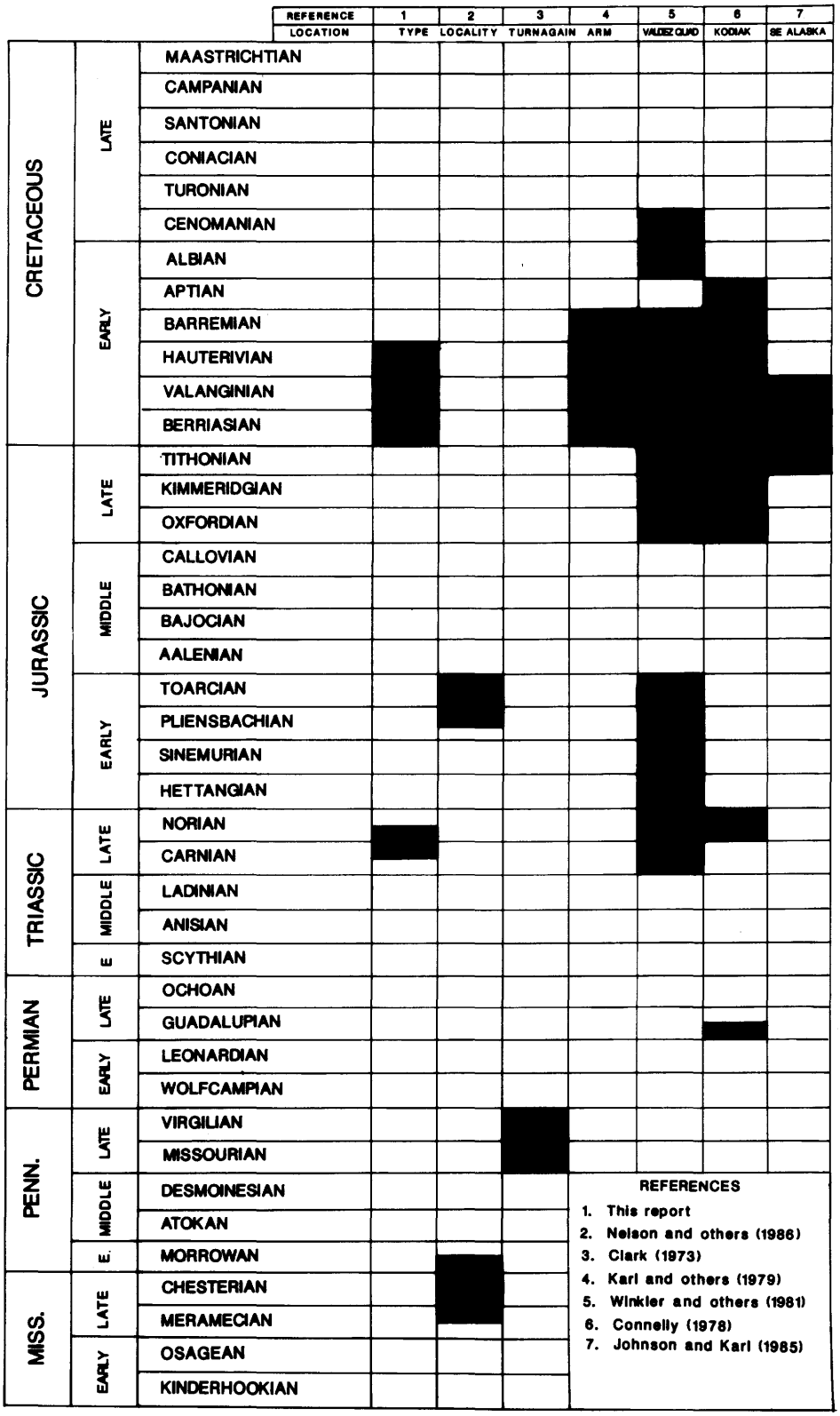

Figure 2.--Age range of fossils from the McHugh Complex and related units.

Seldovia Bay Complex on the Kenai Peninsula (Cowan and Boss, 1978), and the Uyak Complex (Connelly, 1978) on Kodiak Island. Winkler and others (1981) recognized three "belts" of fossil ages within the McHugh Complex in the Valdez quadrangle; a northern belt containing Late Triassic radiolarians only, a middle belt with Jurassic and Cretaceous radiolarians, and a southern belt with radiolarians as young as mid-Cretaceous. On Kodiak Island, Connelly (1978) reported on a hydrozoan from the Uyak Complex that is similar to a Late Triassic (Norian) hydrozoan found on the Alaska Peninsula; he also reported radiolarian ages ranging from Late Jurassic into Early Cretaceous (fig. 2). In the Seldovia Bay Complex, as recognized by Cowan and Boss (1978), Triassic radiolarians were identified from a mappable unit of contorted chert and greenstone (G. Plafker, 1976, oral commun., in Cowan and Boss, 1978). Kelley (1985) however believed that the fault-bounded chert and greenstone belongs to the Kachemak terrane of Jones and others (1981) and that it is separate from the Chugach terrane. Kelley (1985) describes the McHugh Complex in this area as largely composed of an association of graywacke and altered volcaniclastic rocks, chert, and no metavolcanic association.

The presence of Triassic fossils from the type locality of the McHugh Complex suggests that the protolith ages in the McHugh Complex span most of the Mesozoic and may represent diverse pelagic and hemipelagic environments, and that rock units that are elsewhere recognizable as separate map units have been structurally incorporated into the McHugh Complex in the type locality.

The Early Cretaceous fauna reported herein increases the number of radiolarian species of this age identified from the McHugh Complex. Mid-Cretaceous fossils from the Valdez quadrangle (Winkler and others, 1981) are the youngest yet reported and are probably representative of the age of accretion of the McHugh Complex (Plafker and others, 1985). Thus an accretionary age rather than a protolith age may be the most appropriate for the McHugh Complex.

REFERENCES CITED

Clark, S.H.B., 1972, Reconnaissance bedrock geologic map of the Chugach Mountains near Anchorage, Alaska: U.S. Geological Survey Miscellaneous Field Studies Map MF-350, 1 sheet, scale 1:250,000.

____ 1973, The McHugh Complex of south-central Alaska: U.S. Geological Survey Bulletin 1372-D, p. D1-D11.

Connelly, William, 1978, Uyak Complex, Kodiak Islands, Alaska -- A Cretaceous subduction complex: Geological Society of America Bulletin, v. 89, p. 755-769.

Cowan, D.S., and Boss, R.F., 1978, Tectonic framework of the southwestern Kenai Peninsula, Alaska: Geological Society of America Bulletin, v. 89, p. 155-158.

Decker, John, 1980, Geology of a Cretaceous subduction complex, western Chichagof Island, southeastern Alaska: Stanford, Calif., Stanford University, Ph.D. thesis, 135 p.

Johnson, B.R., and Karl, S.M., 1985, Geologic map of western Chichagof and Yakobi Islands, southeastern Alaska: U.S. Geological Survey Miscellaneous Investigations Series Map I-1506, 2 sheets, scale 1:250,000, 15 p.

Jones, D.L., Silberling, N.J., Berg, H.C., and Plafker, George, 1981, Tectonostratigraphic terrane map of Alaska: U.S. Geological Survey Open-File Report 81-792, 2 sheets.

Karl, Susan, Decker, John, and Jones, D.L., 1979, Early Cretaceous radiolarians from the McHugh Complex, south-central Alaska, in Johnson, K.M., and Williams, J.R., eds., The United States Geological Survey in Alaska--Accomplishments during 1978: U.S. Geological Survey Circular 804-B, p. B88-B90.

Kelley, J.S., 1985, Geology of the southwestern tip of the Kenai Peninsula, in Sisson, A., ed., Guide to the geology of the Kenai Peninsula, Alaska: Anchorage, Alaska Geological Society Guidebook, p. 50-68.

Nelson, S.W., Blome, C.D., Harris, A.G., Reed, K.M., and Wilson, F.H., 1986, Late Paleozoic and Early Jurassic fossil ages from the McHugh Complex, Alaska, in Bartsch-Winkler, Susan, and Reed, K.M., eds., Geological Studies in Alaska by the U.S. Geological Survey during 1985: U.S. Geological Survey Circular 978, p. 60-63.

Plafker, George, Jones, D.L., Hudson, Travis, and Berg, H.C., 1976, The Border Ranges fault system in the Saint Elias Mountains and the Alexander Archipelago, in Cobb, E.H., ed., The United States Geological Survey in Alaska--Accomplishments during 1975: U.S. Geological Survey Circular 733, p. 14-16.

Plafker, George, Nokleberg, W.J., and Lull, J.S., 1985, Summary of 1984 TACT geologic studies in the northern Chugach Mountains and southern Copper River Basin, in Bartsch-Winkler, Susan, ed., The United States Geological Survey in Alaska--Accomplishments during 1984: U.S. Geological Survey Circular 967, p. 76-79.

Winkler, G.R., Silberman, M.L., Grantz, Arthur, Miller, R.J., and Mackevett, E.M., Jr., 1981, Geologic map and summary geochronology of the Valdez quadrangle, southern Alaska: U.S. Geological Survey Open-File Report 80-892A, 2 sheets, scale 1:250,000.

Reviewers: J.H. Dover and M.L. Miller

EFFECTS OF WEATHERING ON PETROLEUM-SOURCE EVALUATION OF COALS FROM THE SUNTRANA FORMATION NEAR HEALY, ALASKA

Richard G. Stanley

Rock-Eval pyrolysis is a rapid and effective laboratory method of evaluating the quality and thermal maturity of prospective petroleum source rocks (Peters, 1986). Since its introduction about 10 years ago, the Rock-Eval method has been widely accepted by petroleum geologists and applied to samples from both surface outcrops and wells. The procedure mimics the natural hydrocarbon-generation processes which occur at much slower rates within the earth when sediments containing kerogen (organic matter) are buried progressively deeper and subjected to higher temperatures (Waples, 1985). In Rock-Eval pyrolysis, pulverized samples of rock are gradually heated from 300 °C to 550 °C at 25 °C per minute in an oxygen-free atmosphere (Peters, 1986). Heating causes the release of water, carbon dioxide, and two batches of hydrocarbons from the rock. The first batch of hydrocarbons is released at about 300 °C and consists of volatile organic compounds, such as oil and gas, that are already present in the rock. A detector on the Rock-Eval apparatus measures the quantity of these first hydrocarbons (HC), called S1, in milligrams HC per gram of rock. As the temperature rises above 350 °C, a second batch of hydrocarbons called S2 (also measured in milligrams HC per gram of rock) is released. S2 represents the organic compounds generated by thermal degradation of the remaining kerogen in the rock, and is an important indicator of the remaining ability of the rock to generate oil and gas. The temperature at which S2 is at a maximum--generally about 400 °C to 500 °C--is known as Tmax and is an indicator of thermal maturity. A third quantity, called S3, is the amount of carbon dioxide (in milligrams per gram of rock) that is generated during pyrolysis, stored in a collector, and measured at the end of the procedure. S3 is thought to be related to the amount of oxygen in the kerogen. Other important Rock-Eval parameters include TOC, the total organic carbon in weight percent; HI, the hydrogen index, defined as the product of 100 times (S2/TOC); and OI, the oxygen index, defined as the product of 100 times (S3/TOC).

As part of a project aimed at assessing the petroleum resources of interior Alaska, I am using the Rock-Eval technique to evaluate the petroleum source potential of Tertiary nonmarine coals and mudrocks that crop out in the central Alaska Range (fig. 1). These Tertiary nonmarine strata are believed to be similar in age and lithology to subsurface strata in the middle Tanana basin (fig. 1), a prospective petroleum province (Miller and others, 1959; Hite and Nakayama, 1980). Well samples from this frontier area are scarce, and identification of potential source rocks must therefore be based mainly on outcrop samples. In order to properly evaluate such surface samples, it is important to understand the effects of weathering on organic matter and on the results of Rock-Eval pyrolysis. Published data on this subject are sparse, however. Studies by Clayton and Swetland (1978) and Leythaeuser (1973) used wet-chemical methods (not Rock-Eval pyrolysis) to show that surface weathering can result in a decrease in the amount of organic matter as well as changes in its composition. Peters (1986), in an otherwise thorough discussion of Rock-Eval pyrolysis, noted that weathered samples commonly show depletion in S1 and S2 as well as elevated S3 and Tmax, but provided no data to support these conclusions.

Ten samples of subbituminous coal from fresh excavations and weathered outcrops were collected from coal beds of the middle Miocene Suntrana Formation (Wahrhaftig and others, 1969) and studied using Rock-Eval pyrolysis and thermal alteration index (TAI). (Thermal alteration index is a method of using the color of pollen grains and other kerogen, as viewed through a microscope using transmitted light, to determine the thermal maturity of the rock.) The purposes of this investigation were (1) to evaluate the petroleum source potential of the coals and (2) to determine whether there are any systematic differences in Rock-Eval results between coals collected from fresh excavations and stratigraphically equivalent coals collected from weathered outcrops.

Six relatively fresh samples of coal were obtained from open-pit excavations in the "Poker Flats" area of the Usibelli coal mine near the town of Healy, in the Healy (D-4) quadrangle (fig. 1). Coal bed number 3 was sampled in an excavation about 17 days old, and coal bed number 4 was sampled in an excavation less than 24 hours old (Wendel Parker, Chief Engineer, Usibelli Coal Mine, Inc., oral commun., 1985). Four additional samples of coal were obtained from coal beds 3 and 4 at weathered outcrops along strike and about 800 m east of the Poker Flats excavations. All of the samples were transported from the field to the laboratory in sealed plastic bags to prevent contamination. Splits of the samples were analyzed using Rock-Eval pyrolysis by T.A. Daws (U.S. Geological Survey, Denver, Colo.) and thermal alteration index (TAI) by Hideyo Haga (Micropaleo Consultants, Inc., San Diego, Calif.). The results (tables 1 and 2) allow some preliminary conclusions regarding the quantity, type, and thermal maturity of organic matter in the sampled coals, and also show some systematic differences between fresh and weathered samples.

The quantity of organic matter in the samples is indicated by TOC, S1, and S2. The TOC

Table 1.--Rock-Eval and thermal alteration index (TAI) data for samples of coal from the Suntrana Formation near Healy, Alaska
[See fig. 1 for location of samples. See text for explanation of symbols in headings]

Sample No.	Coal bed No.	TOC (wt. pct.)	HI	OI	Sample weight (mg)	S1 (mg HC/ g rock)	S2 (mg HC/ g rock)	S3 (mg CO_2/ g rock)	S1/(S1+S2)	S2/S3	Tmax (°C)	TAI	Interpretation*
A. "Poker Flats" pit (fresh excavations), lat 63°54'09"N., long 148°55'54"W.:													
A1	4	58.12	156	47	10.9	2.66	91.00	27.88	0.03	3.26	392	2.0	GOP, IM
A2	4	54.26	167	48	12.5	4.08	90.88	26.24	.04	3.46	393	2.0-2.5	GOP, IM
A3	4	55.28	150	55	7.7	2.46	83.11	30.64	.03	2.71	400	2.0	GP, IM
A4	3	59.54	141	54	8.9	2.13	84.49	32.35	.02	2.61	407	2.3?	GP, IM
A5	3	62.19	131	55	11.5	2.17	82.08	34.78	.03	2.35	399	2.5-3.5	GP, IM
A6	3	62.52	141	55	10.4	1.92	88.46	34.61	.02	2.55	409	2.5-3.5?	GP, IM
B. "Poker Flats" area (weathered roadcut), lat 63°54'02"N., long 148°54'50"W.:													
B1	4	57.98	129	56	9.5	3.05	74.94	32.84	0.04	2.28	400	2.0-2.5	GP, IM
B2	4	39.11	185	107	10.5	2.85	72.38	41.90	.04	1.72	400	2.0	GOP, IM
C. "Poker Flats" area (weathered streamcut), lat 63°54'10"N., long 148°54'54"W.:													
C1	3	58.48	126	85	8.3	2.16	74.21	50.12	0.03	1.48	408	2.0-2.3	GP, IM
C2	3	39.07	155	115	10.6	1.32	60.75	45.28	.02	1.34	420	2.0-2.3	GOP, IM

*Abbreviations: GP, gas prone; GOP, gas and oil(?) prone; IM, thermally immature with respect to the oil-generative zone. An interpretation of "GOP" was assigned to any rock that showed HI>150 or S2/S3>3.0.

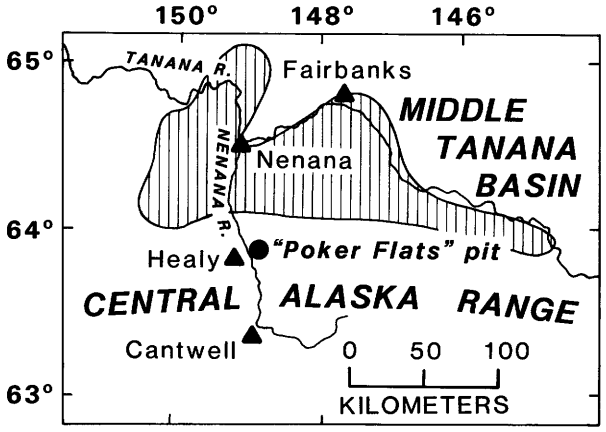

Figure 1.--Location map. Filled circle at "Poker Flats" pit gives general location of sample sites A, B, and C (table 1). Vertical ruling denotes subsurface "middle Tanana basin" as mapped by Miller and others (1959).

of the sampled coals ranges from 39.07 percent to 62.52 percent (table 1), indicating that these rocks have "very good" generative potential according to the classification of Peters (1986). The TOC values of samples from fresh excavations are generally but not consistently higher than those from weathered outcrops (table 2). Both fresh and weathered samples exhibit values of S1 greater than 1.3 and S2 greater than 60, indicating that all of the samples have "good" to "very good" generative potential according to the classification of Peters (1986). Values of S1 are about the same in fresh and weathered samples, but S2 is consistently higher in the fresh coals and S3 higher in the weathered coals (table 2).

The type of organic matter in the samples is shown on a modified van Krevelen diagram (fig. 2) and also is indicated by the hydrogen index (HI), oxygen index (OI), and the ratio S2/S3. A modified van Krevelen diagram (fig. 2) is a plot of HI against OI that is used to compare sample results with four idealized types of kerogen. Type I and Type II kerogens are "oil prone", or capable of generating oil; Type III kerogens are "gas prone", or capable of generating gas but little or no oil; and Type IV kerogens are variously regarded as oil prone, gas prone, or inert (Smyth, 1983; Tissot and Welte, 1984; Peters, 1986). All of the sampled coals from the Suntrana Formation--both fresh and weathered--plot between kerogen types II and III but closer to type III on the van Krevelen diagram (fig. 2), suggesting that the coals are capable of generating gas and perhaps small amounts of oil. In addition, several of the samples exhibit HI greater than 150 or S2/S3 ratios greater than 3 (table 1), also suggesting that these samples have gas and oil generative potential, according to the classification of Peters (1986). However, this interpretation should be viewed with caution because the Rock-Eval technique typically overestimates the oil generative potential of coals due to poorly understood analytical problems (Peters, 1986).

The thermal maturity of organic matter in the samples is indicated by the Tmax (in °C) and thermal alteration index (TAI). Both fresh and weathered samples exhibit Tmax of 420 °C or less and TAI generally less than 2.5 (table 1). Comparison of these values with the maturation

Table 2.--Summary and comparison of Rock-Eval and TAI results from fresh and weathered samples of coal beds in the Suntrana Formation near Healy, Alaska
[See table 1 for complete data set]

		Coal bed No. 3		Coal bed No. 4		
		Fresh excavation (3 samples)	Weathered outcrop (2 samples)	Fresh excavation (3 samples)	Weathered outcrop (2 samples)	Differences: fresh vs. weathered
TOC	range	59.54-62.52	39.07-58.48	54.26-58.12	39.11-57.98	Fresh generally higher
	mean	61.42	48.78	55.89	48.55	
HI	range	131-141	126-155	150-167	129-185	No consistent difference
	mean	138	141	158	157	
OI	range	54-55	85-115	47-55	56-107	Weathered consistently higher
	mean	55	100	50	82	
S1	range	1.92-2.17	1.32-2.16	2.46-4.08	2.85-3.05	No consistent difference
	mean	2.07	1.74	3.07	2.95	
S2	range	82.08-88.46	60.75-74.21	83.11-9i.00	72.38-74.94	Fresh consistently higher
	mean	85.01	67.48	88.33	73.66	
S3	range	32.35-34.78	45.28-50.12	26.24-30.64	32.84-41.90	Weathered consistently higher
	mean	33.91	47.70	28.25	37.37	
S1/ (S1+S2)	range	0.02-0.03	0.02-0.03	0.03-0.04	0.04-0.04	No consistent difference
	mean	0.02	0.03	0.03	0.04	
S2/S3	range	2.35-2.61	1.34-1.48	2.71-3.46	1.72-2.28	Fresh consistently higher
	mean	2.50	1.41	3.14	2.00	
Tmax (°C)	range	399-409	408-420	392-400	400-400	Weathered generally higher
	mean	405	414	395	400	
TAI	range	2.3-2.5	2.0-2.3	2.0-2.5	2.0-2.5	No consistent difference

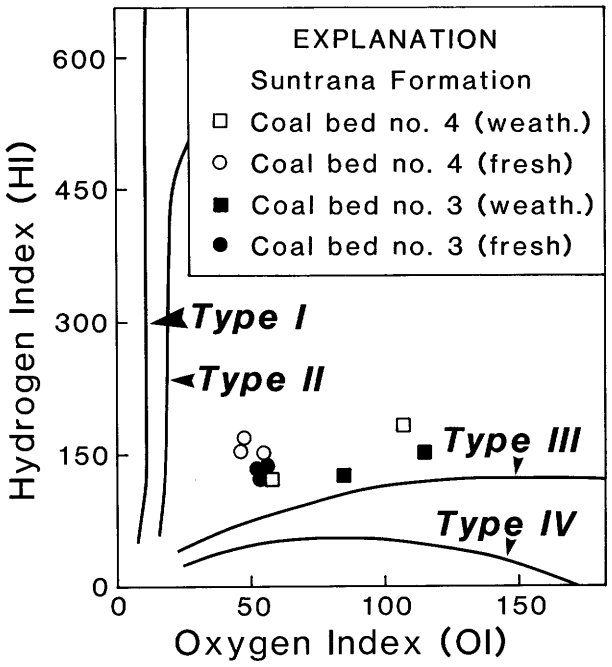

Figure 2.--Modified van Krevelen diagram (Peters, 1986) showing idealized kerogen types (solid lines) and results from weathered and fresh samples of coal from the Suntrana Formation near Healy, Alaska. Type I and Type II kerogens are oil prone; Type III kerogens are gas prone; Type IV kerogens are variously regarded as oil prone, gas prone, or inert (Smyth, 1983; Tissot and Welte, 1984; Peters, 1986).

range chart (fig. 3) indicates that all of the samples are immature to marginally mature with respect to the oil-generative zone. The anomalously high values of TAI (up to 3.5) in samples A5 and A6 (table 1) may be due to contaminants or to the presence of oxidized or recycled organic material that was incorporated into the coals at the time of deposition. Values of Tmax are generally but not consistently higher in the weathered samples, while values of TAI are about the same in both fresh and weathered samples.

In summary, the data presented above indicate that coals in the Suntrana Formation near Healy are potential sources of gas and perhaps oil, but are thermally immature. Similar coals may occur in the subsurface in the middle Tanana basin (Miller and others, 1959); if so, and if the subsurface coals have been buried deeply enough to reach an appropriate level of thermal maturity, they may have generated commercial quantities of gas and oil. Accumulations of gas derived from coal are commercially produced in northwestern Europe, Russia, Alabama, New Mexico, and Colorado (Meissner, 1984; Rightmire, 1984; Tissot and Welte, 1984). Crude oils associated with coals and perhaps derived from them occur in Germany, France, the United Kingdom, Indonesia, Australia, and Venezuela (Tissot and Welte, 1984; Waples, 1985).

Compared to the fresh samples, weathered coals from the Suntrana Formation exhibit lower values of TOC, S2, and S2/S3 and higher values of OI, S3, and Tmax. Apparently, there are no systematic differences between fresh and weathered coals in HI, S1, and TAI. Taken as a whole, the Rock-Eval results indicate gas and oil generative potential for both fresh and weathered samples, but slightly less favorable oil generative potential for the weathered samples.

The differences in Rock-Eval results between fresh and weathered samples most likely are due to oxidation of organic matter during surface weathering, but this interpretation is based on only 10 samples. The lower TOC of the weathered samples may reflect lower initial amounts of organic matter rather than the results of weathering. Another problem is that the sample weights (7.7 to 12.5 mg) are much less than the 75 mg minimum recommended by Peters (1986). Such low sample weights are required because larger amounts of coal would saturate and overload the Rock-Eval apparatus. Nevertheless, the results of this study suggest that weathering can affect the results of Rock-Eval pyrolysis in systematic ways that lead to less favorable estimates of oil-generative potential. Further

Coal Rank	Rock-Eval Tmax (°C)	Vitrinite Reflectance (%Ro)	Thermal Alteration Index (TAI)
PEAT			
LIGNITE & SUB-BITUMINOUS	IMMATURE		
	430-445	0.5-0.7	2.0-2.7
	OIL-GENERATIVE ZONE (OIL WINDOW)		
BITUMINOUS	465-475	1.2-1.4	2.9-3.5
	WET-GAS GENERATIVE ZONE		
	495-500	1.9-2.0	3.3-3.8
SEMI-ANTHRACITE & ANTHRACITE	POST-MATURE (DRY-GAS GENERATIVE ZONE)		
		4.0	4.0
META-ANTHRACITE	LOW-GRADE METAMORPHIC (BARREN)		

Figure 3.--Organic geochemical parameters and levels of thermal maturation, compiled from Hunt (1979), Tissot and Welte (1984), Graham and Williams (1985), Waples (1985), Peters (1986), and Bayliss and Magoon (1987).

research is needed to test this hypothesis on other rock types, to identify the specific geochemical processes involved, and to explain why weathering causes changes in some Rock-Eval parameters (TOC, OI, S2, S3, Tmax) but not others (HI, S1).

REFERENCES CITED

Bayliss, G.S., and Magoon, L.B., in press, Organic facies and thermal maturity in the National Petroleum Reserve in Alaska: Intercalibration of visual kerogen assessment, vitrinite reflectance, and C_1-to-C_4 hydrocarbons, in Gryc, George, ed., Geology of the National Petroleum Reserve in Alaska: U.S. Geological Survey Professional Paper 1399.

Clayton, J.L., and Swetland, P.J. 1978, Subaerial weathering of sedimentary organic matter: Geochimica et Cosmochimica Acta, v. 42, no. 2, p. 305-312.

Graham, S.A., and Williams, L.A., 1985, Tectonic, depositional, and diagenetic history of Monterey Formation (Miocene), central San Joaquin Valley, California: American Association of Petroleum Geologists Bulletin, v. 69, no. 3, p. 385-411.

Hite, D.M., and Nakayama, E.N., 1980, Present and potential petroleum basins of Alaska, in Landwehr, M.L., ed., Exploration and economics of the petroleum industry: New ideas, new methods, new developments: Dallas, Institute on Petroleum Exploration and Economics, p. 511-554.

Hunt, J.M., 1979, Petroleum geochemistry and geology: San Francisco, W.H. Freeman, 617 p.

Leythaeuser, Detlev, 1973, Efects of weathering on organic matter in shales: Geochimica et Cosmochimica Acta, v. 37, no. 1, p. 113-120.

Meissner, F.F., 1984, Cretaceous and lower Tertiary coals as sources for gas accumulations in the Rocky Mountain area, in Woodward, Jane, Meissner, F.F., and Clayton, J.L., eds., Hydrocarbon source rocks of the greater Rocky Mountain region: Denver, Rocky Mountain Association of Geologists, p. 401-431.

Miller, D.J., Payne, T.G., and Gryc, George, 1959, Geology of possible petroleum provinces in Alaska: U.S. Geological Survey Bulletin 1094, 131 p.

Peters, K.E., 1986, Guidelines for evaluating petroleum source rock using programmed pyrolysis: American Association of Petroleum Geologists Bulletin, v. 70, no. 3, p. 318-329.

Rightmire, C.T., 1984, Coalbed methane resource, in Rightmire, C.T., Eddy, G.E., and Kirr, J.N., eds., Coalbed methane resources of the United States: American Association of Petroleum Geologists Studies in Geology 17, p. 1-13.

Smyth, Michelle, 1983, Nature of source material for hydrocarbons in Cooper basin, Australia: American Association of Petroleum Geologists Bulletin, v. 67, no. 9, p. 1422-1428.

Tissot, B.P., and Welte, D.H., 1984, Petroleum formation and occurrence (2nd ed.): Berlin, Springer-Verlag, 699 p.

Wahrhaftig, Clyde, Wolfe, J.A., Leopold, E.B., and Lanphere, M.A., 1969, The coal-bearing group in the Nenana coal field, Alaska: U.S. Geological Survey Bulletin 1274-D, 30 p.

Waples, D.W., 1985, Geochemistry in petroleum exploration: Boston, International Human Resources Development Corporation, 232 p.

Reviewers: L. B. Magoon, K.E. Peters, and Clyde Wahrhaftig

THERMAL MATURITY AND PETROLEUM-SOURCE POTENTIAL OF THE CANTWELL FORMATION (PALEOCENE), ALASKA RANGE

Richard G. Stanley

The Paleocene Cantwell Formation is a highly deformed sequence of nonmarine sedimentary and volcanic rocks that is widely distributed in the central Alaska Range and is more than 3,000 m thick in places (Wolfe and Wahrhaftig, 1970). Mudstone and coal beds in the Cantwell Formation were deposited in a variety of lacustrine, fluvial overbank, and swamp environments and are of interest as potential source rocks of petroleum. Thirty-eight samples of mudstone and bituminous coal were collected from 10 outcrops of the Cantwell Formation and analyzed using Rock-Eval pyrolysis (see preceding article by Stanley, this volume), vitrinite reflectance, and thermal alteration index. The results suggest that these rocks are potential sources of gas and minor amounts of oil.

Rock samples were collected from outcrops along ridge tops and from cuts along streams, highways, and the Alaska Railroad (fig. 1). The rock samples were excavated from depths of 10-30 cm below the outcrop surfaces and transported to the laboratory in sealed plastic bags. Splits of the samples were analyzed using Rock-Eval pyrolysis by T.A. Daws (U.S. Geological Survey, Denver, Colo.), thermal alteration index by Hideyo Haga (Micropaleo Consultants, Inc., San Diego, Calif.), and vitrinite reflectance by M.J. Pawlewicz (U.S. Geological Survey, Denver, Colo.). The basic principles and terminology of Rock-Eval pyrolysis and thermal alteration index are briefly discussed in the preceding article in this volume. Vitrinite reflectance is a method of determining the thermal maturity of a rock by measuring the ability of vitrinite, a type of kerogen formed from terrestrial plant material, to reflect incident light (Tissot and Welte, 1984; Waples, 1985).

The samples were collected from widely scattered geographic locations (fig. 1 and table 1). The relative stratigraphic positions of the samples within the Cantwell Formation are uncertain. Little is known about the internal stratigraphy of the Cantwell except that volcanic rocks are more abundant near the top of the formation (Wolfe and Wahrhaftig, 1970). Stratigraphic correlations within the Cantwell Formation are hampered by the lack of paleontologic and biostratigraphic control, rapid lateral changes in facies and thickness, wide areas of cover between outcrops, and complicated structure that includes numerous faults, igneous intrusions, and tight folds that in places are overturned.

The results of the sample analyses (table 1) allow some preliminary conclusions regarding the quantity, type, and thermal maturity of organic matter in the mudstone and coal beds of the Cantwell Formation.

The quantity of organic matter in the samples is indicated by the TOC (total organic carbon in weight percent) and the quantities S1 and S2. All but one of the 38 samples have TOC greater than 0.5 percent, which generally is regarded as the lower limit for potential source rocks of petroleum (Tissot and Welte, 1984). Twenty-nine of the samples have TOC greater than 1.0 percent, and therefore have good to very good generative potential, according to the classification of Peters (1986). However, the values of S1 and S2 generally are less than 0.5 and 2.5, respectively, suggesting poor generative potential (Peters, 1986). The reasons for this depletion in S1 and S2 are unknown, but may be related to (1) surface weathering of the sampled outcrops and (2) initially poor generative potential due to a high proportion of humic (woody) and inertinitic (oxidized) kerogens. Many but not all of the Cantwell samples contain visible remains of terrestrial plants, including woody stems and leaves; however, no detailed optical studies of kerogen morphology have been done.

The type of organic matter in the Cantwell samples is indicated by the hydrogen index (HI), oxygen index (OI), and the ratio S2/S3. Most of the samples exhibit HI less than 150 and S2/S3 less than 3; comparison of these values with table 2 of Peters (1986) indicates that most of the Cantwell samples are "gas prone", or capable of generating gas but little or no oil. A few of the samples, including some coals, exhibit HI as great as 169 or S2/S3 as great as 18.64 and therefore may be capable of generating oil in addition to gas. However, this interpretation should be viewed with caution because coals may yield spuriously large HI and S2/S3 values due to poorly understood analytical problems that cause the Rock-Eval method to overestimate the liquid hydrocarbon potential of coaly rocks (Peters, 1986).

Plots of HI against OI on a modified van Krevelen diagram (fig. 2) indicate that kerogens in the Cantwell samples are mainly types III and IV. Kerogens of type III are inferred to be gas prone (Tissot and Welte, 1984; Peters, 1986), but the source potential of type IV kerogens is controversial. Smyth (1983) argued that type IV kerogens (also known as "inertinites") can be sources of both oil and gas, while Peters (1986) believed that type IV kerogens have little or no source potential.

The thermal maturity of organic matter in the Cantwell samples is indicated by the Tmax of Rock-Eval pyrolysis (in °C), vitrinite reflectance (percent Ro), and thermal alteration index (TAI).

Table 1-- Rock-Eval, vitrinite reflectance (Ro), and thermal alteration index (TAI) data from the Cantwell Formation

[Rock-Eval parameters (TOC, HI, OI, etc.) are discussed in the preceding article in this volume. See fig. 1 for sample locations]

Sample No.	Rock type	TOC (wt. pct)	HI	OI	Sample weight (mg)	S1 (mg HC/ g rock)	S2 (mg HC/ g rock)	S3 (mg CO_2/ g rock)	$\frac{S1}{S1+S2}$	S2/S3	Tmax (°C)	Median Ro (%)	TAI	Interpretation*
A. Boundary Creek area (ridge top), lat 63°29'29" N., long 150°19'20" W.:														
A1	mdst	1.26	22	68	125.0	0.03	0.28	0.86	0.10	0.32	514	1.18	Barren	GP, OZ
A2	mdst	2.37	28	22	139.6	.05	.68	.53	.07	1.28	488	.89	Barren	GP, OZ
A3	mdst	1.42	18	45	120.6	.03	.26	.64	.11	.40	509	.98	2.3?	GP, OZ
B. Stony Creek area (ridge top), lat 63°30'20" N., long 150°17'12" W.:														
B1	mdst	1.32	12	44	161.4	0.0	0.17	0.59	0.0	0.28	-	1.41	2.5-2.8?	GP, GZ
B2	mdst	1.19	13	36	136.2	.0	.16	.44	.0	.36	-	1.20	No data	GP, OZ
B3	mdst	1.19	10	29	156.2	.0	.12	.35	.0	.34	-	1.13	No data	GP, OZ
C. East Fork Toklat River (stream cut), lat 63°35'06" N., long 149°52'12" W.:														
C1	mdst	0.56	0	33	175.3	0.0	0.0	0.19	0.0	0.0	-	2.89	3.8	PM
C2	mdst	0.46	2	43	198.8	.0	.01	.20	.0	.05	-	Barren	3.8	PM
D. East Fork Toklat River (stream cut), lat 63°35'06" N., long 149°52'12" W.:														
D1	mdst	3.09	55	9	51.4	0.36	1.71	0.29	0.17	5.89	463	1.00	2.5-2.8	GOP, OZ
D2	mdst	6.02	73	5	41.4	.43	4.44	.36	.09	12.33	473	.98	2.5?	GOP, OZ
D3	mdst	6.05	56	7	26.0	.61	3.42	.46	.15	7.43	474	1.13	2.5	GOP, OZ
D4	mdst	9.68	68	5	17.5	.80	6.62	.57	.11	11.61	477	1.18	2.5	GOP, OZ
D5	coal	33.07	169	9	12.3	2.84	55.93	3.00	.05	18.64	470	1.21	2.5-3.0	GOP, OZ
D6	mdst	3.62	31	17	36.9	.10	1.13	.62	.08	1.82	497	1.19	2.5	GP, OZ
E. Polychrome Pass area (road cuts), lat 63°31'36" N., long 149°54'00" W.:														
E1	coal	26.77	67	28	13.9	0.21	18.12	7.62	0.01	2.37	451	0.71	2.8-3.0?	GP, OZ
E2	mdst	1.90	45	60	242.5	.02	.86	1.15	.02	.74	437	.71	3.0?	GP, OZ
E3	mdst	14.17	37	51	10.7	.0	5.32	7.28	.0	.73	448	.74	3.0?	GP, OZ
E4	mdst	2.40	35	67	77.9	.02	.84	1.61	.02	.52	449	.69	3.0?	GP, OZ
F. Cathedral Mountain area (stream cut), lat 63°35'02" N., long 149°36'06" W.:														
F1	mdst	3.52	2	16	75.7	0.01	0.09	0.58	0.10	0.15	-	3.23	3.7	PM
F2	mdst	0.99	6	19	108.1	.01	.06	.19	.17	.31	-	2.0	3.0	PM?
F3	mdst	1.69	24	31	104.5	.02	.42	.54	.05	.77	495	1.34	2.5?	GP, GZ
F4	mdst	1.74	27	43	88.4	.02	.48	.76	.04	.63	457	1.14	2.5-3.0	GP, OZ
F5	mdst	3.73	43	30	94.2	.05	1.61	1.14	.03	1.41	449	1.07	2.5-3.0	GP, OZ
F6	mdst	1.32	28	48	131.0	.01	.38	.64	.03	.59	455	.84	2.5	GP, OZ
F7	mdst	3.37	38	23	82.4	.15	1.31	.80	.10	1.63	461	1.13	3.0?	GP, OZ
G. McKinley Village (railroad cut), lat 63°39'12" N., long 148°50'24" W.:														
G1	mdst	3.76	77	40	71.7	0.06	2.92	1.53	0.02	1.90	443	0.66	2.5-2.8	GP, OZ
G2	mdst	1.28	55	78	75.4	.03	.71	1.00	.04	.71	442	.63	2.5-2.8	GP, OZ
G3	coal	50.18	80	17	10.0	.10	40.40	8.80	.0	4.59	466	.94	2.5-3.0	GOP, OZ
G4	mdst	1.21	31	129	164.7	.0	.38	1.57	.0	.24	442	.70	2.5-3.0	GOP, OZ
H. Yanert coal mine (tailings pile), lat 63°38'40" N., long 148°50'32" W.:														
H1	coal	5.11	87	11	36.4	0.24	4.45	0.60	0.05	7.41	452	0.93	2.5-3.0	GOP, OZ
J. Carlo area (ridge top), lat 63°32'00" N., long 148°45'12" W.:														
J1	mdst	0.51	1	41	187.5	0.0	0.01	0.21	0.0	0.04	-	3.65	3.5	PM
K. Carlo area (ridge top), lat 63°30'27" N., long 148°44'57" W.:														
K1	mdst	8.65	0	54	23.6	0.0	0.04	4.74	0.0	0.0	-	2.93	3.5	PM
K2	mdst	0.99	0	30	75.0	.0	.0	.30	.0	.0	-	2.01	3.8	PM
K3	mdst	0.88	0	26	122.8	.0	.0	.23	.0	.0	-	1.37	3.5-3.8	PM?
K4	mdst	3.86	0	19	33.6	.0	.0	.77	.0	.0	-	2.74	3.5-3.8	PM
K5	mdst	0.77	0	31	72.1	.0	.0	.24	.0	.0	-	1.48	3.5-3.8	PM?
K6	mdst	0.63	0	30	184.4	.0	.0	.19	.0	.0	-	4.28	3.8	PM?
K7	mdst	0.58	0	29	154.8	.0	.0	.17	.0	.0	-	1.99	3.8	PM

*Abbreviations: GP, gas prone; GOP, gas and oil(?) prone; OZ, oil-generative zone ("oil window"); GZ, wet-gas generative zone; PM, post-mature (dry-gas generative zone). An interpretation of "GOP" was assigned to any rock that showed HI>150 or S2/S3>3.0. Tmax values for samples with S2<0.2 were rejected because they are probably unreliable (Peters, 1986).

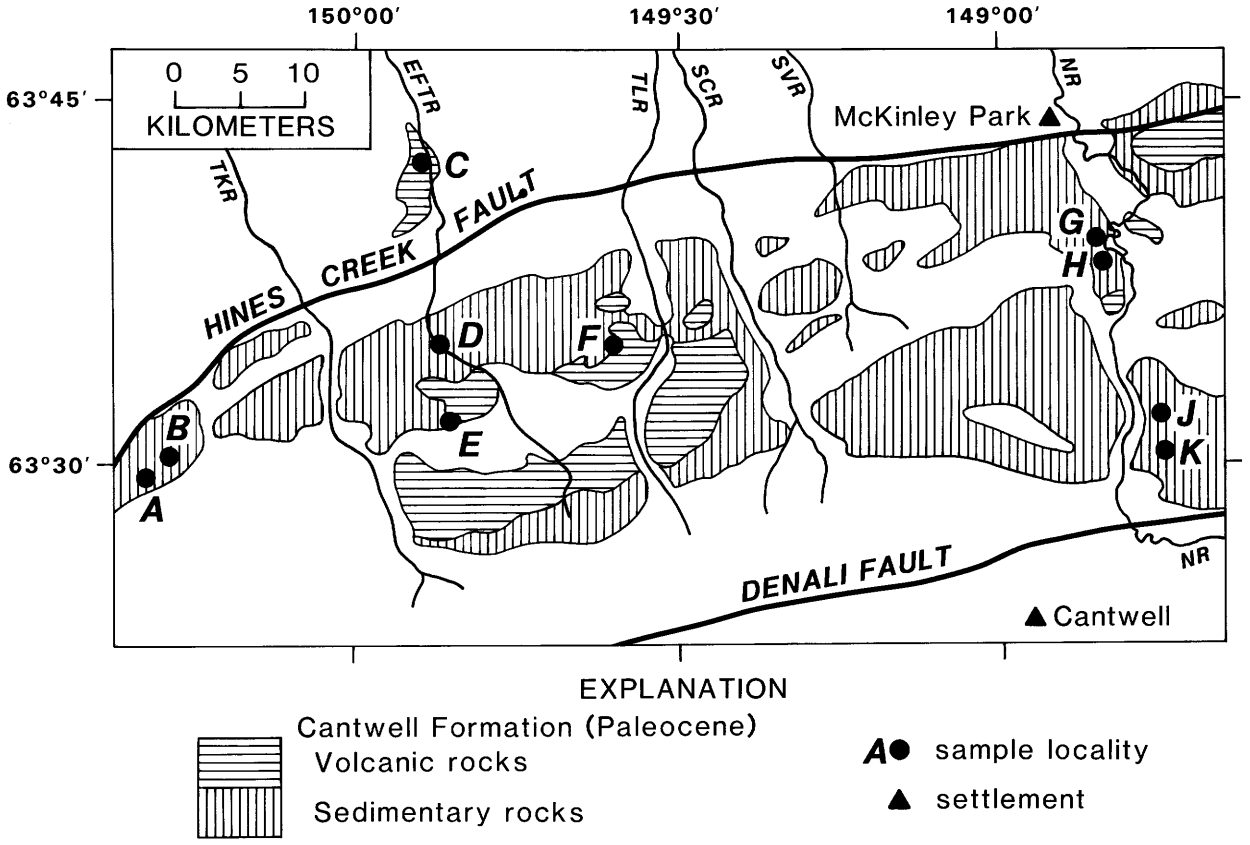

Figure 1.--Sample localities in the Cantwell Formation. Outcrop area generalized from Wolfe and Wahrhaftig (1970) and Jones and others (1983). Major rivers (from west to east): TKR, Toklat River; EFTR, East Fork Toklat River; TLR, Teklanika River; SCR, Sanctuary River; SVR, Savage River; NR, Nenana River.

Comparison of the Cantwell data (table 1) with the maturation range chart (fig. 3) shows that the coals are bituminous and that the thermal maturity of the mudstones ranges from mature to post-mature with respect to the oil and wet-gas generative zones. The reasons for this wide range in thermal maturity are unclear but may be related to variations in burial depth as well as to local heating near igneous intrusions and faults. Another problem is that several of the samples exhibit values of Tmax that are too high compared to Ro and TAI values from the same sample, possibly as a result of oxidation during outcrop weathering (see preceding article by Stanley, this volume). However, Peters (1986) noted that unusually high Tmax can also reflect the presence of highly mature, recycled, or type IV kerogens as well as interference from the clay mineral matrix.

In conclusion, limited data indicate that some but not all nonmarine mudstones and coals in the Paleocene Cantwell Formation are potential sources of gas and minor amounts of oil. These results are encouraging, but little can be said about the overall petroleum resource potential of the Cantwell Formation until more is known about potential reservoirs, trapping conditions, and general structure and stratigraphy. Given the tight folds, abundant faults, igneous intrusions, and rapid lateral facies changes that are evident in outcrop, it seems likely that petroleum accumulations in the Cantwell Formation--if any exist--will be small and difficult to find. However, the presence of potential petroleum source rocks in the Cantwell suggests that other Tertiary nonmarine formations in central Alaska also may include potential petroleum sources. Speculatively, Tertiary nonmarine source rocks similar to those in the Cantwell Formation may occur in the subsurface in sedimentary basins such as the middle Tanana and Yukon Flats basins (shown by Miller and others, 1959) and may have generated hydrocarbons in commercial quantities.

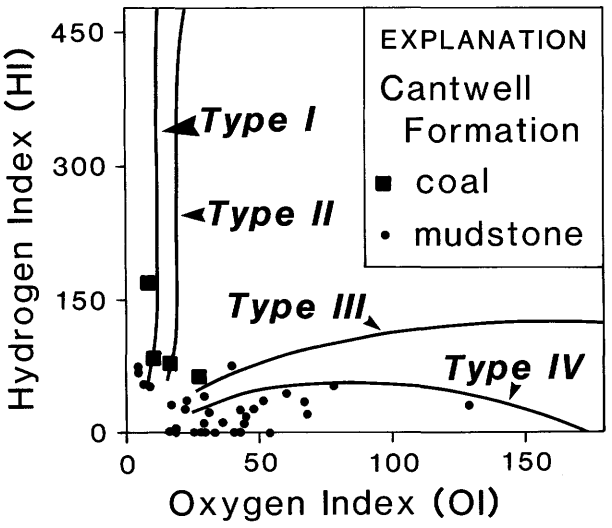

Figure 2.--Modified van Krevelen diagram (Peters, 1986) showing idealized kerogen types (solid lines) and analytic results from the Cantwell Formation. Type I and Type II kerogens are oil prone; Type III kerogens are gas prone; Type IV kerogens are variously regarded as gas prone, oil prone, or inert (Smyth, 1983; Peters, 1986).

Coal Rank	Rock-Eval Tmax (°C)	Vitrinite Reflectance (%Ro)	Thermal Alteration Index (TAI)
PEAT	IMMATURE		
LIGNITE & SUB-BITUMINOUS			
	430-445	0.5-0.7	2.0-2.7
BITUMINOUS	OIL-GENERATIVE ZONE (OIL WINDOW)		
	465-475	1.2-1.4	2.9-3.5
	WET-GAS GENERATIVE ZONE		
	495-500	1.9-2.0	3.3-3.8
SEMI-ANTHRACITE & ANTHRACITE	POST-MATURE (DRY-GAS GENERATIVE ZONE)		
		4.0	4.0
META-ANTHRACITE	LOW-GRADE METAMORPHIC (BARREN)		

Figure 3.--Organic geochemical parameters and levels of thermal maturation, compiled from Hunt (1979), Tissot and Welte (1984), Graham and Williams (1985), Waples (1985), Peters (1986), and Bayliss and Magoon (1987).

REFERENCES CITED

Bayliss, G.S., and Magoon, L.B., in press, Organic facies and thermal maturity in the National Petroleum Reserve in Alaska: Intercalibration of visual kerogen assessment, vitrinite reflectance, and C_1-to-C_4 hydrocarbons, in Gryc, George, ed., Geology of the National Petroleum Reserve in Alaska: U.S. Geological Survey Professional Paper 1399.

Graham, S.A., and Williams, L.A., 1985, Tectonic, depositional, and diagenetic history of Monterey Formation (Miocene), central San Joaquin basin, California: American Association of Petroleum Geologists Bulletin, v. 69, no. 3, p. 385-411.

Hunt, J.M., 1979, Petroleum geochemistry and geology: San Francisco, W. H. Freeman, 617 p.

Jones, D.L., Silberling, N.J., Gilbert, W.G., and Coney, P.J., 1983, Interpretive bedrock geologic map of the Mt. McKinley region: U.S. Geological Survey Open-File Report 83-11, 2 sheets, scale 1:250,000.

Miller, D.J., Payne, T.G., and Gryc, George, 1959, Geology of possible petroleum provinces in Alaska: U.S. Geological Survey Bulletin 1094, 131 p.

Peters, K.E., 1986, Guidelines for evaluating petroleum source rock using programmed pyrolysis: American Association of Petroleum Geologists Bulletin, v. 70, no. 3, p. 318-329.

Smyth, Michelle, 1983, Nature of source material for hydrocarbons in Cooper basin, Australia: American Association of Petroleum Geologists Bulletin, v. 67, no. 9, p. 1422-1428.

Tissot, B.P., and Welte, D.H., 1984, Petroleum formation and occurrence (2nd ed.): Berlin, Springer-Verlag, 699 p.

Waples, D.W., 1985, Geochemistry in petroleum exploration: Boston, International Human Resources Development Corporation, 232 p.

Wolfe, J.A., and Wahrhaftig, Clyde, 1970, The Cantwell Formation of the central Alaska Range: U.S. Geological Survey Bulletin 1294-A, p. A41-A46.

Reviewers: K. J. Bird, L. B. Magoon, and K.E. Peters

AN APPLICATION OF OBLIQUE ROTATION R-MODE FACTOR ANALYSIS IN THE MOUNT HAYES QUADRANGLE, ALASKA (ABSTRACT)

J.D. Hoffman

As part of the Alaska Mineral Resource Assessment Program (AMRAP), a reconnaissance geochemical sampling program was conducted to aid in the evaluation of known mineral resources and the exploration for potential mineral resources in the Mount Hayes quadrangle, eastern Alaska Range. An extreme variable, oblique rotation R-mode factor analysis procedure was used to reduce the analytical data from the sampling program in an attempt to define and locate geochemical signatures that may represent mineralization. Factor analysis can discern subtle relationships among data that may not be readily apparent. As exploration geochemical data may be intercorrelated, the oblique rotation was used to allow for these possible intercorrelations in the data. The oblique rotation, as with other rotations, also has the advantage of maximizing factor loadings. The program used 19 elemental analyses of 1,343 rock outcrop samples, provided by semiquantitative emission spectrography and atomic absorption spectrophotometry.

The ability of factor analysis to generate multielement associations, or factors, that distinguish mineralization signatures from lithologic signatures depends in part on the ratio of regional variance in the data to that of more local variance. To push the factor analysis procedure toward describing mineralization signatures and not simply lithologic signatures, the data were grouped into five lithotectonic subterranes and terranes; the factor analysis procedure was then applied to these separate groups. The number of samples in each group was at least 105.

The elemental associations as shown by factor loadings can be related to mineralization types in the quadrangle; some of the associations may be related to previously unreported mineralization. Plots of the factor scores agree well with the locations of known mineral occurrences and deposits. For example, in the Maclaren terrane, factor 4 (lead, zinc, and manganese) score plots may indicate vein-type base-metal mineralization in the Maclaren metamorphic belt. The Maclaren belt rocks incorporate schist, amphibolite, argillite, and metagraywacke. As another example, in the Slana subterrane, factor 1 (chromium, nickel, cobalt, magnesium, and iron) score plots probably indicate known chromite occurrences in the Mesozoic Nikolai Greenstone. Lastly, in the Jarvis terrane, a terrane of metamorphosed plutonic and volcanic rocks, factor 3 (lead, zinc, and copper) score plots are related to known Kuroko-type massive sulfide deposits and occurrences. These three examples illustrate the capability of factor analysis to discern and locate geochemical signatures that may indicate mineralization.

Reviewers: M. Allen and J.B. Cathrall

SOUTHEASTERN ALASKA

Fairweather Range, Glacier Bay National Monument. Photo by D.A. Brew.

STRUCTURAL FABRIC ANALYSIS OF THE PERSEVERANCE SLATE AND GOLD-BEARING QUARTZ VEINS IN THE SOUTH ORE BODY OF THE ALASKA-JUNEAU LODE SYSTEM, SOUTHEASTERN ALASKA

Christopher C. Barton and Thomas D. Light

The Juneau gold belt extends for almost 200 km along the western flank of the Coast Mountains in southeastern Alaska. The Alaska-Juneau lode system is located near the center of the gold belt in the vicinity of the city of Juneau (fig. 1). The deposit has produced 3.5×10^6 oz (110,000 kg) of gold (Berg, 1984), ranking it as the largest lode gold deposit in the state. We report here on the structural fabric analysis of the host rock and gold veins in order to place vein formation into the context of the tectonic history. Our work has been confined to the southwestern half of the open-pit mine in the south ore body of the Alaska-Juneau lode system (fig. 1) in the Silverbow Basin, 4.5 km east of Juneau. The pit is divided into northeastern and southwestern halves by a northwest-southeast-striking ridge of unmined rock. The southwestern half is ovoid in plan and measures 250 m long, 125 m wide, and 125 m deep; the long axis strikes N. 60° W. The pit walls are subvertical and provide good cross-sectional exposures of the host-rock and vein fabrics. The bottom of the pit was collapsed by block-cave mining from below and is composed of coarse rock debris which slopes away from the walls.

The Perseverance Slate is the host rock for the gold-bearing quartz veins. It is a 1.5-km-wide belt of carbonaceous and graphitic quartz sericite phyllite, schist, and black slate with minor carbonaceous limestone and numerous sill-like lenses of amphibolite (Brew and Ford, 1984 a, b, c). Regionally, the slate strikes N. 50°-70° W., parallel to the regional structural trend (Brew and Ford, 1985). The protolithic age of the Perseverance Slate is now considered as late Triassic, based on ammonites and Halobeid pelecypods from within the unit; it was metamorphosed during latest Cretaceous and early Tertiary time (D. A. Brew, USGS, oral commun., 1986).

The Alaska-Juneau deposit is cut by the Silverbow normal fault, a few tens of meters north of the pit. The fault strikes nearly east-west, dips 75° north, and has oblique normal offset. The north (hanging wall) side has moved down about 550 m and about the same distance to the west (Wayland, 1939).

In the southwestern half of the pit, the Perseverance Slate is silver-black carbonaceous phyllite. The strike of the compositional layering ranges from N. 55° W. to S. 85° E. The dip of layering changes smoothly from 80° NE at the southwest wall of the pit, flattens, and then over a distance of a few meters, bends to 87° SW at the wall dividing the pits. The layering describes an open asymmetric synform whose axis bears S. 81° E. and plunges 36° SE (fig. 2). Two penetrative cleavages are well developed throughout the Perseverance Slate in the pit. The first is parallel to the plane of the quartz veins (fig. 3); it dips vertically and strikes from N. 5° W. to N. 57° W., averaging N. 45° W. The second strikes from N. 46° W. to N. 60° W. and dips 57°-76° NE. Neither cleavage appears to penetrate the gold-quartz veins. Neither cleavage is axial planar to or fans about the synclinal fold axis. Planar zones of intense shearing are also present. They range in width from a few centimeters to as much as 5 m. The rock in the zones contains shear planes spaced millimeters apart. The zones and

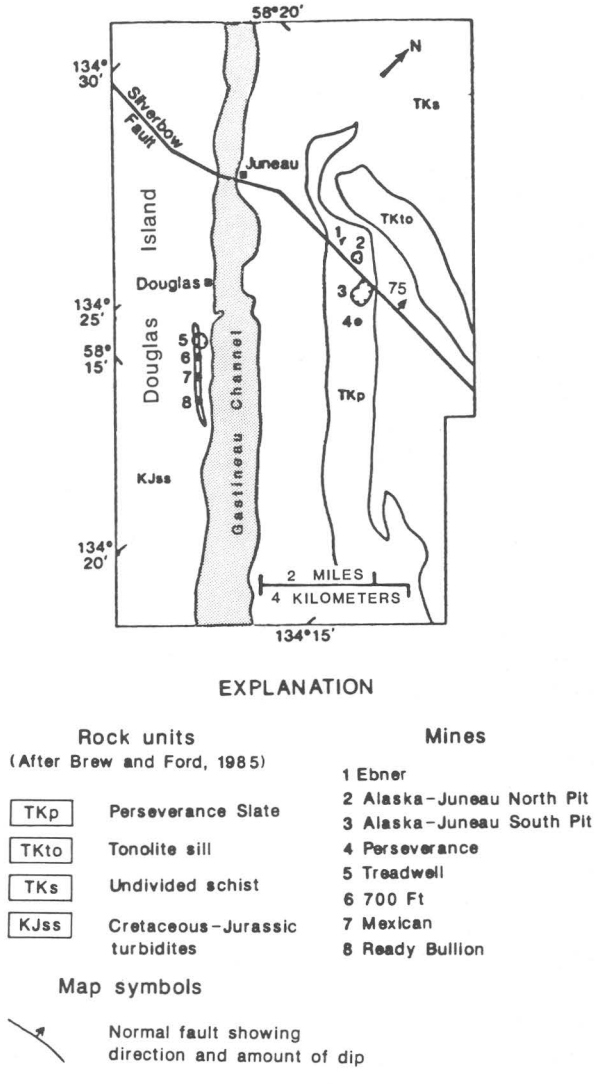

Figure 1.--Generalized geologic map showing the location of major structural features and mines.

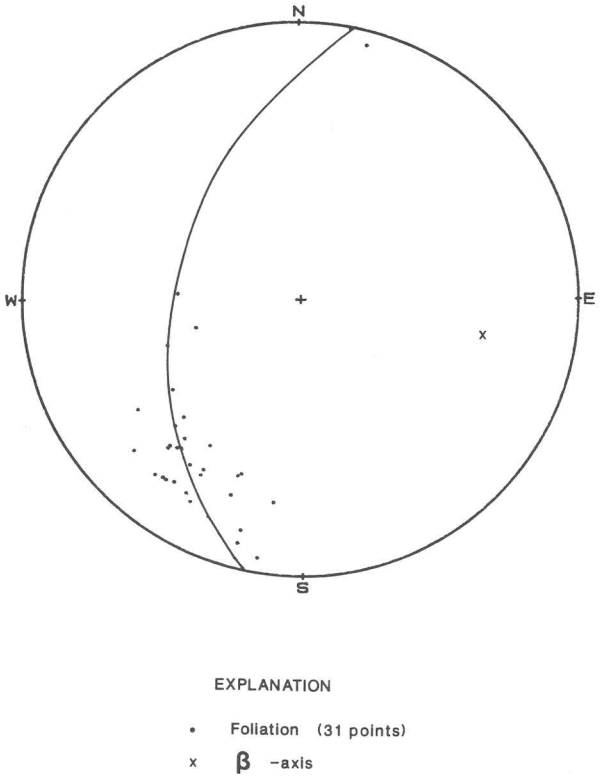

Figure 2.--Lower-hemisphere equal-area projection of poles to compositional layering. B-axis to great circle fit to poles is the bearing and plunge of the synform axis.

the shear planes within them are in the same orientation as the second of the two penetrative cleavages. The sense of shear is up the dip line of the shear planes, as determined by the slickenlines and the offset of veins.

Joints are not pervasive throughout the pit, but rather well-defined sets are developed only in small areas. Only one set of joints is present in each of the areas sampled. The joints are not spatially or genetically related to any other structural elements. The mean orientation for each of the four joint sets sampled are:

(1) N. 30° E., 90°
(2) N. 47° E., 82° SE
(3) N. 25° W., 56° SW
(4) N. 70° W., 65° NE

The Perseverance Slate has been penetrated by a system of noncontiguous sulfide-bearing veins of the Alaska-Juneau system. The veins range in width from a few centimeters to as much as 1 m. The height-to-width ratios of those in the pit walls range from 1:1 to more than 50:1. The spacing between veins ranges from a few centimeters to a few meters. The veins are about 95 percent quartz with subsidiary ankerite, pyrrhotite, galena, sphalerite, arsenopyrite, pyrite, and gold

Figure 3.--Photograph of near-vertical boudinaged gold-bearing quartz vein and, plane-parallel to it, penetrative cleavage in the pit wall.

(Twenhofel, 1952). The gold is concentrated with sulfide minerals along the edges of some of the veins, in fractures in quartz, and in the ankerite which normally bounds the edges of the veins and separates the quartz from the country rock.

The strike of the veins in the pit ranges from N. 5° W. to N. 57° W. and averages N. 45° W. The veins are nearly vertical except within the shear zones, where they have been mechanically sheared and rotated partly or completely into the plane of shearing. We were not able to distinguish different generations of veining based on orientation or crosscutting relations. The veins are not spatially related to either the joints or compositional layering (fig. 4). The veins pinch and swell in both vertical and horizontal sections (fig. 3). We interpret this as "chocolate tablet structure" (Ramsey and Huber, 1983); a type of boudinage where the competent mass is extended in all directions, producing a complex of crossing

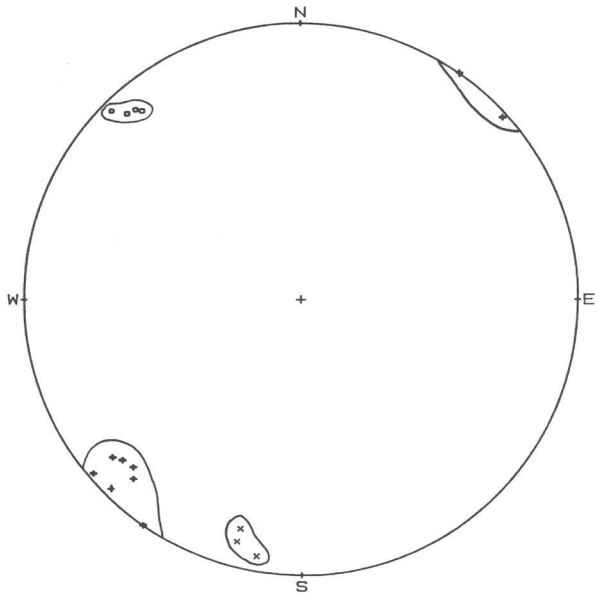

Figure 4.--Lower-hemisphere equal-area projection of poles to foliation, veins, and joints at one of eight stations along the southeast pit wall.

boudin necks. We infer at least one phase of boudinage development with the least principal stress in the plane of the veins.

Our observations of structural overprinting indicate the following stages in the geologic history for the south ore body: (1) deposition of the protoliths of the Perseverance Slate, (2) accretion, metamorphism, and folding of the Perseverance, (3) emplacement of quartz veins, (4) boudinage of veins and development of cleavage parallel to them, (5) development of shear zones and a cleavage parallel to the shear zones, and (6) unroofing and development of joints and formation of the Silverbow fault. Although each stage occurred in sequence, events that are grouped together did not necessarily occur simultaneously.

REFERENCES CITED

Berg, H.C., 1984, Regional geologic summary, metallogenesis, and mineral resources of southeastern Alaska: U.S. Geological Survey Open-File Report 84-572, 299 p.

Brew, D.A., and Ford, A.B., 1984a, Tectonostratigraphic terranes in the Coast plutonic-metamorphic complex, southeastern Alaska, in Bartsch-Winkler, Susan, and Reed, K.M., eds., The United States Geological Survey in Alaska: Accomplishments during 1982: U.S. Geological Survey Circular 939, p. 90-93.

_____ 1984b, Timing of metamorphism and deformation of the Coast plutonic-metamorphic complex near Juneau, Alaska (abs.): Geological Society of America Abstracts with Programs, v. 16, no. 5, p. 272.

_____ 1984c, The northern Coast plutonic-metamorphic complex, southeastern Alaska, and northwestern British Columbia, in Coonrad, W.C., and Elliot, R.L., eds., The United States Geological Survey in Alaska: Accomplishments during 1981: U.S. Geological Survey Circular 868, p. 120-124.

_____ 1985, Preliminary reconnaissance geologic map of the Juneau, Taku River, Atlin, and part of the Skagway quadrangles, southeastern Alaska: U.S. Geological Survey Open-File Report 85-395, scale 1:250,000.

Ramsey, J.G., and Huber, M.I., 1983, The techniques of modern structural geology, volume I: Strain analysis: New York, Academic Press, 307 p.

Twenhofel, W.S., 1952, Geology of the Alaska-Juneau lode system, Alaska: U.S. Geological Survey Open-File Report 52-160, 180 p.

Wayland, R.G., 1939, Geology of the Juneau region, Alaska, with special reference to the Alaska Juneau ore body: Minneapolis, University of Minesota, Ph.D. dissertation, 93 p.

Reviewers: E.R. Verbeek and R.J. Goldfarb

THE MEADE GLACIER FAULT— AN IMPORTANT TECTONIC BOUNDARY IN THE NORTHERN CORDILLERA, SOUTHEASTERN ALASKA

David A. Brew and Arthur B. Ford

One of the persistent questions about the tectonic history of southeastern Alaska concerns the existence and the nature of the boundary separating composite tectonostratigraphic terranes I and II of Monger and others (1982). This boundary must lie within the granitic and metamorphic rocks of the Coast crystalline belt and would separate the Stikine terrane (part of terrane I) on the east from the Alexander terrane and Gravina overlap assemblage (both part of terrane II) on the west (fig. 1). The existence of this boundary has been questioned by Brew (1983) and Brew and Ford (1983, 1984).

Recent fieldwork in the Atlin quadrangle established the existence of a post-Late Triassic, pre-60 Ma north-northwest-trending fault zone with apparently significant right-lateral and west-side-down separation that may be the only remaining exposure of the terrane boundary (Brew and others, 1985; Himmelberg and others, 1985, 1986; D.A. Brew and A.B. Ford, unpub. data). Recognition of this potentially important tectonic boundary in the Atlin quadrangle led us to examine its possible northern and southern extensions. This article reports progress so far in our efforts to trace the informally named Meade Glacier fault.

In its only known exposures (fig. 2), the fault lies close to the southwest side of the northwest-southeast-trending portion of the Meade Glacier and separates simply deformed low-metamorphic-grade Middle and Upper(?) Triassic volcanic, clastic, carbonate, and volcaniclastic rocks on the west from a package of inferred pre-Late Triassic multiply deformed medium- to high-metamorphic grade quartz-rich gneiss and schist, marble, and metavolcanic rocks on the east. The rocks to the west are intruded by an ultramafic body of uncertain (but post-Triassic, pre-Tertiary) age that consists mostly of peridotite (Himmelberg and others, 1985). The rocks to the east are intruded by a crosscutting hornblende-biotite granodiorite pluton whose age is inferred to be 50 Ma on the basis of compositional and structural similarities to dated plutons both north and south of the Meade Glacier area. Rocks in the fault zone include highly tectonized quartz-rich schist, augen gneiss and marble derived from the package to the east, and similarly tectonized peridotite derived from the rocks to the west. Minor structures in the fault zone indicate that some of the movement postdated the major folding of the schist and gneiss, but we were unable to get a consistent sense of vergence from the younger folds or from strain-sense indicators in the augen gneiss. The fault is healed to the north and south of Meade Glacier by granitic plutons that are about 60 Ma in age (G.R. Tilton, University of California at Santa Barbara, written commun., 1986).

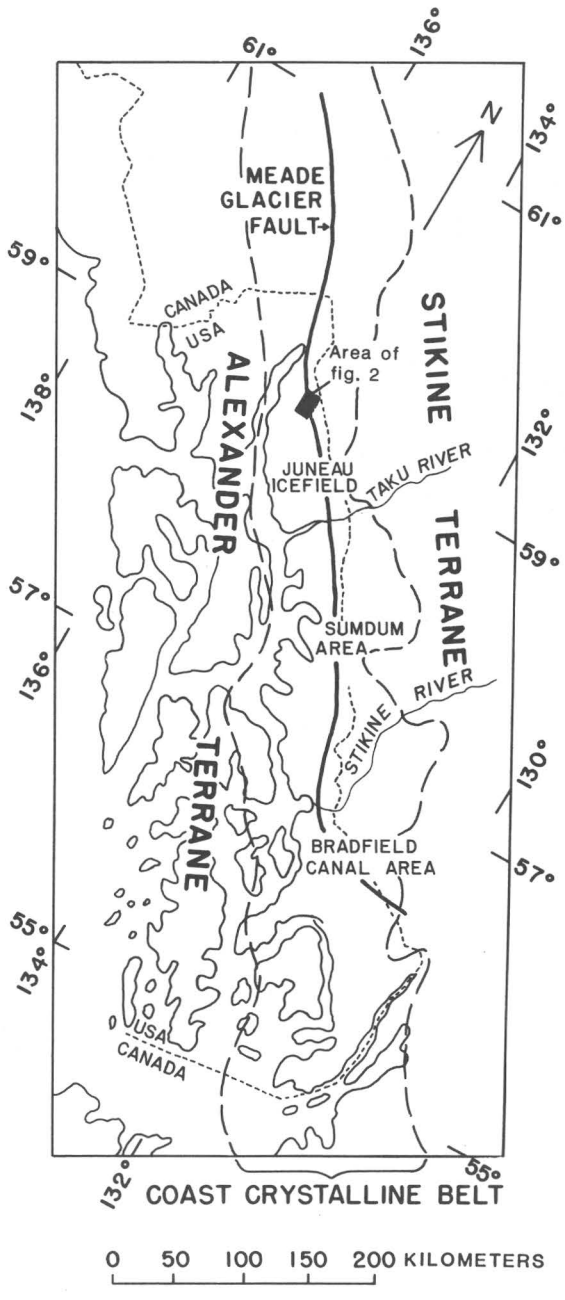

Figure 1.--Map showing boundaries of northern Coast crystalline belt (area between long dash lines), United States and Canada, and extent of Meade Glacier fault (heavy solid line).

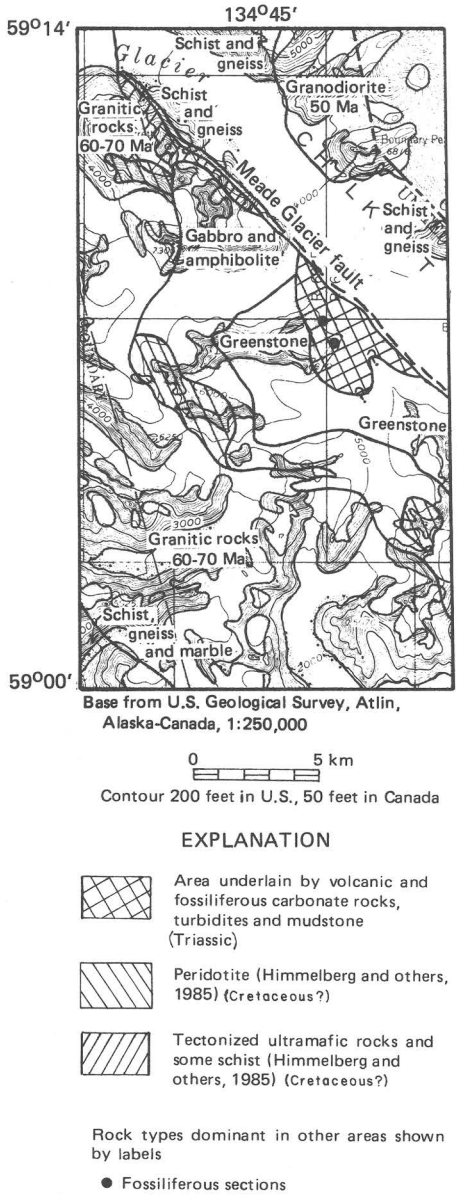

Figure 2.--Map of Meade Glacier area showing known extent of Meade Glacier fault, and rocks on either side.

We have not been able to trace the fault northward into the Skagway quadrangle because of the abundance of younger plutonic rocks and the absence of detailed mapping in that area. Further north, into British Columbia and Yukon Territory, the fault itself is not known to be exposed, but its geologic expression is recognized as far as about latitude 62° N. This is based on the distribution of the Kluane schist and gneiss of probable original Late Jurassic and Cretaceous age on the west and of the Yukon Group of uncertain (but probably early Paleozoic or late Proterozoic) age on the east (Gabrielse and others, 1980; J.O. Wheeler, Geological Survey of Canada, oral commun., 1986). The present interpretation (Gabrielse and others, 1980) of the mapping of Kindle (1953) suggest that near latitude 61° N, Mesozoic age granitic rocks separate two contrasting rock units. The unit to the west consists of quartz-mica schist, quartz-biotite-feldspar gneiss, slate, and minor quartz-sericite-andalusite schist, hornblende schist, sericite-cordierite schist, and garnet-mica schist belonging to the Kluane schist and gneiss unit; the unit to the east consists of somewhat similar rocks, mainly quartz-mica schist, quartz-mica gneiss, quartz-biotite gneiss, and garnet-quartz-biotite gneiss, that are interlayered with distinctive thick coarse-grained white marble and minor limestone and are assigned to the Yukon Group.

To the south, the possible terrane boundary passes through the abundant 50 Ma granitic rocks of the Juneau Icefield (Brew and Ford, 1985) and crosses the Taku River several kilometers downstream from the U.S.-Canada boundary (fig. 1). At this latitude the pre-granitic rocks west of the fault belong to the medium- to high-grade metamorphic package of phyllite, schist, and gneiss, studied in detail near Juneau (Ford and Brew, 1973, 1977; Brew and Ford, 1977; Himmelberg and others, 1984a, b), that includes rocks with original ages ranging from Permian to Cretaceous. The rocks east of the fault are in part higher grade metamorphic rocks like those at the Meade Glacier and in part low- to medium-grade semischists and phyllite. They have been described by Souther (1971) and Brew and Ford (1985). Further south, the boundary passes through more granitic rock into the Sumdum (Tracy Arm-Fords Terror) area described by Brew and Grybeck (1984). There only a few small outcrop areas of metamorphic rocks immediately adjacent to the U.S. - Canada boundary are inferred to belong to the quartz-rich schist and gneiss unit east of the tectonic boundary (D.A. Brew and A.B. Ford, unpub. data). Mapping in the Petersburg area still further south (Brew and others, 1984) and our work in the areas beyond indicate that the boundary probably passes into Canada somewhere in the Bradfield Canal quadrangle. In this region, in the Canadian portions of the Chutine (Souther, 1958) and Bradfield Canal (Geological Survey of Canada, 1957) map-areas, the oldest rocks to the east of the projection of the Meade Glacier fault are schist, gneiss, greenstone, limestone, shale, and clastic sedimentary rocks of original Carboniferous and Permian age. These rocks are all interpreted (Souther and others, 1979) to belong to the same package as those east of the Meade Glacier fault where the fault trace is exposed (fig. 2).

The available evidence is not conclusive as to whether the Meade Glacier fault is the boundary between composite terranes I (Stikine, etc.) and II (Alexander, etc.) of Monger and others (1982). It is strongly suggestive that it may be, however, and more studies along its possible continuations in Canada both north and south of its known extent in Alaska would undoubtedly add to our understanding of its nature and significance in the tectonic development of the northern Cordillera.

REFERENCES CITED

Brew, D.A., 1983, Evaluation of suspect terranes in the Coast plutonic-metamorphic complex, southeastern Alaska and part of British Columbia (abs.): Geological Society of America Abstracts with Programs, v. 15, no. 5, p. 324.

Brew, D.A., and Ford, A.B., 1977, Preliminary geologic and metamorphic-isograd map of parts of the Juneau A-1 and A-2 quadrangles, Alaska: U.S. Geological Survey Map MF-847.

_____1983, Comment on Monger, J.W.H., Price, R.A., and Tempelman-Kluit, D.J., 1982, Tectonic accretion and the origin of the two major metamorphic and plutonic welts in the Canadian Cordillera: Geology, v. 11, p. 427-429.

____1984, Tectonostratigraphic terrane analysis in the Coast plutonic-metamorphic complex, southeastern Alaska (abs.), in Bartsch-Winkler, Susan, and Reed, K.M., eds., The United States Geological Survey in Alaska: Miscellaneous geologic research 1982: U.S. Geological Survey Circular 939, p. 90-93.

____1985, Preliminary reconnaissance geologic map of the Juneau, Taku River, Atlin and part of the Skagway 1:250,000 quadrangles, southeastern Alaska: U.S. Geological Survey Open-File Report 85-395, 23 p., scale 1:250,000, 2 sheets.

Brew, D.A., Ford, A.B., and Garwin, S.L., 1985, Fossiliferous Middle and(or) Upper Triassic rocks within Coast plutonic-metamorphic complex southeast of Skagway, Alaska, in Bartsch-Winkler, Susan, ed., The United States Geological Survey in Alaska: Accomplishments during 1984: U.S. Geological Survey Circular 967, p. 86-89.

Brew, D.A., and Grybeck, Donald, 1984, Geology of the Tracy Arm-Fords Terror wilderness study area and vicinity, in Mineral resources of Tracy Arm-Fords Terror wilderness study area and vicinity, Alaska: U.S. Geological Survey Bulletin 1525, p. 19-52.

Brew, D.A., Ovenshine, A.T., Karl, S.M., and Hunt, S.J., 1984, Preliminary reconnaissance geologic map of the Petersburg and parts of the Port Alexander and Sumdum 1:250,000 quadrangles, southeastern Alaska: U.S. Geological Survey Open-File Report 84-405, 2 sheets, 43 p.

Ford, A.B., and Brew, D.A., 1973, Preliminary geologic and metamorphic-isograd map of the Juneau B-2 quadrangle, Alaska: U.S. Geological Survey Miscellaneous Field Studies Map MF-527, scale 1:31,680.

____1977, Preliminary geologic and metamorphic-isograd map of parts of the Juneau A-1 and A-2 quadrangles, Alaska: U.S. Geological Survey Miscellaneous Field Studies Map MF-847, scale 1:31,680.

Gabrielse, H., Tempelman-Kluit, D.J., Blusson, S.L., and Campbell, R.B., 1980, MacMillan River 1:1,000,000 geological Atlas: Geological Survey of Canada Map 1398A.

Geological Survey of Canada, 1957, Stikine River area, British Columbia: Geological Survey of Canada Map 9-1957, scale 1:253,440.

Himmelberg, G.R., Brew, D.A., and Ford, A.B., 1986, Chemical composition of olivine and orthopyroxene in peridotite in the Coast plutonic-metamorphic complex near Skagway, Alaska, in Bartsch-Winkler, Susan, ed., The United States Geological Survey in Alaska: Accomplishments during 1985: U.S. Geological Survey Circular 978, p. 95-98.

Himmelberg, G.R., Ford, A.B., and Brew, D.A., 1984a, Progressive metamorphism of pelitic rocks in the Juneau area, southeastern Alaska, in Coonrad, W.C., and Elliott, R.L., eds., The United States Geological Survey in Alaska: Accomplishments during 1981: U.S. Geological Survey Circular 868, p. 131-134.

____1984b, Reaction isograds in pelitic rocks of the Coast plutonic-metamorphic complex near Juneau, Alaska (abs.), in Bartsch-Winkler, Susan, and Reed, K.M., eds., The United States Geological Survey in Alaska: Accomplishments during 1982: U.S. Geological Survey Circular 939, p. 105-108.

____1985, Ultramafic bodies in the Coast plutonic-metamorphic complex near Skagway, Alaska, in Bartsch-Winkler, Susan, ed., The United States Geological Survey in Alaska: Accomplishments during 1984: U.S. Geological Survey Circular 967, p. 92-93.

Kindle, E.D., 1953, Dezadeash map-area, Yukon Territory: Geological Survey of Canada Memoir 268, 68 p.

Monger, J.W.H., Price, R.A., and Tempelman-Kluit, D.J., 1982, Tectonic accretion and the origin of the two major metamorphic and plutonic welts in the Canadian Cordillera: Geology, v. 10, p. 70-75.

Souther, J.G., 1958, Chutine, British Columbia, map-area: Geological Survey of Canada Map 7-1959, scale 1:253,440.

____1971, Geology and ore deposits of Tulsequah map area, British Columbia: Geological Survey of Canada Memoir 362, 84 p.

Souther, J.G., Brew, D.A., and Okulitch, A.V., 1979, Iskut River 1:1,000,000 Geological Atlas: Geological Survey of Canada Map 1418A.

Reviewers: G.R. Himmelberg and S.M. Karl

THE WRIGHT GLACIER VOLCANIC PLUG AND DIKE SWARM, SOUTHEASTERN ALASKA

Arthur B. Ford and David A. Brew

The distribution of early and late Cenozoic granitic plutons and of related late Cenozoic dike swarms in the Coast crystalline belt of southeastern Alaska is known from extensive reconnaissance work (Brew and Morrell, 1983; D.A. Brew, unpub. data), but no late Cenozoic plutons or dike swarms have been reported from this belt north of the latitude of Wrangell. These plutons and dike swarms are of interest because of their association with the large molybdenite deposit at Quartz Hill near the southern tip of southeastern Alaska (Hudson and others, 1979) and with molybdenite occurrences at Burroughs Bay, Cone Mountain, and Groundhog Basin near Wrangell (Hudson and others, 1979; Grybeck and others, 1984) (fig. 1). In the vicinity of Juneau, Souther (1971) mapped a northeast-southwest-striking 10-km-wide dike swarm of aplite and felsite on the Canadian side of the international boundary mainly on the north side of Mount Ogden, not far south of the Taku River east of Juneau. Several molybdenite occurrences accompany the swarm. We recently mapped the extension of that swarm into Alaska and found that it consists of rhyolite that is apparently associated with a dacite plug (fig. 2). This report briefly describes that swarm and plug.

The dike swarm is well exposed on both the northeast and southwest sides of the northwest-flowing Wright Glacier, about 7 km above the lake at the terminus of the glacier (fig. 2). The conspicuous, 1- to 5-m-wide, vertically dipping, northeast-southwest-striking dikes occur sporadically over the 6.5 km width of the swarm. Although the dikes are common, there are few localities with a concentration of more than two or three dikes within 100 m. The dikes cut granitic rocks inferred to be about 50 Ma in age as well as the pre-Late Triassic gneiss and schist referred to as the Tulsequah sub-belt (Brew and Ford, 1985). The dikes are well jointed and locally are miarolitic. They weather light yellow and are slightly iron-stained in places. Small quartz phenocrysts are present in almost all samples. Our geochemical sampling to date has not shown any pattern of significantly anomalous concentrations of molybdenum or other metals.

The 0.5-by-1.0-km dacite body that we infer to be plug-like is at an elevation of about 6,500 feet (1,980 m) about 6 km south-southeast of Wright Glacier lake at the terminus of Wright Glacier (fig. 2). It forms the relatively inaccessible peak labelled 6,882 feet (2,098 m) and intrudes 50 Ma granodiorites; most of the contacts with the surrounding rock are concealed by glaciers. The rock is well jointed and is medium gray in color, weathering grayish brown; it is both conspicuously fragmental and consistently plagioclase porphyritic in hand specimen. The maximum size volcanic fragment observed in outcrop was about 15 cm. Small quartz phenocrysts are present, but are rare. In thin section the fragments are seen to be dominantly silicic volcanic rock, some of which have been

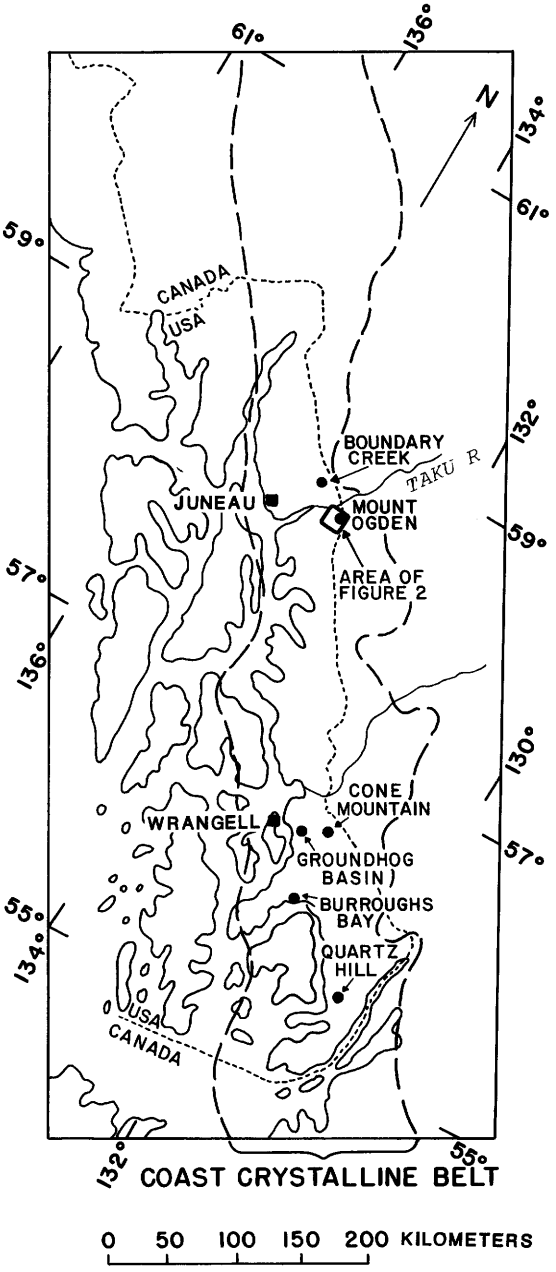

Figure 1.--Map showing significant molybdenite occurrences in Coast crystalline belt (area between long dashes), southeastern Alaska, and area of figure 2.

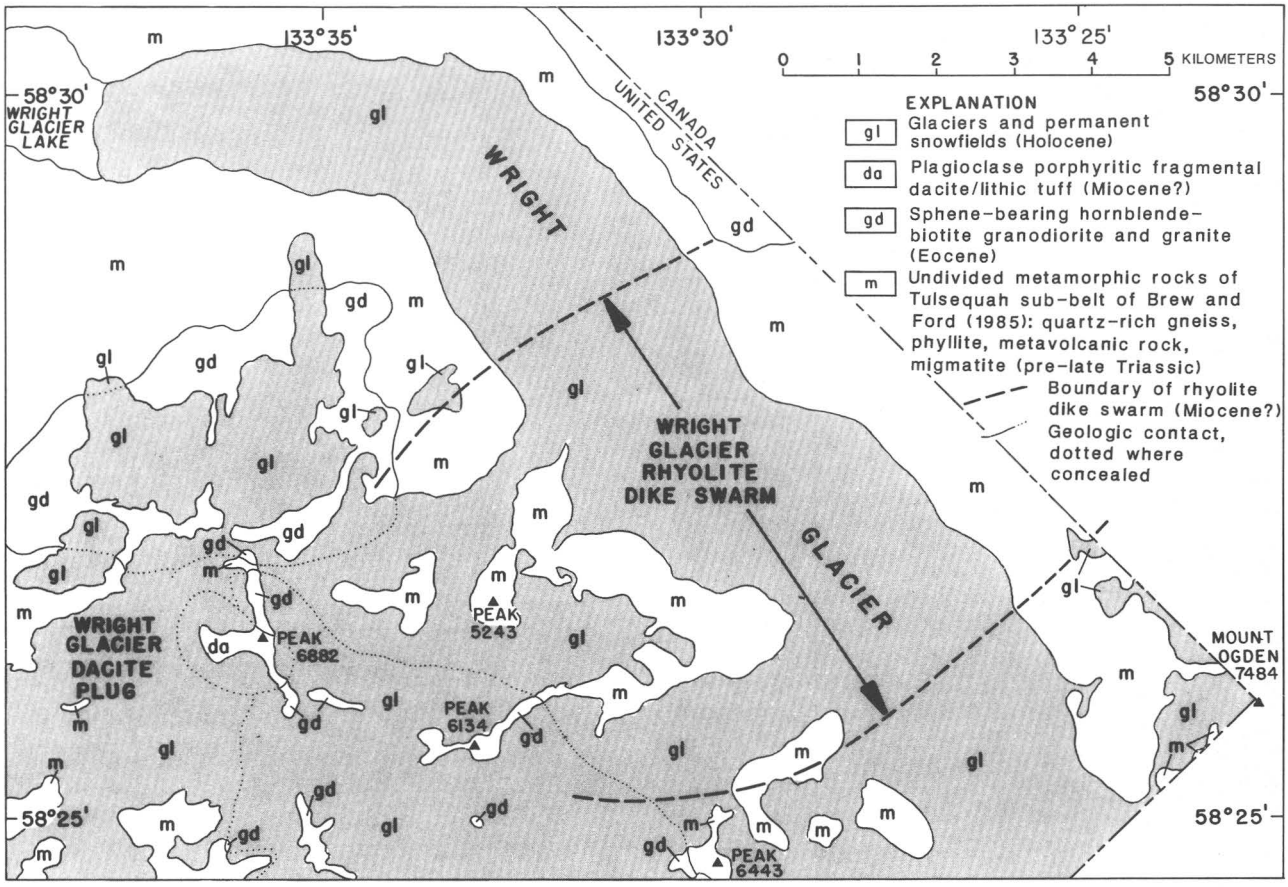

Figure 2.--Map of Wright Glacier area, Coast crystalline belt, showing location of Wright Glacier rhyolite dike swarm and dacite plug. Base map from U.S. Geological Survey Taku River B-5 1:63,360 series topographic map.

subjected to biotitic alteration, but fragments of silicic schist like that exposed nearby are also present. Some fine-grained disseminated sulfide is present. Chemically, the rock has a SiO_2 content of 63.3 percent and is a calcalkalic dacite of average K-content in the classification of Irvine and Baragar (1971). It is a high-K dacite according to Peccarillo and Taylor (1976). Semiquantitative spectrographic analysis indicates that the rock contains amounts of molybdenum that are detectable but less than 5 ppm and contains 10 ppm arsenic (S.J. Sutley and J.D. Hoffman, USGS, written communs., 1986).

We are uncertain of the exact age of the plug and the dikes, but the nature of the lithic fragments in the plug, the intrusive relations with the 50 Ma granitoids, and time inferred to have elapsed between the emplacement of the granite and its uplift and subsequent intrusion by the dacite, all indicate that the plug and dikes are probably appreciably younger than the granitic rocks. The relations between the plug and the dikes have not been observed, although dikes occur in granitic rock close to the plug. We presently interpret them to be of the same age and suggest that the dikes and the plug, which is located at the northwestern end of the dike swarm, came from the same concealed source.

The Wright Glacier dacite plug and rhyolite dike swarm are the northernmost expression of late Cenozoic magmatism reported to date in southeastern Alaska (see also Koch and others, this volume). Their presence suggests that the northwest to southeast crustal extension that localized the somewhat younger dike swarms further south in southeastern Alaska and the volcanic fields of west-central British Columbia was locally active elsewhere in the northern Cordillera and that a concentration of late Cenozoic activity may have occurred in the Coast Mountains east of Juneau.

REFERENCES CITED

Brew, D.A., and Ford, A.B., 1985, Preliminary reconnaissance geologic map of the Juneau,

Taku River, Atlin and part of the Skagway 1:250,000 quadrangles, southeastern Alaska: U.S. Geological Survey Open-File Report 85-395, 23 p.

Brew, D.A., and Morrell, R.P., 1983, Intrusive rocks and plutonic belts in southeastern Alaska, in Roddick, J.A., ed., Circum-Pacific plutonic terranes: Geological Society of America Memoir 159, p. 171-193.

Grybeck, D.J., Berg, H.C., and Karl, S.M., 1984, Map and description of the mineral deposits in the Petersburg and eastern Port Alexander quadrangles, southeastern Alaska: U.S. Geological Survey Open-File Report 84-837, 87 p.

Hudson, Travis, Smith, J.G., and Elliott, R.L., 1979, Petrology, composition, and age of intrusive rocks associated with the Quartz Hill molybdenite deposit, southeastern Alaska: Canadian Journal of Earth Sciences, v. 16, no. 9, p. 1805-1822.

Irvine, T.N., and Baragar, W.R., 1971, A guide to the chemical classification of the common volcanic rocks: Canadian Journal of Earth Sciences, v. 8, no. 5, p. 523-548.

Peccarillo, A., and Taylor, S.R., 1976, Geochemistry of Eocene calcalkalic volcanic rocks from the Kastamonu area, northern Turkey: Contributions to Mineralogy and Petrology, v. 58, p. 63-81.

Souther, J.G., 1971, Geology and ore deposits of Tulsequah map area, British Columbia: Geological Survey of Canada Memoir 362, 84 p.

Reviewers: R.D. Koch and T.G. Theodore

ULTRAMAFIC AND MAFIC SILLS IN THE VICINITY OF THE TREADWELL GOLD DEPOSITS, DOUGLAS ISLAND, SOUTHEASTERN ALASKA

David A. Brew, Glen R. Himmelberg, Arthur B. Ford, and Robert C. Jachens

A group of ultramafic and mafic sills occurs close to the Treadwell deposits of the Juneau Gold Belt (fig. 1). They may have some role in the origin and localization of the deposits and are described here so that workers concerned with the genesis of these important lodes, which produced 3.2 million ounces (about 100,000 kg) of gold between 1881 and 1926 (Wells and others, 1985), may evaluate their significance.

The Treadwell deposits consist of free gold and various sulfide minerals in calcite veins and disseminated in a highly altered felsic granitic rock. Their geology has been described by Becker (1898) and Spencer (1904, 1905a, b, 1906) and their exploration and production history by Cobb (1972), Stone and Stone (1980), Wells and others (1985), and Redman and others (1986). The regional setting is shown on the maps of Ford and Brew (1973) and Brew and Ford (1985). The occurrence and possible significance of the sills was called to our attention by George A. Moerlein in 1986; several of the small areas of mafic rock had been mapped in our previous fieldwork (unit "sdb" of Ford and Brew, 1973), but the extent of the bodies had not been recognized.

The sills are poorly exposed along Gastineau Channel on the northeastern shore of Douglas Island starting just south of the former site of the Alaska-Mexican shoreline facility and extending to the point of land just north of the mouth of Ready Bullion Creek (fig. 1). Their sill-like occurrence is inferred from the distribution of scattered several-meter-wide outcrops of mafic and ultramafic rock in relation to intervening outcrops tens of meters wide of graywacke semischist, slate, and minor greenstone and greenschist that are considered to belong to the Seymour Canal Formation of the Stephens Passage Group of Late Jurassic and Early Cretaceous age (Lathram and others, 1965). It is possible that they are not continuous sills at all, but instead are a series of irregular lumps conformable with the country rock. As discussed below, we infer that the surface outcrops are connected at depth to a major mafic-ultramafic feature.

Field observations indicate that the hanging wall of the northwest-southeast-striking, northeast-dipping Treadwell ore-bearing altered felsic rock sill must locally be within a few meters of the ultramafic sills at the surface, but evidence indicates that there is at least some greenstone-greenschist in between everywhere. We do not know if the now-inaccessible mine workings cut any mafic-ultramafic rock. In addition to the shoreline exposures, another ultramafic sill (not shown on fig. 2) occurs in the country rocks on the footwall side of the Treadwell ore-bearing sill (G.A. Moerlein, Houston Oil and Minerals, Co., oral commun., 1986). The sills appear to be confined to a northwest-southeast-trending zone no more than a kilometer wide adjacent to the Gastineau Channel fault; none were found along the course of Ready Bullion Creek, which affords good exposures across the structure of the footwall for a few kilometers.

The southernmost exposures of the sills contrast with those farther north. At the point of land just north of the mouth of Ready Bullion Creek, a body of magnetite-bearing hornblende diorite and hornblendite a few tens of meters wide has locally well-developed banding and cockscomb layering. These rock types are not exposed to the north, where the dominant sill rocks are the clinopyroxenite described below. Large (to 1 m maximum) boulders of orange-weathering harzburgite (sample 86DB069B) are found in several places on the beach just north of the hornblendite and hornblende diorite outcrops. Their origin is uncertain; they are not likely to belong to the clinopyroxenite-hornblendite-diorite suite. Nevertheless, all of the boulder occurrences that are known are in this one place. No other harzburgite occurrences have been reported from Douglas Island or elsewhere in the vicinity of Juneau, and the provenance of these probably ophiolite-related boulders remains a puzzle.

The ultramafic rocks samples are magnetite-bearing clinopyroxenite, hornblende clinopyroxenite, and plagioclase-bearing clinopyroxenite (samples 86DB064A, 86DB068A, and 86DB069A, respectively on table 1). They are brown weathering, hard, dense, and have a coarse serrate texture with pyroxene grains up to 1 cm maximum dimension. From a distance they look enough like the augite-bearing greenstones in the Douglas Island Volcanics of the Stephens Passage Group to have fooled two of us (DAB and ABF) repeatedly as we walked this stretch of beach. A phenocryst from a sample of those greenstones (86DB066A) just south of the mouth of Ready Bullion Creek was analyzed for comparative purposes. The chemical compositions and structural formulas based on microprobe analyses of the pyroxenes in clinopyroxenite, harzburgite, and greenstone are given in table 1, those of the olivine from the harzburgite in table 2, and the pyroxene compositions are plotted in figures 2 and 3. In general the pyroxene values group closely, differ appreciably from those from the Blashke Islands (Himmelberg and others, 1986), but are similar to those reported from Duke Island (Irvine, 1974) and other southeastern Alaskan-type ultramafic complexes. These diagrams show that the Treadwell suite has petrogenetic affinity with normal alkalic basaltic rocks.

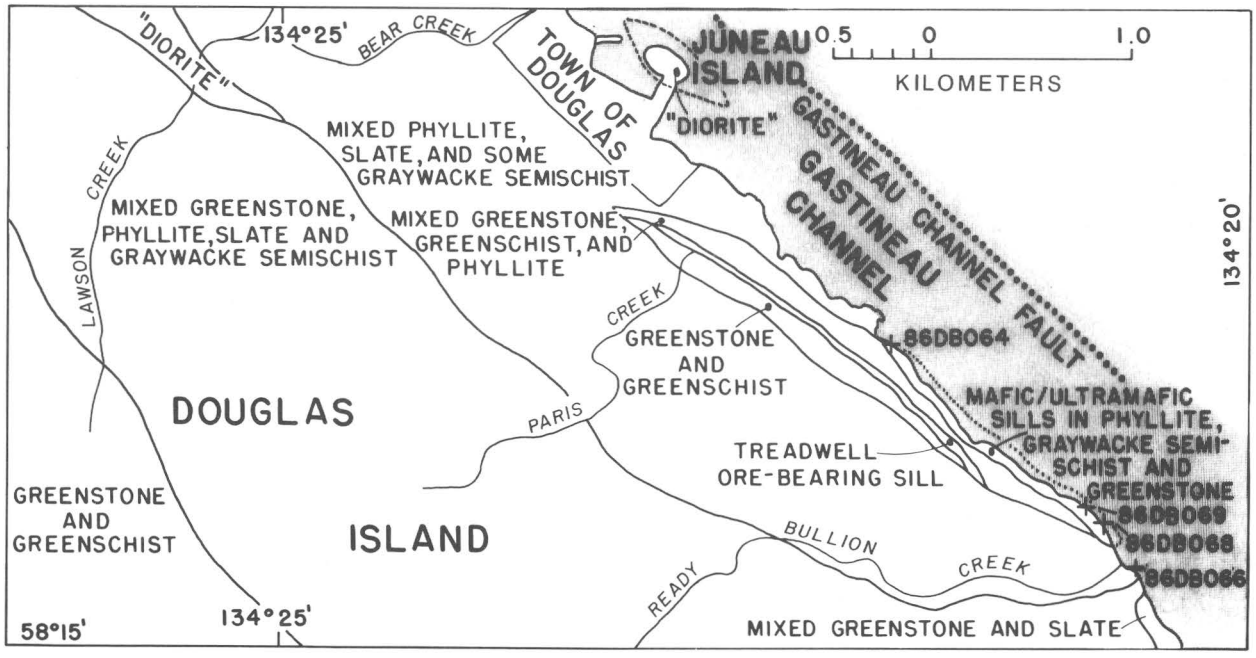

Figure 1.--Generalized geologic map of Treadwell mine area, Douglas Island, showing sample locations (+) and mafic-ultramafic sills.

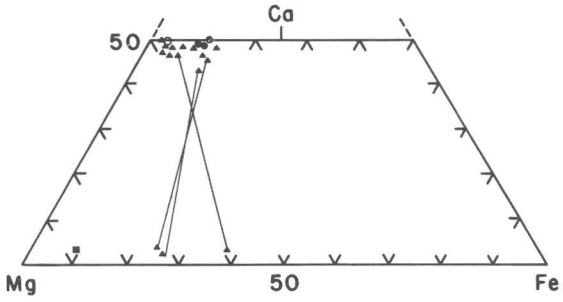

Figure 2.--Mg-Fe-Ca triangular diagram showing compositions of pyroxenes from Treadwell mine area ultramafic sills (solid circles), from the Douglas Island Volcanics (open circle), from harzburgite float (solid square), and from peridotite-gabbro suite at Blashke Islands (solid triangles, Himmelberg and others, 1986). Tie lines connect clinopyroxene and orthopyroxene in the same sample.

The recognition of the mafic-ultramafic sills helps explain a hitherto enigmatic prominent linear aeromagnetic anomaly close to Gastineau Channel (U.S. Geological Survey, 1984). That anomaly extends southeastward to include the exposed magnetite-bearing mafic-ultramafic rocks at the Midway Islands and in Port Snettisham (Jachens, 1984; Brew and Grybeck, 1984) and is more or less in line with an inferred belt of linear magnetic anomalies to the northwest that accompanies the mafic and ultramafic rocks exposed at Haines and Klukwan (Decker and others, 1981). Strong to moderate gravity anomalies accompany all the magnetic anomalies (D.F. Barnes, oral commun., 1986). Although no detailed models have been prepared, preliminary studies of the magnetic properties of oriented samples from the Douglas Island sills indicate that the rocks have susceptibilities that could produce the observed anomaly provided that the sills reflect a larger body with comparable magnetic susceptibility at depth. Preliminary two-dimensional models of the magnetic anomaly southeast of Douglas Island suggest that the source body is about 8 km wide at its top and extends to a significant depth.

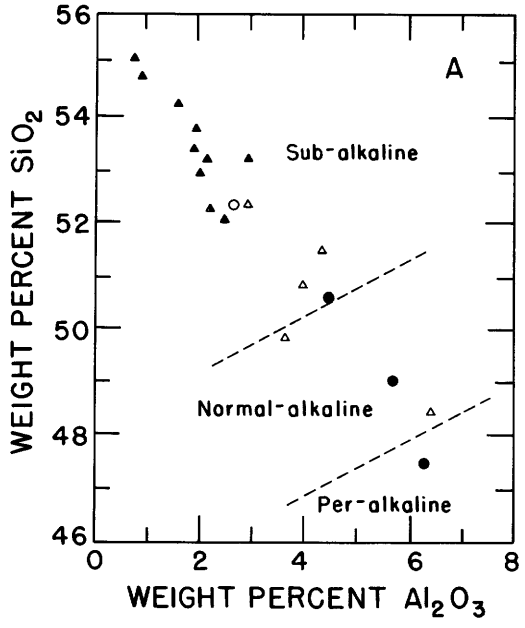

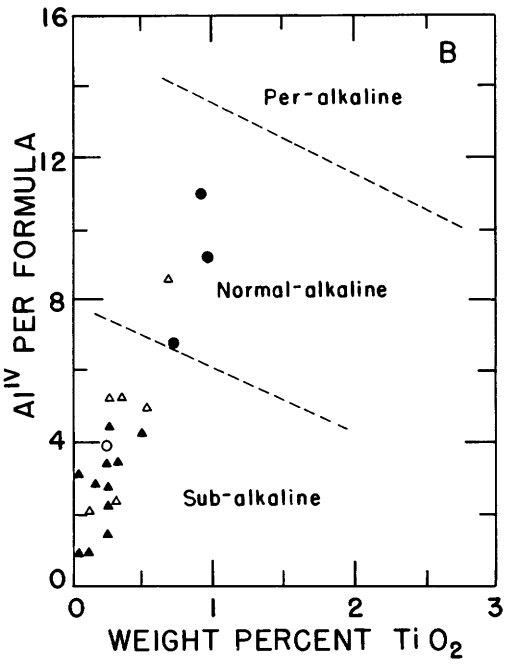

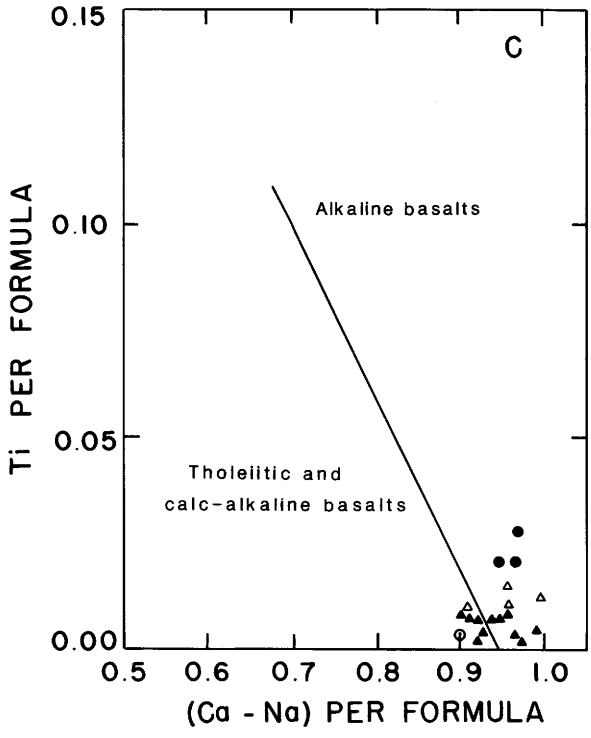

Figure 3.--Clinopyroxene discrimination diagrams. Solid circles Treadwell mine area ultramafic sills; open circle, Douglas Island Volcanics; solid triangles, Blashke Island rocks (Himmelberg and others, 1986); open triangles, Duke Island rocks (Irvine, 1974). A, SiO_2 versus Al_2O_3 (Le Bas, 1962); B, Al^{IV} versus TiO_2 (Le Bas, 1962); C, Ti versus (Ca+Na) (Leterrier and others, 1982).

Table 1.--Chemical composition (in weight percent) and structural formula of pyroxene in Douglas Island ultramafic and volcanic samples

	86DB64A CPX	86DB68A CPX	86DB69A CPX	86DB69B OPX	86DB66A CPX
SiO_2	49.00	50.60	47.50	55.30	52.20
TiO_2	.91	.68	.92	.00	.26
Al_2O_3	5.64	4.24	6.14	4.05	2.66
FeO	7.61	6.62	7.81	6.05	5.80
MnO	.19	.13	.21	.14	.17
MgO	12.60	14.00	12.70	32.40	16.00
CaO	23.70	23.40	23.40	1.00	22.30
Na_2O	.43	.24	.36	.00	.24
Sum	100.08	99.91	99.04	98.94	99.63
Si	1.816	1.870	1.777	1.929	1.919
AlIV	.184	.130	.223	.071	.081
Sum T	2.000	2.000	2.000	2.000	2.000
AlVI	.068	.055	.048	.096	.035
Ti	.025	.019	.026	.000	.007
Fe	.236	.205	.245	.177	.178
Mn	.006	.004	.007	.004	.005
Mg	.697	.772	.709	1.686	.878
Ca	.942	.928	.939	.037	.880
Na	.031	.017	.026	.000	.017
Sum	4.000	4.000	4.000	4.000	4.000
100 Mg/ Mg+Fe+Mn	74.2	78.7	73.8	90.3	82.7

Table 2.--Chemical composition in weight percent and structural formula of olivine in Douglas Island harzburgite
[n.d., not determined]

	86DB69B Olivine
SiO_2	41.90
FeO	9.30
MnO	.14
MgO	48.20
CaO	.00
NiO	n.d.
Sum	99.54
Si	1.033
Fe	.192
Mn	.003
Mg	1.772
Ca	.000
Ni	.000
Sum	3.000
100 Mg/ Mg+Fe+Mn	90.1

As mentioned earlier, the relations (if any) of the ultramafic and mafic sills to the mineralization at the Treadwell mines and perhaps to the Alaska-Juneau mine on the northeast side of Gastineau Channel are not known. The northwestern part of the magnetic anomaly clearly underlies the Treadwell deposits, and the northern edge of the magnetic source beneath almost a top the Alaska-Juneau and nearby gold deposits. It is intriguing to speculate about the possible linkages, however, given the strong similarities among the mesothermal gold deposits throughout the northern Cordillera (Nesbitt and others, 1986) and the spatial association of ultramafic rocks with the most important concentrations of lode deposits in the Sierran foothills (Böhlke and Kistler, 1986). R.P. Ashley (USGS, written commun., 1986) has pointed out that although there are strong associations of Sierran gold deposits with ultramafic rocks on a regional scale and on a local scale in some mining districts, it is entirely possible that those relationships are fortuitous; the low-sulfide gold-quartz vein deposits and the ultramafic rocks may both be controlled by the same major regional structures, but may not necessarily be related to each other.

REFERENCES CITED

Becker, G.F., 1898, Reconnaissance of the gold fields of southern Alaska, with some notes on general geology: U.S. Geological Survey 18th Annual Report, pt. 3, p. 1-86.

Böhlke, J.K., and Kistler, R.W., 1986, Rb-Sr, K-Ar, and stable isotope evidence for the ages and sources of fluid components of gold-bearing quartz veins in the northern Sierra Nevada Foothills metamorphic belt, California: Economic Geology, v. 81, no. 2, p. 296-322.

Brew, D.A., and Ford, A.B., 1985, Preliminary reconnaissance geologic map of the Juneau, Taku River, Atlin and part of the Skagway 1:250,000 quadrangles, southeastern Alaska: U.S. Geological Survey Open-File Report 85-395, 23 p.

Brew, D.A., and Grybeck, Donald, 1984, Geology of the Tracy Arm-Fords Terror wilderness study area and vicinity, in Mineral resources of Tracy Arm-Fords Terror wilderness study area and vicinity, Alaska: U.S. Geological Survey Bulletin 1525, p. 19-52.

Cobb, E.H., 1972, Metallic mineral resources map of the Juneau quadrangle, Alaska: U.S. Geological Miscellaneous Field Studies Map MF-435, scale 1:250,000.

Decker, John, Mullen, M.W., and Schwab, C.E., 1981, Aeromagnetic profile map of southeastern Alaska: U.S. Geological Survey Open-File Report 82-505, scale 1:1,000,000.

Ford, A.B., and Brew, D.A., 1973, Preliminary geologic and metamorphic-isograd map of the Juneau B-2 quadrangle, Alaska: U.S. Geological Survey Miscellaneous Field Studies Map MF-527, scale 1:31,680.

Himmelberg, G.R., Loney, R.A., and Craig, J.T., 1986, Petrogenesis of the ultramafic complex at the Blashke Islands, southeastern Alaska: U.S. Geological Survey Bulletin 1662, 14 p.

Irvine, T.N., 1974, Petrology of the Duke Island ultramafic complex, southeastern Alaska: Geological Society of America Memoir 138, 240 p.

Jachens, R.C., 1984, Interpretation of the aeromagnetic data, in Mineral resources of Tracy Arm-Fords Terror wilderness study area and vicinity, Alaska: U.S. Geological Survey Bulletin 1525, p. 53-62.

Lathram, E.H., Pomeroy, J.S., Berg, H.C., and Loney, R.A., 1965, Reconnaissance geology of Admiralty Island, Alaska: U.S. Geological Survey Bulletin 1181-R, p. R1-R48.

LeBas, M.H., 1962, The role of aluminum in igneous clinopyroxenes with relation to their parentage: American Journal of Science, v. 260, p. 267-288.

Leterrier, Jacques, Maury, R.C., Thonon, Pierre, Girard, Danielle, and Marchal, Michele, 1982, Clinopyroxene composition as a method of identification of the magmatic affinities of paleovolcanic series: Earth and Planetary Science Letters, v. 59, no. 1, p. 139-154.

Nesbitt, B.E., Murowchick, J.B., and Muehlenbachs, K., 1986, Dual origins of lode gold deposits in the Canadian cordillera: Geology, v. 14, p. 506-509.

Redman, E., Roberts, W.S., Clough, A., and Kurtak, J., 1986, Preliminary mine, prospect, and sample location maps and descriptions, Juneau Gold Belt area: U.S. Bureau of Mines Open-File Report 85-86, 68 p.

Spencer, A.C., 1904, The Juneau gold belt, Alaska: U.S. Geological Survey Bulletin 225, p. 28-42.

_____1905a, The geology of the Treadwell ore-deposits, Douglas Island, Alaska: Transactions American Institute of Mining Engineers, v. 35, p. 473-510.

_____1905b, The Treadwell ore deposits, Douglas Island: U.S. Geological Survey Bulletin 259, p. 69-87.

_____1906, The Juneau gold belt, Alaska: U.S. Geological Survey Bulletin 287, p. 1-137.

Stone, David, and Stone, Brenda, 1980, Hard rock gold, the story of the great mines that were the heartbeat of Juneau: Seattle, Wash., Vanguard Press, 108 p. Reprinted in 1983.

U.S. Geological Survey, 1984, Aeromagnetic map of the Juneau area, Alaska: U.S. Geological Survey Open-File Report 84-296, scale 1:250,000.

Wells, D.E., Pittman, T.L., Brew, D.A., and Douglass, S.L., 1985, Map and description of the mineral deposits in the Juneau, Taku River, Atlin, and part of the Skagway quadrangles, Alaska: U.S. Geological Survey Open-File Report 85-717, 332 p.

Reviewers: R.P. Ashley and R.A. Loney

NEWLY DISCOVERED MOLYBDENITE OCCURRENCE NEAR BOUNDARY CREEK, COAST MOUNTAINS, SOUTHEASTERN ALASKA

Richard D. Koch, David A. Brew, and Arthur B. Ford

A previously unknown molybdenite occurrence was discovered during fieldwork in the Coast Mountains east of Juneau during 1986. This occurrence is close to the "Boundary Creek occurrence" discovered and described by Brew and Ford (1969) (fig. 1). Based on very limited data, the mineralization at this newly discovered locality appears to cover a larger area than that at the other locality. This article reports what we presently know of this new "Boundary Creek 2" occurrence. Further surface work is planned to define better the extent and grade of the mineralized rock.

The regional geologic setting of the newly discovered occurrence is shown on the map of Brew and Ford (1985). Compared with "Boundary Creek 1," the local setting of "Boundary Creek 2" is relatively simple; it occurs well within a large mass of granodiorite, granite, and alkali granite rather than near the margin (fig. 2). In detail, the newly discovered occurrence is at an elevation of about 3,800 ft (1,160 m) in alkali leucocratic granite on a broad south-extending shoulder of the main ridge that is north and east of Boundary Creek. Four grab samples were collected in alkali granite near the crest of that shoulder about 1.2 km west of lake 2880 (fig. 2). The alkali granite also occurs at one locality examined east of the occurrence, near lake 2880.

The rock at the newly discovered molybdenite locality is well-jointed, light-gray-weathering, fine- to coarse-grained, seriate-textured biotite alkali granite with a color index of 1. Some potassium feldspar grains are as large as 2 cm. Aplite dikes as wide as 25 cm cut the main rock. The age of the alkali granite is not known, except that it must be no older than the 50 Ma age of the dominant granodiorite pluton with which it is spatially associated (Brew and Ford, 1985); the alkali granite may be a phase of that intrusion or it may be younger. If it is younger and intrusive into the granodiorite, then we favor an age of about 15-30 Ma for it, based on the general compositional analogies with the molybdenite-bearing pluton at Quartz Hill, with the host rocks for the molybdenite occurrence at Burroughs Bay (Hudson and others, 1979), and with molybdenite occurrences at Cone Mountain and Groundhog Basin (Grybeck and others, 1984) in southern southeastern Alaska (fig. 1).

The full extent of the mineralization is not known. Granite in an area of about 100 m by 100 m contains a trace to about 2 volume percent visible molybdenite, and an intensely iron-stained

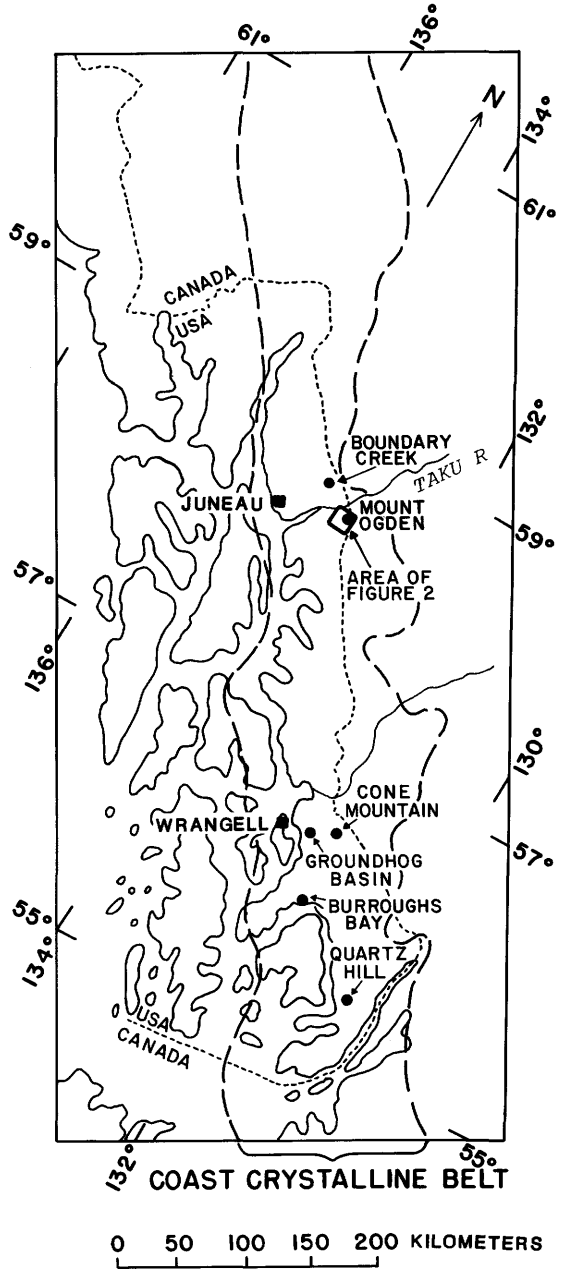

Figure 1.--Significant molybdenite occurrences in Coast crystalline belt, southeastern Alaska.

zone about 2 x 10 m in area contains up to 5 percent molybdenite as disseminated small grains and as composite flakes as large as 5 mm. Pyrite accompanies the molybdenite, and its oxidation is the cause of the iron stain. Widely spaced, narrow, coarse-grained pyrite-bearing quartz veins cut the mineralized rock, but they do not contain molybdenite. Semiquantitative spectrographic analyses of grab samples show that the large expanse of molybdenite-bearing rock contains

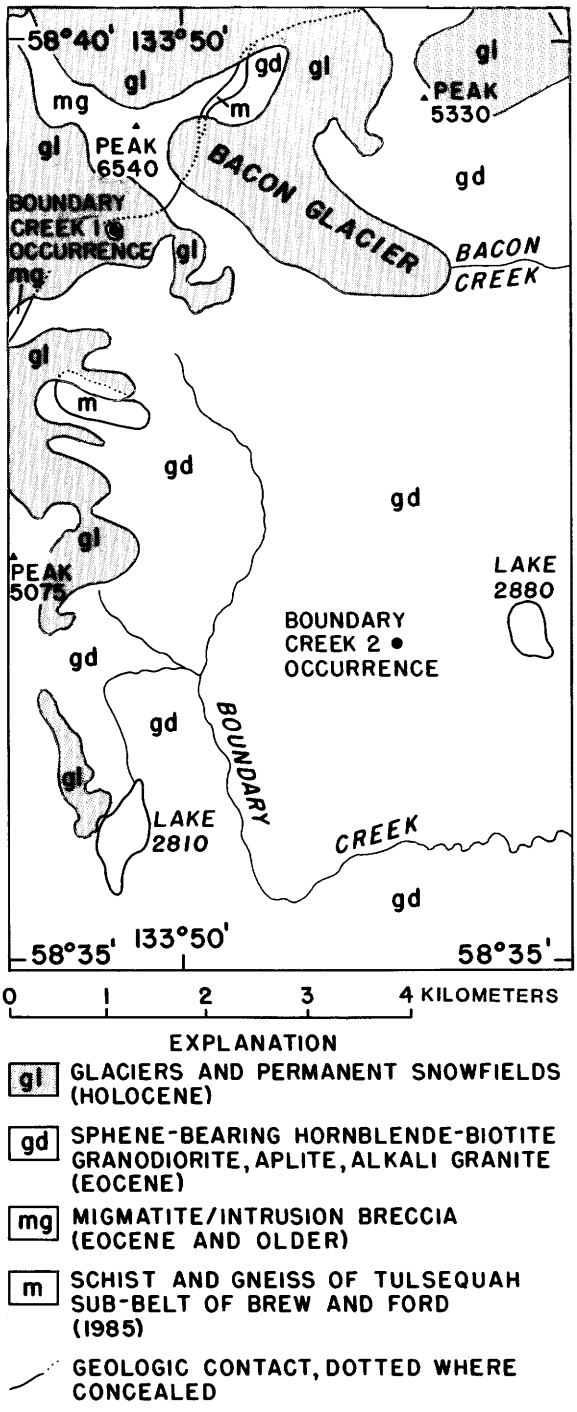

Figure 2.--Sketch map showing Boundary Creek molybdenite occurrences and vicinity. Base from U.S. Geological Survey Taku River (C-6) 1:63,360 series topographic map.

5 ppm Mo and a trace of Ag; the small exposure of higher grade rock contains 1,500 ppm Mo and 1.5 ppm Ag; and the quartz veins contain 30 ppm Mo, 10 ppm Bi, 200 ppm Cu, and 2 ppm Ag (E.A. Bailey, and O. Erlich, written commun., 1986).

The significance of this newly discovered locality cannot be evaluated fully with the data at hand. Given the proximity to the Boundary Creek 1 occurrence, to the molybdenite deposits near Mount Ogden some 25 km to the southeast (Souther, 1971), and to the possible young volcanic plug and dike swarm that is near those deposits but on the Alaska side of the border (see Ford and Brew, this volume), we suggest that an area with both significant late Cenozoic intrusive rocks and potential for molybdenite resources may exist in the Coast Mountains near Juneau.

REFERENCES CITED

Brew, D.A., and Ford, A.B., 1969, Boundary Creek molybdenum-silver occurrence, southeastern Alaska: U.S. Geological Survey Circular 615, p. 12-15.

___1985, Preliminary reconnaissance geologic map of the Juneau, Taku River, Atlin and part of the Skagway 1:250,000 quadrangles, southeastern Alaska: U.S. Geological Survey Open-File Report 85-395, 23 p., scale 1:250,000, 2 sheets.

Grybeck, D.G., Berg, H.C., and Karl, S.M., 1984, Map and description of the mineral deposits in the Petersburg and eastern Port Alexander quadrangles, southeastern Alaska: U.S. Geological Survey Open-File Report 84-837, 87 p.

Hudson, Travis, Smith, J.G., and Elliott, R.L., 1979, Petrology, composition, and age of intrusive rocks associated with the Quartz Hill molybdenite deposit, southeastern Alaska: Canadian Journal of Earth Sciences, v. 16, no. 9, p. 1805-1822.

Souther, J.G., 1971, Geology and ore deposits of Tulsequah map area, British Columbia: Geological Survey of Canada Memoir 362, 84 p.

Reviewers: S.L. Douglass and T.G. Theodore

SALT CHUCK PALLADIUM-BEARING ULTRAMAFIC BODY, PRINCE OF WALES ISLAND

Robert A. Loney, Glen R. Himmelberg, and Nora Shew

The ultramafic intrusive body north of Salt Chuck, at the head of Kasaan Bay, southeastern Prince of Wales Island, forms a tadpole-shaped outcrop that trends west-northwest for a distance of 7.3 km; its maximum width is about 1.6 km at its western end (fig. 1). The ultramafic body intrudes mainly basalt flows and pyroclastic rocks of the Descon Formation (Lower Ordovician through Lower Silurian) (Eberlein and others, 1983), in which it has produced a contact aureole at least a few meters wide. The Salt Chuck Mine, located in the middle part of the intrusion, is the only mine in the body. It operated intermittently from 1905 to 1941 and produced about 300,000 tons (270,000 t) of milling ore (chiefly bornite in clinopyroxenite) estimated to have averaged 0.95 percent Cu, 0.36 oz (12 ppm) Au, 0.17 oz (5.8 ppm) Ag, and 0.63 oz (22 ppm) Pd per ton (Holt and others, 1948).

The intrusive body has been included by previous authors in the belt of Cretaceous ultramafic bodies that extends from Klukwan to Duke Island (Lanphere and Eberlein, 1966; Brew and Morrell, 1980; Himmelberg and others, 1986). These bodies have been called zoned ultramafic complexes of the Ural-Alaskan type (Taylor, 1967) and concentric complexes (Jackson and Thayer, 1972). A recent potassium-argon study on biotite clinopyroxenite from the Salt Chuck body has yielded an age of 429 Ma (chloritized biotite). The K_2O values of the altered biotite are low (table 1), thus making the Paleozoic age suspect. However, the extreme age difference between the Salt Chuck ultramafic body and the others in the Klukwan-Duke Island ultramafic belt implies that it should be considered separately from them.

Our field mapping in 1986 showed the Salt Chuck intrusive body to consist of clinopyroxenite and gabbro that grade irregularly into one another with no regular pattern. Most exposures are massive and homogeneous, although isomodal layers 2 to 8 cm thick with mineral ratio contacts are locally present in some gabbros. The clinopyroxenites are clinopyroxene-magnetite cumulates with late (postcumulus) plagioclase and biotite. Most gabbros are anhedral granular or subhedral granular clinopyroxene-plagioclase-magnetite adcumulates with postcumulus biotite. The postcumulus biotite occurs in clinopyroxenite commonly in a poikilitic texture in which it forms enclosing crystals (oikocrysts) as large as 2 to 3 cm in size. Grain size of all the rocks is generally 1-2 mm, with the exception of the biotite oikocrysts noted above.

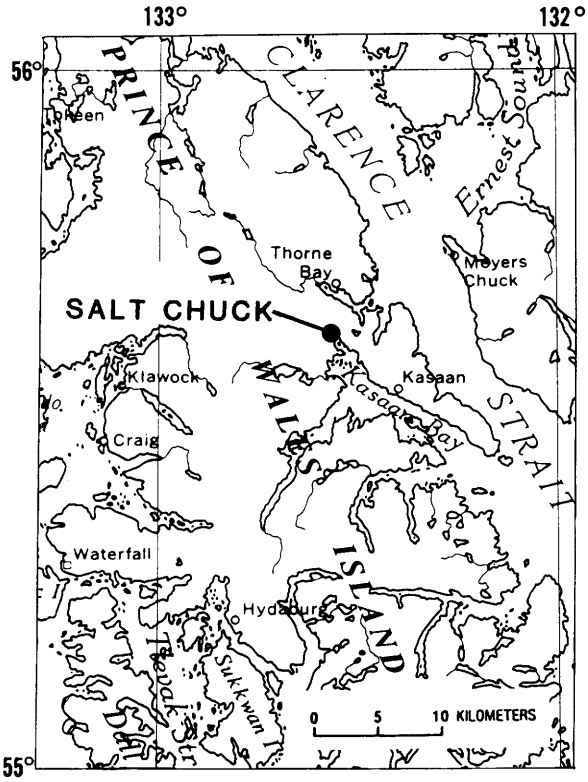

Figure 1.--Location of Salt Chuck ultramafic body.

Our initial petrographic study indicates that although the rocks are extensively altered, a close approximation of the original modal amounts of primary minerals can be made. These amounts are as follows: clinopyroxene, greater than 90 percent to 35 percent; plagioclase, less than 1 percent to 10 percent in clinopyroxenite, 20 to 65 percent in gabbro; magnetite, generally 5 to 10 percent in clinopyroxenite and gabbro, although some gabbros contain as little as 2 percent magnetite; biotite, 1 to 10 percent in clinopyroxenite and gabbro. Trace amounts of hornblende are present in some samples of both rock types, apatite is a common accessory mineral in both types, and interstitial potassium feldspar was noted in one gabbro sample. The rocks are extensively altered and veined by epidote. Plagioclase in most samples is 100 percent altered to mixtures of white mica, zoisite/clinozoisite, epidote, and in some cases minor calcite and prehnite. Unaltered grains of biotite are present in some clinopyroxenite, but in most grains biotite is altered to chlorite, epidote, and prehnite. Clinopyroxenite generally remains unaltered, except for minor chloritic alteration along fractures and cleavage in some samples.

Table 1.--Potassium-argon analytical data, Salt Chuck mine, Alaska
[Constants used: $^{40}K/K = 1.16 \times 10^{-4}$ mol/mol; $\lambda_\varepsilon = 0.581 \times 10^{-10} yr^{-1}$; $\lambda_\beta = 4.962 \times 10^{-10} yr^{-1}$]

Sample No.	Lat. Long.	Rock type	Mineral dated	K_2O (wt pct)	Ar_{rad} ($\times 10^{-9}$ moles/g)	Ar_{rad} (pct)	Age (Ma)
84ASh 35c	55°37'35" N. 132°33'17" W.	Clino-pyroxenite	Biotite (altered)	5.98	4.2436	96.8	429±11
				6.06	4.1527	97.6	
				$\bar{x}$=6.02			

Bornite, the principal ore mineral of the Salt Chuck Mine, occurs as interstitial grains in clinopyroxenite in amounts up to 15 percent; it occurs similarly in gabbro in lesser amounts. Significant bornite occurrences are primarily restricted to the workings of the mine.

REFERENCES CITED

Brew, D.A., and Morrell, R.P., 1980, Intrusive rocks and plutonic belts of southeastern Alaska, U.S.A.: U.S. Geological Survey Open-File Report 80-78, 34 p.

Eberlein, G.D., Churkin, Michael, Jr., Carter, Claire, Berg, H.C., and Ovenshine, A.T., 1983, Geology of the Craig quadrangle, Alaska: U.S. Geological Survey Open-File Report 83-91, 23 p.

Himmelberg, G.R., Loney, R.A., and Craig, J.T., 1986, Petrogenesis of the ultramafic complex at the Blashke Islands, southeastern Alaska: U.S. Geological Survey Bulletin 1662, 14 p.

Holt, S.P., Shepard, J.P., Thorne, R.L., Tolonen, A.W., and Fosse, E.L., 1948, Investigation of the Salt Chuck copper mine, Kasaan Peninsula, Prince of Wales Island, southeastern Alaska: U.S. Bureau of Mines Report of Investigations 4358, 16 p.

Jackson, E.D., and Thayer, T.P., 1972, Some criteria for distinguishing between stratiform, concentric, and alpine peridotite-gabbro complexes: International Geological Congress, 24th, Montreal, Proceedings, section 2, p. 289-296.

Lanphere, M.A., and Eberlein, G.D., 1966, Potassium-argon ages of magnetite-bearing ultramafic complexes in southeastern Alaska: Geological Society of America Special Paper 87, p. 94.

Taylor, H.P., Jr., 1967, The zoned ultramafic complexes of southeastern Alaska, in Wyllie, P.J., ed., Ultramafic and related rocks: New York, John Wiley, p. 96-118.

Reviewers: T.E.C. Keith and W.H. Nelson

THE ALASKA-JUNEAU GOLD DEPOSIT; REMOBILIZED SYNGENETIC VERSUS EXOTIC EPIGENETIC ORIGIN

Rainer J. Newberry and David A. Brew

The Alaska-Juneau (AJ) deposit is the largest lode producer of gold in Alaska. The AJ deposit is located at Juneau, near the northern end of a 10-km-wide, 150-km-long belt of lode gold deposits (the "Juneau gold belt") from which the majority of Alaska's lode gold has been produced. The AJ deposit is a swarm of sub-parallel quartz-ankerite±biotite-muscovite-chlorite-gold-sulfide veins of probable mid-Tertiary age. The deposits are described by Wernecke (1932), Twenhofel (1952), and Wayland (1960). Brew and Ford (1985) summarized the regional geology.

Current and continuing efforts to assess the undiscovered gold endowment of the Juneau gold belt are tied into genetic models of deposit formation. Traditionally, these deposits have been viewed as epigenetic veins and vein swarms, with an origin ascribed to boiling of circulating late metamorphic fluids (Goldfarb and others, 1986). Several industry geologists (for example, T.R. Turner, Calista Corp., written commun., 1986), however, support an origin by remobilization of a gold-enriched chemical sediment formed by volcanogenic ("exhalative") processes. If the epigenetic hypothesis is correct, then localization of orebodies depends principally on the presence of structural foci, and undiscovered endowment can be assessed by consideration of typical deposit densities in other structure-related vein districts (as in the Mother Lode district of California). If the remobilization hypothesis is correct, then there is a strong potential for undiscovered stratiform gold orebodies in the district, and the presence of such stratiform orebodies is a vital prerequisite to the formation of vein ores. In this article we review the evidence for both views and conclude that the deposits are most likely epigenetic in origin.

Several lines of evidence support a remobilized syngenetic model for gold mineralization in the AJ area. (1) The vein swarms are broadly stratabound in the sense that they occur in one lithostratigraphic unit, and may be in one part of that unit as suggested by alignment of the major open-pit orebodies (fig. 1). (2) The deposits occur in a black phyllite unit with many intercalated mafic and felsic rocks, structurally above a thick volcanic unit. (3) Extensive, broadly stratiform zones of ankerite-bearing rocks (units "ags" and "b" on fig. 1) are present in the area, adjacent to both intercalated mafic rocks (unit "a") and to the thick volcanic unit (unit "gs"). Such rocks are compositionally similar to "carbonate exhalites," that is, Fe-carbonate-rich rocks which host disseminated gold ores, as at the Agnico-Eagle deposit in Quebec (Barnett and others, 1982) and the Homestake deposit in South Dakota (Slaughter, 1968)

Four major lines of evidence argue for an epigenetic and against a remobilized syngenetic origin: (1) non-stratabound mineralization, (2) the minor role of syn-sedimentary volcanic activity, (3) evidence for broad-scale post-metamorphic hydrothermal activity, and (4) the lack of evidence for stratiform gold enrichment. Although the major orebodies of the AJ area are broadly stratabound, detailed mapping of the contact between the phyllite (unit "p" on fig. 1) and the greenstone units ("gs", "ags", and "clgs" on fig. 1) shows that the orebodies move away from this contact in the progression Perseverance-South-North pits. The Humboldt prospect, the largest prospect north of the North pit, is still farther upsection from the greenschist-phyllite contact. Structural mapping (Ford and Brew, 1973; Brew and Ford, 1977) indicated the presence of a major overturned antiform in the vicinity of the orebodies with the main pits in one limb of the fold; if the ore was truly stratabound then gold-bearing rocks would be expected to occur on both limbs of the fold. Finally, sampling of quartz veins in the AJ area (table 1) and locations of known prospects and adits (fig. 1) indicate that in detail the mineralization is not stratabound, but rather occurs over a wide stratigraphic interval and in a variety of different rock types.

Mafic bodies in the phyllite unit have been described as either metabasalt (Herreid, 1962) or metamorphosed gabbroic-dioritic sills (Wernecke, 1932). These bodies consist of foliated amphibole and plagioclase with accessory magnetite and ilmenite. Contact relations with the surrounding phyllites are obscure and do not conclusively demonstrate intrusive or extrusive origins. Our mapping, however, indicates (1) that thicker bodies are coarser grained (up to 2 cm) whereas thinner bodies are finer grained (2-4 mm) and (2) all bodies examined have fine-grained margins and coarse-grained interiors. Thus, they are intrusive and not metavolcanic rocks.

Felsic rocks do not show clastic features; locally (fig. 1) they crosscut foliation, indicating either an intrusive or alteration origin and not a syn-sedimentary volcanic origin. The occurrence of graphitic, pyrrhotite-bearing muscovite-quartz schist slightly crosscutting the regional strike of the graphitic phyllite near the Perseverance pits (fig. 1) suggests that the pyrrhotite-bearing schist originated by alteration of the graphitic phyllite in this area. Most of the quartzite and micaceous quartzite in the AJ area is probably of sedimentary origin and is not metamorphosed from volcanic rock.

Although usually well-laminated, ankerite-bearing rocks in the AJ area distinctly show

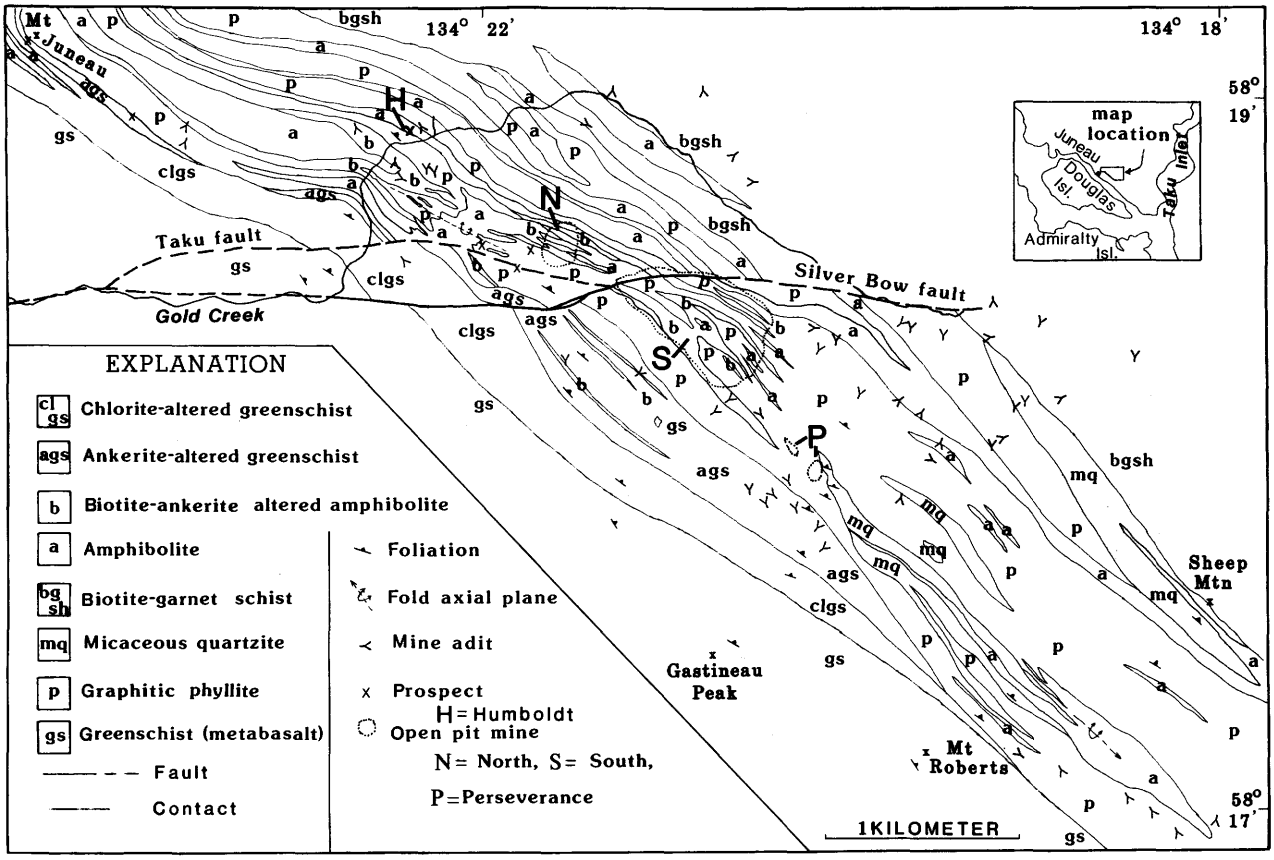

Figure 1.--Bedrock geologic map of Alaska-Juneau mine area, Juneau quadrangle, Alaska. Modified from Wernecke (1932), Twenhofel (1952), Ford and Brew (1973), Brew and Ford (1977), based on mapping 1985-1986. Topographic base and prospect locations from USGS 1:24,000 Juneau and vicinity map, 1948.

crosscutting features. We recognize two major varieties: ankerite-altered amphibolite and ankerite-altered greenschist. Map relations (fig. 1) indicate that biotite-ankerite rocks surround amphibolite (meta-diorite/gabbro) sills in the vicinity of orebodies. Detailed mapping indicates that contacts between foliated amphibolite and laminated biotite-ankerite rock are gradational over 1-3 m; these contacts also commonly cut across foliation. Quartz veins with biotite-ankerite margins are present in amphibolites; although the veins distinctly crosscut foliation in the amphibolite, the biotite-ankerite margins possess the foliation of the rock they replace. Similarly, 1- to 5-m blocks of unaltered, ankerite-free greenstone occur within the ankerite-chlorite-biotite altered greenschist unit (unit "ags" on fig. 1). The presence of unaltered remnant blocks with the same foliation attitude indicates that the foliation is pseudomorphous after the original foliation. Finally, post-metamorphic quartz veins are found only within phyllites, altered greenschists, and altered amphibolites, which implies that the ankerite-biotite alteration is related to the post-metamorphic veins and that both are products of broad-scale post-metamorphic hydrothermal activity.

Pyrrhotite-pyrite relations provide further evidence of a hydrothermal origin for the alteration and veins. Petrographic examination of the altered rocks from the AJ area indicates a consistent alteration assemblage of ankerite-pyrrhotite-ilmenite±biotite-chlorite-muscovite-tourmaline. Pyrite is rare and only occurs as a late phase in quartz veins, whereas pyrrhotite is ubiquitous. The assemblage ilmenite-pyrrhotite is not reported from metamorphosed volcanogenic deposits but is described from mesothermal vein deposits (Ramdohr, 1980). Indeed, pyrrhotite is not the dominant iron sulfide in any unmetamorphosed volcanogenic sulfide deposit, and metamorphism to granulite facies is required to convert the bulk of pyrite to pyrrhotite in volcanogenic sulfide deposits (Rockingham and Hutchison, 1980). For example, the Homestake deposit, which has been metamorphosed to

Table 1.--Gold contents of rocks from the Alaska-Juneau mine area, Juneau quadrangle, southeastern Alaska [Analyses by atomic absorption; N, not detected at 50 ppb (0.05 ppm) detection limit; L, detected, but below 50 ppb; abbreviations: qtz, quartz; po, pyrrhotite; bio, biotite; ank, ankerite; gl, galena; chl, chlorite; tour, tourmaline; alt'd, altered]

Sample No.	Au (ppm)	Rock type and alteration	Location
85Rn116a	N	Black phyllite	300 m SW of N pit
85Rn124b	N	Carbonate rock	N pit
85Rn124c	N	Chert, interlayered with carbonate	N pit
85Rn124d	L	Black phyllite with qtz-po-bio veins	N pit
85Rn124e	N	Alt'd amphibolite	N pit
85Rn124f	0.1	Alt'd amphibolite with qtz-ank veins	N pit
85Rn130b	N	Qtz-po (5%)-musc-cal vein in phyllite	Uground, N orebody
85Rn131a	70	Qtz-po-gl-ank vein in bio-alt'd amphibolite	Uground, N orebody
85Rn140	N	Composite of 500 m of chl-alt'd greenschist	Gold Ck. at the Horn
85Rn140c	N	3 m thick felsic volc in greenschists	Gold Ck. at the Horn
85Rn183b	N	Chl alt'd amphibolite	Near Mt. Juneau
85Rn184a	N	Ankeritic schist (alt'd greenschist)	Mt. Juneau
85Rn192a	N	Chl alt'd amphibolite	Near Sheep Mtn.
85Rn194a	N	Marble	Near Mt. Roberts
86Rn24a	0.1	Qz-ank-tour veins in ank alt'd greenschist	Mt. Juneau

amphibolite facies, contains subequal pyrite and pyrrhotite (Slaughter, 1968). The stratabound Morro Velho gold deposit (Brazil), metamorphosed to mid greenschist facies, also has high pyrite contents (Gair, 1962). Since there is no evidence that rocks of the AJ area have been metamorphosed higher than amphibolite facies (Brew and Ford, 1985), a metamorphic origin for the pyrrhotite is unlikely. Tourmaline has been noted at approximately 18 localities in the AJ area; it occurs exclusively in the altered rocks and is in all of the alteration types. Although tourmaline occurs with some stratabound gold deposits (Slaughter, 1968) and with some volcanogenic sulfide deposits (Taylor and Slack, 1984), it is also very common with mesothermal gold vein deposits (Hodgson and MacGeehan, 1982) and with geothermal systems (Watanabe, 1967) and is thus not a diagnostic feature of either type of deposit. In general, the occurrence of a consistent opaque-silicate assemblage in all the altered rocks of the AJ area points to a single hydrothermal system; the fact that much of this alteration is demonstrably post-metamorphic suggests that it is all post-metamorphic.

We have evaluated the possibility of stratiform gold enrichment by reconnaissance sampling of the rocks in the AJ area; the results (table 1) indicate that (1) altered rocks with quartz veins contain gold values equal or greater than 0.1 ppm, (2) altered rocks (such as foliated ankerite-bearing rocks) which lack quartz veins contain low (less than 0.5 ppm) gold values, and that (3) unaltered rocks (such as metacherts and marbles) also contain low gold values. In contrast, stratabound gold deposits commonly contain gold concentrations of 10 ppm in non-veined rocks (Barnett and others, 1982) and background Au values for most rocks are approximately 0.01-0.005 ppm. Although our conclusions are limited by the detection limits of the analytical method used, the fact that only quartz-carbonate-veined rocks contain significant gold values suggests that gold was introduced into the rocks during veining, not remobilized from the rocks during veining.

In summary, the available evidence supports an epigenetic origin for the alteration and mineralization in the AJ area, and by inference, an exotic origin for the gold in the deposit. The map data also indicate that several cubic kilometers of ankeritic alteration resulted from the large hydrothermal system that operated in the AJ mine area. Goldfarb and others (1986) presented evidence for fluid boiling in the AJ veins and for vein formation at greater than 230° C and 1.5 kilobars. Such boiling results in CO_2 loss and carbonate deposition. We suggest that the accompanying loss of H_2S during boiling would result in Au deposition by decomplexation of Au(HS), as the experimental data on gold solubility in H_2S-bearing fluids (Seward, 1973) indicate that Au solubility drops by 2 orders of magnitude for every order of magnitude decrease in H_2S activity. In addition, gold solubility is sufficiently high under the proposed conditions of deposition (approximately 1-0.1 ppm; Seward, 1973) for circulating fluids to leach gold from any subjacent rock types. The establishment of the required

hydrothermal cell necessitates a major structural anomaly, and we suggest therefore that structural controls probably represent a dominant influence on the development of ores in the area.

REFERENCES CITED

Barnett, E.S., Hutchinson, R.W., Adamcik, Anton, and Barnett, R.J., 1982, Geology of the Agnico-Eagle gold deposit, Quebec, in Hutchinson, R.W., Spence, C.D., and Franklin, J.M., eds., Precambrian sulfide deposits: Geological Association of Canada Special Paper 25, p. 403-426.

Brew, D.A., and Ford, A.B., 1977, Preliminary geologic and metamorphic isograd map of the Juneau B-1 quadrangle, Alaska: U.S. Geological Survey Miscellaneous Field Studies Map MF-846, scale 1:31,680.

_____1985, Preliminary reconnaissance geologic map of the Juneau, Taku River, Atlin, and part of the Skagway 1:250,000 quadrangles, southeastern Alaska: U.S. Geological Survey Open-File Report 85-395.

Ford, A.B., and Brew, D.A., 1973, Preliminary geologic and metamorphic isograd map of the Juneau B-2 quadrangle, Alaska: U.S. Geological Survey Miscellaneous Field Studies Map MF-527, scale 1:31,680.

Gair, J.E., 1962, Geology and ore deposits of the Nova Lima and Rio Acima quadrangles, Minas Gerais, Brazil: U.S. Geological Survey Professional Paper 341-A, p. A1-A65.

Goldfarb, R.J., Light, T.D., and Leach, D.L., 1986, Nature of the ore fluids at the Alaska-Juneau gold deposit, in Bartsch-Winkler, Susan, and Reed, K.M., eds., Geologic studies in Alaska by the U.S. Geological Survey during 1985: U.S. Geological Survey Circular 978, p. 92-94.

Herreid, Gordon, 1962, Preliminary report on geologic mapping in the Coast Range mineral belt: Alaska Division of Mines and Minerals Geologic Report 1, 22 p.

Hodgson, C.J., and MacGeehan, P.J., 1982, A review of the geological characteristics of "gold-only" deposits in the Superior Province of the Canadian shield: Canadian Institute of Mining and Metallurgy, Special Vol. 24, p. 211-229.

Ramdohr, Paul, 1980, The ore minerals and their intergrowths, 2d edition: Oxford, U.K., Pergamon, 1205 p.

Rockingham, C.J., and Hutchison, R.W., 1980, Metamorphic textures in Archean copper-zinc massive sulfide deposits: Canadian Institute of Mining and Metallurgy Bulletin, v. 73, p. 104-112.

Seward, T.M., 1973, Thio complexes of gold and the transport of gold in hydrothermal ore solutions: Geochemica et Cosmochimica Acta, v. 37, p. 379-401.

Slaughter, A.L., 1968, The Homestake mine, in Ridge, J.D., ed., Ore deposits of the United States: New York, American Institute of Mining Engineers, p. 1436-1459.

Taylor, B.E., and Slack, J.F., 1984, Tourmalines from Appalachian-Caledonian massive sulfide deposits: Textural, chemical, and isotopic relationships: Economic Geology, v. 79, p. 1703-1726.

Twenhofel, W.S., 1952, Geology of the Alaska-Juneau lode system, Alaska: U.S. Geological Survey Open-File Report 52-160, 170 p.

Watanabe, Takeo, 1967, Geochemical cycle and concentration of boron in the earth's crust, in Vingradov, A.P., ed., Chemistry of the earth's crust, Vol. II: Jerusalem, Israel Program for Scientific Translations, p. 167-178.

Wayland, R.G., 1960, The Alaska Juneau gold ore body: Neues Jahrbuch für Mineralogie Abhandlungen v. 94, p. 267-279.

Wernecke, Livington, 1932, Geology of the ore zones: Engineering and Mining Journal, v. 133, p. 494-499.

Reviewers: R.P. Ashley and W.H. Nelson

PALEOMAGNETIC EVIDENCE FOR A LATEST PLIOCENE AND EARLY PLEISTOCENE AGE OF THE UPPER YAKATAGA FORMATION ON MIDDLETON ISLAND, ALASKA

Edward A. Mankinen and George Plafker

The Yakataga Formation, along the northern Gulf of Alaska margin, records late Cenozoic glaciation in a sequence with an aggregate outcrop thickness of about 5,000 m (Plafker and Addicott, 1976). The youngest part of the Yakataga Formation (1,170 m thick) exposed in outcrop is on Middleton Island, located in the Gulf of Alaska approximately 130 km southwest of Cordova (fig. 1).

A reconnaissance paleomagnetic sampling of the Yakataga Formation on Middleton Island was made in 1967 by R.R. Doell and George Plafker. Encouraged by preliminary results from that study, we revisited the island with Doell in 1970 to try to sample a geomagnetic polarity transition in this thick and rapidly deposited sequence and to refine the age of the sequence. We collected samples for paleomagnetic analysis from sections exposed on intertidal reefs at the southwest and northeast ends of the island that were well exposed as a result of tectonic uplift of about 4 m during the 1964 Alaskan earthquake. At the same time, we described the stratigraphy of these sections and collected samples for paleontological study. Although we were unable to sample across a polarity transition in detail, our paleomagnetic results provide the best age data presently available on the Middleton Island section and indicate that it is latest Pliocene and early Pleistocene in age.

The Yakataga Formation at Middleton Island is made up mainly of poorly to moderately indurated siliciclastic sedimentary rocks of both marine and glaciomarine origin (Miller, 1953; Plafker and Addicott, 1976; Plafker, 1981; Eyles and others, 1985). Measured sections on the southwest and northeast ends of the island are 1,170 m and 585 m thick, respectively (figs. 1 and 2). The sequence consists primarily of thick, massive beds of till-like, mud-matrix diamictite (86 percent), subordinate amounts of lenticular, channel-fill conglomerate (9 percent) with sand or sandy-mud matrix, and minor sandstone, siltstone, and mudstone. Scattered boulder- to pebble-size clasts, some of which have faceted and striated surfaces and are interpreted as dropstones, are present in all lithologic types, but especially in the diamictite and the laminated siltstone or mudstone. Fine-grained sediment that composes the diamictite matrix, as well as most of the siltstone and mudstone, was primarily derived as glacial rock flour from coastal glaciers and floating ice.

The combined paleontologic and sedimentologic data suggest a cold, shallow-water, inner to middle sublittoral depositional environment for the Yakataga Formation at Middleton Island. Sediment derived from the mainland to the north was deposited in a shallow shelf basin that received variable amounts of glaciomarine detritus. The occurrence of both a massive conglomerate interpreted as a subglacial channel fill and striated pavements in the section indicate that ice sheets extended across the shelf to Middleton Island during deposition of the upper part of the section (Plafker and Addicott, 1976, p. 29-30). Local disconformities in the section are marked by thin horizons of well-sorted sandstone and conglomerate with abundant mollusks (fig. 2).

Paleontologic dating of the abundant fauna in the formation has been inhibited by a high degree of faunal provincialism coupled with the tendency for the late Cenozoic cold-water forms to be unusually long-ranging in time. The base of the formation at Cape Yakataga on the mainland has not been dated more closely than early middle Miocene to late Miocene (Plafker, 1986). Mollusks, foraminifers, siliceous microorganisms, and ostracodes from the highest exposed part of the formation at Middleton Island are considered to be of probable Pleistocene (Miller, 1953; Addicott and others, 1978) or Pliocene and Pleistocene age (Plafker and Addicott, 1976; Rau and others, 1983). A sparse nannofossil fauna, including the short-ranging species *Gephyrocapsa caribbeanica* Boudreaux and Hay from near the top of the section is of Pleistocene age (David Bukry, USGS, written commun., 1972).

Our detailed magnetostratigraphy on Middleton Island was based on one sample per horizon in the northeast section and 3 or 4 samples per horizon, laterally separated by approximately one meter, in the southwest section. A total of 161 separate horizons were sampled throughout the two sections (fig. 2). Paleomagnetic samples were obtained with a portable core drill and were oriented using a magnetic compass. Remanence measurements were made using spinner magnetometers, and samples were magnetically cleaned in alternating fields using tumbling demagnetizers. Only four of the horizons from which multiple cores were obtained had mean magnetization directions that failed to satisfy the Vincenz and Bruckshaw (1960) test for non-randomness, and these were omitted when determining the magnetic stratigraphy. Acceptable mean directions were transformed to virtual geomagnetic poles (VGP) according to the magnetic dipole formula.

A magnetic polarity was initially assigned to each horizon on the basis of its VGP latitude (fig. 2). However, because of the considerable variation in the precision of the magnetic directions and the large deviations away from the expected local field direction in our data set, an erroneous polarity assignment could result if based solely on the VGP latitude. For this reason, a

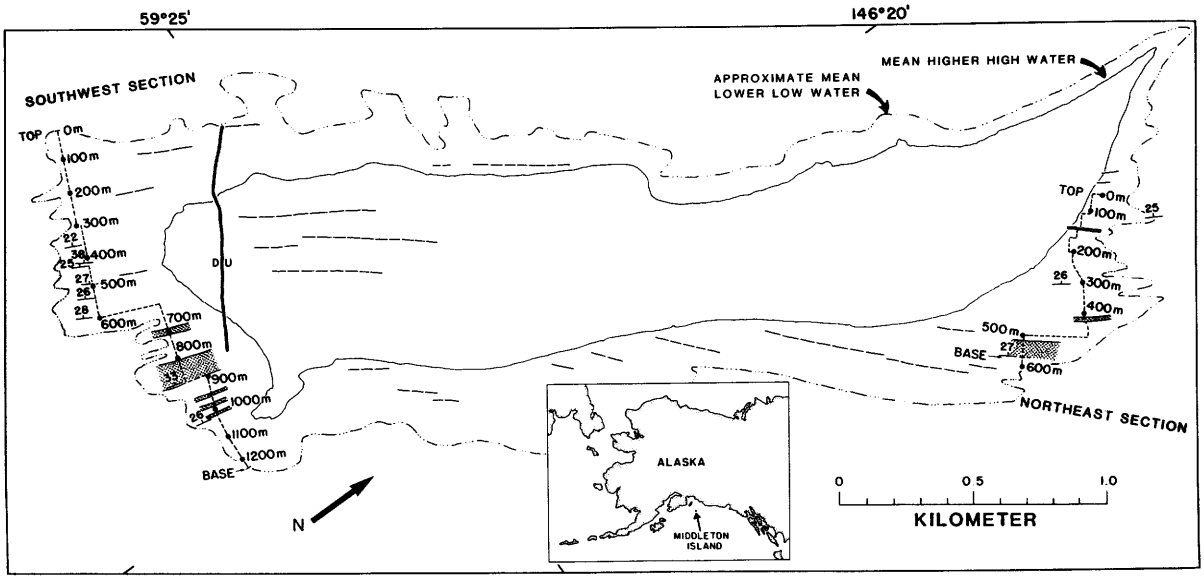

Figure 1.--Map of Middleton Island showing locations of measured and sampled sections of the upper Yakataga Formation (dashed). Numerals indicate thickness in meters and correspond to section thickness shown on figure 2. Dotted intervals are zones of normal polarity corresponding to those shown on figure 2. Long dashed lines indicate strike of resistant beds; heavy black line is a normal fault (D, downthrown; U, upthrown).

reversal of polarity was assumed only if a definite switch in both inclination and declination accompanied a change of VGP latitude from one hemisphere to another.

A similar pattern of magnetozones in both sections (fig. 2) indicates that the normal polarities are not the result of a recent, post-folding remagnetization. However, the magnetozones in the two sections do not appear to match if the bedding trends are extrapolated to the southwest end of the island. The mismatch could result from offset of the sequence by the normal fault at that end of the island (fig. 1) or from an unrecognized angular unconformity. A short, normal-polarity interval was recorded by two horizons with a stratigraphic separation of about 5.5 m in the northeast section, but the same interval was not sampled in the southwest section. The thickness of the reversed magnetozone at about 700-800 m in the southwest section is not well determined because the coarse-grained diamictite in this part of the section made sampling difficult. The sediment character suggests to us that this particular magnetozone may not represent as much time as might be inferred by its apparent thickness. Three short, normal-polarity magnetozones are indicated near the bottom of the southwest section. Because Pliocene and Pleistocene fossils have been found in these sections and no major unconformities are evident, the predominance of reversed polarities throughout the sequence indicates deposition during the latter part of the Matuyama Reversed-Polarity Chron. The Matuyama is the only extended period of reversed polarity during the late Pliocene and Pleistocene (Mankinen and Dalrymple, 1979).

The magnetozones determined for the two sections are compared to the geomagnetic polarity time scale in figure 3. The three short, normal-polarity intervals near the bottom of the southwest section can be correlated with the Reunion Normal-Polarity Subchron. However, the number and durations of the Reunion intervals are still uncertain, although available evidence indicates that there are probably two and possibly three (Mankinen and Dalrymple, 1979). The youngest normal-polarity interval in the northeast section probably represents the Cobb Mountain Subchron, currently the only one identified as occurring in this part of the Matuyama. The interval is too thin to realistically be considered as representing the Jaramillo Normal-Polarity Subchron, especially since other normal-polarity magnetozones in the section are considerably thicker.

The two larger, normal-polarity intervals in both sections can be interpreted in two ways. In the first (alternative 1 in fig. 3), the top of the longest interval is considered to be the top of the Olduvai Normal-Polarity Subchron and the younger interval possibly represents an undocumented episode at about 1.55 Ma. Evidence for the younger episode may have been found in east-central Arizona by Castro and others (1983), who reported several normal-polarity lava flows

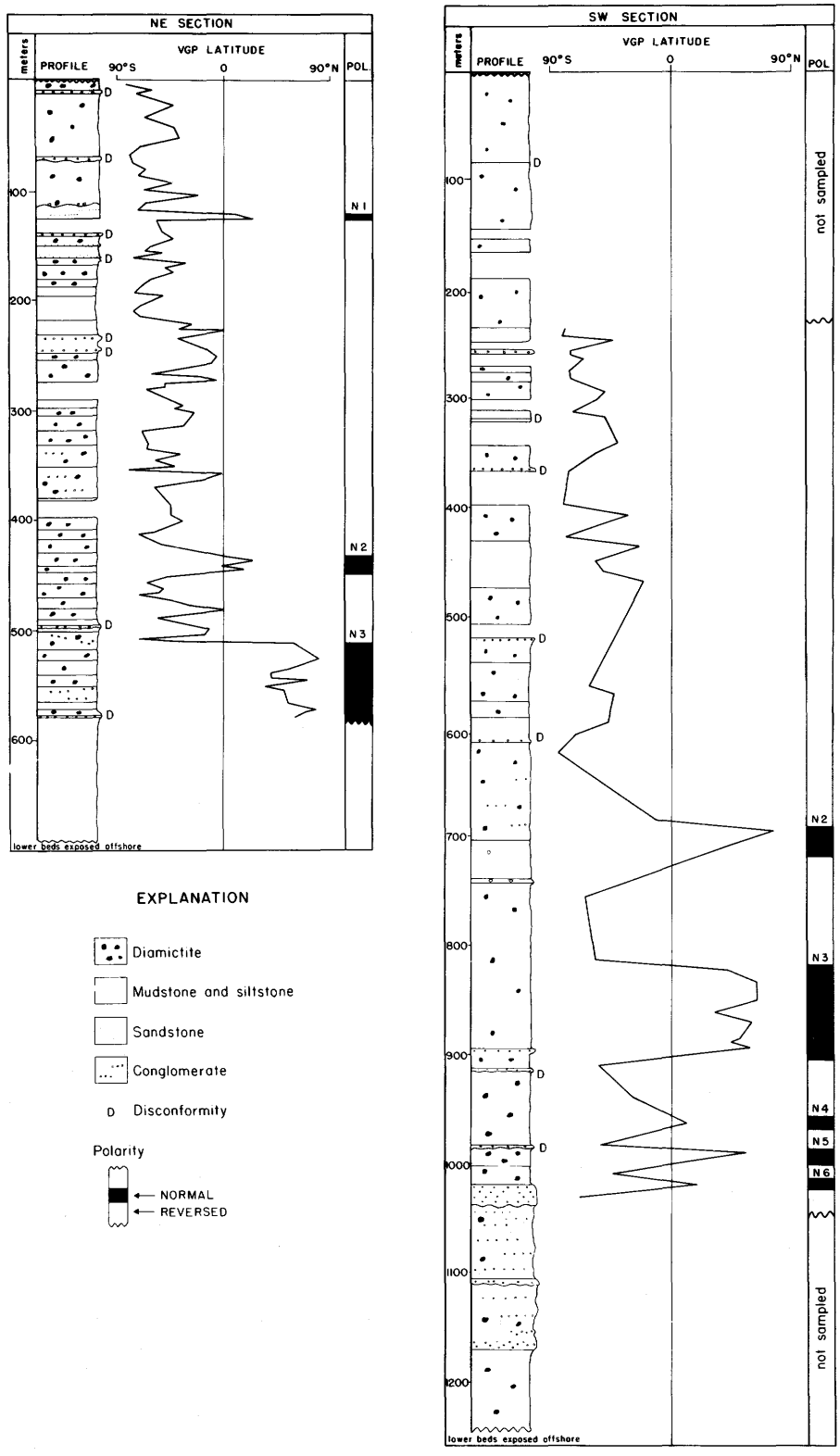

Figure 2.--Generalized stratigraphic sections of the upper Yakataga Formation and corresponding virtual geomagnetic pole (VGP) latitude, and interpreted magnetic polarity (POL). Locations shown on figure 1.

yielding radiometric ages of about 1.5 Ma. However, this possible correlation should be considered tentative because their full report is still unpublished. Additional evidence for a short normal-polarity interval following the Olduvai Subchron has been found in deep-sea cores (Opdyke, 1972; Clement and Kent, 1985) and in an onshore sedimentary sequence in Pakistan (Burbank and Tahirkheli, 1985).

The second alternative (fig. 3) considers the reversed-polarity interval to be an episode within the Olduvai. Some evidence for such an episode has been noted in onshore sedimentary sequences (Theyer and others, 1985; Seward and others, 1986) and appears to be present in some deep-sea cores (Glass and others, 1967). Thus, some evidence to support both alternatives has been published, but none can be considered conclusive.

Regardless of which alternative best explains the two thickest, normal-polarity magnetozones (N2 and N3), it is evident that the sequence that was sampled paleomagnetically spans a period of more than 1 million years from just before the oldest Reunion interval (2.14 Ma) to some time between the Jaramillo (0.97 Ma) and Cobb Mountain (1.10 Ma). This corresponds with the latest Pliocene and early part of the Pleistocene Epochs (Berggren and others, 1985).

If our correlations to the polarity time scale are correct, rough estimates of sedimentation rates for part of the Yakataga Formation on Middleton Island can be made. The interval between the Cobb Mountain and Olduvai in the northeast section must have been deposited at an average rate of about 70 cm/ka (1,000 yr) using alternative 1 in figure 3, or about 60 cm/ka using alternative 2. Only the lower part of the southwest section is well constrained (between the top of the Olduvai and the bottom of the Reunion), and rates of 45 cm/ka or 70 cm/ka can be calculated using alternatives 1 and 2, respectively.

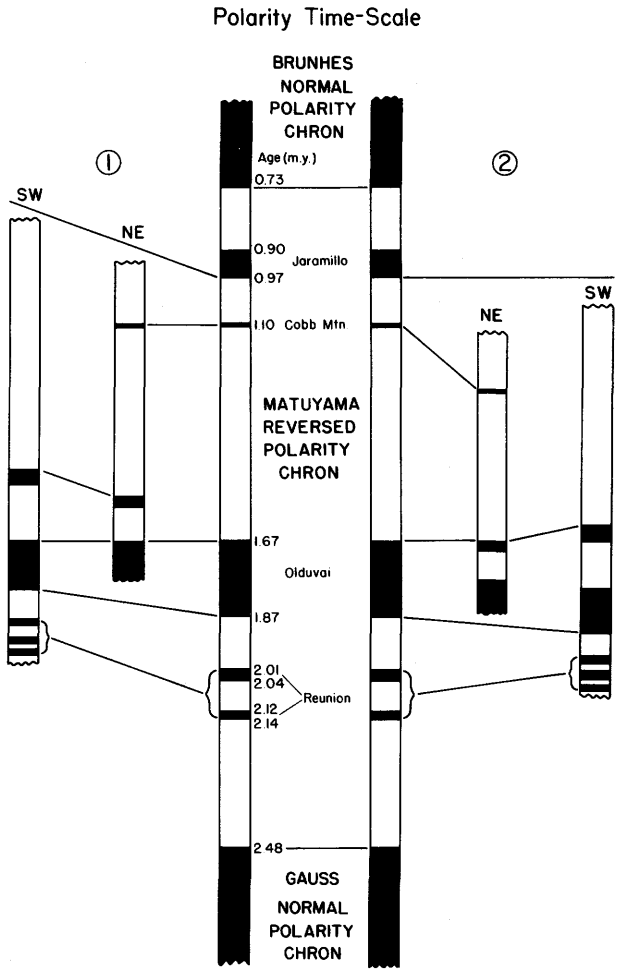

Figure 3. --Correlation of magnetozones of northeast and southwest sections sampled on Middleton Island with portion of geomagnetic polarity time scale of Mankinen and Dalrymple (1979) modified by addition of the Cobb Mountain Normal-Polarity Subchron (Mankinen and others, 1978; Mankinen and Gromme, 1982). Solid intervals correspond to periods of normal polarity. 1 and 2 are alternative interpretations of magnetozones in lower part of both sections (see text).

REFERENCES CITED

Addicott, W.O., Winkler, G.R., and Plafker, George, 1978, Preliminary megafossil biostratigraphy and correlation of selected stratigraphic sections of the Gulf of Alaska Tertiary province: U.S. Geological Survey Open-File Report 78-491, 2 plates.

Berggren, W.A., Kent, D.V., Flynn, J.J., and Van Couvering, J.A., 1985, Cenozoic geochronology: Geological Society of America Bulletin, v. 96, p. 1407-1418.

Burbank, D.W., and Tahirkheli, R.A.K., 1985, The magnetostratigraphy, fission-track dating, and stratigraphic evolution of the Peshawar intermontane basin, northern Pakistan: Geological Society of America Bulletin, v. 96, p. 539-552.

Castro, Joyce, Brown, Laurie, and Condit, C.D., 1983, Paleomagnetic results from the Springerville-Show Low volcanic field, east-central Arizona: Eos (Transactions American Geophysical Union), v. 64, p. 689.

Clement, B.M., and Kent, D.V., 1985, Details of short geomagnetic polarity chronozones as recorded at DSDP site 609: Eos (Transactions American Geophysical Union), v. 66, p. 872.

Eyles, C.H., Eyles, Nicholas, and Miall, A.D., 1985, Models of glaciomarine sedimentation and their application to the interpretation of ancient glacial sequences: Palaeogeography, Palaeoclimatology, Palaeoecology, v. 51, p. 15-84.

Glass, B., Ericson, D.B., Heezen, B.C., Opdyke, N.D., and Glass, J.A., 1967, Geomagnetic reversals and Pleistocene chronology: Nature, v. 216, p. 437-442.

Mankinen, E.A., and Dalrymple, G.B., 1979, Revised geomagnetic polarity time scale for the interval 0-5 m.y. B.P.: Journal of Geophysical Research, v. 84, p. 615-626.

Mankinen, E.A., Donnelly, J.M., and Gromme, C.S., 1978, Geomagnetic polarity event recorded at 1.1 m.y. B.P. on Cobb Mountain, Clear Lake volcanic field, California: Geology, v. 6, p. 653-656.

Mankinen, E.A., and Gromme, C.S., 1982, Paleomagnetic data from the Coso Range, California and current status of the Cobb Mountain normal geomagnetic polarity event: Geophysical Research Letters, v. 9, p. 1279-1282.

Miller, D.J., 1953, Late Cenozoic marine glacial sediments and marine terraces of Middleton Island, Alaska: Journal of Geology, v. 61, p. 17-40.

Opdyke, N.D., 1972, Paleomagnetism of deep-sea cores: Reviews of Geophysics and Space Physics, v. 10, p. 213-149.

Plafker, George, 1981, Late Cenozoic glaciomarine deposits in the Yakataga Formation, Alaska, in Hambrey, M.J., and Harland, W.B., eds., Earth's pre-Pleistocene glacial record: New York, Cambridge University Press, p. 694-699.

_____ in press, Regional geology and petroleum potential of the northern Gulf of Alaska continental margin, in Scholl, D.W., Grantz, Arthur, and Vedder, J.G., eds., Geology and resource potential of the continental margin of western North America and adjacent ocean basins--Beaufort Sea to Baja California: Circum-Pacific Council for Energy and Mineral Resources, Earth Science Series No -

Plafker, George, and Addicott, W.O., 1976, Glaciomarine deposits of Miocene through Holocene age in the Yakataga Formation along the Gulf of Alaska margin, in Miller, T.P., ed., Recent and ancient sedimentary environments in Alaska: Anchorage, Alaska Geological Society, p. Q1-Q23.

Rau, W.W., Plafker, George, and Winkler, G.R., 1983, Foraminiferal biostratigraphy and correlations in the Gulf of Alaska Tertiary province: U.S. Geological Survey Oil and Gas Investigations Chart OC-120.

Seward, Diane, Christoffel, D.A., and Lienert, B., 1986, Magnetic polarity stratigraphy of a Plio-Pleistocene marine sequence of North Island, New Zealand: Earth and Planetary Science Letters, v. 80, p. 353-360.

Theyer, Fritz, Burbank, Doug, Lund, S.P., and McRaney, John, 1985, High-resolution magnetic field transitions and related secular variation from Matuyama-aged lake sediments in Kashmir, India: Eos (Transactions American Geophysical Union), v. 66, p. 872.

Vincenz, S.A., and Bruckshaw, J. McG., 1960, Note on the probability distribution of a small number of vectors: Proceedings Cambridge Philosophical Society, v. 56, p. 21-26.

Reviewers: J.W. Hillhouse and L.N. Marincovich

CENOZOIC MAGMATISM IN SOUTHEASTERN ALASKA (ABSTRACT)

David A. Brew

A recently completed synthesis indicates that late Mesozoic and Cenozoic magmatic belts cover most of southeastern Alaska (fig. 1), but they are concentrated in the Chugach terrane in the western part of the region, in the western part of the Alexander terrane mainly adjacent to the Chugach terrane, and along the Alexander-Stikine terrane boundary in the Coast Mountains. The late Mesozoic and Cenozoic magmatic events are part of a continuum that began in the Jurassic. Early(?) and Middle Jurassic magmatic events formed the roots and extrusive products of a Jurassic-Cretaceous arc developed on the Alexander terrane; these are the 180 Ma to 110 Ma granitic events. Their distribution are not shown on the map. Linear belts of plutons in the middle and Late Cretaceous coincided spatially with the Lower and middle Cretaceous flysch- and volcanic rock-filled rift between the Alexander and Stikine terranes; these are the 110 Ma ultramafic event and the 100 Ma and 90 Ma granitic events. Their distributions are also not shown on the map.

Latest Cretaceous and Cenozoic magmatic events are indicated by mostly plutonic rocks related to the collision of the Chugach terrane with the Alexander/Wrangellia terrane; these are the 70-55 Ma, 55-45 Ma, and 45-35 Ma granitic events (fig. 1). Subsequent volcanic and plutonic activity of the 35-5 Ma events was related to the transition from collision to regional extension. These events were followed by the volcanic and plutonic activity of the 5-0 Ma events, which accompanied transform movement on Pacific plate bounding faults.

The products of these latest Cretaceous and Cenozoic magmatic events form distinct belts that cover much of the region. The 70-55 Ma events were concentrated in a narrow belt inboard (east) of the Alexander terrane and adjacent to (but almost entirely west of) the locus of intrusion of the 55-45 Ma events. Activity then shifted to the Chugach terrane on the outboard (west) side of the Alexander terrane for the 45-35 Ma events and shifted eastward onto the Alexander terrane during the end of that episode. The 35-5 Ma volcanic and plutonic events are concentrated in a lengthy belt that cuts across the previously established regional structures and tectonostratigraphic terranes. The youngest volcanic events (less than 5 Ma) also may be interpreted to form a crude discontinuous belt across all previous emplaced tectonostratigraphic terranes and magmatic belts.

Rocks of the latest Cretaceous through Holocene episodes have a wide variety of chemical and modal compositions, but most are calc-alkalic except for parts of the 5-35 Ma episode, which are alkalic to peralkalic, and the youngest (less than 5 Ma) episode, which is alkalic. Different segments of the linear plutonic belts are dominantly metaluminous, mixed metaluminous and peraluminous, or peraluminous. These compositional contrasts, as well as different orientations of some of the belts, may be related to thickness and composition of the subducted slab and overlying crust. Available rare-earth- and trace-element information shows moderately fractionated patterns and arc affinities for all but the youngest magmatic episode.

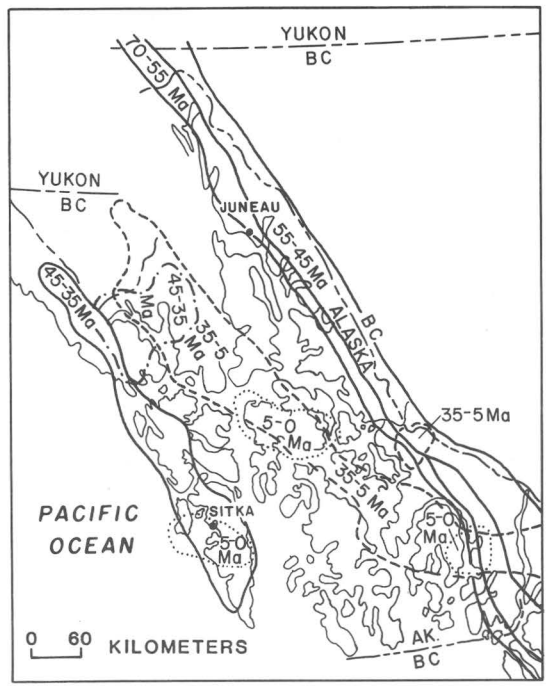

Figure 1.--Cenozoic magmatic belts of southeastern Alaska. 120 km of right-lateral (north-south) separation on Lynn Canal-Chatham Strait fault has been removed.

Reviewers: R.D. Koch and J.G. Smith

OFFSHORE

Diver resting on wave-agitated slush ice during studies of ice rafting in the Beaufort Sea. Photo by P.W. Barnes.

BEAUFORT SEA COASTAL CURRENTS: A DIVERGENCE NEAR BARTER ISLAND, ALASKA?

Peter W. Barnes, Scot Graves, and Erk Reimnitz

Several lines of evidence suggest that water on the Beaufort Sea shelf may flow eastward and westward from a divergence located near Barter Island (fig. 1). First, ice gouges on the Alaskan sector of the shelf are created mostly by ice keels plowing east to west, subparallel to the coastline (Barnes and others, 1984). In contrast, gouges on the Canadian Beaufort shelf are dominantly formed by ice plowing from west to east (Harper and Penland, 1982). Second, on the Alaskan shelf, surface currents are wind-driven and generally flow to the west (Aagaard, 1984), whereas off northwestern Canada, easterly-flowing currents dominate (Harper and Penland, 1982). Third, in 1972 surface drifters were released on the Alaskan shelf between Barter Island and Point Barrow (Barnes and Toimil, 1979). Most of the drifters traveled westward; however, several drifters originating from the easternmost drop-points moved eastward into Canada.

The location and character of the suggested divergence has not been documented, although its presence would have significant impact on the interpretation of westward or eastward pollutant pathways on the shelf of the Alaskan and Canadian Beaufort Sea (Thomas, 1984). As part of an ongoing study of inner shelf circulation patterns, sediment transport, and nearshore processes in the Alaskan Beaufort Sea, we released 1,000 sea-surface and 1,000 seafloor drifters between Camden and Demarcation Bays off northern Alaska in August 1983 (table 1, fig. 2). The drifters were designed to move with the surface and bottom currents, with some portion carried

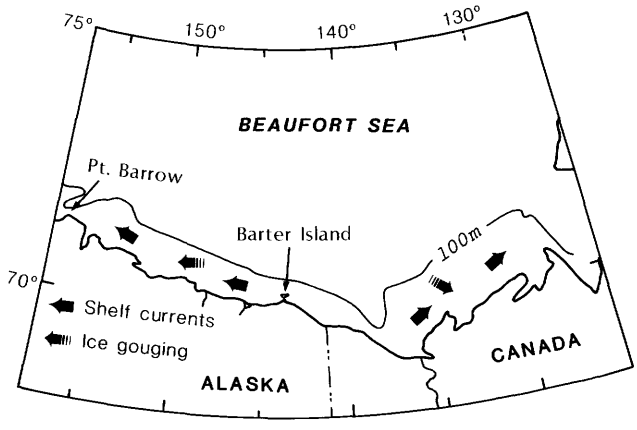

Figure 1.--Location map of study area showing dominant directions of ice gouging and prevailing shelf currents.

Table 1.--Summary information on drifter release and recovery

Date released	Number released	Number recovered	Percent recovered
	Surface drifters		
Released from coastal vessel, 8/7-8/83	400	24	6.0
Released from low flying aircraft, 8/18/83	600	22	3.6
Total	1,000	46	4.6
	Bottom drifters		
Released from coastal vessel, 8/7-8/83	400	33	8.2
Released from low flying aircraft, 8/18/83	600	6	1.0
Total	1,000	39	3.9

ashore where the finder would report the location and serial number. Information on shelf current speed and direction can be inferred from a knowledge of timing and locations of deployment and recovery, and of the assumed drifter trajectories. A major goal of this drifter release was to better define the suggested divergence in water motion between the Alaskan and Canadian Beaufort Seas.

Virtually all of the 85 drifters recovered through the fall of 1985 from the 1983 release traveled east (fig. 2). This is a true representation of the drift as one of us (ER) flew along the entire coastline in 1984 collecting drifters. Coastal travel by the local population (and drifter recovery) commonly occurs westward from the village at Barter Island. A few of the drifters traveled several hundred kilometers to recovery sites well east of Herschel Island while others traveled the few kilometers to the coast (fig. 2). Recoveries indicate the dominance of eastward drift in this part of the Beaufort Sea. Drifters recovered during 1984 and 1985 may have been stranded at their recovery site since 1983.

Recovery locations logged during the two months following drifter release (August and September 1983) and prior to winter freeze-up provided trajectory endpoints for velocity calculations. The data on 15 surface and 9 bottom drifters from 12 release points provide minimum travel time and travel distance, which was used to estimate minimum current velocities during the fall of 1983 (table 2). Estimates of current

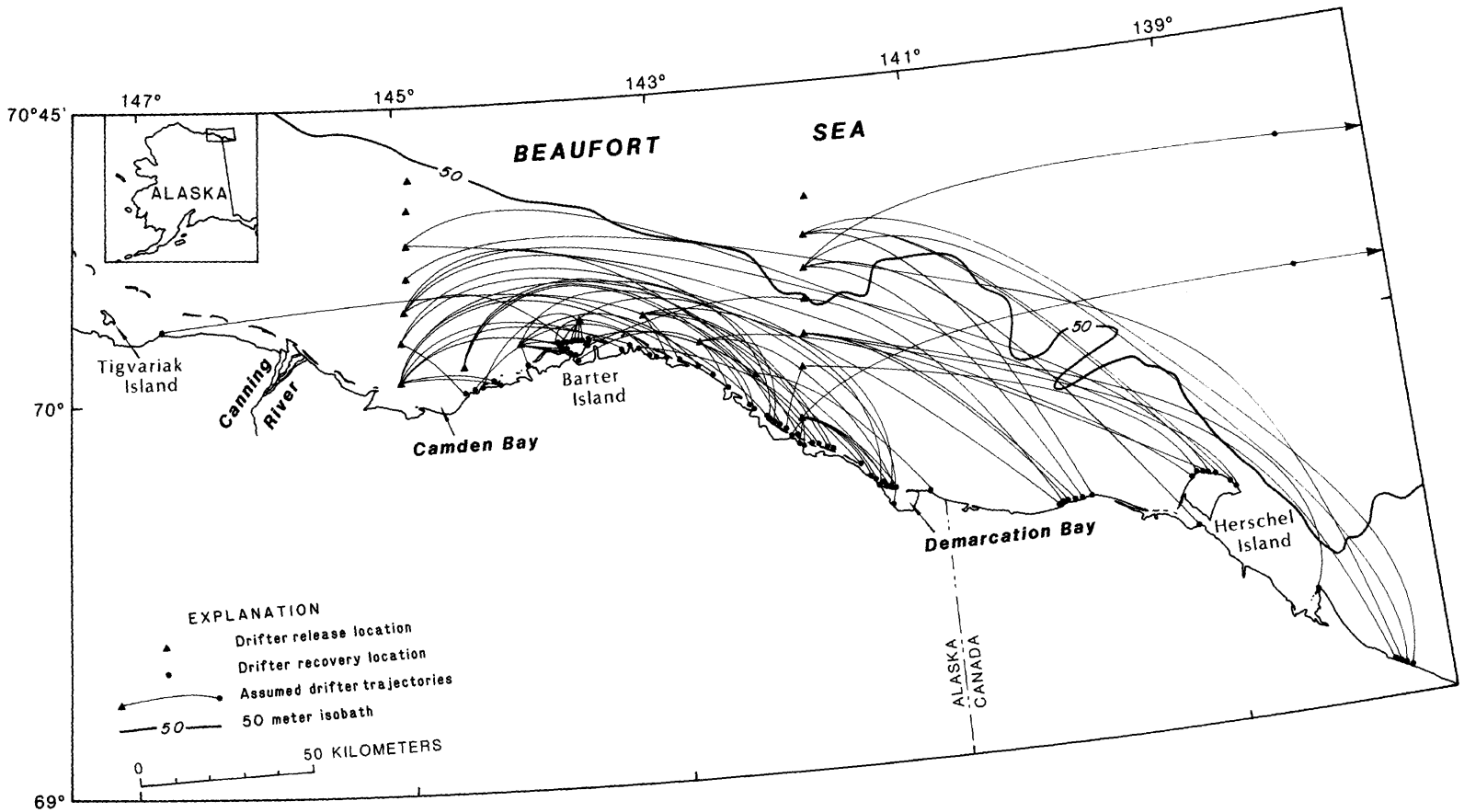

Figure 2.--Regional map of study area locating drifter release stations and idealized trajectories of drifters recovered through 1985.

Table 2.--Drifter speed and displacement

	Surface drifters max.	min.	avg.	Bottom drifters max.	min.	avg.
Speed (cm/s)	18.2	0.3	6.3	16.0	0.3	3.7
Distance (km)	154	9	45.8	137	7	31.8

velocity generated from these data are minimum values as the drifters may have been discovered some time after the drifter had reached shore. Based on drifters recovered prior to the freeze-up in the fall of 1983, the minimum eastward velocities for surface and near-bottom waters are between 0.3 and 18.2 cm/s and averaged about 5 cm/s over distances up to 154 km. The low velocities recorded for most inshore drifters may not reflect slow coastal currents, but may reflect the sparse human population along the coast in the study area. The highest current velocity values calculated were those indicated by the recovery of drifters released along the two offshore lines. The bottom drifters showed no difference in direction of travel, although the velocities averaged about half the speed of the surface drifters.

Prevailing winds have a major impact on shelf currents and sea level in the Alaskan Beaufort Sea, as astronomic tides are only 10-20 cm; strong westerlies raise sea level and easterlies lower it (Barnes and Toimil, 1979). Therefore currents flow parallel to the coast, driven by the winds (Aagaard, 1984). As a result, debris and drifters at the shoreline during westerly storms will strand higher on the beaches than debris left from easterly wind events. Thus, a majority of the flotsam, and drifters, found along the Beaufort Sea coasts may reflect a preservation biasing of eastward transport events from westerly winds.

Although the western Beaufort Sea off Alaska experiences mostly northeasterly winds during the summer (Barnes and Toimil, 1979), the distribution of summer winds along the eastern Beaufort Sea coast indicate winds from both the west and east (fig. 3). The westerly winds at Barter Island are related to the effect of mountain topography (Kozo and Robe, 1986); thus, the movement of our drifters to the east does not violate the summer wind pattern. The wind data (fig. 3), however, also show a significant easterly component that is not seen in the movement of either our surface or bottom drifters (fig. 2). We believe that the the bulk of the recovered drifters moved rather swiftly eastward (table 2) and stranded during the persistent westerly winds that followed their deployment in 1983 (Kozo and Robe, 1986). The lack of westward drift indicated by figure 2 suggests that the drifters stranded during the 1983 period of westerly winds and have not been available for westward transport since that time.

The ocean becomes ice-covered subsequent to freeze-up in October, and surface drifters would be arrested until breakup the following July. Little is known about currents acting beneath the ice canopy on the shelf (Aagaard, 1984), thus the movement of bottom drifters during the period of ice cover is not well understood. Because it is quite conceivable that many of the drifters, both surface and seafloor types, are incorporated in the seasonal ice canopy, our trajectory data may incorporate the motion of ice. In the winter, that portion of the ice cover not held fast to the land may move westward with the prevailing winds and ice motions (Aagaard, 1984; Kozo and Robe, 1986). Drifters incorporated in the ice may be displaced and re-released far to the west or even carried entirely out of the Alaskan Beaufort Sea.

The divergence suggested by the earlier drifter studies (Barnes and Toimil, 1979) and by the ice gouge orientations remains unconfirmed. In the present study the shelf, currents responded to forcing from westerly winds. As westerly winds are a major component of the wind regime in the eastern Beaufort Sea (fig. 3), we predict that eastward flowing currents would be a major component of the current regime. As the wind and current data on the western Beaufort Sea shelf

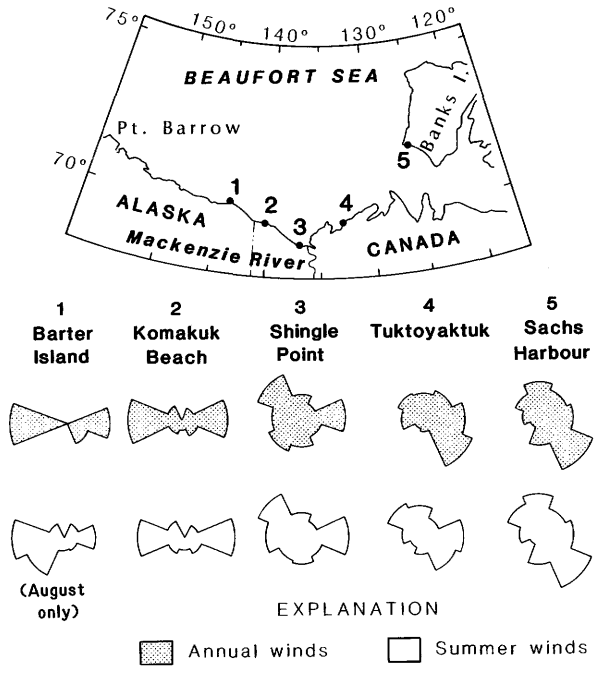

Figure 3.--Beaufort Sea showing annual and summer (open water) winds along coast of eastern Beaufort Sea. Data from NOAA climatologic summaries and Harper and Penland (1982).

(Barnes and Toimil, 1979) indicate that westward currents would dominate, the need for a zone of divergence between these two regimes still exists.

Drifters caught up in the landfast ice, on the other hand, may be held in position during the winter and re-released in the spring, fairly near their position of capture in the autumn. Landfast ice is of shallow draft, and thus, after the early summer breakup, it responds almost solely to the wind effects.

We conclude that waters on the eastern Beaufort Sea shelf moved eastward in the fall of 1983 at velocities which ranged from less than 1 to more than 15 cm/s in response to persistent westerly winds. Suspended sediments and (or) pollutants entrained in the upper waters can be expected to travel at similar speeds, on similar trajectories that commonly move from Alaska into Canada.

This study was funded in part by the Minerals Management Service through an interagency agreement with the National Oceanic and Atmospheric Administration, as part of the Outer Continental Shelf Environmental Assessment Program.

REFERENCES CITED

Aagaard, Knut, 1984, The Beaufort Undercurrent, in Barnes, P.W., Schell, D.M., and Reimnitz, Erk, eds., The Alaskan Beaufort Sea: Ecosystems and Environments: Orlando, Fla., Academic Press, p. 47-71.

Barnes, P.W., Rearic, D.M., and Reimnitz, Erk, 1984, Ice gouging characteristics and processes, in Barnes, P.W., Schell, D.M., and Reimnitz, Erk eds., The Alaskan Beaufort Sea: Ecosystems and Environments, Orlando, Fla., Academic Press, p. 185-212.

Barnes, P.W., and Toimil, L.J., 1979, Inner shelf circulation patterns, Beaufort Sea, Alaska: U.S. Geological Survey Miscellaneous Field Studies Map MF-1125.

Harper, J.R. and Penlana, Shea, 1982, Beaufort Sea sediment dynamics: Geological Survey of Canada, Atlantic Geoscience Centre, Open File Report, 127 p.

Kozo, T.L., and Robe, R.Q., 1986, Modeling winds and open-water bouy drift along the eastern Beaufort Sea coast, including effects of the Brooks Range: Journal of Geophysical Research, v. 91, p. 13011-13032.

Thomas, D.R., 1984, Interaction of oil and arctic sea ice, in Barnes, P.W., Schell, D.W., and Reimnitz, Erk, eds., The Alaskan Beaufort Sea: Ecosystems and environment: Orlando, Fla., Academic Press, p. 441-460.

Reviewers: E.W. Kempema and M.A. Noble

VOLCANIC-ARC DACITE AND EARLY MIOCENE BASALT DREDGED FROM THE SHUMAGIN MARGIN, ALASKA

Terry R. Bruns, Tracy L. Vallier, Leda Beth Pickthorn, and Roland von Huene

The Shumagin continental margin lies along the Alaska Peninsula between Kodiak Island and Unimak Pass. The geology of the shelf islands and interpretations of multichannel seismic-reflection data indicate that much of the Shumagin shelf is underlain by Upper Cretaceous turbidites of the Shumagin Formation and by Paleocene granodiorite. These rocks are in turn overlain above a regional erosional unconformity by sedimentary rocks of late Miocene and younger age. Early Tertiary rocks like those of the Kodiak Island region are not known to crop out on the Shumagin shelf islands, but they presumably extend on strike southwestward and underlie the outer shelf and slope of the Shumagin margin (Bruns and others, in press). However, samples from three dredge sites are the only available evidence with which to characterize the rocks that underlie the outer shelf and slope.

During 1979, sedimentary and igneous rocks were sampled at three dredge sites, numbered 2, 3, and 4, on the Shumagin margin (fig. 1). Dredge sites 2 and 3 were located on the north and south flanks respectively of Unimak Seamount, a prominent midslope bathymetric high about 60 km south of Sanak Island (fig. 2). Unimak Seamount is, in turn, the highest point on Unimak ridge, an extensive bathymetric and structural high that extends about 100 km southwest of Sanak Island to Unimak Pass (Bruns and others, in press; Lewis and others, in press). Dredge site 4 was located on the west wall of a submarine canyon south of the Shumagin Islands.

Dredge site 2 yielded only sedimentary rocks. Dredge sites 3 and 4 yielded basalt and dacite respectively. Detailed descriptions of rock samples from the dredge hauls are given in Bruns and others (1985; in press) and are only summarized here. In this paper, we report the recently determined volcanic-arc chemistry of the igneous rocks and the radiometrically determined early Miocene age of one basalt sample from site 3, and speculate about the implication of finding volcanic-arc basalt on Unimak ridge.

Dredge site 4 yielded undated dacite and nodular limestone and calcareous siltstone, dated by diatoms as Pliocene and Pleistocene. The amount of dacite recovered was too small to radiometrically date the rocks. Chemical analyses of the dacite samples show that they represent three chemically distinct units, possibly individual flow units; samples 4-4 and 4-11 are similar, as are 4-8 and 4-9, and sample 4-12 forms the third unit. The chemistry also indicates that the dacite samples have calc-alkaline affinities that are typical of an island-arc setting (tables 1 and 2, and fig. 3).

Dredge sites 2 and 3 yielded four rock units (Bruns and others, 1985; in press): (1) an Eocene unit indicated by a single mudstone from site 2,

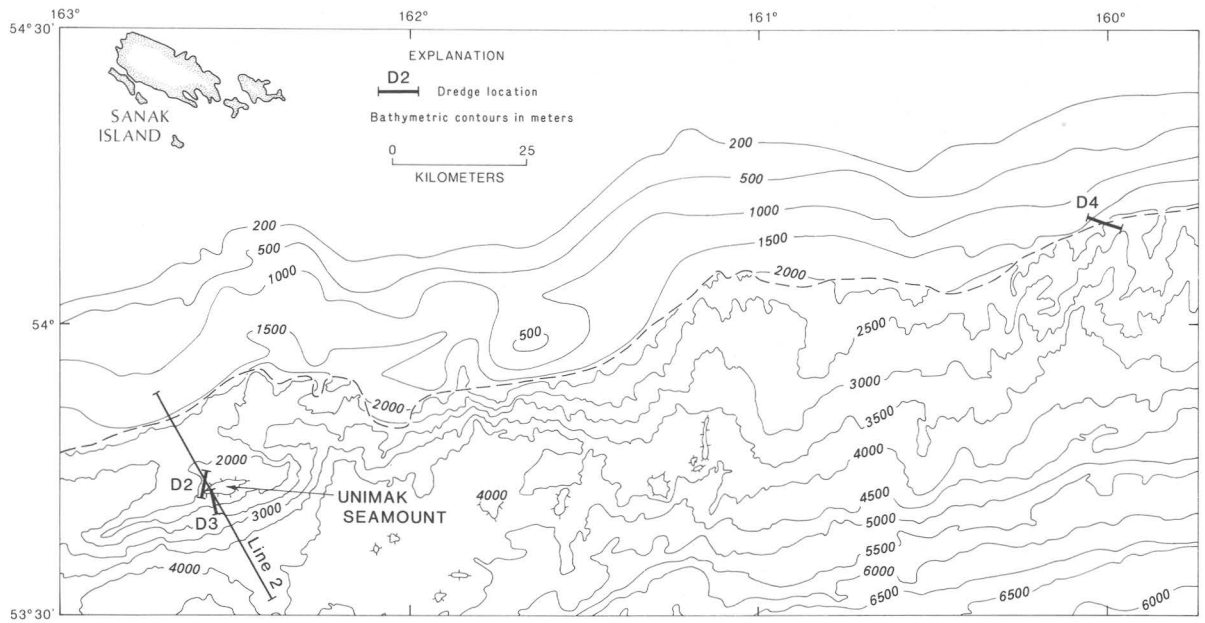

Figure 1.--Locations of dredge hauls from Shumagin margin. Bathymetry south of dashed line from Seabeam data of Lewis and others (in press).

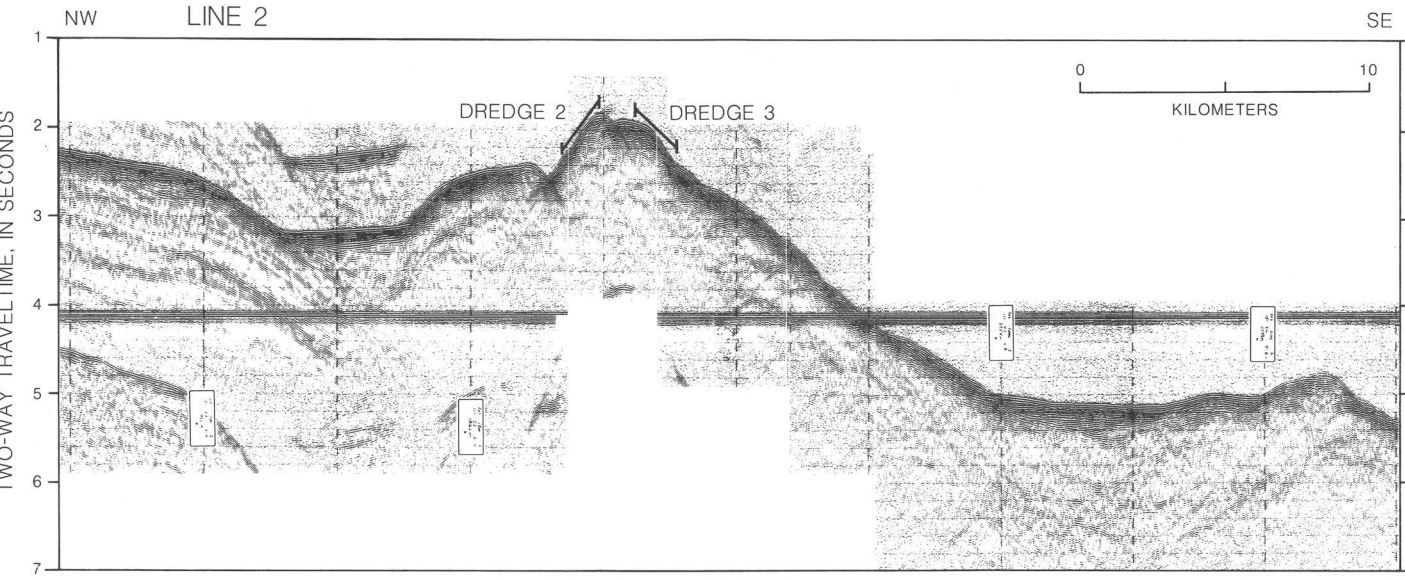

Figure 2.--Single-channel seismic-reflection line showing location of dredge stations 2 and 3 on Unimak Seamount; line location shown in figure 1. Vertical exaggeration about 4:1.

dated by foraminifers, but considered as suspect by Bruns and others (1985; in press) because the sample could be an erratic; (2) a lower and middle Miocene unit from site 2, represented by a large suite of mudstone, siltstone, and sandstone samples dated by abundant diatoms; (3) a Pliocene and younger unit represented by two mudstone cobbles from site 3, also dated by diatoms; and (4) the basalt unit from site 3, represented by two large (30x30x20 cm) angular pieces with fresh-appearing edges. The Miocene sedimentary rocks are apparently locally derived. They contain abundant pumice and glass shards, indicating proximity to an active arc during deposition. The sandstones also contain abundant plutonic debris derived from quartz diorite or granodiorite source rocks, probably the Paleocene granitic batholiths exposed on the nearby Shumagin and Sanak Islands. The basalt samples are moderately altered, containing olivine and glass that is partly converted to clay minerals. The basalt is probably the source rock for a pronounced magnetic anomaly coincident with Unimak ridge (Bruns and von Huene, 1977).

Although a volcanic-arc origin for the dacite samples at site 4 is clear from the obvious calc-alkaline chemistry, the origin of the basalt samples from site 3 is less obvious.

The chemistry of the site 3 basalt samples (tables 1 and 2; fig. 3) indicates that they are more closely related to volcanic-arc basalts than to either mid-ocean ridge basalt (MORB) or ocean island (and seamount) basalt (OIB). Sample 3-1 has higher Al_2O_3 and lower TiO_2 and light rare-earth element (LREE) abundances than OIB, and higher Al_2O_3, K_2O, and Ba contents, lower CaO and TiO_2 values, and enriched LREE contents compared to MORB. Thus, sample 3-1 is unlike both OIB and MORB. Sample 3-3 has alkali (K and Na) element contents that are too high for MORB. It also has higher Al_2O_3, lower TiO_2, and lower contents of high-field-strength trace elements (Zr, Y, Nb) than OIB, and is thereby more similar to volcanic-arc rocks than to OIB. Furthermore, the higher SiO_2, K_2O, rare earth elements (REE), Y, Zr, and Hf contents in sample 3-3 show that it is more

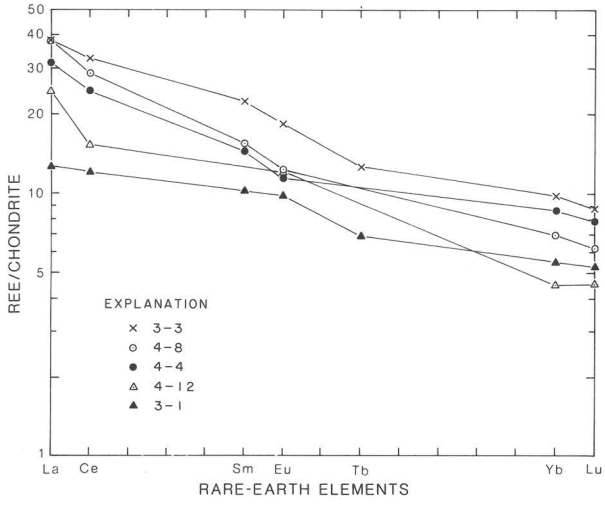

Figure 3.--Plot of rare-earth elements (REE) for dredged volcanic rocks normalized to chondrite values of Masuda and others (1973). Sample numbers in tables 1 and 2. Samples 4-9 and 4-11 are not plotted because of their close REE similarities with samples 4-8 and 4-4 respectively.

fractionated than sample 3-1 and might be better classified as a basaltic andesite. Thus, the REE patterns of both rocks are similar to those from arcs; sample 3-3 is definitely calc-alkaline, and sample 3-1 is transitional between island-arc tholeiite and calc-alkaline basalt. Thus, we believe that samples 3-1 and 3-3 both have a volcanic-arc origin.

Attempts were made to date plagioclase from samples 3-1 and 3-3 by conventional potassium-argon (K-Ar) and by argon 40/39 total fusion techniques. However, because of the altered nature of the basalt and the low potassium content, only sample 3-3 could be dated, and only by the argon 40/39 total fusion technique. Two separate runs yielded an average date of 19.8 ± 1.0 m.y. (early Miocene). The plagioclase looks somewhat altered in thin sections. Thus, the measured date represents a minimum age for the basalt because some argon may have been lost due to alteration of the plagioclase. The age is, however, consistent with that of the associated lower and middle Miocene sedimentary rocks.

If the basalt samples are from bedrock, and if the measured age is correct, then the chemical and age data have important tectonic implications. First, the arc-type chemistry of the dredged basalt shows that Unimak ridge, and hence the entire continental slope landward of the ridge, is underlain by arc-related rocks rather than by accreted sedimentary rocks or an accreted oceanic seamount complex. Second, the basalts were most likely emplaced into the Shumagin margin before deposition of the associated sedimentary rocks,

Table 1.--Trace element concentrations (ppm) in igneous rocks from dredge sites 3 and 4, cruise S7-79-WG [Analysts are L.Schwarz (instrumental neutron activation analysis) and R. Johnson (X-ray fluorescence, XRF). XRF values are noted by *; uranium value for sample 3-1 was below detection limit]

Element	3-1	3-3	4-4	4-8	4-9	4-11	4-12
Rb*	9	10	24	54	51	19	36
Sr*	415	349	358	400	397	354	796
Ba*	101	234	466	619	621	466	386
Th	.67	2.27	3.0	5.82	5.91	3.14	4.01
U	--	.68	1.08	2.10	2.10	1.19	1.2
La	4.8	14.6	12.0	14.6	14.8	11.6	9.3
Ce	11.7	32.2	23.9	27.6	27.5	23.0	15.3
Nd	13	23	13	14	16	14	8
Sm	2.37	5.18	3.24	3.51	3.54	2.99	1.84
Eu	.85	1.59	.99	1.02	1.01	.92	1.04
Tb	.41	.75	.52	.39	.37	.47	.23
Yb	1.38	2.44	2.14	1.75	1.47	2.13	1.12
Lu	.206	.342	.366	.241	.259	.315	.180
Y*	16	27	20	17	16	21	11
Zr*	80	138	134	110	107	134	150
Nb*	6	6	6	7	6	7	6
Hf	1.57	2.97	2.93	2.78	2.85	2.97	3.46
Ta	.27	.29	.35	.22	.27	.36	.31
Co	43	31	14	21	19	14	14
Cr	205	97	21	54	51	19	39
Sc	30	30	15	27	26	14	22
Zn	76	92	86	56	55	84	55

Table 2.--Major and minor element oxides (wt pct) of igneous rocks from dredge sites 3 and 4, cruise S7-79-WG
[Rock elemental oxides summed to 100 percent and H_2O^+, H_2O^-, and CO_2 values included. Analyses by X-ray fluorescence and wet chemical methods; A. Bartel, D. Kobilis, and J. Pastor analysts]

Oxides	3-1	3-3	4-4	4-8	4-9	4-11	4-12
SiO_2	48.79	52.12	61.52	60.51	60.76	62.05	60.27
TiO_2	1.05	1.55	.73	.77	.76	.76	.81
Al_2O_3	18.55	18.74	18.75	18.19	18.10	18.62	17.83
Fe_2O_3	3.97	5.75	3.17	3.91	3.98	3.41	3.01
FeO	4.73	3.79	3.16	1.45	1.35	2.94	2.40
MnO	.15	.18	.12	.05	.05	.11	.08
MgO	8.76	5.59	2.91	2.16	2.21	2.78	3.66
CaO	10.99	7.35	5.01	7.96	7.74	4.65	7.23
Na_2O	2.51	3.67	3.45	3.11	3.07	3.53	3.27
K_2O	.38	1.01	.99	1.84	1.83	.96	1.38
P_2O_5	.12	.25	.19	.15	.15	.19	.06
H_2O^+	1.40	2.40	2.20	.87	.95	2.10	1.10
H_2O^-	.97	2.90	1.20	1.50	1.20	1.30	1.20
CO_2	.02	.02	.02	.02	.02	.02	.02
FeO*/MgO	.95	1.61	2.07	2.25	2.23	2.16	1.40

because (1) the basalt is at least as old or older than the clastics, (2) basalt is not a major constituent of the associated sandstones, and (3) the sedimentary rocks are thermally immature and thus were not affected by an intrusive event (Bruns and others, 1985; in press). Third, the basalts have no clear relation to the bulk of eruptive volcanic rocks along the Aleutian arc, whose ages are dominantly Eocene through Oligocene, corresponding to the major development time of the so-called Meshik arc of Wilson (1985), and late Miocene through Holocene, corresponding to development of the Aleutian Arc. The age of the dredged basalt best corresponds to the youngest recorded age of early Miocene for Meshik arc volcanic rocks, but could also indicate an entirely different and younger volcanic event than the Meshik arc events. Finally, the dredged volcanic- arc rocks from site 3 are at present anomalously close to the Aleutian trench (about 60 km) compared to normal eruption sites of lavas along the Aleutian chain or other island-arc volcanic chains. These basalts could have been emplaced by forearc volcanism during a volcanic episode separate from either the Meshik or Aleutian arc events. Another possibility, and the one that we prefer, is that the basalts were originally emplaced in a normal arc-axis position relative to the early Miocene trench and volcanic arc, and that the outer part of the margin has been subsequently removed by tectonic erosion (Bruns and others, in press).

REFERENCES CITED

Bruns, T.R., and von Huene, Roland, 1977, Sedimentary basins on the Shumagin shelf, western Gulf of Alaska: Ninth Annual Offshore Technology Conference Proceedings, Houston, Tex., v. 1, p. 41-50.

Bruns, T.R., von Huene, Roland, Culotta, R.C., and Lewis, S.D., 1985, Summary geologic report for the Shumagin Outer Continental Shelf (OCS) planning area, Alaska: U.S. Geological Survey Open-File Report 85-32, 58 p.

Bruns, T.R., von Huene, Roland, Culotta, R.C., Lewis, S.D., and Ladd, J.W., in press, Geology and petroleum potential of the Shumagin margin, Alaska, in Scholl, D.W., Grantz, Arthur, and Vedder, J.G., eds., Geology and resource potential of the continental margin of western North America and adjacent ocean basins -- Beaufort Sea to Baja California: Circum-Pacific Council for Energy and Mineral Resources Earth Science Series, 84 p.

Lewis, S.D., Ladd, J.W., Bruns, T.R., and von Huene, Roland, in press, Structural development of an accretionary prism by thrust and strike-slip faulting: Shumagin region, Aleutian Trench: Geological Society of America, Bulletin.

Masuda, A., Nakamura, N., and Tanaka, T., 1973, Fine structures of mutually normalized rare-early patterns of chondrites: Geochimica et Cosmochimica Acta, v. 37, p. 239-248.

Wilson, F.H., 1985, The Meshik arc -- An Eocene to earliest Miocene magmatic arc on the Alaska Peninsula: Alaska Division of Geological and Geophysical Surveys, Professional Report 88, 14 p.

Reviewers: M.A. Fisher and M.S. Marlow

GLORIA IMAGES OF ZHEMCHUG CANYON AND BERING CHANNEL-FAN SYSTEM, BERING SEA

Herman A. Karl, James V. Gardner, and Quentin Huggett

The deep-sea part of the Exclusive Economic Zone (EEZ) of Alaska is being surveyed as a continuation of the EEZ- SCAN project of the U.S. Geological Survey (Gardner, 1984). The primary survey tool is a long-range side-scan sonar, the GLORIA III system (Somers and others, 1978; Swinbanks, 1986). Two-channel digital seismic-reflection profiling, 3.5- and 10-kHz profiling, gravity, and magnetics systems provide ancillary geophysical data. The first of four planned Alaska field seasons began in the summer of 1986 with four cruises. One brief cruise surveyed a small corridor of about 50,000 km^2 in the Gulf of Alaska, and three longer cruises covered approximately 700,000 km^2 of the Beringian continental slope, the abyssal seafloor of the Aleutian Basin, and the north slope of the Aleutian Ridge (fig. 1). We report here only the highlights of preliminary interpretations of the shipboard GLORIA side-scan imagery from cruise F3-86 that covered a rectangular area of approximately 200,000 km^2 in the Bering Sea from Zhemchug Canyon southeastward along the margin to just north of Pribilof Canyon and southwestward across the Aleutian Basin to Bowers Ridge.

Some of the largest submarine canyons in the world incise the Beringian continental margin, and Zhemchug Canyon is the largest of these canyons. Zhemchug Canyon has a volume of at least 5,800 km^3, more than an order of magnitude larger than Astoria Canyon on the Oregon continental margin (425 km^3) and Hudson Canyon on the New York margin (300 km^3) (P.R. Carlson, USGS, oral commun., 1986). Previous investigators recognized evidence of mass transport of sediment in the Beringian canyons (Scholl and others, 1970; Carlson and Karl, 1984). However, the GLORIA images reveal that products of mass transport are much more common than previously interpreted and that mass-wasting is the dominant erosional process on the continental slope (fig. 2). Earlier studies of Zhemchug Canyon utilized seismic-reflection data and sediment samples as interpretive tools. The new perspectives of the canyon provided by the GLORIA images enable us not only to refine previous descriptions of the morphology and evolution of the canyon, but also to offer new insight into the origin of the canyon. For example, there is a large sediment mass at the base of Zhemchug Canyon that is clearly visible on the GLORIA mosaic (fig. 2). Although this mass had been observed on single- channel seismic-reflection records collected on earlier cruises, its dimensions were unknown and its relationship to the canyon was unclear. Our preliminary data suggest that Zhemchug Canyon originated when this large block broke away from the margin and slid intact onto the abyssal plain. Headward erosion by sediment failure progressed northeastward until it reached the southernmost of two parallel normal faults on the outer shelf. These faults were identified on earlier cruises, and we agree with previous interpretations (Scholl and others, 1970) that at this stage of canyon evolution, sediment in the structural basin between the faults was preferentially eroded to the northeast, northwest, and southeast and produced the winged shape of Zhemchug Canyon. As masses of sediment became detached from the slope, the resulting blocks, slumps, and slides clogged major sediment dispersal pathways in the growing gorge and formed a labyrinth of channels. These products of mass sediment transport, in turn, were eroded by numerous gullies. The amount of sediment contributed to the Aleutian Basin from and via Zhemchug Canyon is unknown. However, it appears that the canyon is not presently an important source of modern sediment because no channels from the canyon extend onto the abyssal plain.

The GLORIA mosaic, however, has enabled us to identify the principal routes of sediment transport to the basin. We have recognized a channel that enters the study area from the east, apparently originating from Bering Canyon (fig. 3). Although a channel at the mouth of Bering Canyon had been suggested on bathymetric maps, it was not known that it extends onto the abyssal plain for more than 500 km. Unlike other known deep-sea channels, such as Cascadia channel on the abyssal plain off Oregon and Washington, Bering channel is not deeply incised but, as seen on high- resolution and seismic-reflection profiles, rather shallow and broad, being about 10-20 m deep and and as wide as 25 km, with a low but well-developed levee on the north side. Bering channel terminates in a newly discovered deep-sea fan, informally called Bering fan, which is being constructed in the deepest part of the eastern Aleutian Basin. Bering fan is a very low relief feature with a complex system of distributaries and located in the middle of the abyssal seafloor, whereas most submarine fans are large-volume high-relief sediment bodies built up at the base of the continental slope (Bouma and others, 1985). Moreover, Bering fan lacks the distinctive upper, middle, and lower fan morphology and channel-levee systems that generally are present on other fans. Instead, it is a thin veneer of sediment disgorged by Bering channel. We surmise that most transport and deposition on the fan is by sheet- flow rather than channelized flow as in the traditional models of fan development (Bouma and others, 1985). We cannot yet determine from our initial analysis of the data whether Bering fan

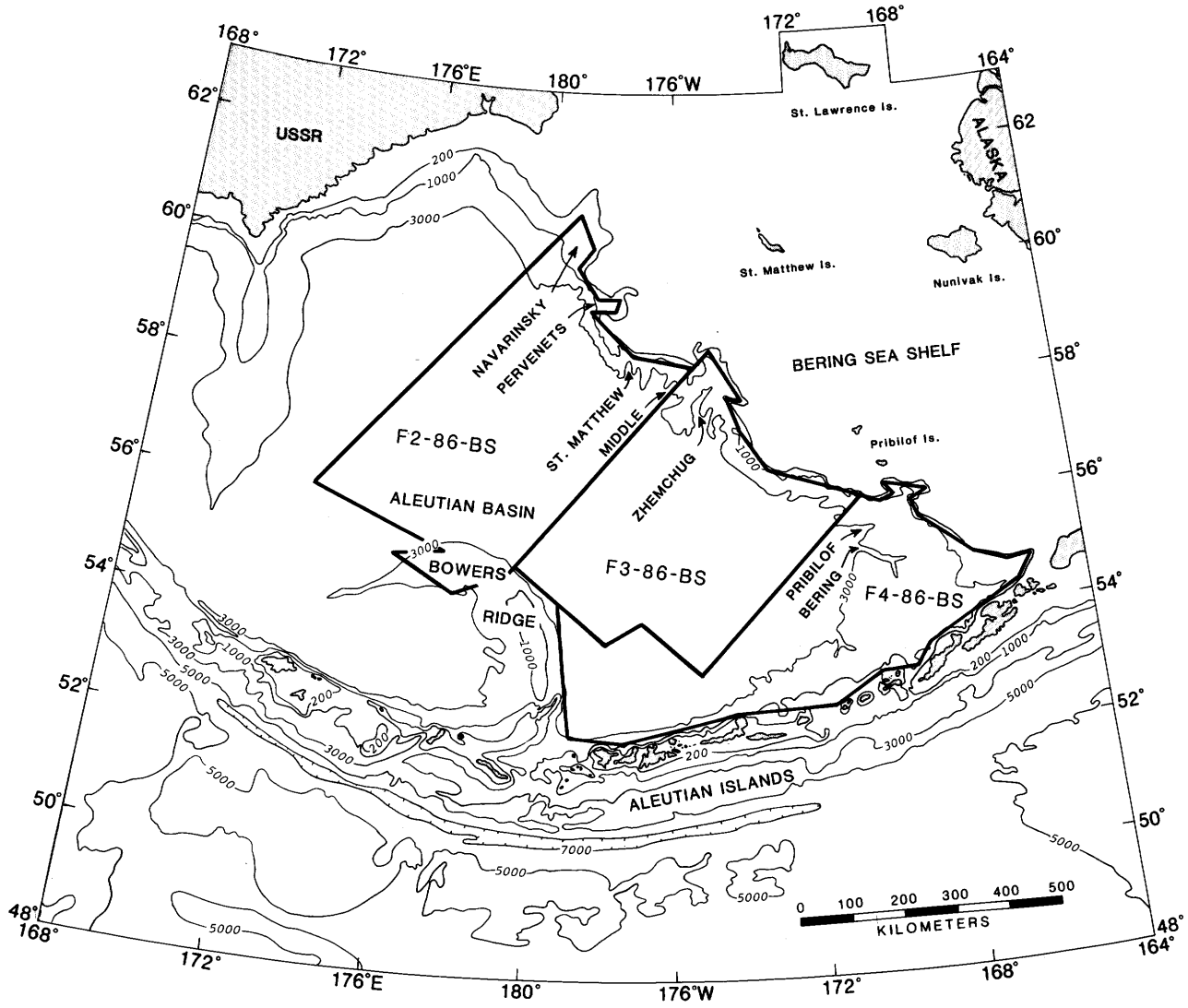

Figure 1.--Location map showing area of each Bering Sea cruise and major canyons that incise Beringian margin. Bathymetric contours in meters.

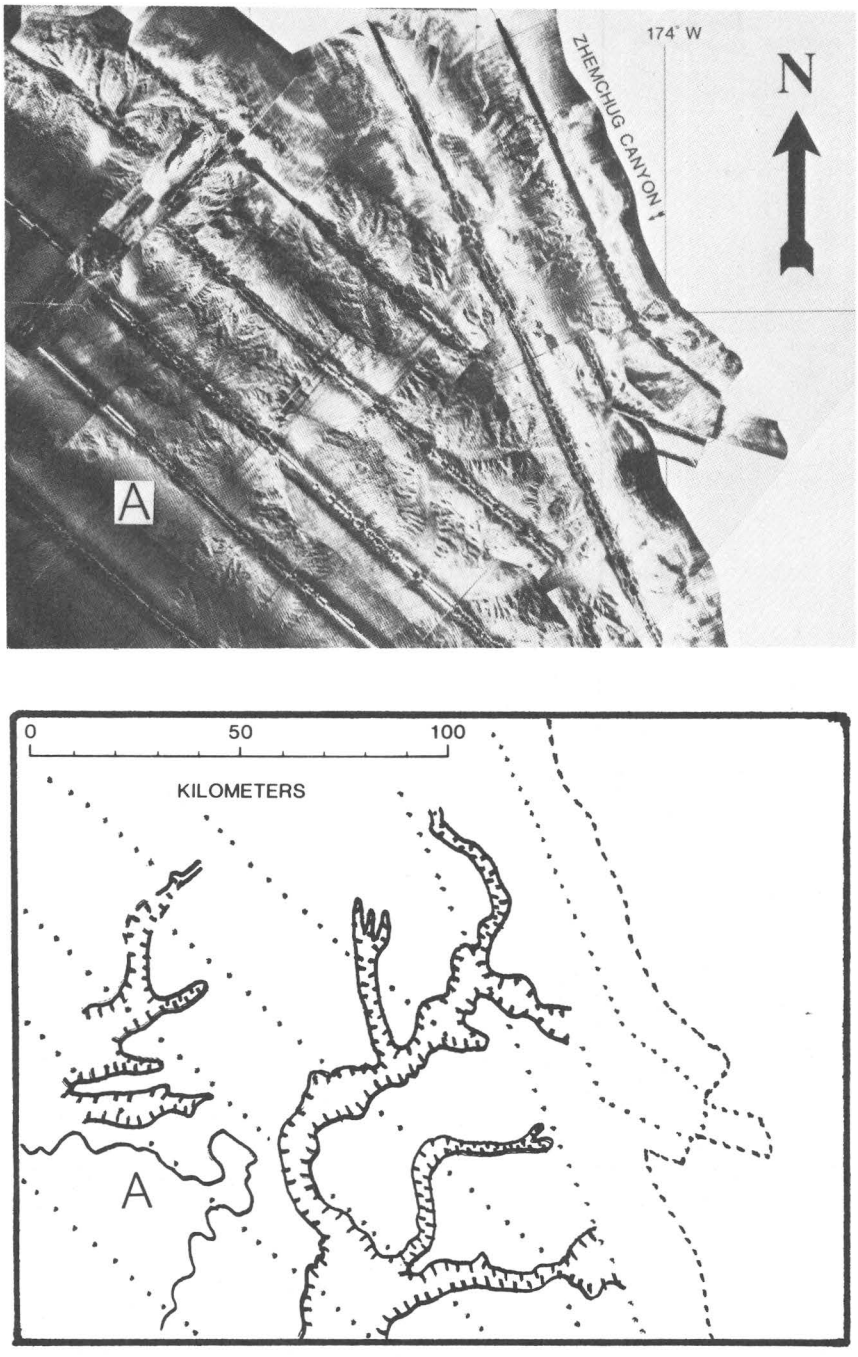

Figure 2.--Top, sonographic mosaic of Zhemchug Canyon and adjacent continental slope and abyssal seafloor. A, large block at base of Zhemchug mentioned in text. Note numerous gullies and sediment masses that evidence mass-wasting. Mosaic constructed onboard ship. Lines signify areas of no data under ship's track. Bottom, line drawing of sonograph showing major channels and outlining large block at base of canyon. Dots indicate ship's track for orientation with features on sonograph.

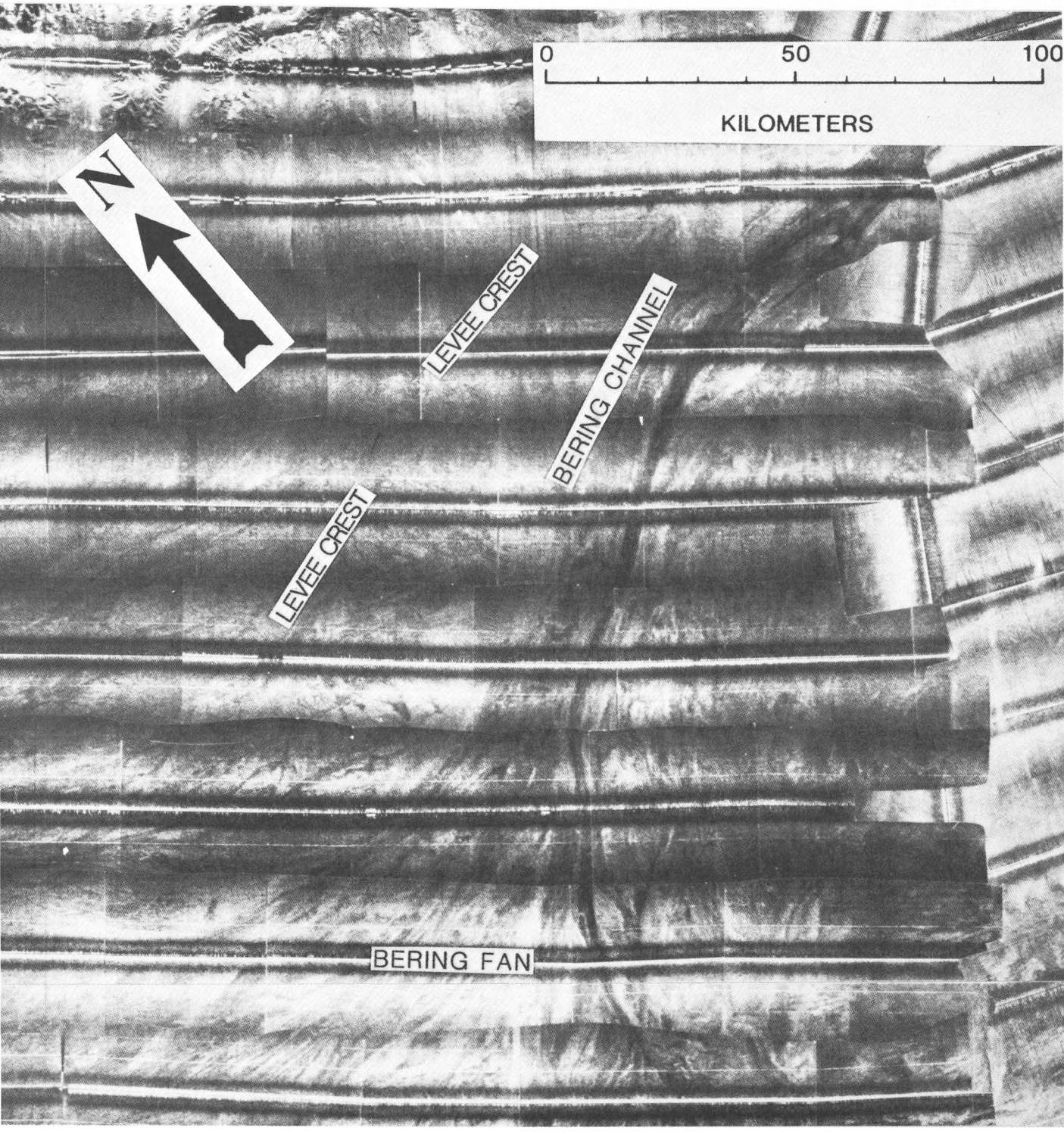

Figure 3.--Bering channel and Bering fan. Note complex backscatter pattern that distinguishes fan. Levee cannot be distinguished easily on the unprocessed sonograph and its approximate position and trend are labeled.

represents an early developmental stage of a normal submarine fan or a new class of deep-sea fan. Debris shed from the Aleutian Ridge and funneled down its flanking canyons appears to accumulate in the immediate vicinity of Bering fan as well (A.J. Stevenson, USGS, written commun., 1986), thus this area seems to be the primary loci of modern deposition in the Bering Sea.

REFERENCES CITED

Bouma, A.H., Normark, W.R., and Barnes, N.E., eds., 1985, Submarine fans and related turbidite systems: New York, Springer-Verlag, 351 p.

Carlson, P.R., and Karl, H.A., 1984, Mass movement of fine-grained sediment to the deep-basin floor, Bering Sea, Alaska: Geo-Marine Letters, v. 4, p. 227-234.

Gardner, J.V., 1984, Program EEZ-SCAN: A reconnaissance view of the western U.S. Exclusive Economic Zone, in Clarke, S.H., ed., U.S. Geological Survey highlights in marine research: U.S. Geological Survey Circular 938, p. 125-132.

Scholl, D.W., Buffington, E.C., Hopkins, D.M., and Alpha, T.R., 1970, The structure and origin of the large submarine canyons of the Bering Sea: Marine Geology, v. 8, p. 187-210.

Somers, M.L., Carson, R.M., Revie, J.A., Edge, R.H., Barrow, B.J., and Andrews, A.G., 1978, GLORIA II--An improved long range side-scan sonar: Oceanology International 78, p. 16-24.

Swinbanks, D., 1986, New GLORIA in record time: Nature, v. 320, p. 568.

Reviewers: B.D. Edwards and T.L Vallier

GLORIA SIDE-SCAN AND GEOPHYSICAL SURVEYS OF THE CENTRAL BERING SEA IN 1986

Michael S. Marlow, Paul R. Carlson, Shawn V. Dadisman, Douglas M. Rearic, Edward J. Maple, and Lindsay M. Parson

During the summer of 1986, about 225,000 km^2 of the central Bering Sea continental slope and abyssal plain were surveyed with the GLORIA side-scan sonar system on the MV Farnella (fig. 1). This cruise was part of a cooperative program between the U.S. Geological Survey and the British Institute of Oceanographic Sciences in which the deep-water parts of the Alaskan EEZ (Exclusive Economic Zone) are being surveyed using the GLORIA system.

Prominent geomorphic features of the Bering Sea were imaged, including Navarinsky, Pervenets, and Zhemchug Canyons along the Beringian margin, the abyssal floor of the Aleutian Basin, and the northern part of Bowers Ridge (Bering Sea EEZ Scan 86 Group, 1987). Large slump and slide features, some measuring kilometers across, occur along the margin, showing that mass movement is a major sediment transport mechanism on the continental slope. A wide variety of slides and flows previously have been identified on the Beringian margin from seismic-reflection profiles (Carlson and Karl, 1984/85), and mass wasting has been inferred to be an important erosional process. The extent of mass wasting, however, was not recognized until the margin was imaged with GLORIA. Evidence of mass transport is common not only on the Beringian slope, but also along Bowers Ridge.

Along the Beringian slope and on both sides of Bowers Ridge, sediment-flow patterns fan out into the basin from the numerous canyons and gullies incised in the slopes. Major channels are absent across that part of the northern Aleutian abyssal plain surveyed by us, suggesting that sheet flow is the dominant mode of sediment transport in the northern Aleutian Basin (Carlson and others, 1986).

Large sand waves, 600 m long and 2-5 m high, are visible on the GLORIA images in Navarinsky and Pervenets Canyons (fig. 2). These sand waves were previously recognized on seismic-reflection profiles and interpreted by Karl and Carlson (1982) and Karl and others (1986). The GLORIA side-scan imagery provides a plan view of the sand waves that allows us to determine the orientation and continuity of these large-scale bedforms. The sand waves cover about 1,400 and 800 km^2 of the heads of Navarinsky and Pervenets Canyons, respectively. These sand waves, some of which are relict, buried features, reach a maximum stratigraphic thickness of 120 m and consist of several crossbedded sets (fig. 2).

Along with the GLORIA survey, we also collected two-channel seismic-reflection, gravity, gradiometer (magnetic), and bathymetric data. The seismic-reflection data show that the western Aleutian Basin is underlain by six linear basement ridges, 30 to 140 km long, which are buried by an average of 1.5 to 2.0 km of sediment (fig. 1 and table 1). Two of the ridges, Sounder and Bartlett, were discovered by Cooper and others (1976b, 1979). The other four subsurface ridges, A, B, Farnella and Pear, were discovered in 1986 by seismic-reflection profiling on the MV Farnella. The six ridges occupy an area south of the continental margin of eastern Siberia (USSR) extending southwest toward the junction of Bowers, Shirshov, and the western Aleutian Ridges (fig. 1). The ridges are built on oceanic crust of presumed Mesozoic age interpreted to be part of the Kula plate (Cooper and others, 1976a, b). Two of the ridges, Sounder and Bartlett, have associated positive and negative magnetic anomalies, respectively. Local buried basement highs associated with several of the ridges, including Farnella ridge, extend to within a few hundred meters of the sea floor (fig. 3). Farnella ridge shows two such local highs, which are draped by differentially compacted sediment over the tops of the highs. These local highs are probably ancient seamounts rising along the linear basement ridges.

The basement ridges range from being oblique to perpendicular to the north-south-striking linear magnetic anomalies of presumed Mesozoic origin that were first described by Cooper and others (1976b). For instance, the spreading anomalies in the Aleutian Basin are interrupted or possibly terminated to the northwest by Sounder ridge, which may occupy an ancient fracture zone now trending nearly east-west. The basement ridges could be the same age or younger than the underlying oceanic crust.

The north-south-striking linear magnetic anomalies fan to the southwest. These spreading anomalies, which originate from the oceanic crust beneath the Aleutian Basin (Cooper and others, 1976a, b), may have formed along a propagating rift system similar to rift systems suggested for the fanning Mesozoic magnetic anomalies in the northern central Pacific, which were first noted by Larson and others (1972) and discussed by Tamaki and others (1979).

The seismic-reflection data collected in 1986 also revealed 280 acoustic anomalies in the reflection horizons beneath the Aleutian Basin (Rearic and others, 1986). Over 88 percent of these anomalous reflectors are distinguished as VAMPs, the velocity-amplitude anomalies of Scholl and Cooper (1978), and exhibit velocity or time-based pulldowns such as that shown in fig. 4. Maximum amplitude of the pulldowns averages 25 ms and can be more than 70 ms. The

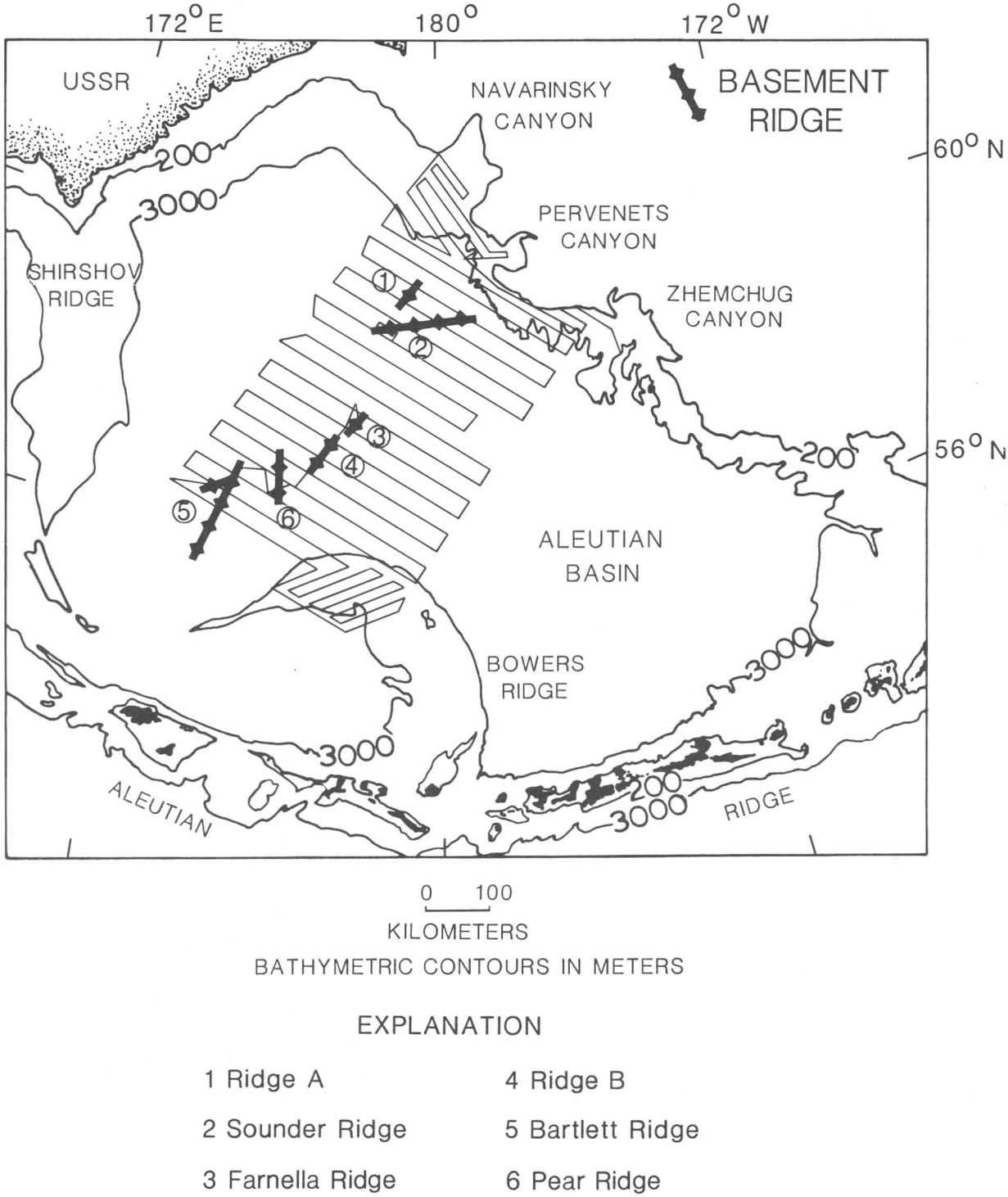

Figure 1.--Ship's tracks for first GLORIA leg in Bering Sea in 1986. Note location of buried basement ridges in western Aleutian Basin. Albers equal-area projection.

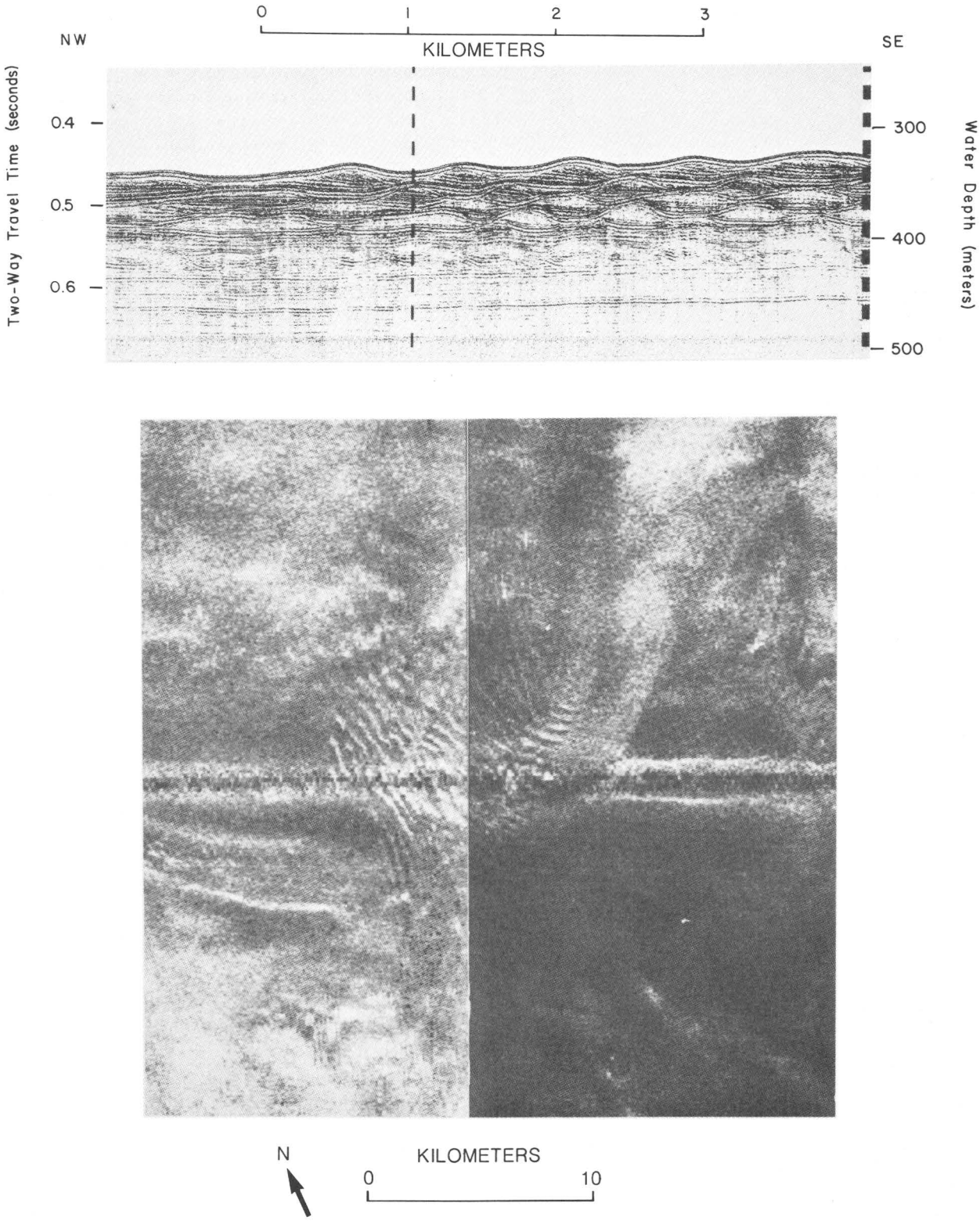

Figure 2.--Minisparker seismic-reflection profile (top) and unprocessed GLORIA imagery across Navarinsky sand-wave field.

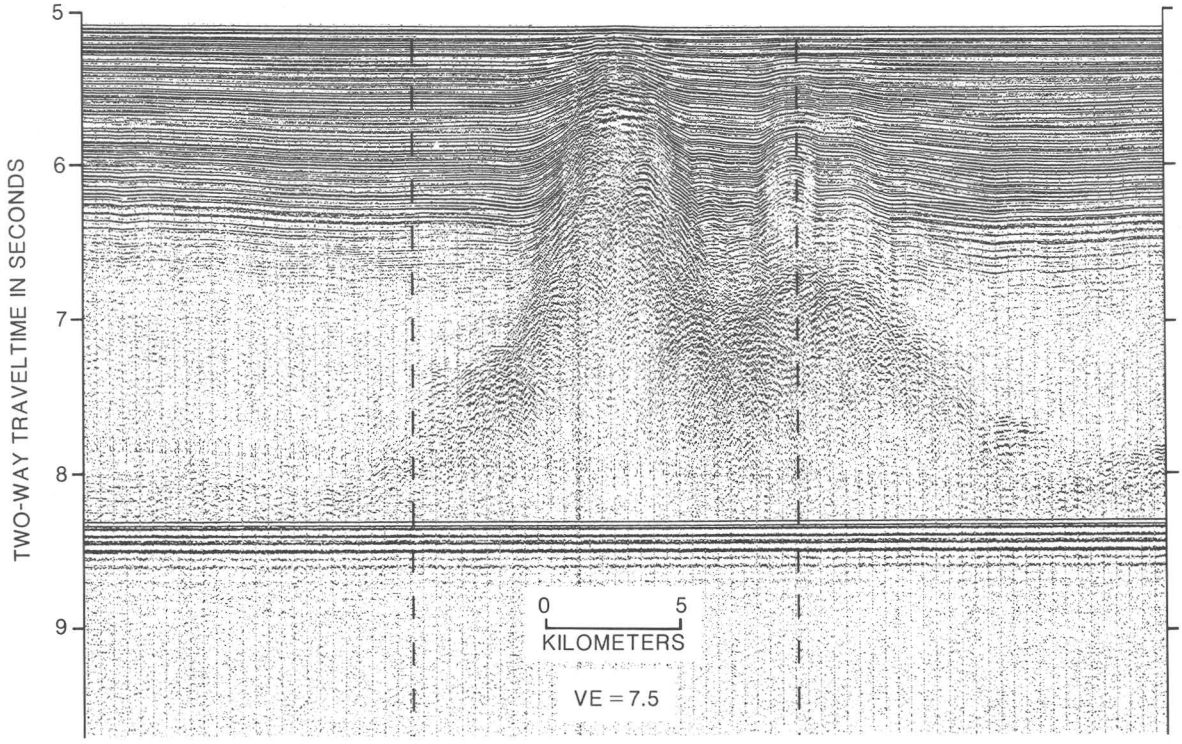

Figure 3.--Single-channel seismic-reflection profile across Farnell ridge. Ridge is buried by 450-500 m of sediment. Note associated magnetic anomaly across ridge, which trends obliquely to regional magnetic anomaly trends. Note the two basement highs.

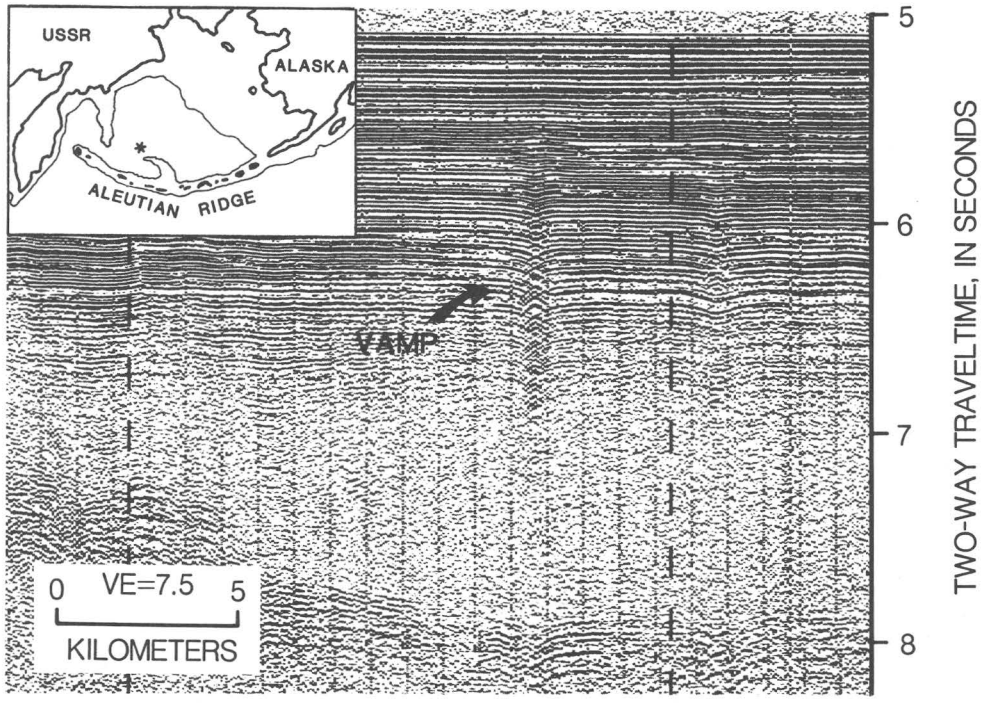

Figure 4.--Seismic-reflection profile from southern Aleutian Basin. VAMP at center exhibits many characteristics commonly observed in anomalous reflectors in Aleutian Basin (pull-down, phase inversion, arching of overlying reflectors, and diffraction hyperbola with bowtie structure).

anomalous reflectors range in width from 0.5 km to 9 km and average 1.5 km. The anomalies are interpreted as indicating gas-charged sediment.

Table 1.--Basement ridges beneath western Aleutian Basin

NAME	FROM	TO	LENGTH(km)
Ridge A	58.92 N. 179.86 E.	58.75 N. 179.44 E.	30
Sounder ridge	58.65 N. 179.33 E.	58.43 N. 178.52 E.	140
Farnella ridge	57.34 N. 177.96 E.	57.12 N. 177.74 E.	30
Ridge B	56.95 N. 177.28 E.	56.49 N. 176.78 E.	60
Pear ridge	56.85 N. 175.71 E.	56.20 N. 175.83 E.	75
Bartlett ridge	56.49 N. 174.97 E.	55.35 N. 173.90 E.	140

REFERENCES CITED

Bering Sea EEZ Scan Group 86, in press, Long-range side-scan sonar and geophysical survey of Aleutian Basin: Eos (Transactions American Geophysical Union).

Carlson, P.R., and Karl, H.A., 1984/85, Mass movement of fine-grained sediment to the basin floor, Bering Sea, Alaska: Geo-Marine Letters, v. 4, p. 221-225.

Carlson, P.R., Marlow, M.S., Rearic, D.M., Dadisman, S.V., and Parson, L.M., 1986, GLORIA side-scan imagery of central Bering Sea EEZ: Eos (Transactions American Geophysical Union), v. 67, p. 1228-1229.

Cooper, A.K., Scholl, D.W., and Marlow, M.S., 1976a, A plate tectonic model for evolution of the eastern Bering Sea Basin: Geological Society of America Bulletin, v. 87, p. 1119-1126.

_____ 1976b, Mesozoic magnetic lineations in the Bering Sea marginal basin: Journal of Geophysical Research, v. 81, p. 1916-1934.

Cooper, A.K., Scholl, D.W., Marlow, M.S., Childs, J.R., Redden, G.D., Kvenvolden, K.A., and Stevenson, A., 1979, Hydrocarbon potential of Aleutian Basin, Bering Sea: American Association of Petroleum Geologists Bulletin, v. 63, p. 2070-2087.

Karl, H.A., Cacchione, D.A., and Carlson, P.R., 1986, Internal-wave currents as a mechanism to account for large sand waves in Navarinsky Canyon head, Bering Sea: Journal of Sedimentary Petrology, v. 56, p. 706-714.

Karl, H.A. and Carlson, P.R., 1982, Large sand waves in Navarinsky Canyon head, Bering Sea: Geo-Marine Letters, v. 2, p. 157-162.

Larson, R.L., Smith, S.M., and Chase, C.G., 1972, Magnetic lineations of Early Cretaceous age in the Western Equatorial Pacific Ocean: Earth and Planetary Science Letters, v. 15, p. 315-319.

Rearic, D.M., Williams, S., and Carlson, P.R., 1986, VAMPs and other acoustic evidence of gas-charged sediment in the abyssal Aleutian Basin, Bering Sea, Alaska (abs.): Eos (Transactions American Geophysical Union), v. 67, p. 1211.

Scholl, D.W., and Cooper, A.K., 1978, VAMPs -- Possible hydrocarbon-bearing structures in Bering Sea basin: American Association of Petroleum Geologists Bulletin, v. 62, p. 2481-2488.

Tamaki, K., Joshima, M., and Larson, R.L., 1979, Remanent Early Cretaceous spreading center in the Central Pacific Basin: Journal of Geophysical Research, v. 84, p. 4501-4510.

Reviewers: S.L. Eittreim and H.A. Karl

VIBRACORE STRATIGRAPHY OF THE NORTHEASTERN CHUKCHI SEA

R. Lawrence Phillips and Mitchell W. Colgan

Shallow epicontinental seas, such as the Cretaceous intercontinental seaway, are common throughout geologic history, but there are few modern analogs. The Chukchi Sea is one such analog. In this paper we present our preliminary findings of the stratigraphy of the northeastern part of that water body.

The Chukchi Sea is a shallow (<60 m deep) epicontinental sea that is ice-covered for 9 to 10 months a year. Sediment input is low because few rivers enter the Chukchi Sea, and an extensive barrier island system traps much of their sediment (Grantz and others, 1982). Consequently, a thin sediment cover (generally less than 6 m thick) overlies gently to steeply dipping folded and faulted bedrock. A northward-flowing shore-parallel current (the Alaska Coastal Current) dominates the Chukchi Sea's eastern flank; converging currents off Cape Lisburne, Icy Cape, and Point Franklin deposit the thickest sediment cover in the eastern Chukchi Sea. Storms, ice gouging, and local currents rework the shelf sediments.

In September and October 1985, we used the NOAA RV Discoverer to conduct geological and geophysical surveys of the Chukchi Sea. Our study area is bounded by Point Hope to Point Barrow on the east, the US-USSR 1867 Convention Line to the west, and the shelf break to the north (fig. 1). Our data are based on seismic records obtained from a high-resolution seismic system and a 3.5-kHz sub-bottom profiler along 2,600 km of trackline and 22 vibracore samples of 9 cm diameter and up to 6 m long. This report examines the shelf stratigraphy from 14 of those cores taken at 26-48 m water depth. We examined core subsamples for texture, mineralogy, and fossils (diatoms, sponge spicules, foraminifers, ostracodes, mollusks, and insects) to define the stratigraphic units. Clay mineralogy was determined by X-ray diffraction.

Our high-resolution seismic records were used to define the bedrock surface on which the younger sediments were deposited. A series of channels of unknown age incise the bedrock (fig. 2). The vibracores record a sedimentary history of erosion and limited deposition. At least five major laterally continuous stratigraphic units -- volcanic ash, pebbly mud, pebbly to muddy sand, iron stained sand, and pebbly muddy sand -- occur above bedrock. In addition, two minor units, a consolidated silty clay and a laminated sand, are recognized.

The deepest stratigraphic unit is 204 cm of consolidated silt and clay, which rests on inclined bedrock and coarsens upward (core 53 in fig. 2). The silt fraction is composed of glass shards, quartz grains, and biotite and is suspended in a mixed clay that consists of smectite, illite, and chlorite. This unit contains horizontal parallel laminations, black organic-rich beds, and large burrows.

Volcanic ash is found at the base of five cores over a distance of 160 km north-south and 97 km east-west, and it blankets directly or rests within 2 m of an irregular bedrock surface that causes the deposit to thicken or thin above it. The thickness of the ash ranges from 152 cm in core 53 to a possible maximum thickness of 6 m (determined from high-resolution seismic records at station 62). Horizontal parallel graded laminations of volcanic glass and black organic material form the major sedimentary structures. The ash, where not altered, consists of greater than 95 percent glass shards that range from 425 μm (medium sand) to 4 μm (very fine silt) with a median size of 62.5-125 μm (fine sand). Mineralogy consists of rhyolite vitric ash (SiO_2 = 76.1 percent) and altered tephra (clay). The vitric ash is colorless and consists of a mixture of bubble wall junction shards, vesicular shards, and bubbles; the shards have a refractive index of 1.500 ± 0.002. The altered tephra contains a clay mixture of smectite-illite, kaolinite, and chlorite with zeolites. Marine microfossils of diatoms, sponge spicules, and foraminifers are sparsely distributed in the ash deposit. The upper 1 m of the deposit contains scattered rounded quartz and chert pebbles as well as two pebble beds.

Overconsolidated cobbly to pebbly sandy mud containing gravel clasts (up to 6 cm in length), ash beds (up to 12 cm thick), and bioturbated mud conformably overlies altered tephra, and in one case (core 66) may rest directly on or near bedrock. The deposit ranges in thickness from 30 cm to at least 180 cm, and pinches out to the east (toward shore) and the north. Quartz grains, biotite, glass shards, diatoms, rare foraminifers, and sponge spicules are found in the sand-size fraction.

The pebbly to muddy sand unit was found only in five northwestern cores (51, 54, 56, 57, and 58). The vibracore did not penetrate below this unit at any of those stations, and its lower contact therefore could not be determined. The unit ranges in thickness from 17 cm (core 51) to 220 cm (core 56). The sand-size fraction is composed of quartz grains, abundant muscovite, glass shards, sponge spicules, and foraminifers (locally abundant *Elphidium* sp.). Horizontal parallel laminations, thin organic-rich beds, scattered pebbles (up to 1 cm diameter), shell beds, and abundant bioturbation are common. In the thickest section, in core 56, sediment texture coarsens upward.

The lowermost unit of core 67 is a 155-cm-thick sequence of repeated parallel sand laminae that rests on or near bedrock. Sand grains consist

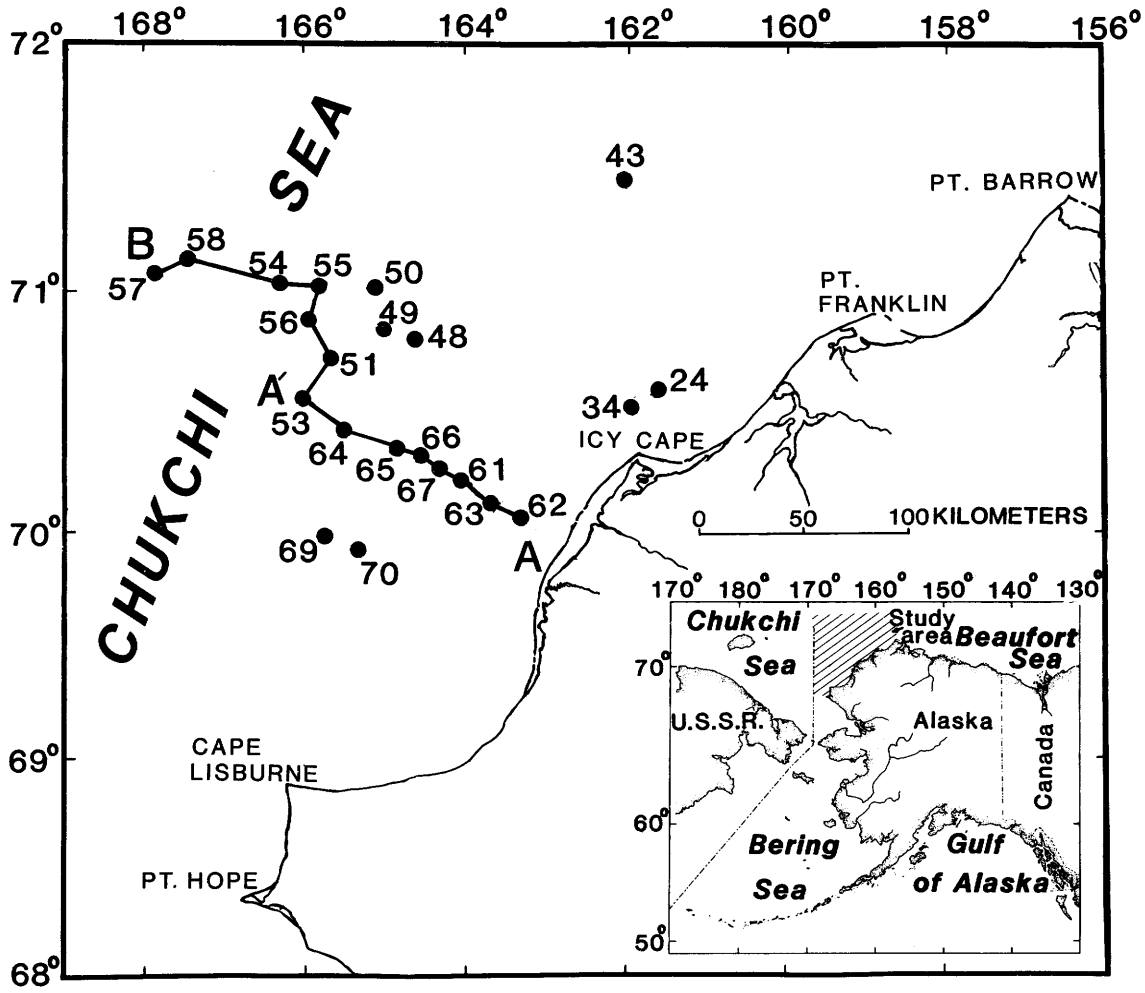

Figure 1.--Vibracore locations in northeastern Chukchi Sea. A-A' and A'-B designate core profiles.

of white and clear quartz, amphiboles, pyroxenes, and books of biotite. Heavy-mineral content (specific gravity >2.96) ranges from 13.4 to 15.7 percent, with heavy minerals concentrated in laminae. Neither fossils nor biogenic structures are evident.

Iron-stained, quartz-rich sand to locally pebbly sand is found in eight cores (fig. 2). Thickness varies from 19 cm (core 56) to 245 cm (core 67), and the unit thins to the west. The iron-stained sand rests on an erosional contact above either weathered tephra, laminated sand, pebbly mud, or pebbly muddy sand (fig. 2). Well-rounded quartz sand, brown peat laminae and beds, scattered isolated pebbles and pebble lags, and thin muddy gravel beds characterize this sequence. The organic-rich laminae contain abundant insect remains, ostracodes (nonmarine), algal filaments, seeds, and wood, but macrofossils are absent.

Silty mud to sandy gravel deposited since the last transgression forms the uppermost sequence. These sediments range in thickness from 50 to 440 cm and rest on either iron stained sand, pebbly mud, or pebbly to muddy sand. The unit consists of bioturbated horizontal laminae to intensely bioturbated massive sediment with a few scattered pebbles. Sediment texture fines westward. All cores from 65 westward have a thin surface mud layer over sand, but the mud layer is absent to the east, where the Alaska Coastal Current erodes the sea bed (cores 66 to 68). Quartz grains, glass shards, macrofossils (bivalves, gastropods, barnacles, and echinoids), and microfossils (ostracodes, foraminifers, diatoms, and sponge spicules) occur in the sand fraction. A gravel-shell lag usually marks the base of this sequence.

Although direct correlation of our units is tentative pending age determination, core

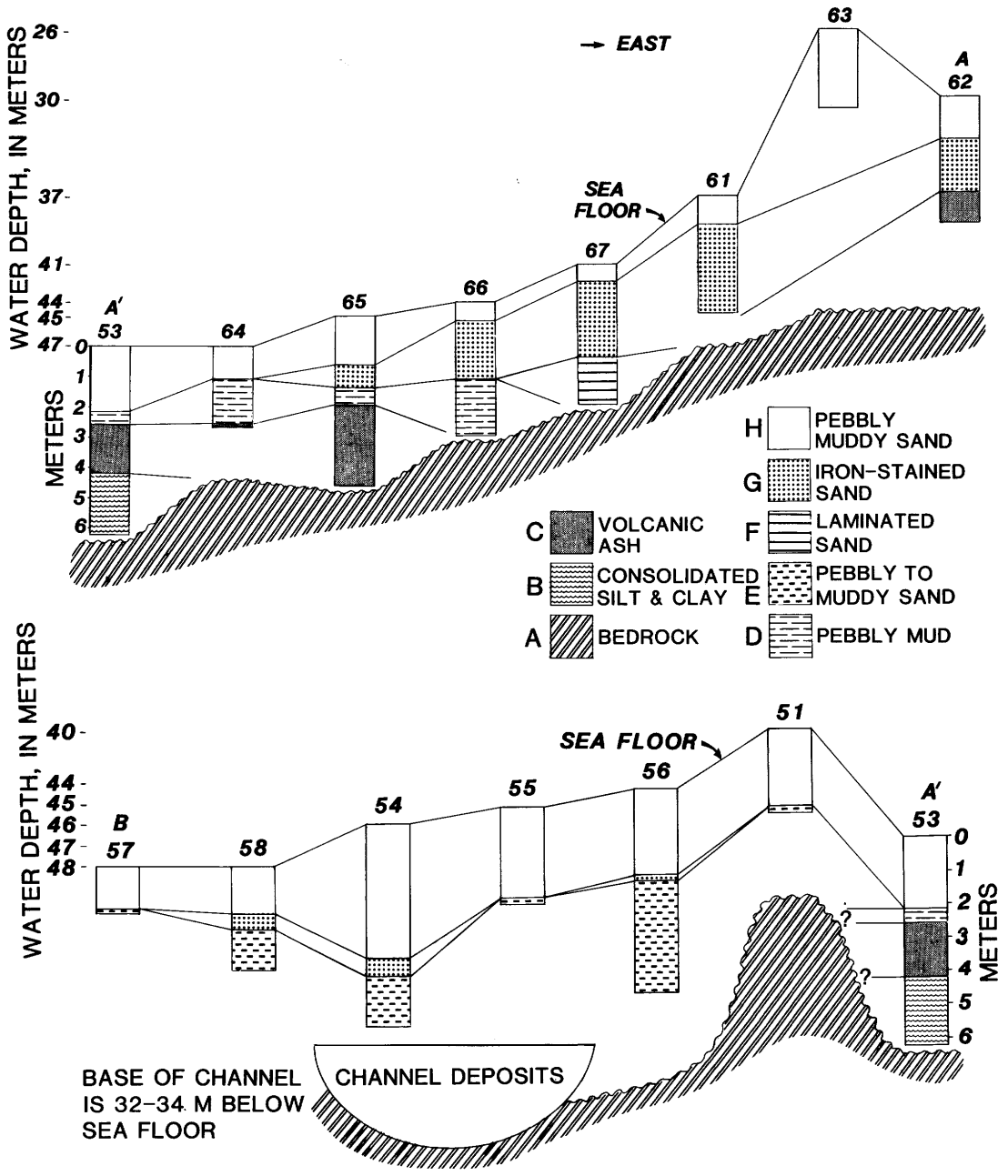

Figure 2.--Vibracore stratigraphy across northeastern Chukchi Sea. See figure 1 for core locations. Depth to bedrock surface determined from high-resolution seismic records. Core meter scale is on core 53.

stratigraphy suggests a consistent regional sequence. The origin of the deepest depositional unit, unit B in core 53, is uncertain because of its limited areal distribution and the lack of fossils. However, the presence of abundant glass shards and laminated sediment suggest either an altered tephra or weathered bedrock with ash contamination from the overlying tephra. The general absence of sediment between bedrock and tephra reveals that erosion was the predominant shelf process prior to deposition of the tephra. The ash fell into the ocean where currents redistributed it, resulting in locally abnormally thick deposits (unit C, fig. 2) The presence of well-rounded detrital quartz grains and pebbles in the uppermost section of the ash signals the initiation of ice-rafted sedimentation during the later stage of ash deposition. The end of ash deposition was followed by marine clastic sedimentation with continued ice-rafting of pebbles and cobbles (unit D).

A transgressive-regressive cycle best explains the deposition of units overlying the tephra and marine pebbly mud. A transgression resulted in deposition of marine sediment (unit E) and a possibly related beach sand (unit F). Later sea-level lowering exposed the shelf, and eolian and fluvial sediment were deposited (unit G). The last transgression eroded most of the previously deposited units and deposited the uppermost marine sequence (unit H). Modern shelf processes (storms, currents, ice, and bioturbation) then reworked these sediments, resulting in areas of thin sediment cover (cores 66, 67, and 68) and areas of deposition (core 63).

This study was funded in part by the Minerals Management Service through interagency agreement with the National Oceanic and Atmospheric Administration as part of the Outer Continental Shelf Environmental Assessment Program. We thank Captain Peterson, the officers, and crew of the RV Discoverer for their help.

REFERENCE CITED

Grantz, A., Dinter, D.A., Hill, E.R., Hunter, R.E., May, S.D. McMullin, R.H., and Phillips, R.L., 1982, Geologic framework, hydrocarbon potential, and environmental conditions for exploration and development of proposed oil and gas lease sale 85 in the central and northern Chukchi Sea: U.S. Geological Survey Open-File Report 82-1053, 84 p.

Reviewers: P.J. Quinterno and Erk Reimnitz

THIRTY-FOUR-YEAR SHOREFACE EVOLUTION AT A RAPIDLY RETREATING ARCTIC COASTAL SITE

Erk Reimnitz and Edward W. Kempema

Erosion rates for vast stretches of circum-Arctic coastlines are among the highest on the globe. Long-term erosion rates in arctic USSR typically are 5-10 m/yr, commonly 15 m/yr, and in places as high as 50 m/yr (Are, 1980; Zenkovich, 1985). Similarly high average erosion rates occur along much of northern Alaska and the Yukon Territory in Canada (Reimnitz and others, 1985; Forbes and Frobel, 1985). The high coastal retreat rates in arctic regions are commonly attributed to processes of thermal erosion (Are, 1980; National Research Council, Marine Board, 1982), driven by the temperature differential between frozen sediments of surrounding coastal plains and the relatively warm sea.

Recognizing that the advancing sea dramatically slices off the coastal plains above sea level around the Arctic Ocean, and that the same processes have acted at least since sea level approached its present position about 5,000 years ago, inevitably leads to considerations of the adjoining shelf profile (for example, Harper, 1978). At the seaward limit of modern erosion, a break in slope or ramp should form, and given the high rates of coastal retreat, such ramps should be wide. Wide, well-developed terraces do not surround the Arctic basin at sea level. Therefore, submarine processes must be maintaining the typically concave-upward continental shelf profile in some type of equilibrium. But the precise mechanisms of profile maintenance remain obscure (Reimnitz and others, 1985).

Russian scientists believe that thermal energy and related processes play the most important role in shaping the arctic shelf profile. Tomirdiaro (1975) stated "The eastern Arctic seas are largely young Holocene bodies of water formed by thermo-abrasional processes." Thus the seafloor simply settles as ice-rich underlying sediments thaw, and therefore little lateral transport of clastic detritus is required. In fact, thaw settlement of the inner shelf should produce depositional basins for concurrent sediment supply (Harper, 1978). In contrast, Reimnitz and others (1985) argued that mechanical energy is more important than thermal energy for the maintenance of the dynamic equilibrium profile, but they lacked proof in the form of long-term comparisons of shoreface profiles. Knowledge of how the shoreface responds to extensive shoreline displacement is important not only for evaluating whether the seafloor provides a sediment sink or sediment source, but also for evaluating such problems as the fate of inundated archaeological sites and the design of oil pipeline crossings of arctic coasts. In this report we present the results of a shoreface study from a site where the coast locally retreated 400 m over a 30-year period (fig. 1).

The earliest bathymetry in the study area (fig. 1) stems from Hydrographic Survey 7922, done by the U.S. Coast and Geodetic Survey in July and August 1951 at a scale of 1:40,000. Most of the dense trackline pattern of that survey, shown in an inset of figure 1, was controlled by the use of Shoran, and the soundings were referenced to mean lower low water (MLLW). The original reference tidal bench marks still exist about 25 km west of the study site. The coastline was remapped by the State of Alaska and the National Ocean Survey, and again referenced to the same bench marks, in 1981. This new coastline is also shown on figure 1. The 30-yr average retreat rate for a 23-km-long coastal segment centered on figure 1 is 7.5 m/yr (Reimnitz and others, 1985).

In 1985 we used the RV Karluk and a skiff to run a hydrographic transect perpendicular to the coast and regional isobaths. From the beach to 2-m depth, the skiff, equipped with an echo sounder and an acoustic ranging system, was rowed along a range-line, and distances to a transponder moored on the crest of a nearshore bar (fig. 2) were recorded (distance errors less than 0.5 m). The emergent crest of the bar (fig. 3) on either side near our transect was surveyed by the State of Alaska in 1984 and 1985. Therefore this inner part of our depth profile is accurate for the purpose of a comparison with the original hydrographic survey. Seaward from a depth 1.5 m on that same range, partly overlapping the inner profile, the RV Karluk was positioned at 2-min intervals by means of a range/range navigation system using three shore stations. Shore stations A and B (fig.1) are survey monuments, positioned according to national mapping standards. Trading post Esook is located within 3 m of such a monument. Problems with the ranging system resulted in poor closures, which were satisfactorily resolved by adding 321 m to the distances from station B. This resulted in an excellent match in water depths in the overlapping parts of the two separate surveys. Because of navigational uncertainties farther than 3 km from the coast, that part of our survey will not be discussed.

We adjusted the water depths recorded in our surveys with reference to MLLW. The datum was carried to the study area from the previously mentioned bench marks by use of a skiff in radio contact with the RV Karluk, while it continued monitoring water level at the bench marks until the skiff party had established new ones. The possible datum error for our hydrographic survey is probably less than 10 cm.

Figure 2 shows the changes that occurred in the shoreface profile from the beach 3.2 km seaward to the 6-m isobath over the 34-yr

interval. At the very shoreline is a possible uncertainty of 25 m, as the coast continued to retreat an unknown amount since mapped in 1981, and the acoustic ranging system failed shortly before the beach was reached. The comparison shows a profile that deepened substantially during the time period, and maintenance of a bar system that advanced shoreward at a rate comparable to that of the coastal retreat. At 6 m depth the two profiles merge, but from 2 m seaward, our forcing of navigational closure may have displaced the recent profile seaward. The deepening indicated between 2 and 6 m water depths, therefore, is very conservative.

To calculate that portion of the deepening that may have resulted from thaw settlement, we used published data from a geologically similar part of the coastal plain west of the study area (Sellmann and others, 1975) to remove excess ice content (interstitial ice exceeding 37.5 percent of the frozen sediment volume) from the 1951 profile. By doing this, we found, that from the 1951 shoreline to the 1-m water depth (3-4 m below the tundra surface), only 14 percent of the indicated deepening can be attributed to thaw settlement. At more than 1.5 m water depth, none of the profile deepening can be due to thaw settlement. From the upper 3 m of the section eroded since 1951 we subtracted an additional 20 percent to account for the maximum volume of ice that may occur in the form of ice wedges (Sellmann and others, 1975). Figure 2 shows that

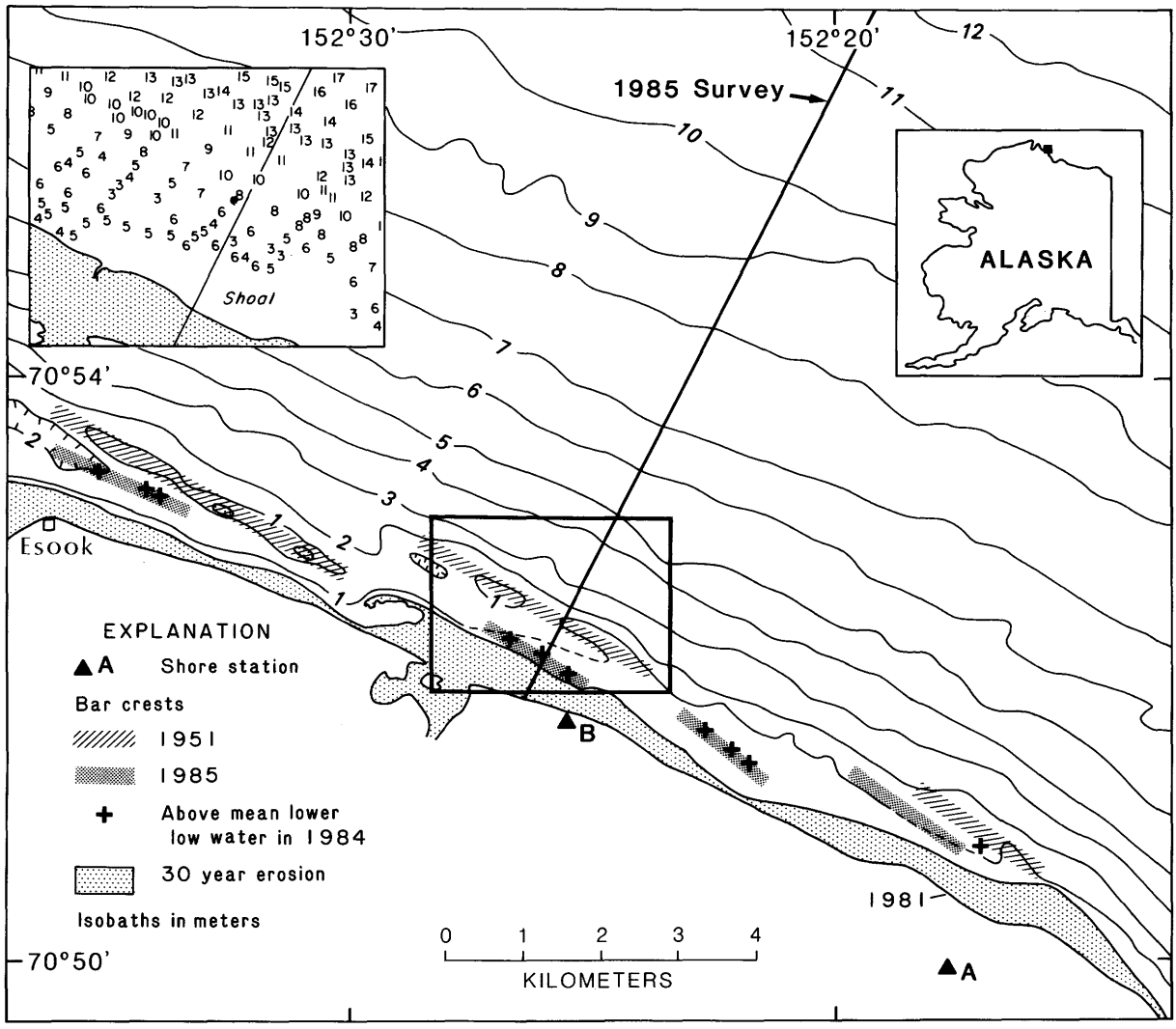

Figure 1.--Water depths of study area, contoured from Hydrographic Survey number 7991 of 1951, and coastlines as mapped in 1951 and 1981. Inset shows typical density of data points defining former bars over inner part of our 1985 survey. Bars in 1985 are sketched from our field observations, and from surveys of emergent points by State of Alaska in 1984 (N. Johnson, written commun., 1986).

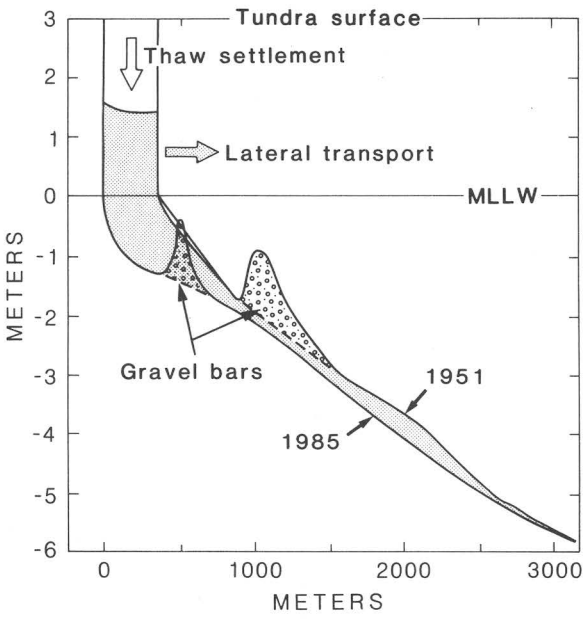

Figure 2.--Shoreface evolution from 1951 to 1985 along transect shown in figure 1. Portion of profile change that can be attributed to thaw settlement is indicated (blank areas). In submerged portion of profile virtually no thaw settlement occurs, and most change is due to mechanical energy and sediment transport.

the maximum amount of thaw settlement possible according to the wealth of published data can account for only a small portion of the section that is eroded below sea level. We therefore conclude that the shoreface is an important sediment source rather than a sediment sink, a finding that is supported by shallow seismic profiles, borings, mapping of outcrops, and other kinds of evidence (Reimnitz and others, 1985).

During the course of our fieldwork we also discovered a series of elongated gravel bars that reach sealevel and higher (fig. 3) in numerous locations at distances of 250 to 1,000 m from coastal bluffs. At four locations (A, B, Esook, and the site of the tidal bench marks west of figure 1) we managed to cross a bar and find relatively deep water in a trough that provides safe anchorage protected against storms and ice. The islets along the crests, important for defining coastal boundaries, were surveyed by the State of Alaska in 1984 and 1985, and served as aids to locate the bars in figure 2. A study of the 1951 soundings reveals the existence of a similar system of troughs and bars, locally emergent, at a slight angle to the coast. The bars consist of sand and gravel, materials absent in local bluffs, and probably migrate obliquely shoreward. The islet north of A, consisting of "sticky clay, apparently bulldozed by pack ice" (N. Johnson, oral commun., 1986), was very different from the elongated, wave-washed gravel bars (fig. 3), and had disappeared by the following year. This observation suggests that ice gouging of strata exposed on the shoreface, and subsequent winnowing by waves and currents, may provide coarse material for bar construction where such materials are absent in coastal bluffs. In any case, such a migrating mini-lagoon system, which here spans a distance of at least 40 km of shoreline, has not been described previously, and apparently is an important component of the shoreface.

The deepening of the shoreface by over 1 m, of which only a small portion can be attributed to melting of excess ice, and the migrating bar system, demonstrate that mechanical energy is far more important than thermal energy for the landward shift of the arctic shoreface. The deepening extends seaward to at least the 6-m isobath. If erosion terminated at the 6-m isobath, a bench roughly 10 km wide would have formed there during the last 1,000 yr. A study of shelf bathymetry nowhere reveals a flat bench which can be interpreted as the seaward limit of modern erosion, and that question therefore remains unanswered.

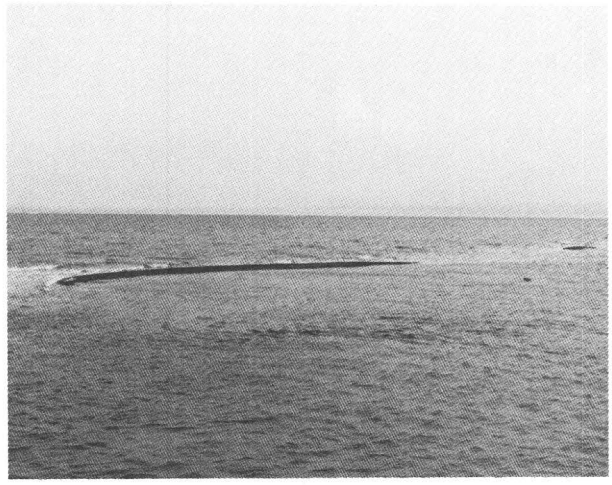

FIGURE 3.--View north to 12-m-long gravel islet due north of shore station B in 1985.

REFERENCES CITED

Are, F.E., 1980, Thermal abrasion of sea shores (in Russian): Moscow, Nauka, 157 p.

Forbes, D.L., and Frobel, D., 1985, Coastal erosion and sedimentation in the Canadian Beaufort Sea, in Current Research, Part B: Geological Survey of Canada Paper 85-1B, p. 69-80

Harper, J.R., 1978, The physical processes affecting the stability of tundra cliff coasts: Baton Rouge, Louisiana State Univesity, Ph.D. dissertation, 212 p.

National Research Council, Marine Board, 1982, Understanding the Arctic sea floor for engineering purposes: Washington, D.C., National Academy Press, Committee on Arctic Seafloor Engineering, 141 p.

Reimnitz, Erk, Graves, S.M., and Barnes, P.W., 1985, Beaufort Sea coastal erosion, shoreline evolution and sediment flux: U.S. Geological Survey Open-File Report 85-380, 74 p.

Sellmann, P.V., Brown, Jerry, Lewellen, R.I., McKim, H., and Merry, C., 1975, The classification and geomorphic implications of thaw lakes on the arctic coastal plain, Alaska: Hanover, N.H., U.S. Army Cold Region Research and Engineering Laboratory, Research Report 344, 21 p.

Tomirdiaro, S.V., 1975, Thermo abrasion-induced shelf formation in the eastern arctic seas of the USSR during the Holocene: Earth Science Sections, v. 219, no. 1-6, p. 23-26.

Zenkovich, V.P., 1985, Arctic USSR, in Bird, E.C.F. and Schwartz, M.L., eds., The world's coastline: New York, Van Nostrand Reinhold, p. 863-871.

Reviewers: J.R. Dingler and H.A. Karl

PETROLOGY, AGE, AND ORIGINAL TECTONIC SETTING OF BASALT FROM THE ST. GEORGE BASIN COST NO. 1 WELL, SOUTHERN BERING SEA

Tracy L. Vallier and Bruce M. Herman

The St. George COST No. 1 well is about 25 km south of the St. George graben on the outer continental shelf of the southern Bering Sea (fig. 1). St. George graben extends from near the Pribilof Islands southeast 300 km towards the Alaska Peninsula. Sediment thickness in places exceeds 12 km (Comer and others, in press). The graben probably opened in response to strike-slip motion related to oblique subduction of the Kula Plate beneath the Beringian margin in the early Tertiary (Marlow and Cooper, 1980). The major phase of opening occurred in the early Paleogene to late Paleogene (late Oligocene) interval when extensive vertical and strike-slip movement occurred along a fault that now forms the graben's north boundary (Comer and others, in press). Subsequent vertical displacement along the fault has offset the seafloor. Other young faults within the St. George graben also offset the seafloor (Gardner and Vallier, 1981). Outside the St. George graben, near the COST No. 1 well, faults younger than probable middle Eocene are rare (Comer and others, in press).

The COST No. 1 well penetrated more than 3 km of Cenozoic sediments and sedimentary rocks that unconformably overlie a volcanic rock sequence (Turner and others, 1984). The sedimentary section ranges in age from middle Eocene through Pleistocene (fig. 2) and consists mostly of well-stratified sandstone and siltstone beds that were deposited in an inner neritic to middle bathyal environment (Bolm, 1984a; Larson, 1984a). A middle Eocene or older basalt and tuff sequence was encountered below the unconformity at a depth below sea level of 3,164 m (10,380 ft) and subsequently was drilled to a total depth of 4,198 m (13,771 ft). Regional magnetic studies indicate that this igneous sequence is less than 30 km across (Comer and others, in press).

Highly vesicular basalt was sampled for chemical analyses from depths of 3,326.1 m (10,912.5 ft; sample SG-2), 3,327.4 m (10,916.8 ft; sample SG-3), 3,328.8 m (10,921.2 ft; sample SG-4), and 4,195.3 m (13,764 ft; sample SG-6). We were interested in the petrology, age, and original tectonic setting of these rocks, which provide clues for interpreting the evolution of the Beringian margin.

The highly vesicular nature of the basalt and the large diameter (>1 cm) of some vesicles suggest that the flows were erupted either subaerially or in shallow water. Textures are

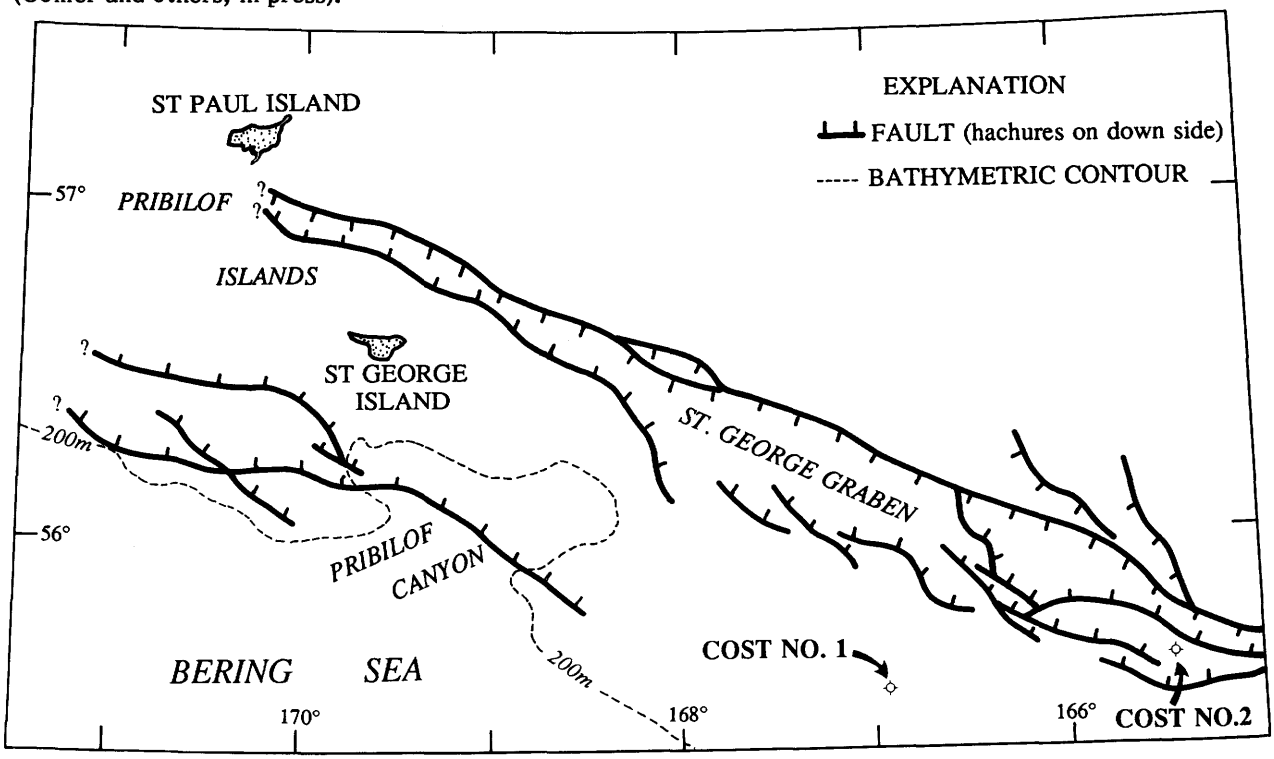

Figure 1.--Index map of St. George Basin area showing locations of major faults, Pribilof Islands, and two COST wells.

porphyritic, hyalopilitic, pilotaxitic, and intersertal. All are altered by weathering and low-grade metamorphism. Glass in the groundmasses has been replaced by chlorite, calcite, smectite, and zeolites. Plagioclase crystals in some samples are partly replaced by zeolites and calcite. Mafic minerals are replaced predominantly by chlorite and zeolites. High H_2O and CO_2 contents (table 1) support the petrographic evidence for extreme alteration. The alteration probably has affected some of the major-element contents, except possibly titanium and total iron. Therefore, the major-element data alone are not adequate for interpreting either the tectonic setting of eruption or the original magma characteristics of the rocks.

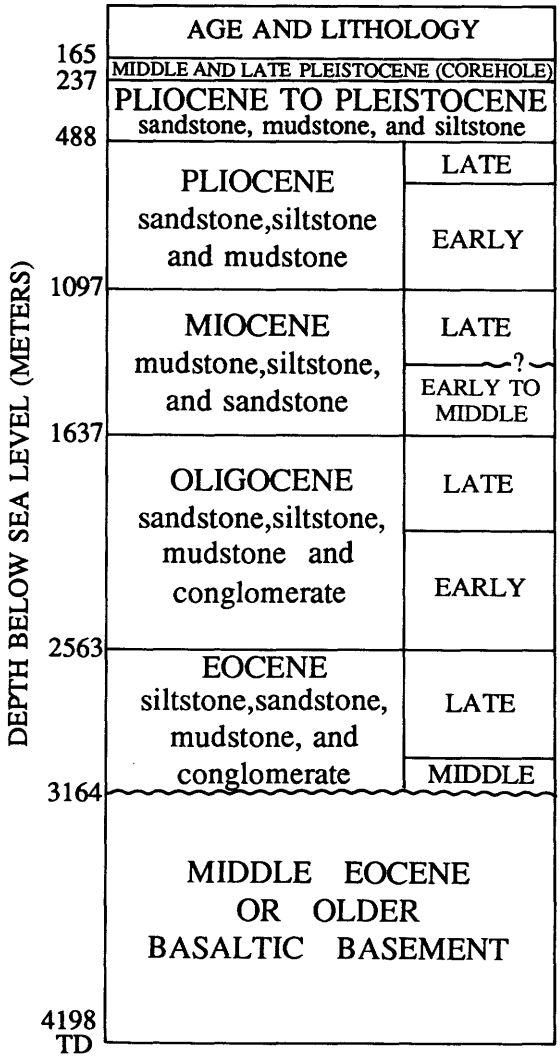

Figure 2.--Stratigraphic summary of St. George COST No. 1 well (modified from Larson, 1984a). Middle and late Pleistocene sediments are sand and silt. Order of lithology gives relative abundance with first lithology dominant.

The TiO_2 contents (table 1), too high for volcanic arc basalt (Gill, 1981), are comparable to ocean island, continental plateau, and rift basalts. Even after considering the possible mobility of major elements, the high alkali (Na_2O + K_2O) content of sample 6 suggests that it is an alkalic basalt. The consistently low K_2O contents in samples 2, 3, and 4 suggest that they are tholeiitic. Furthermore, K contents of 19 other rocks from the well are low (Bolm, 1984a, tables 2 and 3; range, 0.027 to 1.5 percent; average, 0.38 percent), which also suggests that they are tholeiitic.

We can assume that, in addition to Ti, many of the trace elements (table 2) were essentially immobile during rock alteration, particularly the high field strength elements (HFSE) such as Nb, Zr, and Ta (Pearce and Cann, 1973); others that may have been essentially immobile are the heavy rare earth elements (HREE) Lu and Yb, plus the elements Y, Th, U, and Hf. The elements Sr, Ba, Rb, Cs and some of the light rare earth elements (LREE), such as La, Ce, and Nd, may have been mobilized by small amounts during alteration. Normalized plots of rare earth elements (figure 3) show LREE enrichments in all four samples with La_N/Yb_N ratios of 2.1 to 2.6. Sample 6 is more enriched in all rare earth elements than the other samples: La is about 60 and Lu about 20 times chondrite values. The other samples (2, 3, and 4) have similar REE contents and their plots are essentially parallel, with La about 30 and Lu about

Table 1.--Major and minor element oxides (wt pct) of COST well No. 1 samples, St. George Basin region, Bering Sea
[Analyses by X-ray fluorescence (J. Ardith, J. Bartel, J. Stewart, and J. Taggart, USGS, analysts). Volatiles and FeO determined by gravimetric and wet chemical techniques (S. MacPherson, analyst). Major and minor element oxides are recalculated to 100 percent after subtracting volatiles]

Oxide	SG-2	SG-3	SG-4	SG-6
SiO_2	46.04	52.04	45.45	48.25
TiO_2	2.72	2.54	3.11	3.77
Al_2O_3	16.33	16.64	17.08	15.00
Fe_2O_3	8.64	9.80	6.20	4.81
FeO	5.84	2.99	7.09	9.56
MgO	11.62	7.26	9.30	4.16
MnO	.19	.10	.45	.39
CaO	4.45	4.48	7.81	7.91
Na_2O	3.15	3.36	2.71	3.35
K_2O	.69	.47	.45	2.00
P_2O_5	.33	.32	.35	.80
H_2O^+	5.12	3.26	3.92	3.02
H_2O^-	3.39	2.48	2.63	.75
CO_2	.26	.23	.18	.92

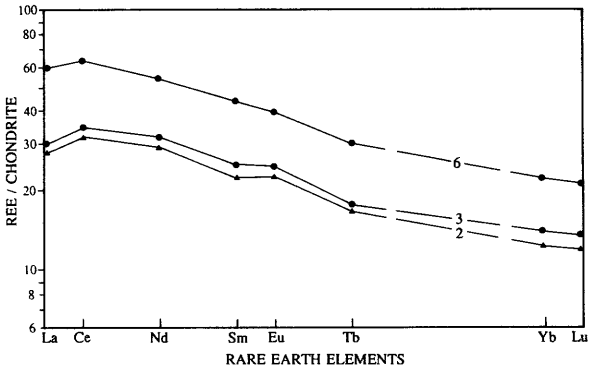

Figure 3. --Rare earth elements (REE) normalized to chondrite values of Masuda and others (1973). Sample SG-4 values plot very close to those of sample SG-2 and are not shown on the diagram.

10-12 times chondrite values. Based in part on the higher Na_2O and K_2O contents and enriched LREE patterns, and particularly on the high Y, Zr, Ti, Nb, and Hf contents, it is apparent that sample SG-6 is alkalic. Trace-element data for the other samples indicate that they most likely are tholeiitic, but the LREE enrichments suggest that they possibly are transitional between tholeiitic and alkalic.

Table 2.--Trace elements (ppm) in basaltic rocks from the COST well No. 1, St. George Basin region, Bering Sea
[Methods are X-ray fluorescence (T. Frost, analyst) and neutron activation analysis (F. Frey, analyst). ---, means not determined]

Element	SG-2	SG-3	SG-4	SG-6
Rb	4.8	---	1.7	---
Cs	---	---	---	0.8
Sr[1]	175	275	265	275
Ba[1]	65	65	60	460
Sc	35	36	41	36
Cr	85	82	79	4
Co	43	46	47	30
Ga	22	---	21	---
Y[1]	29	28	26	58
Zr[1]	140	160	175	335
Nb[1]	12	12	10	19
Hf	3.7	3.9	4.3	8.0
Ta	.59	.58	.72	1.1
Th	.5	.5	.4	1.6
La	11.5	11.6	10.4	22.5
Ce	32.2	34.8	29.7	63.6
Nd	20.0	23.0	19.2	39.3
Sm	5.2	5.92	5.27	10.4
Eu	2.04	2.31	1.99	3.62
Tb	1.01	1.03	.99	1.83
Ho	1.4	1.2	1.3	2.2
Yb	3.17	3.61	3.15	5.81
Lu	.49	.54	.47	.87

[1] X-ray fluorescence techniques

Fourteen rocks, 12 from the volcanic sequence and 2 clasts in the overlying conglomerate beds, were radiometrically dated by conventional K-Ar methods (table 3). Duplicate samples were dated for four of the rocks to provide a measure of analytic precision. Ages range from about 23 to 136 m.y., but the two oldest reported ages are from rocks with very low K_2O contents, and therefore can be discounted. The ages of 10 samples cluster between 23 and 38 m.y. and are thereby younger than the overlying sedimentary rocks. Furthermore, two basalt clasts from middle Eocene conglomerate beds (the uppermost two samples in table 3) show extreme variability in ages, and the 27 ± 4 m.y. age is definitely too young. Although we did not examine thin sections of the samples listed in table 3, we believe that most of the K-Ar ages are unreliable because of extensive alteration. If all of the radiometrically dated basalts are flows (based on their highly vesicular character and their association with tuffs), then they must be middle Eocene or older (older than about 40 million years). However, if some of the dated samples are sills and are not as altered as the samples we examined, then many of the young ages could be reliable. This would mean that Oligocene igneous intrusive activity took place within the basement volcanic sequence. Such a thermal event could account for the low-grade metamorphism.

Unreliable K-Ar ages and an absence of fossils in the volcanic rock sequence below the regional unconformity make it necessary to estimate age by a different technique. Comer and others (in press) used seismic-reflection profiles to determine interval velocities in acoustically stratified rocks beneath the unconformity 10 to 20 km north of the COST well. Because these rocks are from an area beyond the magnetic anomaly associated with the volcanics at the well, they are believed to be sedimentary. Based on the structural and stratigraphic relationships between these strata and the volcanic strata at the COST No. 1 well, Comer and others (in press) concluded that the volcanic rocks are also of Tertiary age.

Analysis of seismic velocities and magnetic field data elsewhere in the region, however, show that in many places the rocks beneath the unconformity have relatively high interval velocities and low magnetic signatures, thereby suggesting the presence of upper Mesozoic sedimentary rocks (Comer and others, in press). At the COST No. 2 well (fig. 1), Oligocene or older (possible Eocene) strata unconformably overlie Lower Cretaceous and Upper Jurassic sandstone and siltstone (Bolm, 1984b; Larson, 1984b). These data and the occurrence of Upper Jurassic sedimentary rocks dredged from the Pribilof Ridge, which are thought to be the volcanic-lithic equivalent of the Naknek Formation (Vallier and others, 1980; Marlow and Cooper, 1983; Comer and others, in press), suggest that rocks beneath the

regional unconformity probably have different ages and are more complex than previously has been recognized.

We used the Ti/100-Yx3-Zr discrimination diagram (fig. 4) of Pearce and Cann (1973) to interpret the original tectonic setting of the basalt. The diagram indicates that the basalts were erupted in a within-plate setting (field D on fig. 4), but the diagram does not discriminate between oceanic island (and seamount) and continental plateau or rift basalts. The chemical data including HFSE contents and high TiO_2 values, plus the plotted points on the Ti/100-Yx3-Zr diagram (fig. 4), clearly show that the rocks are not related to convergent margin (volcanic arc) or to mid-ocean ridge volcanism (fields A, B, and C). All but sample 6 are overlapped by the Pribilof basalt field.

Basalt sampled at the COST No. 1 well had a different magma source than the Pliocene and Pleistocene alkalic basalts from the Pribilof region, but probably erupted in a similar rift setting. Samples 2, 3, and 4 from the COST well have lower Sr, Ba, Cr, Th, and light REE, and higher Zr, Y, and HREE contents than most of the Pribilof samples (Lee-Wong and others, 1979; T.L. Vallier, unpub. data). Sample 6, an alkalic basalt, has TiO_2, Nb, La, and Th contents comparable to the Pribilof basalts, but has high Ba, Y, Zr, and HREE concentrations. When plotted on the Ti/100-Yx3-Zr discrimination diagram (fig. 4), the Pribilof basalt samples generally have higher Ti values and thereby plot closer to the Ti apex than the COST well samples.

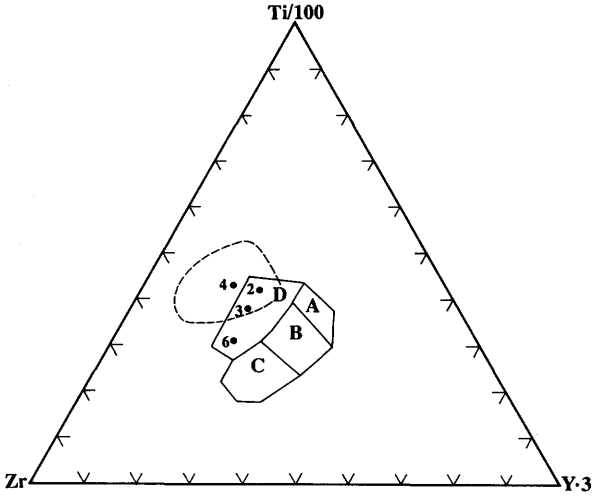

Figure 4.--Ti/100-Yx3-Zr discrimination diagram of Pearce and Cann (1973). Fields shown are: B, ocean floor basalt; A and B, low-potassium tholeiite; C and B, calc-alkalic basalt; and D, within-plate basalt. Basalt from mid-ocean ridge generally plots within fields A and B. Basalt from volcanic arcs plots in fields A, B, or C. Field D basalt may have erupted either on oceanic seamounts, oceanic islands, or within continental framework. Numbered samples are from COST No. 1 well. Dashed field is basalt from the Pribilof Islands (N=36; Lee-Wong and others, 1979; T.L. Vallier, unpub. data).

The COST well basalts most likely are rift-related and were erupted along the continental margin during transtension related to the transform or strike-slip tectonic regime that occurred in the early Tertiary. In the COST No. 1 well area, eruption of basalt along the early Tertiary rifted Beringian continental margin built a large volcanic edifice which was subsequently eroded and then was buried by middle Eocene sediments as the margin subsided.

Table 3.--K-Ar radiometric ages of basalt samples from St. George Basin COST No. 1 well (Bolm, 1984a, p. 60)

[The two shallowest samples are clasts from a conglomerate at the base of the sedimentary section; all others are from the volcanic basement. Analyses by Teledyne Isotopes (T) and Mobil Research and Development Corporation (M). Duplicate samples indicate precision]

Depth below sea level		K	Age	
m	ft	(wt pct)	($\times 10^6$ yr)	Laboratory
3149.5	10,333	0.027	120 ± 16	T
3162.3	10,375	1.50	27 ± 4	T
3324.5	10,907.2	.297	25.7 ± 1.3	M
3324.5	10.907.2	.297	22.9 ± 1.2	M
3330	10,925.3	.410	35.5 ± 1.7	M
3330	10,925.3	.410	35.1 ± 1.7	M
3331.5	10,930.2	.386	31.7 ± 1.5	M
3331.5	10,930.2	.386	32.4 ± 1.6	M
3332.7	10,934	.35	38 ± 6	T
3335.3	10,942.6	.372	29.2 ± 1.5	M
3335.3	10,942.6	.372	31.1 ± 1.5	M
3986.8	13,080	.589	33.7	T
3991.7	13,096	1.08	28.2	T
3995.9	13,110	.298	27.3	T
3999.9	13,123	.086	63.3	T
4194.1	13,760	.878	30.2 ± 1.5	T
4196.5	13,768	.094	136.4 ± 6.9	T
4196.9	13,769.5	.226	52.2 ± 2.6	T

REFERENCES CITED

Bolm, J.G., 1984a, Lithology and well log interpretation, in Turner, R.F., ed., Geological and operational summary, St. George Basin COST No. 1 well, Bering Sea, Alaska: U.S. Minerals Management Service OCS Report MMS 84-0016, p. 41-78.

____ 1984b, Lithology and well log interpretation, in Turner, R.F., ed., Geological and operational summary, St. George Basin COST No. 2 well, Bering Sea, Alaska: U.S. Minerals Management Service OCS Report MMS 84-0018, p. 42-72.

Comer, C.D., Herman, B.M., and Zerwick, S.A., in press, Geologic report for the St. George Planning Area, Bering Sea, Alaska: U.S. Minerals Management Service OCS Report.

Gardner, J.V., and Vallier, T.L., 1981, Faulting in the outer continental shelf of southern Bering Sea: American Association of Petroleum Geologists Bulletin, v. 65, p. 1568-1573.

Gill, J.B., 1981, Orogenic andesites and plate tectonics: New York, Springer-Verlag, 390 p.

Larson, J.A., 1984a, Paleontology and biostratigraphy, in Turner, R.F., ed., Geological and operational summary, St. George Basin COST No. 1 well, Bering Sea, Alaska: U.S. Minerals Management Service OCS Report MMS 84-0016, p. 24-40.

_____ 1984b, Paleontology and biostratigraphy, in Turner, R.F., ed., Geological and operational summary, St. George Basin COST No. 2 well, Bering Sea, Alaska: U.S. Minerals Management Service OCS report MMS 84-0018, p. 28-37.

Lee-Wong, F., Vallier, T.L., Hopkins, D.M., and Silberman, M.L., 1979, Preliminary report on the petrography and geochemistry of basalt from the Pribilof Islands and vicinity, southern Bering Sea: U.S. Geological Survey Open-File Report 79-1556, 51 p.

Marlow, M.S., and Cooper, A.K., 1980, Mesozoic and Cenozoic structural trends under the southern Bering Sea shelf: American Association of Petroleum Geologists Bulletin, v. 64, p. 2139-2155.

_____ 1983, Wandering terranes in southern Alaska: The Aleutia microplate and implications for the Bering Sea: Journal of Geophysical Research, v. 88, p. 3439-3446.

Masuda, A., Nakamura, N., and Tanaki, T., 1973, Fine structures of mutually normalized rare-earth patterns of chondrites: Geochimica et Cosmochimica Acta, v. 37, p. 239-248.

Pearce, J.A., and Cann, J.R., 1973, Tectonic setting of basic volcanic rocks determined using trace element analyses: Earth and Planetary Science Letters, v. 19, p. 290-300.

Turner, R.F., McCarthy, C.M., Comer, C.D., Larson, J.A., Bolm, J.G., Banet, A.C., and Adams, A.J., 1984, Geological and operational summary, St. George Basin COST No. 1 well, Bering Sea, Alaska: U.S. Minerals Management Service OCS Report MMS 84-0016, 105 p.

Vallier, T.L., Underwood, M.B., Jones, D.L., and Gardner, J.V., 1980, Petrography and geologic significance of Upper Jurassic rocks dredged near the Pribilof Islands, southern Bering Sea continental shelf: American Association of Petroleum Geologists Bulletin, v. 64, p. 945-950.

Reviewers: A.K. Cooper and M.S. Marlow

GLORIA IMAGES OBTAINED IN THE TACT CORRIDOR OF THE ALEUTIAN CONVERGENT MARGIN, NORTHERN GULF OF ALASKA (ABSTRACT)

Terry R. Bruns, Michael A. Fisher, Paul R. Carlson, Douglas M. Rearic, and Lindsay M. Parson

The Geological Long-Range Inclined Asdic (GLORIA) side-scanning sonar system was used during June 1986 in the northern Gulf of Alaska to acquire images of the seafloor over the continental slope and rise in the vicinity of Middleton Island, at the southern end of the Trans-Alaska Crustal Transect (TACT) corridor. The GLORIA images provide data on details of structural development and continuity, slope morphology, and depositional processes along an active margin which are not resolvable from available coarse bathymetric data or widely spaced seismic-reflection data. The tectonic setting changes markedly within this region. East of Middleton Island, the continental margin includes the allochthonous Yakutat terrane which is presently colliding with southern Alaska. Southwest of Middleton Island, the continental margin is part of the Aleutian convergent margin and is characterized by compressional deformation associated with subduction along the Aleutian Trench. The two tectonic regimes have very different surface morphologies.

East of Middleton Island, the continental slope is characterized by well-developed dendritic drainage patterns that are located between major glacially-carved shelf sea valleys, and by large sediment masses which have accumulated on the upper slope below the sea valleys. These late Quaternary(?) sediments bury older dendritic drainages. Compressional structures of Pamplona Spur, Khitrov Ridge, and associated structures caused by the ongoing Yakutat terrane collision are clearly visible on the GLORIA images. These structures in part form lower-slope barriers to downslope sediment transport.

Southwest of Middleton Island, dendritic drainages are absent. The slope is characterized by a succession of partly buried, slope-parallel, anticlinal ridges with relief of up to 1,000 m. These ridges are structurally continuous along the 100-km-long slope covered by the GLORIA images, but are broken into morphologically discontinuous segments about 20 to 25 km long. Sediment pathways from the shelf break to the Aleutian trench are clearly discernible on the slope and pass between these ridge segments. The slope sediment largely originates at the mouths of the shelf sea valleys, and is subsequently either deposited around the anticlinal ridges of the slope or funneled circuitously downslope between the discontinuous ridge segments into the trench. In plan view, the initial deformation front at the base of the slope is scalloped, a form also evident at other convergent margins. Multichannel seismic data across the Aleutian convergent margin in this region do not resolve whether some of the slope structures are compressional anticlines or diapiric structures. The extensive continuity of these structures expressed on the GLORIA data indicates that the structures are most likely caused by folding associated with the ongoing Pacific plate subduction, rather than by diapirism.

Reviewers: H.A. Karl and D.S. McCulloch

BIBLIOGRAPHIES

Alaska Range

Reports about Alaska in USGS publications released in 1986

compiled by Ellen R. White

Some reports dated 1985 did not become available until 1986; they are included in this listing

Affolter, R.H., and Stricker, G.D., 1986, Geochemistry of some Tertiary alluvial lowland coals from the Capps and Chuitna coal fields, Cook Inlet region, Alaska, in Garbini, Susan and Schweinfurth, S.P., eds., Symposium proceedings; a national agenda for coal-quality research: U.S. Geological Survey Circular 979, p. 215.

Alger, C.S., and Brabb, E.E., 1985, Bibliography of United States landslide maps and reports: U.S. Geological Survey Open-File Report 85-585, 119 p.

Anders, D.E., and Magoon, L.B., 1986, Geochemical study of surface oil shows and potential source rocks in the Arctic National Wildlife Refuge (North Slope Alaska) (abs.), in Carter, L.M.H., ed., 1986, USGS research on energy resources 1986, program and abstracts: U.S. Geological Survey Circular 974, p. 1-2.

Angeloni, L.M., Wilson, F.H., and Sutley, Stephen, 1986, Map and tables showing preliminary rock geochemical data, Port Moller, Stepovak Bay, and Simeonof Island quadrangles, Alaska: U.S. Geological Survey Open-File Report 85-470, 180 p., scale 1:250,000, 1 sheet.

Bader, J.W., and Bird, K.J., 1986, Geologic map of the Demarcation Point, Mt. Michelson, Flaxman Island, and Barter Island quadrangles, northeastern Alaska: U.S. Geological Survey Miscellaneous Investigations Series Map I-1791, scale 1:250,000, 1 sheet.

Barnes, D.F., 1986, Gravity data indicate large mass and depth of the gabbro body at Haines, in Bartsch-Winkler, Susan, and Reed, K.M., eds., Geologic studies in Alaska by the U.S. Geological Survey during 1985: U.S. Geological Survey Circular 978, p. 88-92.

Barnes, P.W., 1986, Sedimentology and stratigraphy in the Beaufort Sea, in Miley, J.M., and Barnes, P.W., eds., 1985 field studies, Beaufort and Chukchi Seas, conducted from the NOAA ship DISCOVERER: U.S. Geological Survey Open-File Report 86-202, p. 29-30.

Barnes, P.W., Miley, J.M., and Phillips, R.L., 1986, Introduction, methods, and equipment, in Miley, J.M., and Barnes, P.W., eds., 1985 field studies, Beaufort and Chukchi Seas, conducted from the NOAA ship DISCOVERER: U.S. Geological Survey Open-File Report 86-202, p. 2-28.

Bartsch-Winkler, Susan, 1986, Channel migration in Turnagain Arm, in Bartsch-Winkler, Susan, and Reed, K.M., eds., Geologic studies in Alaska by the U.S. Geological Survey during 1985: U.S. Geological Survey Circular 978, p. 29-33.

Bartsch-Winkler, Susan and Reed, K.M., eds., 1986, Geologic studies in Alaska by the U.S. Geological Survey during 1985: U.S. Geological Survey Circular 978, 173 p.

Bartsch-Winkler, Susan, and Reed, K.M., 1986, Geologic studies in Alaska by the U.S. Geological Survey during 1985; abstract, introduction, in Bartsch-Winkler, Susan, and Reed, K.M., eds., Geologic studies in Alaska by the U.S. Geological Survey during 1985: U.S. Geological Survey Circular 978, p. 1-2.

Bird, K.J., Magoon, L.B., and Molenaar, C.M., 1986, Advance in understanding North Slope oil and gas accumulations (abs.), in Carter, L.M.H., ed., 1986, USGS research on energy resources - 1986, program and abstracts: U.S. Geological Survey Circular 974, p. 6.

Blodgett, R.B., Clough, J.G., Dutro, J.T., Jr., Ormiston, A.R., Palmer, A.R., and Taylor, M.E., 1986, Age revisions for the Nanook Limestone and Katakturuk Dolomite, northeastern Brooks Range, in Bartsch-Winkler, Susan, and Reed, K.M., eds., Geologic studies in Alaska by the U.S. Geological Survey during 1985: U.S. Geological Survey Circular 978, p. 5-10.

Blome, C.D., and Reed, K.M., 1986, Triassic and early Jurassic radiolarian faunas, Brooks Range, Alaska: U.S. Geological Survey Open-File Report 86-120, 27 p.

Blueford, J.R., 1986, New radiolarian data from the Orca Group, Prince William Sound, in Bartsch-Winkler, Susan, and Reed, K.M., eds., Geologic studies in Alaska by the U.S. Geological Survey during 1985: U.S. Geological Survey Circular 978, p. 33-34.

Bolm, J.G., and McCulloh, T.H., 1986, Sandstone diagenesis, in Magoon, L.B., ed., Geologic studies of the lower Cook Inlet COST No. 1 well, Alaska Outer Continental Shelf: U.S. Geological Survey Bulletin 1596, p. 51-53.

Bouma, A.H., and Hampton, M.A., 1986, Environmental geology, in Magoon, L.B., ed., Geologic studies of the lower Cook Inlet COST No. 1 well, Alaska Outer Continental Shelf: U.S. Geological Survey Bulletin 1596, p. 11-15.

Brown, C.S., Rosenblum, L.A., and Meier, M.F., 1986, Bed topography inferred from airborne radio-echo sounding of Columbia Glacier, Alaska: U.S. Geological Survey Professional Paper 1258-G, 26 p.

Brunett, J.O., 1986, Ground-water levels in Alaska, water year 1983: U.S. Geological Survey Open-File Report 86-56, 225 p.

Buck, R.A., 1986, Federal response planning in Alaska, in Hays, W.W., and Gori, P.L., eds., Proceedings of Conference XXXI, a workshop

on "evaluation of regional and urban earthquake hazards and risk in Alaska": U.S. Geological Survey Open-File Report 86-79, p. 215-219.

Buck, R.A., 1986, Social effects and disaster response, in Hays, W.W., and Gori, P.L., eds., Proceedings of Conference XXXI, a workshop on "evaluation of regional and urban earthquake hazards and risk in Alaska": U.S. Geological Survey Open-File Report 86-79, p. 249-255.

Cady, J.W., 1986, Geophysics of the Yukon-Koyukuk province, in Bartsch-Winkler, Susan, and Reed, K.M., eds., Geologic studies in Alaska by the U.S. Geological Survey during 1985: U.S. Geological Survey Circular 978, p. 21-25.

Campbell, D.L., and Nokleberg, W.J., 1986, Magnetic model of a profile across northern Copper River basin, northeastern Gulkana quadrangle, in Bartsch-Winkler, Susan, and Reed, K.M., eds., Geologic studies in Alaska by the U.S. Geological Survey during 1985: U.S. Geological Survey Circular 978, p. 35-38.

Carté, G.W., 1986, Improving tsunami preparedness in Alaska, in Hays, W.W., and Gori, P.L., eds., Proceedings of Conference XXXI, a workshop on "evaluation of regional and urban earthquake hazards and risk in Alaska": U.S. Geological Survey Open-File Report 86-79, p. 193-199.

Carter, L.D., and Galloway, J.P., 1986, Engineering geologic maps of northern Alaska, Umiat quadrangle: U.S. Geological Survey Open-File Report 86-335, 17 p., scale 1:250,000, 2 pls.

Carter, L.D., Ferrians, O.J., Jr., and Galloway, J.P., 1986, Engineering-geologic maps of northern Alaska coastal plain and foothills of the Arctic National Wildlife Refuge: U.S. Geological Survey Open-File Report 86-334, 10 p., scale 1:250,000, 2 pls.

Carter, L.M.H., ed., 1986, USGS research on energy resources - 1986, program and abstracts: U.S. Geological Survey Circular 974, 84 p.

Case, J.E., and Nelson, W.H., 1986, Maps showing aeromagnetic survey and geologic interpretation of the Lake Clark quadrangle, Alaska: U.S. Geological Survey Miscellaneous Field Studies Map MF 1114-E, 2 sheets.

Case, J.E., Burns, L.E.,and Winkler, G.R., 1986, Maps showing aeromagnetic survey and geologic interpretation of the Valdez quadrangle, Alaska: U.S. Geological Survey Miscellaneous Field Studies Map MF-1714, scale 1:250,000, 2 sheets.

Case, J.E., Fisher, M.A., Moore, G.W., Moore, J.C., and Nelson, S.W., 1986, Preliminary geologic interpretation of the aeromagnetic map of Afognak and Shuyak Islands, Alaska: U.S. Geological Survey Miscellaneous Field Studies Map MF-1718, scale 1:250,000, 1 sheet.

Childs, J.R., Magistrale, H.W., and Cooper, A.K., 1985, Free-air gravity anomaly map of the Bering Sea: U.S. Geological Survey Miscellaneous Field Studies Map MF 1728, scale 1:2,500,000, 1 sheet.

Church, S.E., Gray, J.E., and Delevaux, M.H., 1986, Use of Pb-isotopic signatures for geochemical exploration in the Healy quadrangle, eastern Alaska Range, in Bartsch-Winkler, Susan, and Reed, K.M., eds., Geologic studies in Alaska by the U.S. Geological Survey during 1985: U.S. Geological Survey Circular 978, p. 38-41.

Clark, S.D., 1986, Bathymetry in the western Beaufort Sea, in Miley, J.M., and Barnes, P.W., eds., 1985 field studies, Beaufort and Chukchi Seas, conducted from the NOAA ship DISCOVERER: U.S. Geological Survey Open-File Report 86-202, p. 47-48.

Claypool, G.E., 1986, Petroleum geochemistry, in Magoon, L.B., ed., Geologic studies of the lower Cook Inlet COST No. 1 well, Alaska Outer Continental Shelf: U.S. Geological Survey Bulletin 1596, p. 33-39.

Collett, T.S., Bird, K.J., Magoon, L.B., Kvenvolden, K.A., and Claypool, G.E., 1986, Gas hydrates, North Slope of Alaska (abs.), in Carter, L.M.H., ed., 1986, USGS research on energy resources - 1986, program and abstracts: U.S. Geological Survey Circular 974, p. 11-12.

Combellick, R.A., 1986, Geologic-hazards mitigation in Alaska: a review of federal, state, and local policies, in Hays, W.W., and Gori, P.L., eds., Proceedings of Conference XXXI, a workshop on "evaluation of regional and urban earthquake hazards and risk in Alaska": U.S. Geological Survey Open-File Report 86-79, p. 262-373.

Cooper, A.K., Marlow, M.S., and Mann, D.M., 1986, Multichannel seismic-reflection profiles collected in 1977 in the northern Bering Sea: U.S. Geological Survey Open-File Report 86-207, 4 p., scale 1:2,500,000, 1 pl.

Cooper, A.K., Marlow, M.S., and Scholl, D.W., 1986, Future hydrocarbon studies in the Bering Sea (abs.), in Carter, L.M.H., ed., 1986, USGS research on energy resources - 1986, program and abstracts: U.S. Geological Survey Circular 974, p. 12.

Cooper, A.K., Stevenson, Andrew, Kenyon, Neil, and Bishop, Derek, 1986, GLORIA study of the Exclusive Economic Zone off Alaska - southern Bering Sea: initial report for cruise F4-86-BS, 3 September 1986: U.S. Geological Survey Open-File Report 86-596, 19 p.

Csejtey, Bela, Jr., Mullen, M.W., Cox, D.P., Gilbert, W.G., Yeend, W.E., Smith T.E., Wahrhaftig, Clyde, Craddock, Campbell, Brewer, W.M., Sherwood, K.W., Hickman,

R.G., Stricker, G.D., St.Aubin, D.R., and Goerz, D.J., III, 1986, Geology and geochronology of the Healy quadrangle, Alaska: U.S. Geological Survey Open-File Report 86-396, 96 p., scale 1:250,000, 4 pls.

Czamanske, G.K., Bennett, P.C., Zientek, M.L., and others, 1986, Comprehensive bibliographies on mineralized and unmineralized layered mafic intrusions in the United States: U.S. Geological Survey Open-File Report 86-589-A, 97 p.

Davies, J.N., 1986, Seismicity, seismic gaps and earthquake potential in Alaska, in Hays, W.W., and Gori, P.L., eds., Proceedings of Conference XXXI, a workshop on "evaluation of regional and urban earthquake hazards and risk in Alaska": U.S. Geological Survey Open-File Report 86-79, p. 43-63.

Detterman, R.L., and Miller, J.W., 1986, A widespread catastrophic event in the Naknek Formation, Alaska Peninsula, in Bartsch-Winkler, Susan, and Reed, K.M., eds., Geologic studies in Alaska by the U.S. Geological Survey during 1985: U.S. Geological Survey Circular 978, p. 27-29.

Detterman, R.L., Miller, J.W., and Case, J.E., 1986, Megafossil locality map, checklists, and pre-Quaternary stratigraphic sections of Ugashik, Bristol Bay, and part of Karluk quadrangles, Alaska: U.S. Geological Survey Miscellaneous Field Studies Map MF 1539-B, scale 1:250,000.

Dillon, J.T., Brosgé, W.P., Jr., and Dutro, J.T., Jr., 1986, Generalized geologic map of the Wiseman quadrangle, Alaska: U.S. Geological Survey Open-File Report 86-219, scale 1:250,000, 1 sheet.

Duttweiler, K.A., 1986, Sulfide occurrences in the Itkillik River region, southeast Chandler Lake quadrangle, Brooks Range, in Bartsch-Winkler, Susan, and Reed, K.M., eds., Geologic studies in Alaska by the U.S. Geological Survey during 1985: U.S. Geological Survey Circular 978, p. 10-13.

Egbert, R.M., 1986, Petrography, provenance, and tectonic significance of Middle and Upper Jurassic sandstone from Tuxedni Bay, in Magoon, L.B., ed., Geologic studies of the lower Cook Inlet COST No. 1 well, Alaska Outer Continental Shelf: U.S. Geological Survey Bulletin 1596, p. 61-63.

Ehrlich, Edward, 1986, Geology of the calderas of Kamchatka and Kurile Islands with comparison to calderas of Japan and the Aleutians, Alaska: U.S. Geological Survey Open-File Report 86-291, 303 p.

Erickson, B.M., Severson, R.C., and Crock, J.G., 1986, Analytical results of plant and soil samples collected near Flat, Iditarod, and Livengood, Alaska, in 1984: U.S. Geological Survey Open-File Report 86-473, 24 p.

Espinosa, A.F., Brockman, S.R., and Michael, J.A., 1986, Modified Mercally intensity distribution for the most significant earthquakes in Alaska, 1899-1981: U.S. Geological Survey Open-File Report 86-203, 1 sheet.

Espinosa, A.F., Schmoll, H.R., Brockman, S.R., Yehle, L.A., Odum, J.K., Michael, J.A., and Rukstales, K.S., 1986, Seismic hazard studies, Anchorage, Alaska, in Hays, W.W., and Gori, P.L., eds., Proceedings of Conference XXXI, a workshop on "evaluation of regional and urban earthquake hazards and risk in Alaska": U.S. Geological Survey Open-File Report 86-79, p. 161-177.

Fisher, M.A., 1986, Correlation of the COST No. 1 well data and the marine seismic data, in Magoon, L.B., ed., Geologic studies of the lower Cook Inlet COST No. 1 well, Alaska Outer Continental Shelf: U.S. Geological Survey Bulletin 1596, p. 23-27.

Fisher, M.A., von Huene, Roland, and Hampton, M.A., 1986, (release date), Summary geologic report for petroleum lease sale #100, Kodiak shelf, Alaska: U.S. Geological Survey Open-File Report 84-24, 51 p., scale 1:500,000, 1 pl.

Fogleman, K.A., Stephens, C.D., Lahr, J.C., and Rogers, J.A.,1986, Catalog of earthquakes in southern Alaska for 1984: U.S. Geological Survey Open-File Report 86-99, 106 p.

Fuis, G.S., and Ambos, E.L., 1986, Deep structure of the contact fault and Prince William terrane - preliminary results of the 1985 TACT seismic-refraction survey, in Bartsch-Winkler, Susan, and Reed, K.M., eds., Geologic studies in Alaska by the U.S. Geological Survey during 1985: U.S. Geological Survey Circular 978, p. 41-45.

Fukuhara, C.R., 1986 (1987), Description of plutons in the western part of the Juneau and parts of the adjacent Skagway 1:250,000 quadrangles, southeastern Alaska: U.S. Geological Survey Open-File Report 86-393, 58 p., scale 1:250,000, 1 pl.

Galloway, J.P., 1986, Landslides in Alaska: A bibliography of the literature describing landslides and other forms of slope instability: U.S. Geological Survey Open-File Report 86-329, 57 p.

Glass, R.L., 1986, Hydrologic conditions in Connors Bog area, Anchorage, Alaska: U.S. Geological Survey Water-Resources Investigations 86-4044.

Glass, R.L., 1986, Hydrologic conditions in the Klatt Bog area, Anchorage, Alaska: U.S. Geological Survey Water-Resources Investigations Report WRI 85-4330.

Goldfarb, R.J., Light, T.D., and Leach, D.L., 1986, Nature of the ore fluids at the Alaska-Juneau gold deposit, in Bartsch-Winkler, Susan, and Reed, K.M., eds., Geologic studies in Alaska by the U.S. Geological Survey during 1985: U.S. Geological Survey Circular 978, p. 92-95.

Grantz, Arthur, Mann, D.M., and May, S.D., 1986, Multichannel seismic-reflection data collected in 1978 in the eastern Chukchi Sea: U.S. Geological Survey Open-File Report 86-206, 4 p., scale 1:1,000,000, 1 pl.

Grantz, Arthur, Mann, D.M., and May, S.D., 1986, Multichannel seismic-reflection data collected in 1980 in the eastern Chukchi Sea: U.S. Geological Survey Open-File Report 86-405, 4 p., scale 1:1,000,000, 1 pl.

Gray, J.E., Church, S.E., and Delevaux, M.H., 1986, Lead-isotope results from gold-bearing quartz veins from the Valdez and Orca Groups, Chugach National Forest, in Bartsch-Winkler, Susan, and Reed, K.M., eds., Geologic studies in Alaska by the U.S. Geological Survey during 1985: U.S. Geological Survey Circular 978, p. 45-50.

Harris, A.G., Tailleur, I.L., and Lane, H.R., 1986, Conodont thermal maturation patterns in Paleozoic and Triassic rocks, northern Alaska - geologic and exploration implications (abs.), in Carter, L.M.H., ed., 1986, USGS research on energy resources - 1986, program and abstracts: U.S. Geological Survey Circular 974, p. 21.

Hays, J.L., 1986, Earthquakes and public policy, in Hays, W.W., and Gori, P.L., eds., Proceedings of Conference XXXI, a workshop on "evaluation of regional and urban earthquake hazards and risk in Alaska": U.S. Geological Survey Open-File Report 86-79, p. 1-3.

Hays, W.W., and Gori, P.L., 1986, Background and summary of the workshop on "Evaluation of regional and urban earthquake hazards and risk in Alaska", in Hays, W.W., and Gori, P.L., eds., Proceedings of Conference XXXI, a workshop on "evaluation of regional and urban earthquake hazards and risk in Alaska": U.S. Geological Survey Open-File Report 86-79, p. 4-37.

Hays, W.W., and Gori, P.L., eds., 1986, Proceedings of Conference XXXI, A workshop on "Evaluation of regional and urban earthquake hazards and risk in Alaska", September 5-7, 1985, Anchorage, Alaska: U.S. Geological Survey Open-File Report 86-79, 388 p., Appendices.

Hill, P.L., 1986, Bibliographies and location maps of aeromagnetic and aeroradiometric publications for Alaska and Hawaii: U.S. Geological Survey Open-File Report 86-525-E, 26 p.

Himmelberg, G.R., Brew, D.A., and Ford, A.B., 1986, Chemical composition of olivine and orthopyroxene in peridotite of the Coast plutonic-metamorphic complex near Skagway, in Bartsch-Winkler, Susan, and Reed, K.M., eds., Geologic studies in Alaska by the U.S. Geological Survey during 1985: U.S. Geological Survey Circular 978, p. 95-98.

Himmelberg, G.R., Ford, A.B., and Brew, D.A., 1986, The occurrence and chemical composition of chloritoid in the metamorphic rocks of the Coast plutonic-metamorphic complex near Juneau, in Bartsch-Winkler, Susan, and Reed, K.M., eds., Geologic studies in Alaska by the U.S. Geological Survey during 1985: U.S. Geological Survey Circular 978, p. 99-102.

Hodel, K.L., 1986, The Sagavanirktok River, North Slope Alaska: Characterization of an arctic stream:U.S. Geological Survey Open-File Report 86-267, 29 p.

Hudson, Travis, 1986, Plutonism and provenance; implications for sandstone compositions, in Magoon, L.B., ed., Geologic studies of the lower Cook Inlet COST No. 1 well, Alaska Outer Continental Shelf: U.S. Geological Survey Bulletin 1596, p. 55-60.

Hunt, S.J., 1986, Structural analysis of plutonic and metamorphic rocks in an area east of Wrangell, Alaska: U.S. Geological Survey Open-File Report 86-50, 25 p.

Hunt, S.J., and Brew, D.A., 1986, Geometric structural analysis of part of the western Coast plutonic-metamorphic complex east of Wrangell, in Bartsch-Winkler, Susan, and Reed, K.M., eds., Geologic studies in Alaska by the U.S. Geological Survey during 1985: U.S. Geological Survey Circular 978, p. 102-108.

Jennings, P.C., 1986, Formulating earthquake resistant design criteria, in Hays, W.W., and Gori, P.L., eds., Proceedings of Conference XXXI, a workshop on "evaluation of regional and urban earthquake hazards and risk in Alaska": U.S. Geological Survey Open-File Report 86-79, p. 148-160.

Kaufman, D.S., 1986, Surficial geologic map of the Solomon, Bendeleben, and southern part of the Kotzebue quadrangles, western Alaska: U.S. Geological Survey Miscellaneous Field Studies Map MF 1838-A, scale 1:250,000, 1 sheet.

Kayen, R.E., 1986, Geotechnical sampling, in Miley, J.M., and Barnes, P.W., eds., 1985 field studies, Beaufort and Chukchi Seas, conducted from the NOAA ship DISCOVERER: U.S. Geological Survey Open-File Report 86-202, p. 49-51.

Knott, J.M., Lipscomb, S.W., and Lewis, T.W., 1986, Sediment transport characteristics of selected streams in the Susitna River basin, Alaska, October 1983 to September 1984: U.S. Geological Survey Open-File Report 86-424W.

Kockelman, W.J., 1986, Reducing losses from earthquakes through personal preparedness, in Hays, W.W., and Gori, P.L., eds., Proceedings of Conference XXXI, a workshop on "evaluation of regional and urban earthquake hazards and risk in Alaska": U.S. Geological Survey Open-File Report 86-79, p. 374-388, Appendices.

Lahr, J.C., Stephens, C.D., and Page, R.A., 1986, Regional seismic monitoring in southern Alaska: application to earthquake hazards assessment, in Hays, W.W., and Gori, P.L., eds., Proceedings of Conference XXXI, a workshop on "evaluation of regional and urban earthquake hazards and risk in Alaska": U.S. Geological Survey Open-File Report 86-79, p. 64-75.

Long, C.L., and Thompson, Bill, 1986, Audio-magnetotelluric resistivity traverses in the Baird Mountains quadrangle, in Bartsch-Winkler, Susan, and Reed, K.M., eds., Geologic studies in Alaska by the U.S. Geological Survey during 1985: U.S. Geological Survey Circular 978, p. 13-16.

McLean, Hugh, 1986, Sandstone petrography, in Magoon, L.B., ed., Geologic studies of the lower Cook Inlet COST No. 1 well, Alaska Outer Continental Shelf: U.S. Geological Survey Bulletin 1596, p. 47-49.

Magoon, L.B., 1986, Conclusions, in Magoon, L.B., ed., Geologic studies of the lower Cook Inlet COST No. 1 well, Alaska Outer Continental Shelf: U.S. Geological Survey Bulletin 1596, p. 91-99.

Magoon, L.B., ed., 1986, Geologic studies of the lower Cook Inlet COST No. 1 well, Alaska Outer Continental Shelf: U.S. Geological Survey Bulletin 1596, 99 p.

Magoon, L.B., 1986, Introduction, in Magoon, L.B., ed., Geologic studies of the lower Cook Inlet COST No. 1 well, Alaska Outer Continental Shelf: U.S. Geological Survey Bulletin 1596, p. 5-9.

Magoon, L.B., 1986, Present-day geothermal gradient, in Magoon, L.B., ed., Geologic studies of the lower Cook Inlet COST No. 1 well, Alaska Outer Continental Shelf: U.S. Geological Survey Bulletin 1596, p. 41-46.

Magoon, L.B., 1986, Stratigraphic units of the COST No. 1 well, in Magoon, L.B., ed., Geologic studies of the lower Cook Inlet COST No. 1 well, Alaska Outer Continental Shelf: U.S. Geological Survey Bulletin 1596, p. 17-22.

Magoon, L.B., and Egbert, R.M., 1986, Framework geology and sandstone composition, in Magoon, L.B., ed., Geologic studies of the lower Cook Inlet COST No. 1 well, Alaska Outer Continental Shelf: U.S. Geological Survey Bulletin 1596, p. 65-90.

March, R.S., Mayo, L.R., and Trabant, D.C., 1986, Geodetic survey stations near Mount Spurr Volcano, Alaska: U.S. Geological Survey Open-File Report 86-137, 14 p.

Marston, S.A., 1986, Evaluation of the workshop on "evaluation of regional and urban earthquake hazards and risk in Alaska", in Hays, W.W., and Gori, P.L., eds., Proceedings of Conference XXXI, a workshop on "evaluation of regional and urban earthquake hazards and risk in Alaska": U.S. Geological Survey Open-File Report 86-79, p. 38-42.

May, S.D., and Grantz, Arthur, 1985, Digital marine gravity data collected in the Chukchi Sea in 1982: U.S. Geological Survey Open-File Report 85-742, 4 p.

Mayo, L.R., and Trabant, D.C., 1986, Recent growth of Gulkana Glacier, Alaska Range, and its relation to glacier-fed river runoff, in Subitzky, Seymour, ed., Selected papers in the hydrologic sciences 1986; January 1986: U.S. Geological Survey Water-Supply Paper 2290, p. 91-99.

McLean, Hugh, 1986, Tectonics and the potential for hydrocarbons in offshore basins of western North America (abs.), in Carter, L.M.H., ed., 1986, USGS research on energy resources 1986, program and abstracts: U.S. Geological Survey Circular 974, p. 39-40.

Meador, P.J., Ambos, E.L., and Fuis, Gary, 1986, Data report for the North and South Richardson Highway profiles, TACT, seismic-refraction survey, southern Alaska: U.S. Geological Survey Open-File Report 86-274, 53 p., scale 1:500,000, 1 sheet.

Menzie, W.D., Reed, B.L., Foster, H.L., Sutley, S.J., Cushing, G.W., and Jones, G.M., 1986, Analyses of selected rock samples from the Lime Peak area, Circle C-6 quadrangle, Alaska: U.S. Geological Survey Open-File Report 86-358, 35 p., scale 1:63,360, 1 pl.

Menzie, W.D., Reed, B.L., and Keith, T.E.C., 1986, Lime Peak - an evolved granite with tin-enriched alteration, in Bartsch-Winkler, Susan, and Reed, K.M., eds., Geologic studies in Alaska by the U.S. Geological Survey during 1985: U.S. Geological Survey Circular 978, p. 25-27.

Miley, J.M., and Barnes, P.W., eds., 1986, 1985 field studies, Beaufort and Chukchi Seas, conducted from the NOAA ship DISCOVERER: U.S. Geological Survey Open-File Report 86-202, 57 p., 5 pls.

Molenaar, C.M., Bird, K.J., and Collett, T.S., 1986, Regional correlation sections across the North Slope of Alaska (abs.), in Carter, L.M.H., ed., 1986, USGS research on energy resources - 1986, program and abstracts: U.S. Geological Survey Circular 974, p. 43.

Molenaar, C.M., Bird, K.J., and Collett, T.S., 1986, Regional correlation sections across the North Slope of Alaska: U.S. Geological Survey Miscellaneous Field Studies Map MF 1907, 1 sheet.

Morgenson, L., Vallier, T., and Lamothe, P., 1985 (1986), Chemical data from Tertiary igneous rocks, Atka and Amlia Islands, central Aleutian Island arc, Alaska: U.S. Geological Survey Open-File Report 85-741, 28 p.

Mosier, E.L., and Lewis, J.S., 1986, Analytical results, geochemical signatures, and sample locality map of lode gold, placer gold, and heavy-mienral concentrates from the Koyukuk-Chandalar mining district, Alaska: U.S. Geological Survey Open-File Report 86-345, 174 p., scale 1:250,000.

Mull, C.G., and Nelson, S.W., 1986, Anomalous thermal maturity data from the Orca Group (Paleocene and Eocene), Katalla-Kayak Island area, in Bartsch-Winkler, Susan, and Reed, K.M., eds., Geologic studies in Alaska by the U.S. Geological Survey during 1985: U.S. Geological Survey Circular 978, p. 50-55.

Mullen, M.W., and Csejtey, Béla, Jr., 1986, Recognition of a Nixon Fork terrane equivalent in the Healy quadrangle, in Bartsch-Winkler, Susan, and Reed, K.M., eds., Geologic studies in Alaska by the U.S. Geological Survey during 1985: U.S. Geological Survey Circular 978, p. 55-60.

Nelson, S.W., Blome, C.D., Harris, A.G., Reed, K.M., and Wilson, F.H., 1986, Late Paleozoic and Early Jurassic fossil ages from the McHugh Complex, in Bartsch-Winkler, Susan, and Reed, K.M., eds., Geologic studies in Alaska by the U.S. Geological Survey during 1985: U.S. Geological Survey Circular 978, p. 60-64.

Nelson, S.W., Dumoulin, J.A. and Miller, M.L., 1986, Geologic map of the Chugach National Forest, Alaska: U.S. Geological Survey Miscellaneous Field Studies Map MF 1645-B, scale 1:250,000.

Nishenko, S.P., and Jacob, Klaus, 1986, Hazards evaluation for large and great earthquakes along the Queen Charlotte-Alaska-Aleutian seismic zone: 1985-2005, in Hays, W.W., and Gori, P.L., eds., Proceedings of Conference XXXI, a workshop on "evaluation of regional and urban earthquake hazards and risk in Alaska": U.S. Geological Survey Open-File Report 86-79, p. 83-92.

Nokleberg, W.J., Aleinikoff, J.N., and Lange, I.M., 1986, Cretaceous deformation and metamorphism in the northeastern Mount Hayes quadrangle, eastern Alaska Range, in Bartsch-Winkler, Susan, and Reed, K.M., eds., Geologic studies in Alaska by the U.S. Geological Survey during 1985: U.S. Geological Survey Circular 978, p. 64-69.

Nokleberg, W.J., Wade, W.M., Lange, I.M., and Plafker, George, 1986, Summary of geology of the Peninsular terrane, metamorphic complex of Gulkana River, and Wrangellia terrane, north-central and northwestern Gulkana quadrangle, in Bartsch-Winkler, Susan, and Reed, K.M., eds., Geologic studies in Alaska by the U.S. Geological Survey during 1985: U.S. Geological Survey Circular 978, p. 69-74

Odum, J.K., 1986, Compilation of field and laboratory geotechnical test data for U.S. Geological Survey drill holes 1C-79, 2C-80, CW81-2,and CE82-1, Beluga resource area, upper Cook Inlet region, Alaska: U.S. Geological Survey Open-File Report 86-382, 10 p., 4 pls.

Odum, J.K., Yehle, L.A., Schmoll, H.R., and Gilbert, Chuck, 1986, Description and interpretation of geologic materials from shotholes drilled for the Trans-Alaska Coastal Transect Project, Copper River basin, Alaska, May 1985: U.S. Geological Survey Open-File Report 86-408, 18 p.

O'Leary, R.M., Hoffman, J.D., Risoli, D.A., and Tripp, R.B., 1986, Analytical results and sample locality map of stream-sediment and heavy-mineral-concentrate samples from the Circle quadrangle, Alaska: U.S. Geological Survey Open-File Report 86-204, 126 p., scale 1:250,000, 1 pl.

Olsen, H.W., 1986, Sensitive clays in the Bootlegger Cove Formation, in Hays, W.W., and Gori, P.L., eds., Proceedings of Conference XXXI, a workshop on "evaluation of regional and urban earthquake hazards and risk in Alaska": U.S. Geological Survey Open-File Report 86-79, p. 119-133.

Page, R.A., and Basham, P.W., 1985, Earthquake hazards in the offshore environment: U.S. Geological Survey Bulletin 1630, 69 p.

Page, R.A., Campbell, D.L., Plafker, George, Fuis, G.S., Nokleberg, W.J., Ambos, E.L., Mooney, W.D., and Fisher, M.A., 1986, Accretion, subduction, and underplating in southern Alaska - Initial results from the Trans-Alaska Crustal Transect (abs.), in Carter, L.M.H., ed., 1986, USGS research on energy resources - 1986, program and abstracts: U.S. Geological Survey Circular 974, p. 50.

Parrish, J.T., 1986, The Shublik Formation - A model for deposition in an ancient marine upwelling zone (abs.), in Carter, L.M.H., ed., 1986, USGS research on energy resources 1986, program and abstracts: U.S. Geological Survey Circular 974, p. 54.

Phillips, R.L., 1986, Sedimentology and stratigraphy in the Chukchi Sea, in Miley, J.M., and Barnes, P.W., eds., 1985 field studies, Beaufort and Chukchi Seas, conducted from the NOAA ship DISCOVERER: U.S. Geological Survey Open-File Report 86-202, p. 52-53.

Plafker, George, and Jacob, K.H., 1986, Seismic sources in Alaska, in Hays, W.W., and Gori, P.L., eds., Proceedings of Conference XXXI, a workshop on "evaluation of regional and urban earthquake hazards and risk in Alaska": U.S. Geological Survey Open-File Report 86-79, p. 76-82.

Plafker, George, Nokleberg, W.J., Lull, J.S., Roeske, S.M., and Winkler, G.R., 1986, Nature and timing of deformation along the contact fault system in the Cordova, Bering Glacier, and Valdez quadrangles, in Bartsch-Winkler, Susan, and Reed, K.M., eds., Geologic studies in Alaska by the U.S. Geological Survey during 1985: U.S. Geological Survey Circular 978, p. 74-77.

Prensky, S.E., 1986, List of released wells and availability of digital well-log data for Atlantic, Pacific and Alaskan OCS regions through December 31, 1985: U.S. Geological Survey Open-File Report 86-48, 42 p.

Preuss, Jane, 1986, Implementation framework to reduce potential losses from tsunami hazards in Alaska, in Hays, W.W., and Gori, P.L., eds., Proceedings of Conference XXXI, a workshop on "evaluation of regional and urban earthquake hazards and risk in Alaska": U.S. Geological Survey Open-File Report 86-79, p. 93-107.

Ramirez, P.C., 1986, Pebble lithology in the Chukchi Sea, in Miley, J.M., and Barnes, P.W., eds., 1985 field studies, Beaufort and Chukchi Seas, conducted from the NOAA ship DISCOVERER: U.S. Geological Survey Open-File Report 86-202, p. 54-57.

Rearic, D.M., 1986, Beaufort Sea ice gouge studies, in Miley, J.M., and Barnes, P.W., eds., 1985 field studies, Beaufort and Chukchi Seas, conducted from the NOAA ship DISCOVERER: U.S. Geological Survey Open-File Report 86-202, p. 41-46.

Rearic, D.M., 1986, Temporal and spatial character of newly formed ice gouges in eastern Harrison Bay, Alaska, 1977-1982: U.S. Geological Survey Open-File Report 86-391, 54 p.

Reed, K.M., and Blome, C.D., 1986, Use of radiolarian biostratigraphy in stratigraphic problems in the Otuk Formation, in Bartsch-Winkler, Susan, and Reed, K.M., eds., Geologic studies in Alaska by the U.S. Geological Survey during 1985: U.S. Geological Survey Circular 978, p. 16-19.

Reimnitz, Erk, Kempema, E.W., and Barnes, P.W., 1986, Anchor ice and bottom freezing in high-latitude marine sedimentary environments: observations from the Alaskan Beaufort Sea: U.S. Geological Survey Open-File Report 86-298, 22 p.

Robb, James, 1986, Geophysical data from the upper continental slope in the Beaufort Sea, in Miley, J.M., and Barnes, P.W., eds., 1985 field studies, Beaufort and Chukchi Seas, conducted from the NOAA ship DISCOVERER: U.S. Geological Survey Open-File Report 86-202, p. 31-40.

Rogers, J.A., 1986, Increasing dynamic range in analog seismic data systems used in Alaska: U.S. Geological Survey Open-File Report 86-78, 17 p.

Sable, E.G., Stricker, G.D., and Affolter, R.H., 1986, Nanushuk Group coal investigations - North Slope of Alaska (abs.), in Carter, L.M.H., ed., 1986, USGS research on energy resources 1986, program and abstracts: U.S. Geological Survey Circular 974, p. 59-60.

Schmidt, J.M., and Folger, P.F., 1986, Pb-Zn-Ag mineralization in Paleozoic dolostones, Powdermilk Prospect, Baird Mountains B-4 quadrangle, in Bartsch-Winkler, Susan, and Reed, K.M., eds., Geologic studies in Alaska by the U.S. Geological Survey during 1985: U.S. Geological Survey Circular 978, p. 19-21.

Schmoll, H.R., 1986, USGS engineering geology projects in the Anchorage area, Alaska: a review, in Hays, W.W., and Gori, P.L., eds., Proceedings of Conference XXXI, a workshop on "evaluation of regional and urban earthquake hazards and risk in Alaska": U.S. Geological Survey Open-File Report 86-79, p. 134-147.

Seitz, H.R., Thomas, D.S., and Tomlinson, Bud, 1986, The storage and release of water from a large glacier-dammed lake: Russell Lake near Yakutat, Alaska, 1986: U.S. Geological Survey Open-File Report 86-545, 10 p.

Selkregg, L.L., 1986, A planning and administrative model for risk and mitigation, in Hays, W.W., and Gori, P.L., eds., Proceedings of Conference XXXI, a workshop on "evaluation of regional and urban earthquake hazards and risk in Alaska": U.S. Geological Survey Open-File Report 86-79, p. 238-248.

Selkregg, L.L., 1986, Present planning for, and management of seismic risk mitigation, in Hays, W.W., and Gori, P.L., eds., Proceedings of Conference XXXI, a workshop on "evaluation of regional and urban earthquake hazards and risk in Alaska": U.S. Geological Survey Open-File Report 86-79, p. 229-237.

Shearer, C.F., 1986, Minutes of the National Earthquake Prediction Evaluation Council, September 8 and 9, 1985, Anchorage, Alaska: U.S. Geological Survey Open-File Report 86-92, 268 p.

Sheinberg, B.J., 1986, Recent and anticipated changes in utilization of earthquake hazard information for siting considerations; Anchorage, Alaska, in Hays, W.W., and Gori, P.L., eds., Proceedings of Conference XXXI, a workshop on "evaluation of regional and urban earthquake hazards and risk in Alaska": U.S. Geological Survey Open-File Report 86-79, p. 190-192.

Silverstein, B.L., Brady, A.G., and Mork, P.N., 1986, Processed strong-motion records from the southern Alaska earthquake of January 1, 1975 0355GMT: U.S. Geological Survey Open-File Report 86-191, 101 p.

Simpson, S.L., 1986, Selected geological and geophysical remotesensing publications by U.S. Geological Survey authors, 1961-1984: U.S. Geological Survey Open-File Report 86-41, 60 p.

Sloan, C.E., Emery, P.A., and Fair, Diana, 1986, Effect of glacier ablation on the Snettisham hydroelectric project, Long Lake and Crater Lake basins, Alaska, with a section on Streamflow records, by R.D. Lamke: U.S. Geological Survey Water-Resources Investigations WRI 85-4315, 22 p., 1 pl.

Sloan, C.E., Kernodle, D.R., and Huntsinger, Ronald, 1986, Hydrologic reconnaissance of the Unalakleet River basin, Alaska 1982-83: U.S. Geological Survey Water-Resouces Investigations Report 86-4089.

Stanley, W.D., 1986, Magnetotelluric study of a compressed flysch system in the Healy and adjacent quadrangles, in Bartsch-Winkler, Susan, and Reed, K.M., eds., Geologic studies in Alaska by the U.S. Geological Survey during 1985: U.S. Geological Survey Circular 978, p. 78-81.

Steinbrugge, K.V., 1986, Earthquake damage - 1964 lessons learned and relearned, in Hays, W.W., and Gori, P.L., eds., Proceedings of Conference XXXI, a workshop on "evaluation of regional and urban earthquake hazards and risk in Alaska": U.S. Geological Survey Open-File Report 86-79, p. 178-189.

Stephens, C.D., Fogleman, K.A., Lahr, J.C., and Page, R.A., 1986, Seismicity in southern Alaska, October 1984 - September 1985, in Bartsch-Winkler, Susan, and Reed, K.M., eds., Geologic studies in Alaska by the U.S. Geological Survey during 1985: U.S. Geological Survey Circular 978, p. 81-85.

Stone, D.B., Page, R.A., and Davies, J.N., eds., 1986, Trans-Aalska lithosphere investigation - Program prospectus: U.S. Geological Survey Circular 984, 24 p.

Stricker, G.D., Affolter, R.H., and Brownfield, M.E., 1986, Geochemical characterization of selected coals from the Beluga energy resource area, south-central Alaska: Site of a proposed coal mine (abs.), in Carter, L.M.H., ed., 1986, USGS research on energy resources - 1986, program and abstracts: U.S. Geological Survey Circular 974, p. 65-66.

Sutley, S.J., O'Leary, R.M., and Goldfarb, R.J., 1986, Analytical results and sample locality map of moraine-sediment, stream-sediment, and heavy-mineral-concentrate samples from the Cordova and Middleton Island 1 by 3 qudrangles, Alaska: U.S. Geological Survey Open-File Report 86-381, 117 p., scale 1:250,000, 1 pl.

Till, A.B., Dumoulin, J.A., Gamble, B.M., Kaufman, D.S., and Carroll, P.I., 1986, Preliminary geologic map and fossil data, Solomon, Bendeleben, and southern Kotzebue quadrangles, Seward Peninsula, Alaska: U.S. Geological Survey Open-File Report 86-276, 69 p., scale 1:250,000, 3 pls.

Turner, L.I., and Sey, Jim, 1986, Emergency preparedness planning in Alaska, in Hays, W.W., and Gori, P.L., eds., Proceedings of Conference XXXI, a workshop on "evaluation of regional and urban earthquake hazards and risk in Alaska": U.S. Geological Survey Open-File Report 86-79, p. 220-228.

Turner, R.F., 1986, Paleontology and biostratigraphy of the COST No. 1 well, in Magoon, L.B., ed., Geologic studies of the lower Cook Inlet COST No. 1 well, Alaska Outer Continental Shelf: U.S. Geological Survey Bulletin 1596, p. 29-31.

U.S. Geological Survey, 1986, 1986 annual report on Alaska's mineral resources: U.S. Geological Survey Circular 983, 47 p.

Updike, R.G., 1986, Engineering geologic maps of the Government Hill area, Anchorage, Alaska: U.S. Geological Survey Miscellaneous Investigations Series Map I-1610, scale 1:48,000.

Updike, R.G., 1986, Status of earthquake hazard research in the Anchorage area and upper Cook Inlet, Alaska, in Hays, W.W., and Gori, P.L., eds., Proceedings of Conference XXXI, a workshop on "evaluation of regional and urban earthquake hazards and risk in Alaska": U.S. Geological Survey Open-File Report 86-79, p. 108-118.

Updike, R.G., and Carpenter, B.A., 1986, Engineering geology of the Government Hill area, Anchorage, Alaska: U.S. Geological Survey Bulletin 1588, 32 p.

von Huene, Roland, 1986, Potential gas generation in subducted sediments of the eastern Aleutian Trench area (abs.), in Carter, L.M.H., ed., 1986, USGS research on energy resources 1986, program and abstracts: U.S. Geological Survey Circular 974, p. 69.

Vyas, Y.K., 1986, An assessment of earthquake hazards offshore southern Alaska, in Hays, W.W., and Gori, P.L., eds., Proceedings of Conference XXXI, a workshop on "evaluation of regional and urban earthquake hazards and risk in Alaska": U.S. Geological Survey Open-File Report 86-79, p. 200-214.

Wade, W.M., Nokleberg, W.J., Ferrians, O.J., and Williams, J.R., 1986, Geologic bibliography of the Gulkana quadrangle, Alaska: U.S. Geological Survey Open-File Report 86-332, 17 p.

White, E.R., Galloway, J.P., and Booth, S.E., 1986, Reports about Alaska in non-USGS publications released in 1985 that include USGS authors, in Bartsch-Winkler, Susan, and Reed, K.M., eds., Geologic studies in Alaska by the U.S. Geological Survey during 1985:

U.S. Geological Survey Circular 978, p. 160-168.

White, E.R., Galloway, J.P., and Booth, S.E., 1986, Reports about Alaska in USGS publications released in 1985, in Bartsch-Winkler, Susan, and Reed, K.M., eds., Geologic studies in Alaska by the U.S. Geological Survey during 1985: U.S. Geological Survey Circular 978, p. 146-159.

Wiggins, J.H., 1986, Legal liability problems in earthquake preparedness, in Hays, W.W., and Gori, P.L., eds., Proceedings of Conference XXXI, a workshop on "evaluation of regional and urban earthquake hazards and risk in Alaska": U.S. Geological Survey Open-File Report 86-79, p. 256-261.

Wiley, T.J., 1986, Sedimentary basins of offshore Alaska and adjacent regions: U.S. Geological Survey Open-File Report 86-35, 122 p., scale 1:2,500,000, 1 pl.

Wiley, T.J., 1986, Tectonics - First-order control of sediment distribution and hydrocarbon potential: Examples from the western margin of North America (abs.), in Carter, L.M.H., ed., 1986, USGS research on energy resources - 1986, program and abstracts: U.S. Geological Survey Circular 974, p. 74-75.

Williams, J.R., 1986, New radiocarbon dates from the Matanuska Glacier bog section, in Bartsch-Winkler, Susan, and Reed, K.M., eds., Geologic studies in Alaska by the U.S. Geological Survey during 1985: U.S. Geological Survey Circular 978, p. 85-88.

Williams, J.R., and Galloway, J.P., 1986, Map of western Copper River basin, Alaska, showing lake sediments and shorelines, glacial moraines, and location of stratigraphic sections and radiocarbon-dated samples: U.S. Geological Survey Open-File Report 86-390, 33 p., scale 1:250,000, 1 pl.

Wilson, F.H., Gajewski, S.Z., and Angeloni, L.A., 1986, Geological literature of the Alaska Peninsula to 1985: U.S. Geological Survey Open-File Report 86-176, 114 p.

Wilson, F.H., and O'Leary, R.M., 1986, Maps and tables showing data and analyses of semiquantitative emission spectrometry and atomic absorption spectrophotometry of rock samples, Ugashik, Bristol Bay, and part of Karluk quadrangles, Alaska: U.S. Geological Survey Miscellaneous Field Studies Map MF 1539-C, scale 1:250,000.

Winkler, G.R., 1986, Data releases and folio reports prepared for the Alaska Mineral Resource Assessment Program and the Regional Alaska Mineral Resource Assessment Program listed alphabetically by quadrangle, in Bartsch-Winkler, Susan, and Reed, K.M., eds., Geologic studies in Alaska by the U.S. Geological Survey during 1985: U.S. Geological Survey Circular 978, p. 110-145.

Winkler, G.R., and Grybeck, D.J., 1986, The Alaska Mineral Resource Assessment Program in 1985, in Bartsch-Winkler, Susan, and Reed, K.M., eds., Geologic studies in Alaska by the U.S. Geological Survey during 1985: U.S. Geological Survey Circular 978, p. 3-5.

Wolf, S.C., Barnes, P.W., Rearic, D.M., and Reimnitz, Erk, 1986, Shallow seismic stratigraphy between the Canning River and Demarcation Bay, Beaufort Sea, Alaska: U.S. Geological Survey Open-File Report 86-582, 37 p.

Yehle, L.A., Odum, J.K., Schmoll, H.R., and Dearborn, L.L., 1986, Overview of the geology and geophysics of the Tikishla Park drill hole, USGS A-84-1, Anchorage, Alaska: U.S. Geological Survey Open-File Report 86-293, 12 p., 1 pl.

Reports about Alaska in non-USGS publications released in 1986 which include USGS authors, marked by an asterisk (*)

compiled by Ellen R. White

Some reports dated 1985 did not become available until 1986; they are included in this listing

*Ager, T.A., 1986, Ice-marginal vegetation development in southern Alaska during the late Pleistocene and early Holocene: Pollen evidence from Cook Inlet region (abs.), in American Quaternary Association, Biennial meeting, 9th, Urbana, University of Illinois-Champaign, 1985, Program and Abstracts, p. 11-12.

*Ager, T.A., and Brubaker, Linda, 1985, Quaternary palynology and vegetational history of Alaska, in Bryant, V.M., Jr., and Holloway, R.G., eds., Pollen records of Late-Quaternary North American sediments: American Association of Stratigraphic Palynologists Foundation, p. 353-384.

*Ager, T.A., *Edwards, L.E., and *Oftedahl, O., 1985, Eocene palynomorphs from the Franklin Bluffs, Arctic Slope, northeast Alaska (abs.), in American Association of Stratigraphic Palynologists, Inc., Annual Meeting, 18th, El Paso, Tex., 1985, Program and Abstracts, no. 18, p. 7.

*Albert, N.R., Evitt, W.R., and Stein, J.A., 1986, Lacrymodinium, n. gen., a gonyaulacoid dinoflagellate with intercalary archeopyle from the Jurassic and Early Cretaceous of California and Alaska: Micropalentology, v. 32, no. 4, p. 303-315, pls. 1-2.

*Aleinikoff, J.N., *Dusel-Bacon, Cynthia, and *Foster, H.L., 1986, Geochronology of augen gneiss and related rocks, Yukon-Tanana terrane, east-central Alaska: Geological Society of America Bulletin, v. 97, no. 5, p. 626-637.

*Arth, J.G., *Barker, Fred, *Stern, T.W., and *Zmuda, Clara, 1986, The Coast batholith near Ketchikan, southeast Alaska: geochronology and geochemistry (abs.): Geological Society of America, Abstracts with Programs, v. 18, no. 6, p. 529.

*Barker, Fred, *Arth, J.G., and *Stern, T.W., 1986, Evolution of the coast batholith along the Skagway Traverse, Alaska and British Columbia: American Mineralogist, v. 71, no. 3-4, p. 632-643.

*Barker, Fred, and *Stern, T.W., 1986, An arc-root complex of Wrangellia, E. Alaska Range (abs.): Geological Society of America, Abstracts with Programs, v. 18, no. 6, p. 534.

*Barnes, D.F., 1986, Gravitational expression of terranes crossed by the southern TACT profile, Alaska (abs.): Eos (American Geophysical Union Transactions), v. 67, no. 44, p. 1197.

*Bernstein, L.R., and *Cox, D.P., 1986, Geology and sulfide mineralogy of the Number One orebody, Ruby Creek copper deposit, Alaska: Economic Geology, v. 81, no. 7, p. 1675-1689.

*Bird, K.J., 1985, The framework geology of the North Slope of Alaska as related to oil-source rock correlations, in *Magoon, L.B., and *Claypool, G.E., eds., Alaska North Slope oil-rock correlation study; Analysis of North Slope crude: Tulsa, Okla., American Association of Petroleum Geologists Studies in Geology 20, p. 3-29.

Biswas, N.N., *Lahr, J.C., and *Page, R.A., 1986, Some results on the seismicity of Alaska (abs.): Eos (American Geophysical Union Transactions), v. 67, no. 44, p. 1236.

Blodgett, R.B., Clough, J.G., *Dutro, J.T., Jr., Palmer, A.R., *Taylor, M.E., and Ormiston, A.R., 1986, Age revision of the Katakturuk Dolomite and Nanook Limestone, northeastern Brooks Range, Alaska (abs.): Geological Society of America, Abstracts with Programs, v. 18, no. 2, p. 87.

*Blome, C.D., 1986, Late Triassic radiolarian paleogeography for western Cordilleran accreted terranes (abs.): Geological Society of America, Abstracts with Programs, v. 18, no. 2, p. 87.

*Box, S.E., 1986, Early Cretaceous shoshonites in western Alaska: changing mantle sources during arc-continent collision (abs.): Eos (American Geophysical Union Transactions), v. 67, no. 44, p. 1278.

*Brewer, M.C., 1985, Petroleum exploration and environmental protection on the Alaskan National Petroleum Reserve, in Gerwick, B.C., ed., Arctic Ocean engineering for the 21st century, Spilhaus Symposium, 1st, Williamsburg, Va., 1984, Proceedings: Marine Technology Society, p. 203-205.

*Brooks, P.D., and *O'Brien, T.J., 1986, The evolving Alaska mapping program: PE & RS (Photogrammetric Engineering, Remote Sensing), v. 52, no. 6, p. 769-777.

*Bruns, T.R., *Fisher, M.A., *Carlson, P.R., and Parson, L.M., 1986, The Yakutat terrane and Aleutian convergent margin, northern Gulf of Alaska - GLORIA images obtained in the TACT corridor (abs.): Eos (American Geophysical Union Transactions), v. 67, no. 44, p. 1197.

*Bruns, T.R., *von Huene, R., *Culotta, R.D., Lewis, S.D., and Ladd, J.W., 1986, Geology and petroleum potential of Shumagin continental margin, western Gulf of Alaska (abs.): American Association of Petroleum Geologists Bulletin, v. 70, no. 7, p. 915.

Bundtzen, T.K., *Miller, M.L., and Kline, J.T., 1985, Geology of heavy mineral placer deposits of the Iditarod and Innoko precincts, western Alaska, in Madonna, J.A., ed., Alaskan placer mining, Annual conference, 7th, Fairbanks, 1985, Proceedings: Fairbanks, Alaskan Prospectors Publishing, p. 35-41.

*Campbell, D.L., *Barnes, D.F., and *Jachens, R.C., 1986, Models using isostatic gravity anomaly of structures near the northeastern edge of the subducting Pacific plate, south-central Alaska (abs.): Eos (American Geophysical Union Transactions), v. 67, no. 44, p. 1195.

*Carlson, P.R., *Marlow, M.S., *Rearic, D.M., *Dadisman, S.V., and Parson, L.M., 1986, GLORIA side-scan imagery of central Bering Sea EEZ (abs.): Eos (American Geophysical Union Transactions), v. 67, no. 44, p. 1228-1229.

*Carter, L.D., Brigham-Grette, Julie, *Marincovich, Louie, Jr., *Pease, V.L., and *Hillhouse, J.W., 1986, Late Cenozoic Arctic Ocean sea ice and terrestrial paleoclimate: Geology, v. 14, no. 8, p. 675-678.

*Cathrall, John, *Antweiler, John, *Mosier, Elwin, *Tripp, Richard, and Lueck, Larry, 1985, Progress report on U.S. Geological Survey Alaskan Gold Project, in Madonna, J.A., ed., Alaskan placer mining, Annual conference, 7th, Fairbanks, 1985, Proceedings: Fairbanks, Alaskan Prospectors Publishing, p. 42-47.

*Colburn, R.H., and *Fuis, G.S., 1986, Velocity structure across the northern boundary of the Peninsular terrane, Copper River basin, Alaska (abs.): Eos (American Geophysical Union Transactions), v. 67, no. 44, p. 1198.

*Collett, T.S., *Bird, K.J., *Kvenvolden, K.A., and *Magoon, L.B., 1986, The effect of freezing-point depression on ice-bearing permafrost, North Slope, Alaska (abs.): Eos (American Geophysical Union Transactions), v. 67, no. 44, p. 949.

*Cooper, A.K., *Marlow, M.S., and *Scholl, D.W., 1986, Frontier basins of Bering Sea (abs.): American Association of Petroleum Geologists Bulletin, v. 70, no. 7, p. 917.

*Davis, A.S., and *Plafker, George, 1986, Eocene basalts from the Yakutat terrane: evidence for the origin of an accreting terrane in southern Alaska (abs.): Eos (American Geophysical Union Transactions), v. 67, no. 44, p. 963-966.

*Detterman, R.L., 1986, Glaciation of the Alaska Peninsula, in *Hamilton, T.D., *Reed, K.M., and Thorson, R.M., eds., Glaciation in Alaska, the geologic record: Anchorage, Alaska Geological Society, p. 151-170.

Dijkmans, W.A., Koster, E.A., *Galloway, J.P., and Mook, W.G., 1986, Characteristics and origin of calcretes in a subarctic environment, Great Kobuk Sand Dunes, northwestern Alaska, U.S.A.: Arctic and Alpine Research, v. 18, no. 4, p. 377-387.

*Drake, D.E., and *Cacchione, D.A., 1986, Field observations of bed shear stress and sediment resuspension on continental shelves, Alaska and California: Continental Shelf Research, v. 6, no. 3, p. 415-429.

Eichelberger, J.C., and *Hildreth, Wes, 1986, Research drilling at Katmai, Alaska: Eos (American Geophysical Union Transactions), v. 67, no.41, p. 778-780.

*Engdahl, E.R., 1986, Aseismic extension of the central Aleutian slab (abs.): Eos (American Geophysical Union Transactions), v. 67, no. 16, p. 380.

*Engdahl, E.R., 1986, Relocation of teleseismically recorded earthquakes in the region of the May 7, 1986, Andreanof Islands earthquake (abs.): Eos (American Geophysical Union Transactions), v. 67, no. 44, p. 1081.

*Engdahl, E.R., and Billington, Selena, 1986, Focal depth determination of central Aleutian earthquakes: Bulletin of the Seismological Society of America, v. 76, no. 1, p. 77-93.

*Espinosa, A.F., and *Rukstales, K.S., 1986, Seismological mapping of the Benioff Zone in Alaska and the Aleutian Islands and in central western South America (abs.): Eos (American Geophysical Union Transactions), v. 67, no. 16, p. 303.

*Fierstein, Judy, and *Hildreth, Wes, 1986, Ejecta dispersal and dynamics of the 1912 eruptions of Novarupta, Katmai National Park, Alaska (abs.): Eos (American Geophysical Union Transactions), v. 67, no. 44, p. 1246.

*Fisher, M.A., *Brocher, T.M., *Page, R.A, *Plafker, George, *Fuis, G.S., *Nokleberg, W.J., and *Campbell, D.L., 1986, Seismic reflection images of deep-crustal features of south-central Alaska: preliminary results of a survey for TACT (abs.): Eos (American Geophysical Union Transactions), v. 67, no. 44, p. 1196.

Folger, P.F., and *Schmidt, J.M., 1986, Geology of the carbonate-hosted Omar copper prospect, Baird Mountains, Alaska: Economic Geology, v. 81, no. 7, p. 1690-1695.

*Frederiksen, N.O., *Ager, T.A., and *Edwards, L.E., 1986, Comment on "Early Tertiary marine fossils from northern Alaska: implications for Arctic Ocean paleogeography and faunal evolution": Geology, v. 14, no. 9, p. 802-803.

*Frederiksen, N.O., *Ager, T.A., *Oftedahl, O.G., and *Edwards, L.E., 1985, Palynological samples near the Cretaceous/Tertiary boundary, North Slope of Alaska (abs.), in

SEPM Annual Midyear Meeting, 2nd, Golden, Colo., 1985, Abstracts: Tulsa, Okla., Society of Economic Paleontologists and Mineralogists, p. 31.

*Fuis, G.S., *Ambos, E.L., *Mooney, W.D., *Page, R.A., and *Campbell, D.L., 1985, Crustal structure of southern Alaska - Preliminary results of the TACT 1984 seismic refraction experiment (abs.): Earthquake Notes, v. 55 (sic), v. 56, no. 1, p. 23.

*Gardner, J.V., *Karl, H.A., and Huggett, Q., 1986, Origin and development of Zhemchug Canyon (Bering Sea), adjacent continental margin, and abyssal plain as revealed by GLORIA (long-range side-scan sonar) and seismic data (abs.): Eos (American Geophysical Union Transactions), v. 67, no. 44, p. 1229.

*Godson, R.H., 1985, Preparation of magnetic anomaly maps of Alaska and Hawaii, in Hinze, W.J., ed., The utility of regional gravity and magnetic anomaly maps: Tulsa, Okla., Society of Exploration Geophysicists, p. 25-32.

Goodwin, E.B., *Ambos, E.L., *Fuis, G.S., *Mooney, W.D., *Page, R.A., and *Campbell, D.L., 1986, The crustal structure of Wrangellia, southern Alaska, from seismic refraction measurements (abs.): Eos (American Geophysical Union Transactions), v. 67, no. 44, p. 1196.

*Gryc, George, 1985, Arctic minerals, in Gerwick, B.C., ed., Arctic Ocean engineering for the 21st century, Spilhaus Symposium, 1st, Williamsburg, Va., 1984, Proceedings: Marine Technology Society, p. 87-88.

*Hamilton, T.D., 1986, Late Cenozoic glaciation of the central Brooks Range, in *Hamilton, T.D., *Reed, K.M., and Thorson, R.M., eds., Glaciation in Alaska, the geologic record: Anchorage, Alaska Geological Society, p. 9-49.

*Hamilton, T.D., *Reed, K.M., and Thorson, R.M., 1986, Glaciation in Alaska - Introduction and overview, in *Hamilton, T.D., *Reed, K.M., and Thorson, R.M., eds., Glaciation in Alaska, the geologic record: Anchorage, Alaska Geological Society, p. 1-8.

*Hamilton, T.D., *Reed, K.M., and Thorson, R.M., eds., 1986, Glaciation in Alaska - The geologic record: Anchorage, Alaska Geological Society, 265 p.

*Hampton, M.A., (1983) 1986, Geotechnical framework study of the Kodiak Shelf, Alaska, in Environmental Assessment of the Alaskan Continental Shelf Final Reports of Principal Investigators: U.S. Department of Commerce, NOAA, OCSEAP Final Report v. 48, U.S. Department of the Interior OCS Study, MMS 86-0065, p. 1-94.

Harbert, William, *Scholl, D.W., *Vallier, T.L., *Stevenson, A.J., and *Mann, D.M., 1986, Major evolutionary phases of a forearc basin of the Aleutian terrace: relation to North Pacific tectonic events and the formation of the Aleutian subduction complex: Geology, v. 14, no. 9, p. 757-761.

*Hildreth, Wes, and *Fierstein, Judy, 1986, Near-vent ejecta around Novarupta, eruption of 1912, Katmai National Park, Alaska (abs.): Eos (American Geophysical Union Transactions), v. 67, no. 44, p. 1246.

*Hillhouse, J.W., *Gromme, C.S., and *Csejtey, Béla, Jr., 1985, Tectonic implications of paleomagnetic poles from Lower Tertiary volcanic rocks, south central Alaska: Journal of Geophysical Research, v. 90, no. B14, p. 12,523-12,535.

Hitzman, M.W., Proffett, J.M., Jr., *Schmidt, J.M., and Smith, T.E., 1986, Geology and mineralization of the Ambler district, northwestern Alaska: Economic Geology, v. 81, no. 7, p. 1592-1618.

*Howell, D.G., *Jones, D.L., and *Schermer, E.R., 1985, Tectonostratigraphic terranes of the Circum-Pacific region, in Howell, D.G., ed., Tectonostratigraphic terranes of the Circum-Pacific region: Houston, Tex., Circum-Pacific Council for Energy and Mineral Resources, p. 3-30.

*Jones, D.L., *Silberling, N.J., and Coney, P.J., 1986, Collision tectonics in the Cordillera of western North America: examples from Alaska, in Coward, M.P., and Ries, A.C., eds., Collision tectonics, Special Publication 19 of the Geological Society of London: Palo Alto, Calif., Blackwell Scientific Publications, p. 367-387.

*Karl, H.A., *Cacchione, D.A., and *Carlson, P.R., 1986, Internal-wave currents as a mechanism to account for large sand waves in Navarinsky Canyon head, Bering Sea: Journal of Sedimentary Petrology, v. 56, no. 5, p. 706-714.

*Kaufman, D.S., and Hopkins, D.M., 1986, Glacial history of the Seward Peninsula, in *Hamilton, T.D., *Reed, K.M., and Thorson, R.M., eds., Glaciation in Alaska, the geologic record: Anchorage, Alaska Geological Society, p. 51-77.

*Keith, T.E.C., 1986, Distribution of hydrothermal alteration associated with Novarupta caldera, Katmai National Park, Alaska (abs.): Eos (American Geophysical Union Transactions), v. 67, no. 44, p. 1246.

Kienle, J., Davies, J.N., *Miller, T.P., and *Yount, M.E., 1986, 1986 eruption of Augustine Volcano: public safety response by Alaskan geologists: Eos (American Geophysical Union Transactions), v. 67, no. 29, p. 580-582.

*Kvenvolden, K.A., and *von Huene, Roland, 1985, Natural gas generation in sediments of the convergent margin of the eastern Aleutian trench area, in Howell, D.G., ed., Tectonostratigraphic terranes of the Circum-Pacific region: Houston, Tex., Circum-Pacific Council for Energy and Mineral Resources, p. 31-49.

*Lachenbruch, A.H., and *Marshall, B.V., 1986, Changing climate: geothermal evidence from permafrost in the Alaska Arctic: Science, v. 234, no. 4777, p. 689-696.

*Lahr, J.C., *Page, R.A., *Fogleman, K.A., and *Miller, T.P., 1985, The 1984 Sutton earthquake: New evidence for activity of the Castle Mountain fault (abs.): Earthquake Notes, v. 55 (sic), v. 56, no. 1, p. 23.

*Lahr, J.C., *Page, R.A., *Stephens, C.D., and *Fogleman, K.A., 1986, Sutton, Alaska, earthquake of 1984: Evidence for activity on the Talkeetna segment of the Castle Mountain fault system: Bulletin of the Seismological Society of America, v. 76, no. 4, p. 967-983.

Lange, I.M., *Nokleberg, W.J., Plahuta, J.T., Krouse, H.R., and *Doe, B.R., 1985, Geologic setting, petrology, and geochemistry of stratiform sphalerite-galena-barite deposits, Red Dog Creek and Drenchwater Creek areas, northwestern Brooks Range, Alaska: Economic Geology, v. 80, no. 7, p. 1896-1926.

*Lee, H.J. and *Schwab, W.C., 1983 (1986), Geotechnical framework, northeast Gulf of Alaska, in Environmental Assessment of the Alaskan Continental Shelf Final Reports of Principal Investigators: U.S. Department of Commerce, NOAA, OCSEAP Final Report, v.48, U.S. Department of the Interior OCS Study, MMS 86-0065, p. 95-547.

*Lee, H.J., Asce, M., and *Edwards, B.D., 1986, Regional method to assess offshore slope stability: Journal of Geotechnical Engineering, v. 112, no. 5, p. 489-509. (Covers Yakutat slump, and Icy Bay - Malaspina slump.)

*Leonard, B.F., 1986, Memorial of A.F. Buddington, November 29, 1890 - December 25, 1980: American Mineralogist, v. 71, no. 9-10, p. 1268-1273.

Lewis, S.D., Ladd, J.W., *Bruns, T.R., and *von Huene, Roland, 1986, Structural development of the accretionary prism, Shumagin region of the Aleutian trench, from SEABEAM and seismic reflection curves (abs.): Eos (American Geophysical Union Transactions), v. 67, no. 44, p. 1197.

*Lisowski, Michael, and *Savage, J.C., 1986, Extremely high shear strain rate measured across the Fairweather fault near Yakutat, Alaska (abs.): Eos (American Geophysical Union Transactions), v. 67, no. 44, p. 907.

Little, T.A., *Blome, C.D., and *Wolfe, J.A., 1986, Paleocene - Eocene sedimentation and wrench tectonics along the Border Ranges fault system, north-central Chugach Mountains, Alaska (abs.): Geological Society of America, Abstracts with Programs, v. 18, no. 2, p. 127.

*Magoon, L.B., and *Bird, K.J., 1985, Alaskan North Slope petroleum geochemistry for the Shublik Formation, Kingak Shale, pebble shale unit, and Torok Formation, in *Magoon, L.B., and *Claypool, G.Ed., eds., Alaska North Slope oil-rock correlation study; Analysis of North Slope crude: Tulsa, Okla., American Association of Petroleum Geologists Studies in Geology 20, p. 31-48.

*Magoon, L.B., and *Claypool, G.E., eds., 1985, Alaska North Slope oil-rock correlation study; Analysis of North Slope crude: Tulsa, Okla., American Association of Petroleum Geologists Studies in Geology 20.

Marincovich, Louie, Jr., and Kase, Tomoki, 1986, An occurrence of *Turritella (Hataiella) sagai* in Alaska: implications for the age of the Bear Lake Formation: Tokyo, Japan, Bulletin of the National Science Museum, Series C (Geology and Paleontology), v. 12, no. 2, p. 61-66.

*Marincovich, Louie, Jr., *Brouwers, E.M., and *Carter, L.D., 1986, Reply to comment by *Frederiksen, N.O., and others, on "Early Tertiary marine fossils from northern Alaska: implications for Arctic Ocean paleogeography and faunal evolution": Geology, v. 14, no. 9, p. 803-804.

*Markon, Carl, and Strong, Laurence, 1985, Development of land cover and terrain data bases for the Arctic National Wildlife Refuge, Alaska, using Landsat and digital terrain data (abs.), in International Symposium on Remote Sensing of Environment, 19th, Ann Arbor, Mich., 1985, Proceedings: Ann Arbor, Mich., Environmental Research Institute of Michigan, v. 1, p. 333-334.

*Marlow, M.S., Parson, L.M., *Carlson, P.R., and *Cooper, A.K., 1986, Buried basement ridges and linear magnetic anomalies in the western Aleutian basin, Bering Sea (abs.): Eos, (American Geophysical Union Transactions), v. 67, no. 44, p. 1227.

*McDougall, Kristin, 1986, Maestrichtian benthic foraminifers from Ocean Point, Alaska (abs.): Geological Society of America, Abstracts with Programs, v. 18, no. 6, p. 688.

*Molnia, B.F., 1986, Glacial history of the northeastern Gulf of Alaska - A synthesis, in *Hamilton, T.D., *Reed, K.M., and Thorson, R.M., eds., Glaciation in Alaska, the geologic record: Anchorage, Alaska Geological Society, p. 219-235.

*Moore, T.E., 1986, Stratigraphic framework and tectonic implications of pre-Mississippian rocks, northern Alaska (abs.): Geological Society of America, Abstracts with Programs, v. 18, no. 2, p. 159.

Morley, J.J., and *Robinson, S.W., 1986, Improved method for correlating late Pleistocene/Holocene records from the Bering Sea: application of a biosiliceous/geochemical stratigraphy: Deep-Sea Research, v. 33, no. 9, p. 1203-1211.

Motyka, R.J., Kodosky, L.G., and *Evans, W., 1986, A review of gas sampling at Augustine Volcano, Alaska: 1982-1986 (abs.): Eos (American Geophysical Union Transactions), v. 67, no. 44, p. 1260.

*Nokleberg, W.J., and *Plafker, George, 1986, Structural and tectonic analysis of major sutures, eastern Chugach Mountains, Alaska (abs.): Eos (American Geophysical Union Transactions), v. 67, no. 44, p. 1195.

*Nokleberg, W.J., *Plafker, George, and *Roeske, S.M., 1986, Structural analysis and accretionary tectonics of Cretaceous and early Tertiary flysch sequences juxtaposed along the Contact fault, eastern Chugach Mountains, Alaska (abs.): Geological Society of America, Abstracts with Programs, v. 18, no. 2, p. 164.

*Page, R.A., *Fuis, G.S., *Ambos, E.L., and *Stephens, C.D., 1986, Relocated earthquakes along the TALI corridor in the Chugach Mountains, southern Alaska (abs.): Eos (American Geophysical Union Transactions), v. 67, no. 44, p. 1197-1198.

*Page, R.A., *Plafker, George, *Fuis, G.S., *Nokleberg, W.J., *Ambos, E.L., *Mooney, W.D., and *Campbell, D.L., 1986, Accretion and sub-duction tectonics in the Chugach Mountains and Copper River basin, Alaska: Initial results of the Trans-Alaska Crustal Transect: Geology, v. 14, no. 6, p. 501-505.

Peteet, D.M., and *Rubin, Meyer, 1986, Paleoecology of the Malaspina and Bering Glacier districts, Alaska (abs.), in American Quaternary Association, Biennial meeting, 9th, Urbana, University of Illinois-Champaign, 1985, Program and Abstracts, p. 13.

*Phillips, R.L., *Barnes, P.W., *Colgan, M.W., and *Miley, J.M., 1986, Quaternary stratigraphy of northern Chukchi Sea, Alaska (abs.): American Association of Petroleum Geologists, Annual Convention, Atlanta, Ga., 1986, Book of Abstracts, p. 632.

*Phillips, R.L., *Barnes, P.W., *Colgan, M.W., and *Miley, J.M., 1986, Quaternary stratigraphy of northern Chukchi Sea, Alaska (abs.): American Association of Petroleum Geologists Bulletin, v. 70, no. 5, p. 632.

*Plafker, George, *Ambos, E.L., *Fuis, G.S., *Mooney, W.D., *Nokleberg, W.J., and *Page, R.A., 1986, Late Mesozoic and Early Tertiary accretion and subduction along the southern Alaska continental margin (abs.): Geological Society of America, Abstracts with Programs, v. 18, no. 2, p. 171.

*Plafker, George, and *Nokleberg, W.J., 1986, Evolution of the continental margin of southern Alaska along the Trans Alaska Crustal Transect (TACT) (abs.): Eos (American Geophysical Union Transactions), v. 67, no. 44, p. 1195.

*Rearic, D.M., Williams, S., and *Carlson, P.R., 1986, VAMP's and other acoustic evidence for gas-charged sediment in the abyssal Aleutian basin, Bering Sea, Alaska (abs.): Eos (American Geophysical Union Transactions), v. 67, no. 44, p. 1211.

*Reynolds, R.L., *Karachewski, J.A., *Fishman, N.S., and *Rosenbaum, J.G., 1986, Magnetic properties of greigite-bearing Cretaceous strata, North Slope, Alaska (abs.): Eos (American Geophysical Union Transactions), v. 67, no. 44, p. 923.

*Roeske, S.M., and Mattinson, J.M., 1986, Early Jurassic blueschists and island arc volcanism in southern Alaska: A paired metamorphic belt? (abs.): Geological Society of America, Abstracts with Programs, v. 18, no. 2, p. 178.

*Roeske, S.M., *Nokleberg, W.J., and *Plafker, George, 1986, Structural analysis of the Orca Group on the east limb of the Alaska orocline, Cordova, eastern Prince William Sound (abs.): Geological Society of America, Abstracts with Programs, v. 18, no. 2, p. 178.

*Savage, J.C., and *Lisowski, M., 1986, Strain accumulation in the Shumagin seismic gap, Alaska: Journal of Geophysical Research, v. 91, no. B7, p. 7447-7454.

*Savage, J.C., and *Lisowski, M., 1986, Strain accumulation in the Yakataga seismic gap, southern Alaska: Journal of Geophysical Research, v. 91, no. B9, p. 9495-9506.

*Savage, J.C., *Lisowski, M., and *Prescott, W.H., 1986, Strain accumulation in the Shumagin and Yakataga seismic gaps, Alaska: Science, v. 231, no. 4738, p. 585-587.

*Schmidt, J.M., 1986, Stratigraphic setting and mineralogy of the Arctic volcanogenic massive sulfide prospect, Ambler district, Alaska: Economic Geology, v. 81, no. 7, p. 1619-1643.

*Schmoll, H.R., and *Yehle, L.A., 1986, Pleistocene glaciation of the Upper Cook Inlet basin, in *Hamilton, T.D., *Reed, K.M., and Thorson, R.M., eds., Glaciation in Alaska, the geologic record: Anchorage, Alaska Geological Society, p. 193-218.

*Scholl, D.W., and *Ryan, H.F., 1986, Crustal structure and evolution of the Aleutian forearc in the vicinity of the Andreanof earthquake (abs.): Eos (American Geophysical Union Transactions), v. 67, no. 44, p. 1081.

*Scholl, D.W., *Vallier, T.L., and *Stevenson, A.J., 1986, Terrane accretion, production, and continental growth: A perspective based on the origin and tectonic fate of the Aleutian-Bering Sea region: Geology, v. 14, no. 1, p. 43-47.

*Scholl, D.W., *Vallier, T.L., *Stevenson, A.J., and *Ryan, H.F., 1986, Contrasting processes controlling basin formation in Cenozoic island arcs, Tonga and Aleutian ridges (abs.): American Association of Petroleum Geologists Bulletin, v. 70, no. 5, p. 646.

*Scholl, D.W., *Vallier, T.L., *Stevenson, A.J., and *Ryan, H.F., 1986, Contrasting processes controlling basin formation in Cenozoic island arcs, Tonga and Aleutian ridges (abs.): American Association of Petroleum Geologists, Annual Convention, Atlanta, Ga., 1986, Book of Abstracts, p. 646.

Shasby, Mark, and *Carneggie, David, 1986, Vegetation and terrainmapping in Alaska using Landsat MSS and digital terrain data: PE & RS (Photogrammetric Engineering, Remote Sensing), v. 52, no. 6, p. 779-786.

*Silberling, N.J., 1985, Biogeographic significance of the Upper Triassic bivalve Monotis in Circum-Pacific accreted terranes, in Howell, D.G., ed., Tectonostratigraphic terranes of the Circum-Pacific region: Houston, Tex., Circum-Pacific Council for Energy and Mineral Resources, p. 63-70

Sisson, V.B., Hollister, L.S., and *Plafker, George, 1986, Rapid two-stage metamorphism of the eastern Chugach Mountains, southern Alaska (abs.): Geological Society of America, Abstracts with Programs, v. 18, no. 2, p. 186.

Spicer, R.A., and *Parrish, J.T., 1986, Fossil woods from northern Alaska and climate near the middle Cretaceous North Pole (abs.): Geological Society of America, Abstracts with Programs, v.18, no. 6, p. 759.

Stephens, G.C., Evenson, E.B., Clinch, J.M., and *Detra, D.E., 1985, In Alaska; geochemical research program underway: Geotimes, v. 30, no. 7, p. 14-17.

*Stevenson, A.J., and *Vallier, T.L., 1986, Evolution, structure, and petroleum potential of Aleutian subduction complex (abs.): American Association of Petroleum Geologists Bulletin, v. 70, no. 7, p. 935.

Taber, J.J., *Fuis, G.S., *Ambos, E.L., *Mooney, W.D., and *Page, R.A., 1986, Seismic velocity structure of the Prince William terrane, Alaska (abs.): Eos (American Geophysical Union Transactions), v. 67, no. 44, p. 1196.

Taber, J.J., Jacob, K.H., and *Engdahl, E.R., 1986, Seismicity of the Aleutian Arc (abs.): Eos (American Geophysical Union Transactions), v. 67, no. 44, p. 1236.

Thorson, R.M., and *Hamilton, T.D., 1986, Glacial geology of the Aleutian Islands. Based on contributions of Robert F. Black, in *Hamilton, T.D., *Reed, K.M., and Thorson, R.M., eds., Glaciation in Alaska, the geologic record: Anchorage, Alaska Geological Society, p. 171-191.

Tolbert, G.E., and *Ericksen, George, 1986, Memorial to Helmut Wedow, Jr. 1917-1984: Geological Society of America Memorials, v. 16.

*Torresan, M.E., *Schwab, W.C., and *Oscarson, R.L., 1985, Controls on the formation of fabric in marine sediment from the Gulf of Alaska (abs.), in SEPM Annual Midyear Meeting, 2nd, Golden, Colo., 1985, Abstracts: Tulsa, Okla., Society of Economic Paleontologists and Mineralogists, p. 89.

Underwood, M.B., and *Stevenson, A.J., 1986, Dispersal of volcanic sediment in central Aleutian forearc and trench (abs.): American Association of Petroleum Geologists Bulletin, v. 70, no. 5, p. 657-658.

Underwood, M.B., and *Stevenson, A.J., 1986, Dispersal of volcanic sediment in central Aleutian forearc and trench (abs.): American Association of Petroleum Geologists, Annual Convention, Atlanta, Ga., 1986, Book of Abstracts, p. 657-658.

*Vallier, T.L., 1986, Tectonic implications of arc-axis (Wallowa terrane) and back-arc (Vancouver Island) volcanism in Triassic rocks of Wrangellia (abs.): Eos (American Geophysical Union Transactions), v. 67, no. 44, p. 1233.

*von Huene, Roland, *Box, Stephen, *Detterman, Bob, *Fisher, Michael, *Moore, Casey, and *Pulpan, Hans, 1985, Centennial Continent/Ocean Transect #6: A-2 Kodiak to Kuskokwim, Alaska: Geological Society of America, 14 p.

*von Huene, Roland, *Keller, G., *Bruns, T.R., and *McDougall, K., 1985, Cenozoic migration of Alaskan terranes indicated by paleontologic study, in Howell, D.G., ed., Tectonostratigraphic terranes of the Circum-Pacific region: Houston, Tex., Circum-Pacific Council for Energy and Mineral Resources, p. 121-136.

*Weber, F.R., 1986, Glacial geology of the Yukon-Tanana Upland, in *Hamilton, T.D., *Reed, K.M., and Thorson, R.M., eds., Glaciation in Alaska, the geologic record: Anchorage, Alaska Geological Society, p. 79-98.

Wolf, L.W., Levander, A.R., and *Fuis, G.S., 1986, Upper crustal velocity structure of the accreted Chugach terrane, Alaska (abs.): Eos (American Geophysical Union Transactions), v. 67, no. 44, p. 1195.

*Yeend, Warren, 1985, Experimental abrasion of detrital gold, in Madonna, J.A., ed., Alaskan placer mining, Annual conference, 7th, Fairbanks, 1985, Proceedings: Fairbanks, Alaskan Prospectors Publishing, p. 1-8.

SUBJECT INDEX

COAL GEOLOGY

ECONOMIC GEOLOGY

GENERAL GEOLOGY

GEOCHEMISTRY

GEOPHYSICS

MARINE GEOLOGY

MINERALOGY

PALEONTOLOGY/MICROPALEONTOLOGY

PETROLEUM GEOLOGY

PETROLOGY - IGNEOUS

PETROLOGY - METAMORPHIC

PETROLOGY - SEDIMENTARY

QUATERNARY GEOLOGY

SEDIMENTOLOGY

STRATIGRAPHY

STRUCTURAL GEOLOGY - TECTONICS

VOLCANOLOGY

AUTHOR INDEX

AUTHORS ADDRESSES

U.S. Geological Survey
Geologic Division Mail Stop --
345 Middlefield Road
Menlo Park, CA 94025

	Mail Stop
Barnes, P.W.	999
Bird, K.J.	999
Box, S.E.	904
Brew, D.A.	904
Bruns, T.R.	999
Carlson, P.R.	999
Carter, Claire	915
Collett, T.S.	999
Dadisman, S.V.	999
Fisher, M.A.	999
Ford, A.B.	904
Foster, H.L.	904
Galloway, J.P.	917
Gardner, J.V.	999
Graves, Scot	999
Huber, D.F.	984
Jachens, R.C.	989
Karl, H.A.	999
Keith, T.E.C.	910
Kempema, E.W.	999
Koch, R.D.	904
Kvenvolden, K.A.	999
Leonard, K.R.	984
Loney, R.A.	904
Magoon, L.B.	999
Mankinen, E.A.	937
Maple, E.J.	979
Marlow, M.S.	999
Meyer, C.E.	975
Mullen, M.W.	917
Murphy, J.M.	904
Oscarson, R.L.	916
Page, N. J	941
Phillips, R.L.	999
Pickthorn, Leda Beth	999
Plafker, George	904
Rearic, D.M.	999
Reimnitz, Erk	999
Rinehart, C.D.	901
Stanley, R.G.	999
Trimble, D.A.	937
Vallier, T.L.	999
von Huene, Roland	999
White, E.R.	955
Yeend, Warren	904

U.S. Geological Survey
Branch of Alaskan Geology
4200 University Drive
Anchorage, AK 99508-4667

Gamble, B.M.
Hamilton, T.D.
Karl, S.M.
Lancaster, G.A.
Miller, T.P.
Nelson, S.W.
Riehle, J.R.
Schmidt, J.M.
Shew, Nora
Yount, M.E.
Zayatz, M.R.

U.S. Geological Survey
Branch of Alaskan Geology
PO Box 80586
Fairbanks, AK 99708

Weber, F.R.
Wheeler, K.L.

U.S. Geological Survey
Geologic Division Mail Stop --
Box 25046, DFC
Denver, CO 80225

	Mail Stop
Barton, C.C.	913
Blome, C.D.	919
Cady, J.W.	964
Duttweiler, K.A.	973
Hoffman, J.D.	955
Light, T.D.	955
Parrish, J.T.	971
Schmoll, H.R.	972

U.S. Geological Survey
5946 McIntyre Street
Golden, CO 80403

Goldfarb, R.J.

U.S. Geological Survey
Museum Natural History E-503
Washington, D.C. 20560

Dutro, J.T., Jr.
Harris, A.G.
Repetski, J.E.

U.S. Geological Survey
National Center Mail Stop --
12201 Sunrise Valley Drive
Reston, VA 22092

	Mail Stop
Ager, T.A.	970
Bartsch-Winkler, Susan	920
McCammon, R.B.	920

U.S. Mineral Management Service
949 E. 36th Avenue Rm 110
Anchorage, AK 99508-4302

Herman, B.M.

Ackerman, R.E.
Washington State University
Department of Anthropology
Pullman, WA 99164

Blodgett, R.B.
Oregon State Unviersity
Department of Geology
Corvallis, OR

Colgan, M.W.
University of Santa Cruz
Earth Sciences Board,
Santa Cruz, CA 95064

Folger, P.F.
University of Montana
Department of Geology
Missoula, MT 59812

Forbes, R.B.
Division of Geological and Geophysical Surveys
400 Willoughby Bldg
Juneau, AK 99801

Himmelberg, G.R.
University of Missouri
Geology Department,
Columbia, MO 65201

Huggett, Quentin
Parson, L.M.
Institute of Oceanographic Sciences
Wormley, London
United Kingdom

Kaufman, D.S.
University of Washington
Department of Geological Sciences
Seattle, WA 98195

Newberry, R.J.
University of Alaska
Department of Geology and Geophysics
Fairbanks, AK 99775-0760

Rohr, D.M.
Sul Ross State University
Department of Geology
Alpine, TX 79830

Spicer, R.A.
Goldsmiths' College
University of London
London SE8 3BU
United Kingdom